REPORT 1339

CONTENTS

	Page
SUMMARY	1391
INTRODUCTION	1391
SYMBOLS AND TERMINOLOGY	1392
SYMBOLS	1392
Subscripts	1392
Abbreviations	1392
TERMINOLOGY	1392
PRESENTATION OF DATA	1392
FLOW CONSIDERATIONS	1393
TRAILING-EDGE SEPARATION	1393
LEADING-EDGE SEPARATION	1394
MIXED SEPARATION	1397
ROUGHNESS	1398
LONGITUDINAL STABILITY	1399
GEOMETRIC CONSIDERATIONS	1399
STALL CONTROL	1400
Devices	1401
Fences or vanes	1401
Nacelles and stores	1403
Extensible leading-edge flaps	1403
Extensible leading-edge slats	1406
Droop nose	1406
Boundary-layer control	1406
Chord extensions	1407
Variable sweep	1410
Contra flaps	1410
Wing Geometry	1411
Camber and twist	1411
Inverse taper	1412
Cranked wings	1412
Composite (A, M, and W) wings	1413
HORIZONTAL TAIL	1413
Effectiveness	1414
Wing-Fuselage-Tail Combinations	1417
LIFT	1418
PLAIN WING	1418
Lift-Curve Slope	1418
Maximum Lift	1418
Type of flow separation	1419
Influence of camber	1420
Reynolds number and Mach number effects	1420
Effect of aspect ratio	1420
Inflection or Usable Lift Coefficient	1420
HIGH-LIFT AND STALL-CONTROL DEVICES	1423
Linear Lift Range	1423
Maximum Lift	1425
Trailing-edge flaps	1425
Leading-edge stall-control devices	1425
Trailing-edge flaps in combination with leading-edge stall-control devices	1426
DRAG	1426
PLAIN WING	1426
Induced Drag	1426
Profile Drag	1427
Span Efficiency	1427
HIGH-LIFT AND STALL-CONTROL DEVICES	1429
SUMMARY OF RESULTS	1429
REFERENCES	1430
TABLES	1434

REPORT 1339

A SUMMARY AND ANALYSIS OF THE LOW-SPEED LONGITUDINAL CHARACTERISTICS OF SWEPT WINGS AT HIGH REYNOLDS NUMBER [1]

By G. Chester Furlong and James G. McHugh

SUMMARY

The low-speed longitudinal characteristics of swept wings derived primarily from investigations at high Reynolds numbers are summarized and analyzed. Two basically different types of flow separation, trailing-edge separation and leading-edge separation, are identified and discussed; and it is shown that in the case of a sweptback wing, either type or a mixture of the two types of separation may occur. The type of separation encountered on any particular wing is dependent primarily on the leading-edge radius, leading-edge sweep angle, Reynolds number, and aspect ratio. When the type of flow separation is defined, generalized trends in the lift, drag, and pitching moment can be established.

Methods of stall control applicable to each type of flow separation are discussed and the effectiveness of the various methods (devices and wing geometry) currently available is indicated. The important influence that the vertical position of the horizontal tail has on the over-all stability of airplane configurations both with and without stall-control devices is considered, and generalized procedures for predicting tail effectiveness are presented.

The effectiveness of various high-lift devices in the linear lift range and at maximum lift has been summarized, and the advantages of the various types are noted.

For the convenience of the designer, the more significant available data, as of August 15, 1951, on the longitudinal characteristics of swept, delta, and thin straight wings are compiled in convenient tabular form. In general, the tabulated data were obtained at a Reynolds number of 6.0×10^6, but, for a few significant configurations where such high Reynolds number data were not available, the results of tests at Reynolds numbers as low as 4.0×10^6 have been included.

INTRODUCTION

At the time when the swept wing was first proposed for high-speed flight (refs. 1 to 9), it was recognized that the induced angle-of-attack distribution and the characteristic boundary-layer growth on such wings would promote tip stall. In addition, simple sweep theory indicated the lift capabilities of swept wings to be materially less than for comparable straight wings. Both the tip-stalling tendencies and low values of attainable lift of swept wings constituted landing and take-off problems requiring considerable research at low speeds.

In an early summary of the longitudinal stability characteristics of swept wings, Shortal and Maggin (ref. 10) established a relation between wing plan-form parameters and the type of longitudinal stability that existed at or prior to maximum lift and, on the basis of such a correlation, showed that longitudinal instability due to tip stalling was dependent primarily on aspect ratio and sweep angle. With the data available at that time, they established an empirical variation of aspect ratio with sweep angle that defined a stability boundary.

In the ensuing years, the low-speed research effort has been directed toward determining the characteristics of swept wings, understanding the basic flow phenomena, and developing means to improve the stability characteristics of those wings the geometry of which was such as to place them on the unstable side of the stability boundary of reference 10. Much work has also been directed toward obtaining satisfactory longitudinal characteristics with horizontal tails in combination with wings falling on either side of the stability boundary.

As a result of this intensive research effort, a large amount of literature has accumulated in which the characteristics of many wings are described both with and without various devices for improving the characteristics. Inasmuch as the literature is comprised of many individual investigations, the present authors have undertaken to provide a comprehensive review of the present knowledge of the low-speed characteristics of swept wings. The present report has two specific purposes. The first is to make an analysis and generalization of these data in order to show the basic effects and trends of sweep and thus provide greater usefulness of the data by permitting reasonable interpolation and extrapolation. The second is to summarize in tabular form the basic results obtained at large Reynolds numbers (above 4.0×10^6) at low Mach numbers (less than 0.25). Two deviations from the stated purposes are noted in that unpublished data available to the authors have been used to supplement the literature on swept wings and also that data available (published and unpublished) on straight low-aspect-ratio wings suitable for supersonic speeds have been included with the

[1] Supersedes recently declassified NACA Research Memorandum L52D16 by G. Chester Furlong and James G. McHugh, 1952.

tabulated data on swept wings. Insofar as possible all large-scale data available as of August 15, 1951 have been included in the tables.

The static-longitudinal-stability problem is analyzed in terms of the effects of such parameters as aspect ratio, sweep, and leading-edge radius. The influence of stall-control devices, high-lift devices, and a horizontal tail on the stability of swept wings is considered in detail. The lift characteristics of swept wings are analyzed with respect to the same parameters and devices. A few remarks have also been included concerning the drag of swept wings. The high Reynolds number data are summarized with very little discussion in tables 1 to 47.

Deficiencies and inadequacies may, of course, be noted in the present accumulation of data, and the possibility exists that the schemes of analysis presented herein may undergo revision as the apparent gaps are filled.

SYMBOLS AND TERMINOLOGY

SYMBOLS

C_L	lift coefficient
L	lift
ΔC_L	increment of lift coefficient at $\alpha=0°$
$C_{L_{max}}$	maximum lift coefficient
$\Delta C_{L_{max}}$	increment of maximum lift coefficient
C_{L_α}	lift-curve slope
c_l	section lift coefficient
$c_{l_{max}}$	section maximum lift coefficient
C_m	pitching-moment coefficient about $0.25c'$
C_D	drag coefficient
D	drag
C_{D_i}	induced-drag coefficient
$C_{D_{min}}$	minimum-drag coefficient
C_{D_0}	profile-drag coefficient
Wake c_{d_0}	section profile-drag coefficient obtained by momentum method
P	pressure coefficient
C_Q	suction flow coefficient
R	Reynolds number
M	Mach number
$\frac{dw}{d\alpha}$	rate of rise of wake center location relative to extended wing-chord plane with angle of attack
α	angle of attack
$\alpha_{C_{L_{max}}}$	angle of attack at maximum lift coefficient
ϵ	downwash angle
δ_f	trailing-edge-flap deflection
δ_n	deflection of leading-edge flap, slat or droop
η	aspect-ratio correction factor (see ref. 11)
J	tail factor depending on aspect ratio, taper ratio, and flap span (see ref. 12)
τ	tail effectiveness parameter (see ref. 13)
e	wing efficiency factor
S	wing area
S'	wing area affected by suction
b	wing span
c'	mean aerodynamic chord $\left(\frac{2}{S}\int_0^{b/2} c^2\,dy\right)$
$\bar{c}$	average chord
c	local chord parallel to the plane of symmetry
c''	ratio of chord of leading-edge flap to local wing chord
y	lateral coordinate
A	aspect ratio
Λ	angle of sweepback
λ	taper ratio
z	vertical distance from extended wing-chord plane
V	tail volume
i	incidence

Subscripts:

$c/4$	quarter-chord line
LE	leading edge
e	effective
w	wing
t	tail
max	maximum

Abbreviations:

L. E.	leading edge
T. E.	trailing edge
a. c.	aerodynamic center
c. g.	center of gravity

TERMINOLOGY

A certain latitude has been necessary in the definition of various terms and in the nomenclature of various devices. For example, some references use the term "usable" maximum lift, whereas others use the term "inflection" lift. In both cases the terms usable and inflection are used to designate the lift coefficient at which there is a decided shift in aerodynamic center. Differences in definition and nomenclature have been pointed out where comparison with the reference report might not be clearly understood.

PRESENTATION OF DATA

All pitching-moment data, unless otherwise specified, are computed about the 0.25 mean aerodynamic chord. For convenience, this moment center will be considered the center of gravity and hence the longitudinal stability may be referred to as either stable or unstable.

Insofar as possible, a tabular form has been used to summarize the large amount of data available (refs. 13 to 67). An index to the tabulated data is given in table 1. The tables 2 to 47 are for the most part self-explanatory; some data which were repetitious and overlapping have been excluded. All data have been referenced so that the reader may easily refer to the detailed conditions under which the tests were made. It will be noted that values of R_{max} and M_{max} are listed in a headnote of each table. These values of Reynolds number and Mach number represent the highest values at which the wing was tested. Inasmuch as tests of the wing plus gadgets were in most cases confined to lower values of Reynolds number and Mach number, the data in the tables were restricted to a Reynolds number range

between 6.0×10^6 and 7.0×10^6. In some cases data were available only at Reynolds numbers lower than 6.0×10^6 and in such cases the values of R_{max} and M_{max} define the test conditions for the tabulated data.

The column headings have the following general significance:

Span of L.E. device ($b/2$): The span of the leading-edge device (slat, flap, etc.) is given in fraction of wing semispan. The outboard end of the device is located between 97 percent and 100 percent of semispan.

Span of T.E. device ($b/2$): The span of the trailing-edge high-lift device is given in fraction of wing semispan. With few exceptions the inboard end of the device is located at the plane of symmetry when a fuselage is not present. Some investigators measured the flap deflection in a plane parallel to the air stream whereas others measured it in a plane perpendicular to constant percent line on the swept panel. Reference to the original report should be made when such details are required.

Configuration: The sketches shown assist in interpreting the table, although plan-form details are unavoidably lacking except in those cases where deemed absolutely necessary.

$C_{L_{max}}$: In many cases the tops of the lift curves were relatively flat and the selection of the maximum value was difficult. In such cases consideration was given to the angle-of-attack range involved and the value was selected at the angle of attack at which the lift effectively leveled off.

$\alpha_{C_{L_{max}}}$: This angle represents the angle of attack at which the tabulated value of $C_{L_{max}}$ was first obtained.

L/D at $0.85C_{L_{max}}$: The values of lift-drag ratio obtained at a lift coefficient of $0.85C_{L_{max}}$ are presented in order to provide a comparison among the configurations in the high-lift range.

C_m characteristics: The longitudinal stability characteristics are easily compared from these compressed plots of C_m against C_L.

The data presented in the figures are intended to illustrate the trends indicated by the tabular data. In addition to the data from the tables, data from references 28 and 68 to 89 have been used in the preparation of the figures. Unfortunately, sweep is only one of the variables and hence its influence on the aerodynamic characteristics cannot be isolated quantitatively except in the most general degree. An index to the figures is presented in table 48.

FLOW CONSIDERATIONS

Fundamental to the improvement of both the stability and maximum lift characteristics of swept wings is a knowledge of those factors which both influence and induce flow separation. It has been found that on certain sweptback wings leading-edge separation may precede or accompany trailing-edge separation, with the result that the variations of pitching-moment coefficient with lift coefficient are quite unlike those obtained when only trailing-edge separation is involved. Similarly, appreciable differences in the maximum lift characteristics exist between swept wings exhibiting trailing-edge separation and those exhibiting leading-edge separation. Inasmuch as the stability and lift characteristics and the required methods of flow control associated with leading-edge separation are so different from those associated with trailing-edge separation, an attempt has been made, in the following sections, to present the basic phenomena of the different types of flow separation.

One effect attributable to sweep is a change in the spanwise distribution of induced angle of such nature as to cause the load on the wing of a given aspect ratio and taper ratio to be concentrated further outboard when the sweep angle is increased (fig. 1). Flow separation and consequent loss in lift over the outboard sections would necessarily precede that over the inboard sections.

The induced camber which exists on either a swept or unswept wing is negative at the tip and positive at the root. The negative induced camber at the tip sections produces adverse pressure gradients very conducive to flow separation; whereas the positive induced camber at the root sections minimizes the adverse pressure gradients so that the flow over these sections is very resistant to flow separation. The significant effect of induced camber is, therefore, its influence on the chordwise pressure gradients across the span.

TRAILING-EDGE SEPARATION

Another factor that promotes tip stall and is attributable to sweep, or at least is accentuated by it, is the manner in which the boundary layer flows on the wing. Elementary considerations of the pressures on a straight wing indicate an outflow of the boundary layer on the lower surface and an inflow of the boundary layer on the upper surface. When sweep is introduced, the respective chordwise pressure distributions are staggered so that, on any line perpendicular

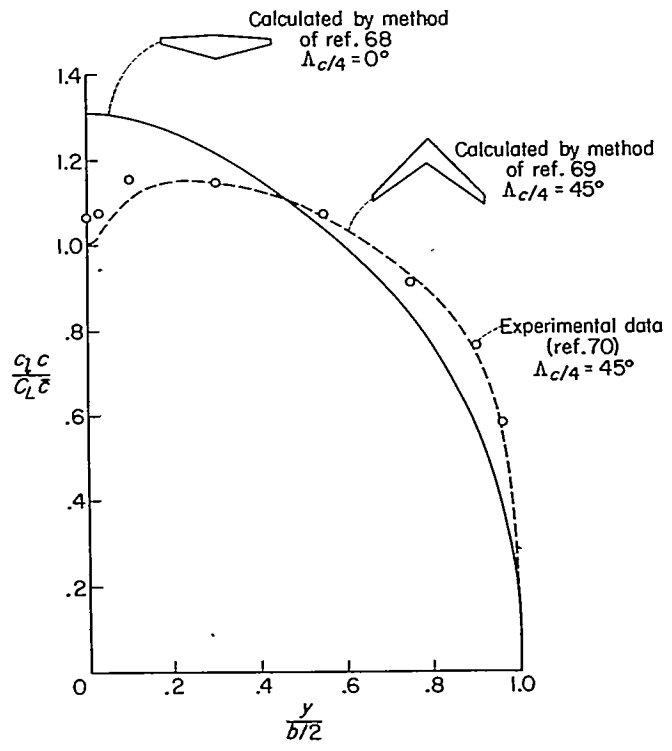

FIGURE 1.—Effect of sweep on the load distribution of a wing having an aspect ratio of 8.02 and a taper ratio of 0.45.

to the plane of symmetry, the pressures on the upper surface become more negative with an increase in distance from plane of symmetry. A pressure gradient, therefore, exists from root to tip, which induces a boundary-layer flow from root to tip.

The degree to which the outflow is established at any given value of lift coefficient is dependent primarily on the sweep angle involved. The outflow of the boundary layer produces over the tip sections excessively thick boundary layers, which separate more easily than those of normal thicknesses. This outflow effectively removes the boundary layer from the inboard sections so that the boundary layer over these sections is more resistant to separation.

The combined effects of the induced-angle distribution on the spanwise loadings, induced camber, and boundary-layer growth over the tip sections on the section-lift characteristics of a high-aspect-ratio, highly sweptback wing are indicated by the data presented in figure 2. The airfoil sections incorporated in the wing were 12 percent thick and the chordwise pressure distributions indicated that flow separation progressed from the trailing edge to the leading edge of the tip sections. The maximum lift coefficients of the tip sections fall far short of the maximum lift coefficients of the root sections.

Some interesting boundary-layer studies made at low Reynolds numbers on a 35° sweptback wing (ref. 90) reveal the complexities which arise from the outflow of the boundary layer. The results presented in reference 90 show that the outflow may be as much as 25° on the surface of the wing, whereas the flow at the upper edge of the boundary layer may be directed toward the plane of symmetry as much as 10°. In many investigations of wings having sweep angles greater than 35°, surface tufts have indicated outflow much in excess of 25°. The development, growth, and separation of a turbulent boundary layer, complex in two-dimensional flow, becomes even more complex when sweep is introduced.

The variations of pitching moment with lift to be obtained when the tip separation is present are indicated in figure 3. The data indicate the extent to which the wing will become longitudinally unstable at the stall if the sweep angle is increased whereas all other parameters are held constant. Further increases in sweep angle for this particular wing would result in unstable tendencies at progressively lower values of lift coefficient.

LEADING-EDGE SEPARATION

When sweep is incorporated in a wing, the airfoil sections of which exhibit a pronounced leading-edge-separation bubble, a conical vortex lying on the wing surface can be observed (ref. 72). The existence of such a vortex flow is not limited

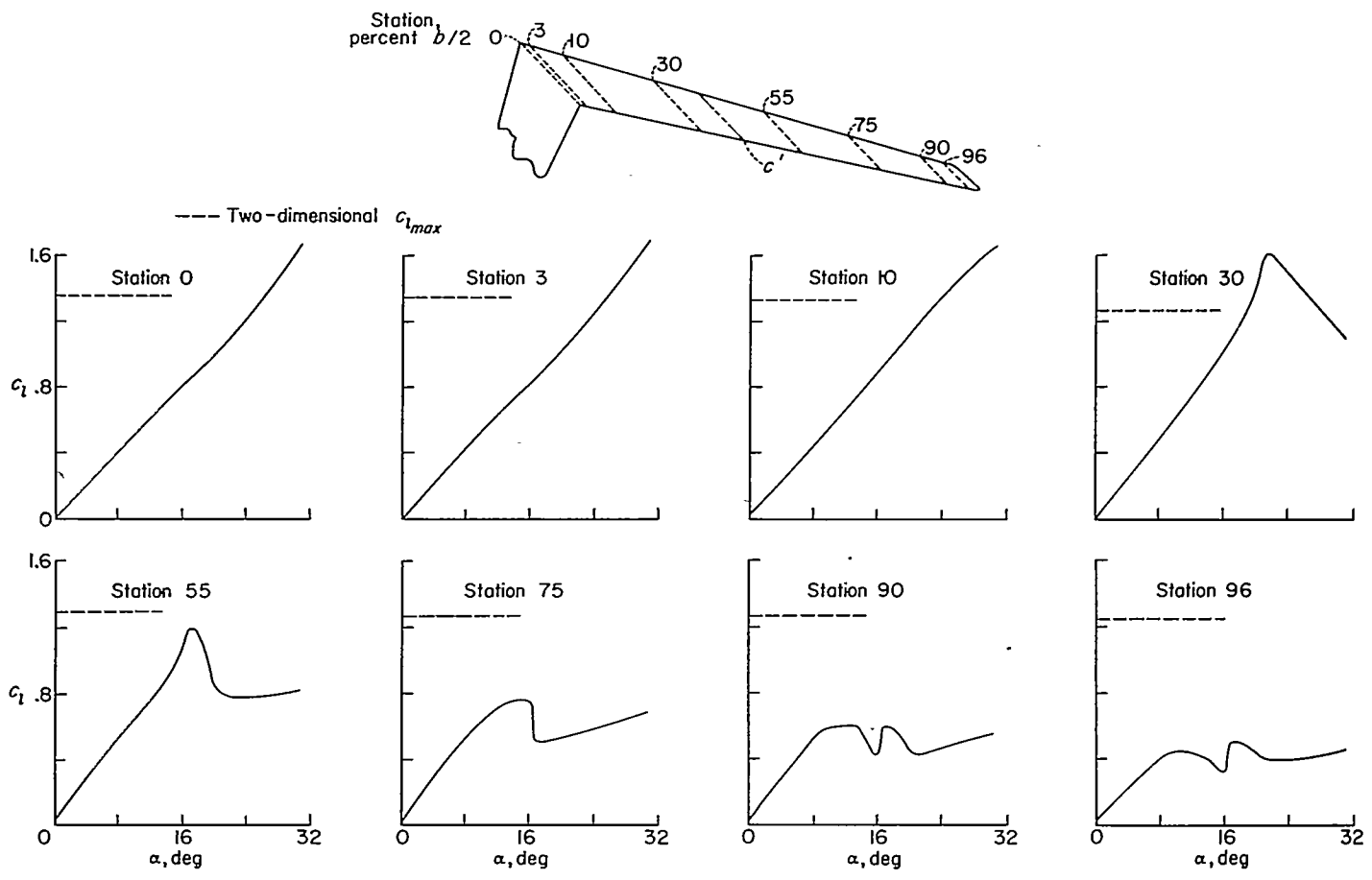

FIGURE 2.—Stall progression on a sweptback wing ($\Lambda_{c/4}=45°$) having an aspect ratio of 8.02, a taper ratio of 0.45, and NACA 63_1A012 airfoil sections as indicated by the section lift characteristics. (Data obtained from ref. 70.)

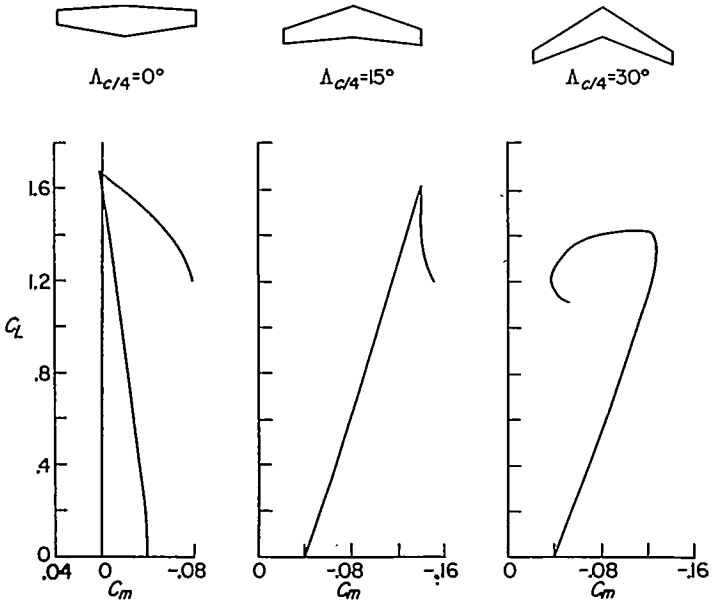

FIGURE 3.—Variations of pitching-moment coefficient with lift coefficient for a family of wings having aspect ratio of 6.0, taper ratio of 0.5, NACA 2415 airfoil sections, and various amounts of sweep. (Data taken from ref. 71.)

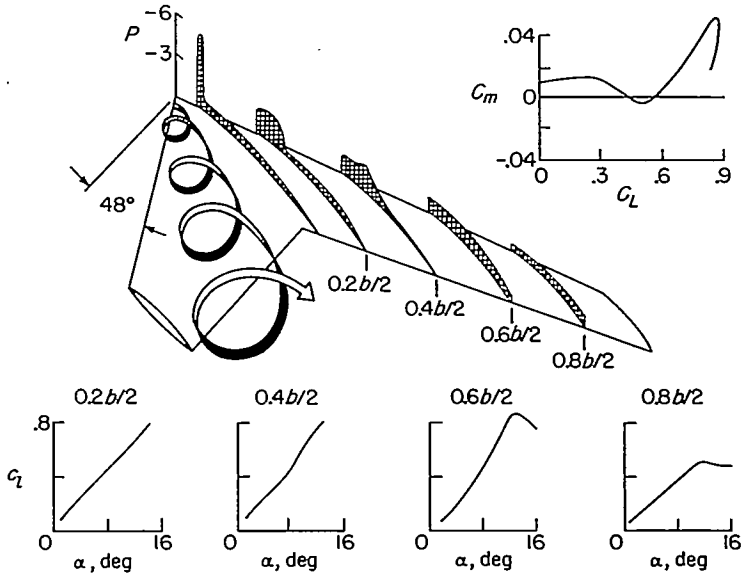

FIGURE 4.—Schematic view of leading-edge vortex flow and its effect on the pressure distribution and the lift and pitching-moment characteristics of a sweptback wing ($\Lambda_{c/4}=45°$) of aspect ratio 3.5 and incorporating circular-arc airfoil sections. $C_L=0.67$. (Data obtained from ref. 72.)

to only those wings incorporating airfoil sections which exhibit a separation bubble, but its presence on them is more easily predicted. For example, if the induced camber effect on a swept wing is great enough, it may cause an airfoil section which stalls in two-dimensional flow from the trailing edge to stall in three-dimensional flow from the leading edge. The result may be that a leading-edge-separation bubble necessary to the formation of the vortex flow is developed. The spanwise extent of the localized leading-edge vortex due to the induced camber over the tip sections probably depends most directly on the values of leading-edge radii involved. The influence of leading-edge radius on the formation of a leading-edge-vortex flow of sufficient strength to affect materially the aerodynamic characteristics of swept wings will be discussed subsequently.

The leading-edge-vortex flow results from both the leading-edge separation bubble and the spanwise pressure gradient introduced by sweep and has been observed to be conical in cross section perpendicular to the leading edge with the diameter of the cone increasing in the tip direction. This shape arises from the fact that at the tip sections the vortex contains an accumulation of the dead air that has drained from the more inboard sections. Probe studies made on the DM-1 glider modified to provide a sharp leading edge indicated the presence of a vortex lying on the wing surface (ref. 91); however, the pressure-distribution tests on a 48° sweptback wing of aspect ratio 3.5 and incorporating circular-arc airfoil sections (ref. 72) seem to be the first to illustrate the mechanics of this type of separation. The results of this investigation have been schematically illustrated in figure 4. The presence of the vortex flow reduces the leading-edge pressures but at the same time broadens the regions of high chordwise loading and causes rearward shifts in center of pressure. Although the section lift characteristics presented in figure 4 do not indicate a strong influence of the vortex flow at the outermost station, pressure-distribution data of reference 72 show it to exist. It is probable that the concentration of boundary-layer air over the rear part of the tip sections separates early and hence tends to nullify the effects of the vortex flow, so that the resulting lift is low but varies fairly linearly with angle of attack to the stall for this section. With an increase in angle of attack, the vortex becomes stronger over the more inboard stations and the boundary-layer concentration is swept off as the vortex is shed from the wing. The result is that these stations experience an increase in lift-curve slope as indicated by the data of the $0.60b/2$ station. With further increase in angle of attack the vortex moves inboard along the trailing edge and leaves more of the tip sections in a diffused region of vortex flow; whereas the inboard sections are experiencing an increase in lift-curve slope because of the increased strength of the vortex flow.

These changes in lift characteristics brought about by the vortex flow produce rather severe changes in the pitching-moment characteristics through the lift range. As can be seen in figure 4, the initial dip in the pitching-moment curve occurs when the vortex has formed with appreciable strength over the outboard sections. The vortex moves inboard along the trailing edge with an increase in angle of attack, thus the tip sections are in a diffused region of vortex flow and their lift-curve slopes are decreased. At the same time the inboard sections are experiencing an increase in lift-curve slope. The changes in span loading associated with these effects cause a destabilizing pitching-moment variation through the moderate lift range. At maximum lift it is possible that the vortex has moved inboard sufficiently to cause a rearward shift in the centers of pressure so that

a stable pitching-moment break at maximum lift is obtained or that the stable pitching moment merely results from the tendency of the wing to assume the pitching-moment coefficient for the stalled flat-plate plan form for this wing.

Although a sharp leading-edge wing is an extreme case used to illustrate the mechanics of vortex flow, recent pressure-distribution tests on a wing of NACA 64A006 series airfoil sections (ref. 92) permits the same analysis.

The sweep angle at which vortex flow assumes a contributing role appears to be related to the leading-edge radius of the airfoil sections employed. (It is necessary at this point to state that the lift coefficient at which the vortex flow is initially formed is also a variable to be considered. Of immediate concern, however, is the rather broad grouping of those wings which are subject to the influences of vortex flow and those wings which are not, and lift considerations will be dealt with subsequently.) The leading-edge radius decreases rapidly with airfoil thickness; hence, the thinner the wing, the lower the sweep angle at which the vortex flow is observed. Figure 5 has been prepared from admittedly meager data, but it does indicate regions influenced by vortex flow and not influenced by vortex flow. Although additional data could have been used in the preparation of this figure, they were not used because probe studies were lacking or there was a doubt as to whether or not the two-dimensional section would exhibit a separation bubble. It should be pointed out that two values of leading-edge radius are shown for several of the wings used to establish this boundary. In such cases, the wings were not constructed with their theoretical airfoil sections parallel to the air stream. The smaller leading-edge radius shown in figure 5 for each of these wings was obtained by multiplying the normal radius of the theoretical section by the cosine of the angle through which the airfoil sections were rotated. This result is believed to give a fair approximation of the streamwise radius.

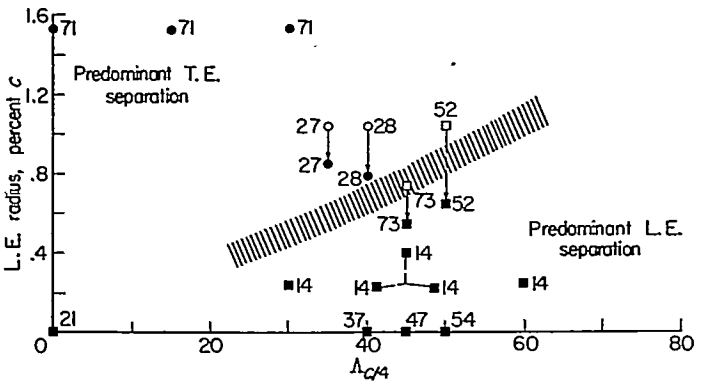

FIGURE 5.—An approximate boundary for the formation of a leading-edge vortex resulting from leading-edge separation expressed in terms of leading-edge radius and sweep angle for uncambered wings. Data obtained at a Reynolds number of 6.0×10^6. Open symbol denotes radius perpendicular to $c/4$ line; solid symbol denotes radius parallel to plane of symmetry. (Numbers adjoining symbols denote references.)

Inasmuch as leading-edge separation is dependent on Reynolds number (ref. 93), the vortex flow that results when sweep is introduced is also dependent on Reynolds number. For example, in figure 6 the variations in inflection lift coefficient with Reynolds number are presented for two 50° sweptback wings having aspect ratios approximately 2.9. One wing incorporates circular-arc airfoil sections, and the other incorporates NACA 64_1–112 airfoil sections. The inflection lift coefficients were found to be concurrent with a vortex flow lying along the leading edge and of such a size as to be visible in probe studies. Actually, the probe studies gave the impression of a rather sudden formation of the leading-edge vortex concurrent with the inflection in lift-curve slope, but it is probable that the formation grows over a finite lift range to a size great enough to influence the section lift characteristics. The results indicate that, whereas the inflection lift of the wing of circular-arc airfoil sections is not influenced by variation in Reynolds number, the inflection lift for the wing incorporating the NACA 64_1–112 airfoil sections is greatly affected. This result implies that the boundary of vortex flow illustrated in figure 5 for data at approximately 6.0×10^6 Reynolds number would probably have a lower slope for data at higher test Reynolds number and a higher slope for data at lower test Reynolds number.

It has been indicated that the presence of the vortex flow produces undesirable pitching-moment characteristics. This must be qualified, however, as indicated by the data presented in figures 7 and 8. Figure 7 shows the influence of sweep on the pitching-moment characteristics of a wing the airfoil sections of which exhibit a separation bubble in two-dimensional flow and which at 30° sweep would be expected to have a spanwise pressure gradient sufficiently strong to result in vortex flow. The data presented in figure 7 show that the effects of vortex flow are beneficial with regard to both the maximum lift and pitching-moment characteristics at a sweep angle of 30°. Figure 8 shows the

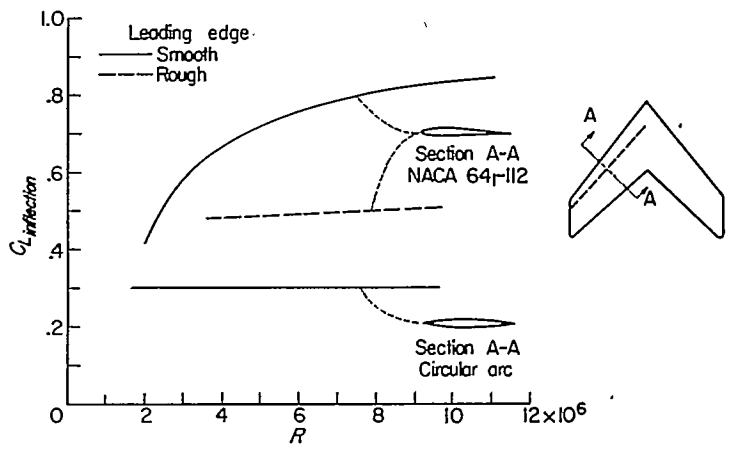

FIGURE 6.—Effect of Reynolds number on the inflection lift coefficient resulting from leading-edge vortex flow for wings incorporating round-nose and sharp-nose airfoils. $\Lambda_{c/4}=50°$; $A=2.9$; $\lambda=0.625$. (Data obtained from refs. 54 and 74.)

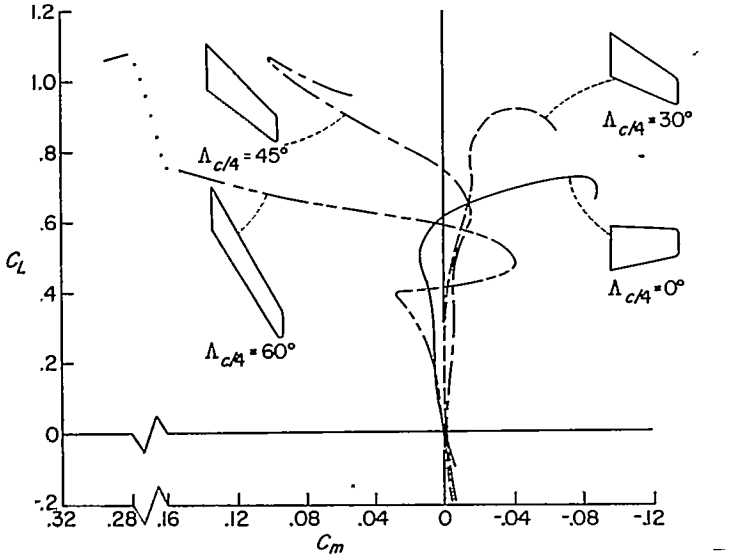

FIGURE 7.—An example of the effects of sweep on the variation of pitching-moment coefficient with lift coefficient when leading edge separation is present. The wings have aspect ratios of 4, taper ratios of 0.6, and NACA 65A006 airfoil sections. (Data obtained from ref. 14.)

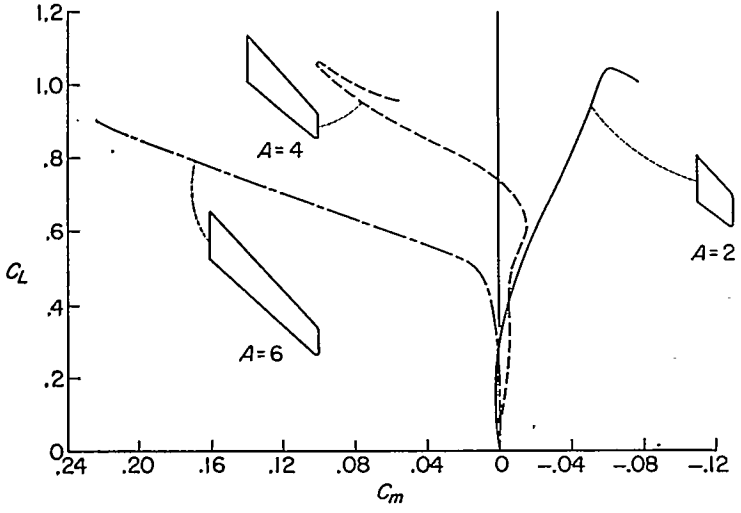

FIGURE 8.—An example of the effect of aspect ratio on the variation of pitching-moment coefficient with lift coefficient when leading-edge separation is present. The wings are sweptback ($\Lambda_{c/4}=45°$), have taper ratios of 0.6, and incorporate NACA 65A006 airfoil sections. (Data obtained from ref. 14.)

influence of aspect ratio on the pitching-moment characteristics of a wing which exhibits leading-edge vortex flow. The data presented in figure 9 indicate that vortex flow can be used to improve the longitudinal trim and maximum lift of the delta type of wing.

MIXED SEPARATION

Although those wings which fall far to either side of the boundary defined in figure 5 are definitely characterized either by trailing-edge separation or by leading-edge separation, the stability characteristics of wings having geometric

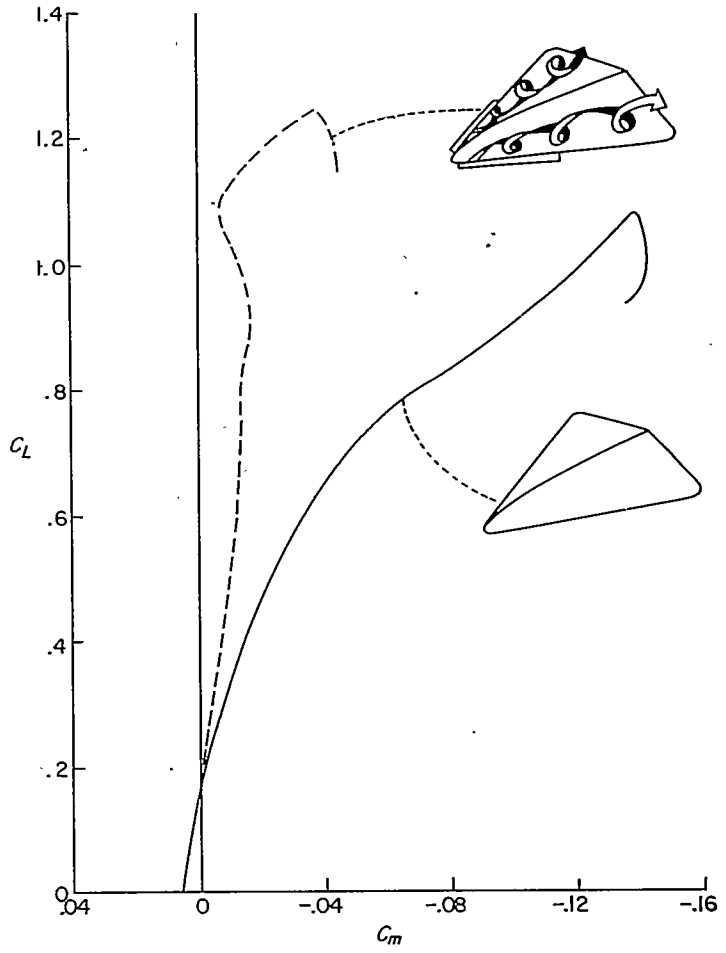

FIGURE 9.—An example of the reduction of the longitudinal stability and out-of-trim pitching moment of a delta wing ($\Lambda_{LE}=60°$) by the leading-edge vortex flow resulting from leading-edge separation. (Data obtained from ref. 56.)

characteristics which place them in the vicinity of the boundary conditions of figure 5 will be influenced by both types of separation. For example, vortex flow was observed on a 47° sweptback wing of aspect ratio 5.1 and incorporating round leading-edge airfoil sections (ref. 73) at a lift coefficient of 0.35 for the test Reynolds number of 1.1×10^6 (fig. 10). The increase in stability at this value of lift coefficient is, as previously discussed, obtained when the vortex flow is present over the tip sections. When the Reynolds number was increased to 6.0×10^6, the formation of the vortex flow was delayed to higher lift coefficients and separation of flow over the tip sections produced the unstable break in pitching moment noted at a lift coefficient of 0.85. The vortex flow did form over the inboard sections at higher lift coefficients, as indicated by the probe studies, and probably contributed to the large positive moments measured in the vicinity of $C_{L_{max}}$. In this particular case, then, Reynolds number greatly influences the type of separation obtained. Figure 11 has been prepared to show schematically how the lift coefficients at which leading-edge vortex flow and tip

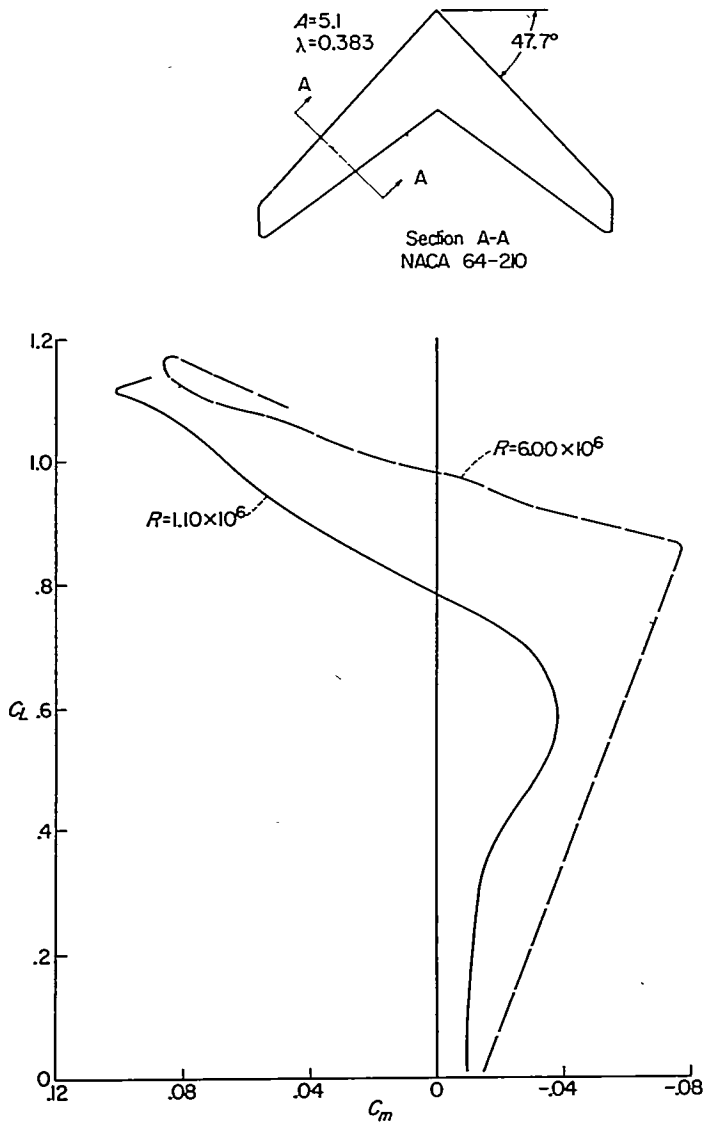

FIGURE 10.—An example of the effect of mixed-flow separation resulting from an increase in Reynolds number from 1.10 to 6.00×10^6 on the pitching-moment characteristics. (Data obtained from ref. 73.)

separation become contributing factors to the variations of pitching-moment coefficient with lift coefficient obtained at various Reynolds numbers. The force data available in reference 73 and unpublished probe studies have been utilized in the preparation of figure 11. The probe studies were limited by physical conditions to a maximum Reynolds number of 3.5×10^6 and, hence, it is not possible to state whether the vortex flow would have been totally eliminated in the Reynolds number range of the force tests. It is important to realize that any data obtained on thin round-nose airfoils (fig. 5) at low Reynolds number or, in fact, at any Reynolds number below the flight value, can be very misleading, or at least should be interpreted in terms of the Reynolds number effect just described, as concerns the stability changes through the lift range.

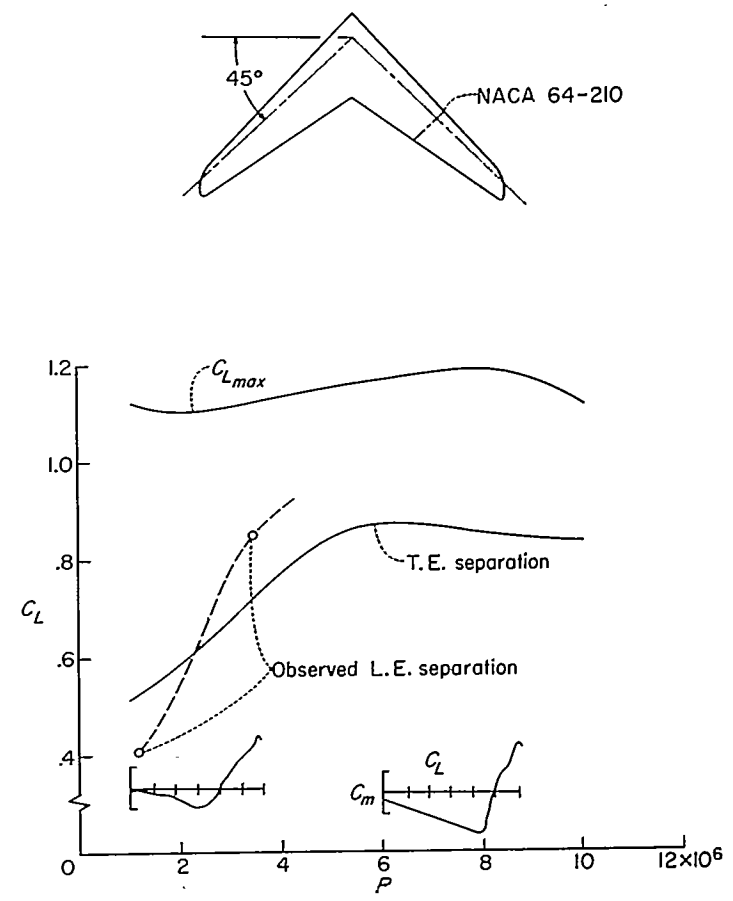

FIGURE 11.—Variation of the lift coefficients with Reynolds number at which trailing-edge separation and leading-edge separation occur. $A=5.1$; $\lambda=0.383$. (Data obtained from ref. 73 and unpublished probe data.)

ROUGHNESS

Although present-day standards for fabricating the leading edges of high-speed aircraft approach those for wind-tunnel models in a smooth condition, it is necessary to consider the adverse effects of roughness on the types of flow separation just discussed. The degree of roughness currently employed in wind-tunnel roughness tests is entirely too severe to be representative of that found on production aircraft, but it may be that the aerodynamic changes are indicative of those to be obtained with a lesser degree of roughness. In any case, experimental studies are required to determine the effects of various degrees of roughness on swept wings.

From the limited data available on tests of swept wings with roughness, it appears that on wings exhibiting trailing-edge separation, roughness eliminates the beneficial effects to be obtained by an increase in Reynolds number. In the case of a $\Lambda_{LE}=42°$ wing having an aspect ratio of 4 and incorporating NACA 64_1–112 airfoil sections (ref. 94) the stall progression for the smooth wing at the lowest Reynolds number (1.7×10^6) and the progression for the rough wing at Reynolds numbers up to the highest (9.5×10^6) were very similar. This similarity was also borne out by the force data.

When roughness was applied to a wing having $\Lambda_{c/4}=50°$, an aspect ratio of 2.9, an NACA 64_1–112 airfoil section, and exhibiting a leading-edge vortex flow when in a smooth condition, the inflection lift coefficient remained approximately constant through the Reynolds number range of the tests (ref. 74). Although probe studies were not made when roughness was applied at the leading edge, the similarity of the pitching-moment characteristics with those obtained on the smooth wing indicates that the leading-edge vortex was present and was due entirely to the effects of the roughness. It is interesting that, from these data, it can be conjectured that a region of laminar boundary layer exists on the rough wing which separates and reattaches in order to form the core of the leading-edge vortex. In order to illustrate the magnitude of the roughness effects on the inflection lift coefficient the results presented in reference 74 are reproduced in figure 6.

LONGITUDINAL STABILITY

GEOMETRIC CONSIDERATIONS

Separation on swept wings initially occurs over the tip sections and is a result of leading-edge separation, trailing-edge separation, or a combination of leading- and trailing-edge separation. Tip stalling could obviously result in a loss in lift behind the moment center of such a magnitude as to cause a nose-up or unstable pitching-moment variation. The compilation work of Shortal and Maggin (ref. 10) showed that whether or not instability would be obtained on a wing of given sweep depended primarily on aspect ratio (see the INTRODUCTION). Although this empirical study did not differentitate between the types of flow separation encountered on swept wings, the stability boundary constructed does provide a general classification of the stability of any particular wing; however, inadequacies were to be found.

In order to provide at least a qualitative explanation for this stability boundary, a re-evaluation of the data presented in reference 10, together with an evaluation of more current data, has been made (fig. 12). It was found that the stability boundary as presented in reference 10 was quite adequate for wings having taper ratios of 1.0 (or nearly 1.0) but was inadequate for wings having very small taper ratios. (See, for example, the pointed wing data presented in fig. 12.) In an effort to correlate this additional effect of taper, it was found that the geometric ratio of the area rearward of the $0.25c'$ to the total wing area could be used as a single stability criterion in place of the three parameters sweep, aspect ratio, and taper ratio. If this area ratio exceeds 0.69, the wing is in the stable region and if it is less than 0.69 the wing is in the unstable region. In figure 12 are shown two stability boundaries based on this criterion, one for a taper ratio of 1.0 and one for a taper ratio of 0. The first curve agrees very well with that from reference 10 except in the low-sweep range where the experimental data upon which

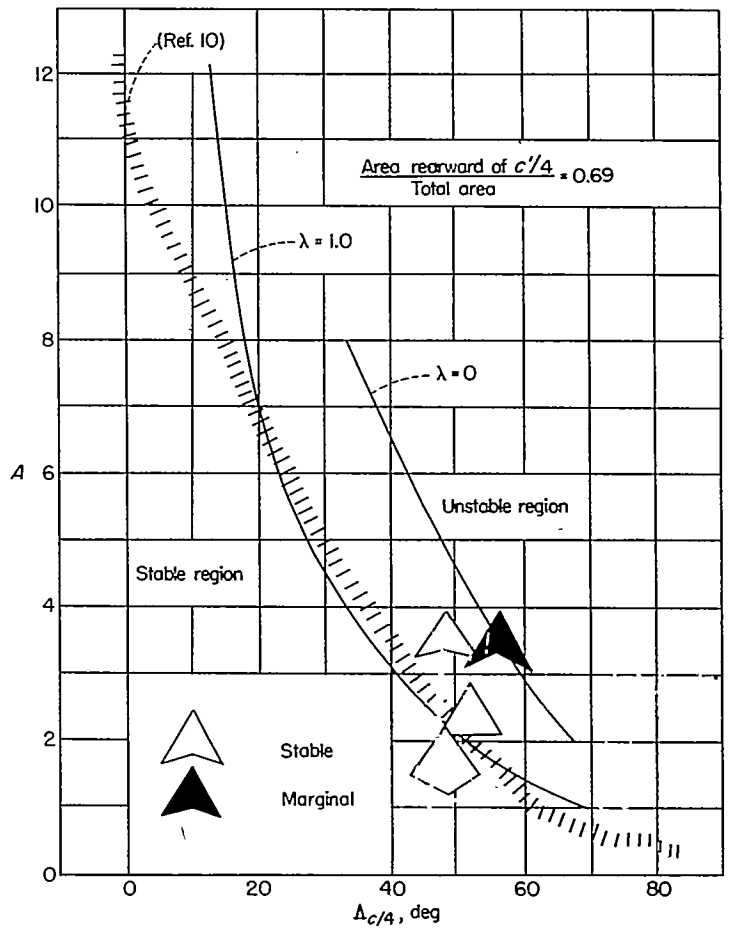

FIGURE 12.—Empirical longitudinal-stability boundary of reference 10 and its relationship to lines of constant area ratio. (Experimental data obtained from refs. 56 and 75.)

the stability boundary is based are meager (fig. 12); whereas the second curve, which lies above that of reference 10, provides considerably improved agreement with the experimental data for wings with taper ratio of 0.

The spanwise distributions of lift obtained for families of wings having taper ratios of 1.0 and 0 and which are defined by this area-ratio value of 0.69 (corresponding to the two stability boundaries in fig. 12) have been presented in figure 13. The spanwise loadings for the family of wings of different sweep but having taper ratios of 1.0 are somewhat more similar than for the family of wings having taper ratios of zero.

The outward shift in the stability boundary for the family of wings having taper ratios of 0 indicates that an unbalance of the moment areas is the more important factor with regard to stability than the occurrence and severity of the tip stall. Inasmuch as the tip sections of highly tapered wings operate at higher values of lift coefficients relative to the root sections than those on untapered wings, separation occurs earlier and, thus, the tip-stalling tendencies are more severe on the tapered wings. If the severity of the tip stall were of primary concern, therefore, the boundary might be expected to be displaced toward the left.

469104—58——89

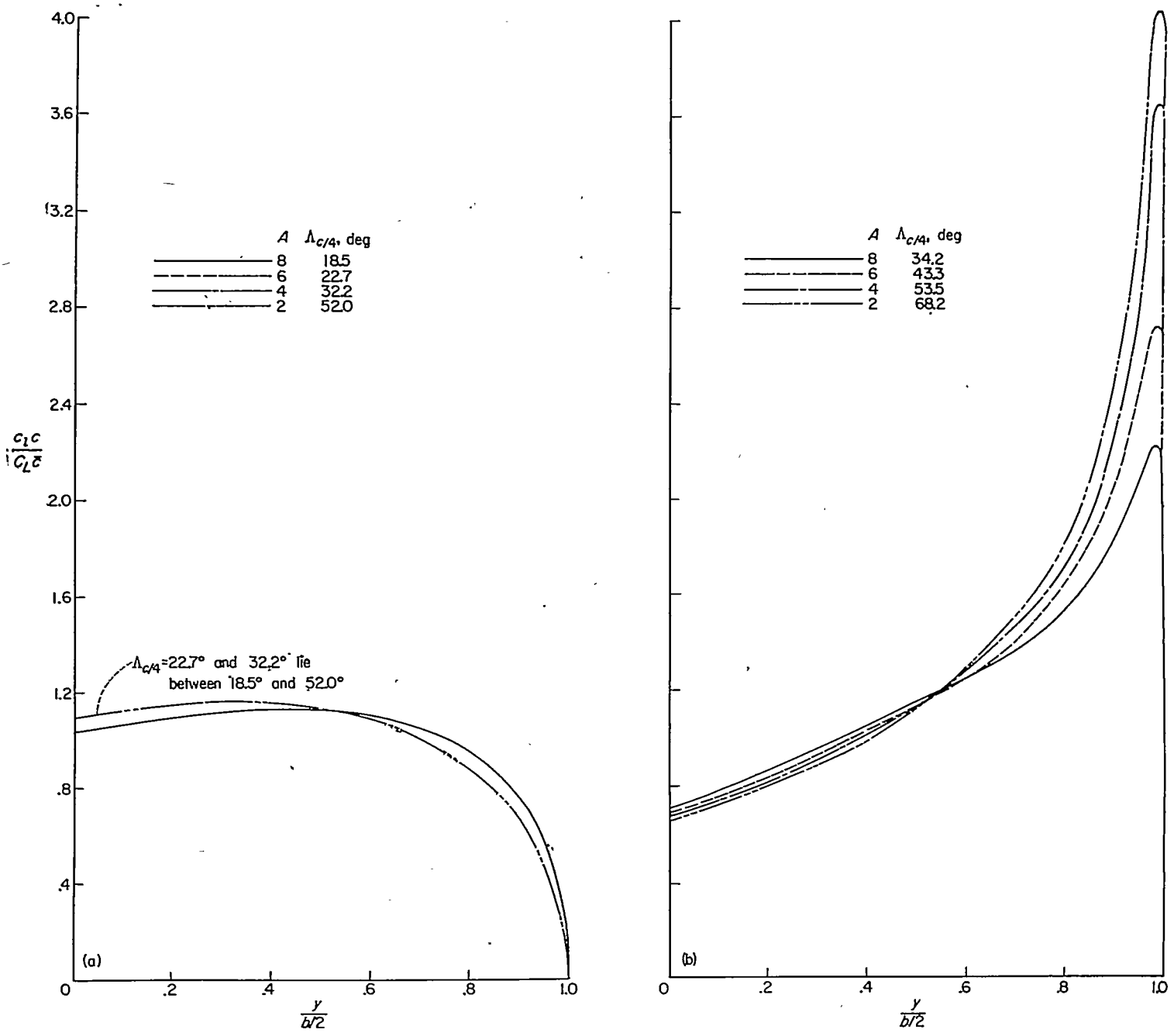

(a) Taper ratio=1.0.

(b) Taper ratio=0.

FIGURE 13.—Load distribution for families of wings defined by the lines of constant area ratio in figure 12. (Loadings obtained from ref. 76.)

STALL CONTROL

The study of the flow characteristics on sweptback wings makes possible a rational approach to the problem of stall control. The delay or prevention of flow separation over the trailing edge or leading edge of a wing may utilize a device attached to or built into the wing or may be embodied in the aerodynamic design of the wing itself. In the following discussion each approach will be considered separately. Such a procedure necessarily results in some duplication because in many applications two or more possible solutions are employed in an attempt to obtain the desired pitching-moment characteristics.

Some remarks pertinent to the attainment of adequate stall control on wings exhibiting the types of flow separation previously discussed are considered. For example, in the case of a wing having trailing-edge separation, it is necessary to prevent trailing-edge flow separation over the tip sections until lift has been lost forward of the moment center. In the case of leading-edge separation extending across the entire leading edge, a full-span device would be required for its elimination. Obviously, such control would merely create a wing then subject to trailing-edge separation at the tip sections and which, in turn, would require further control in order to provide satisfactory stability. It will be shown later, however, that instead of completely eliminating the vortex flow, a simpler and more direct approach would be to direct or diffuse the vortex off the tip

sections in such a way as to obtain linear pitching-moment characteristics.

DEVICES

Fences or vanes.—Data on fences and vanes are presented in tables 7, 19, 20, 21, 25, 26, 29, 33, 34, and 38 from references 13, 14, 19, 27, 34, 36, 39, 41, 48, and 52. Additional information, obtained for the most part at low Reynolds numbers, is contained in references 80, 95, 96, 97, 98, and 99.

Preliminary considerations of stall control for either type of flow separation discussed suggest placing a restriction on the outflow of the boundary-layer air on sweptback wings. A fence (vane) can be used to provide a physical boundary to the outflow of boundary-layer air. Thus, in the case of trailing-edge separation the boundary-layer build-up over the tip sections would be eliminated and hence these sections would not stall prematurely. When leading-edge separation is present, the fence would be required to redirect or to diffuse the leading-edge vortex at a spanwise station such that linear moment characteristics are obtained.

For the fence to be effective in controlling trailing-edge separation, the spanwise accumulation of boundary-layer air is shed off the wing at the location of the fence at a rate sufficient to prevent the accumulated boundary layer from spilling over the fence in the spanwise direction. In some installations employing fences of reasonable height, it might be necessary to employ several fences in order to prevent the boundary-layer build-up over the tip section. Another condition that would necessitate the use of a multiple-fence arrangement would be that in which the aspect ratio is so great that the distance outboard of a single fence (size not a limiting factor) is sufficient to allow another accumulation of boundary-layer air to occur at the tip sections. From the literature it is apparent that the fence should be located over the rear part of the chord in order to be effective in controlling trailing-edge separation. Just how far forward the fence should extend cannot be stated, but it appears from available experimental data that in order to delay the instability to maximum lift, the fence should extend to about the 5-percent-chord point. Although restrictions to the outflow of the boundary-layer air can materially improve the pitching-moment characteristics through the lift range, the induced downwash effects are still such that separation occurs first over the tip portions of the wing which exhibits trailing-edge separation and, if the wing plan form is such as to place it above the boundary of figure 12, an unstable pitching-moment break at maximum lift is obtained.

For the fence to be effective in controlling the effects of leading-edge separation, it is apparent that the fence must be located over the forward part of the chord. Actually experience has shown that the fence should extend around the leading edge to the lower surface. It appears that the size should be large enough to contain the leading-edge vortex, but as there are no data available on the size of such vortices it is not possible to state the size requirements for such a fence. One investigation has been made at low Reynolds numbers to determine the minimum size of fence required to give the maximum increase in stability for a wing which without fences was stable through the stall (ref. 95). These data might be applicable as a guide to the size required on an unstable wing at high Reynolds numbers.

Inasmuch as the fence has no appreciable effect on the spanwise variation of induced downwash and must, in most applications, be of small height, it serves only as a delaying device for the instability. Exceptions have been found where besides delaying the onset of instability, fences have actually caused stable pitching-moment breaks at maximum lift. In one case the application of a leading-edge stall-control device to a swept wing reduced a condition of severe instability to one of marginal instability which was eliminated by the further addition of a fence (ref. 52). In another case, a wing-fuselage-tail combination exhibited instability through the high lift region. A recent analysis of these data offers the explanation that the instability was not chargeable to the pitching-moment characteristics of the wing but rather to the destabilizing effect of the horizontal tail in the downwash field of the wing (effect of tail on the over-all stability will be discussed in a later section). It was found, however, that properly located fences on the wing could so alter the flow characteristics at the tail that the instability due to the tail was significantly reduced (ref. 95).

There has been a question raised from time to time as to whether or not the improvements in stability obtained in wind-tunnel tests of wings with fences are to be realized at flight Reynolds numbers. It would appear that any empirical relationship between the influence of fences and the effects of variation in Reynolds number would involve the wing-thickness-ratio as a parameter. Thus, on thin wings whose leading-edge radii are such as to place them well below the boundary shown in figure 5, large increases in Reynolds number would not eliminate the need for fences as determined from wind-tunnel tests. If the wing thickness (leading-edge radius) approaches or lies above the boundary of figure 5, increases in Reynolds number might necessitate a relocation to maintain their effectiveness and in some instances their need might be eliminated.

The data presented in reference 39 show that fences can be used to control the boundary-layer outflow to such an extent that linear pitching-moment characteristics are obtained on a relatively high-aspect-ratio sweptback wing. As suggested in the previous paragraph, the required number and position of fences may be somewhat different at flight Reynolds numbers. The effects of several fence arrangements on the pitching-moment and section-lift characteristics of this wing are shown in figure 14 (refs. 39 and 70). These results may appear optimistic in light of a similar investigation on a wing of the same sweep but having a lower aspect ratio (5.1) (ref. 48) where both single- and multiple-fence arrangements did not provide very significant improvements in the pitching-moment characteristics. In the latter tests, however, leading-edge separation was present as evidenced by the fact that the leading-edge fence (extended to the lower surface) caused an improvement in the pitching-moment characteristics that was not materially changed by an extension of the fences to the trailing edge. The data of reference 48 may point out that greater difficulty is to be expected in selecting the size, number, and position of fences to control this type of separation.

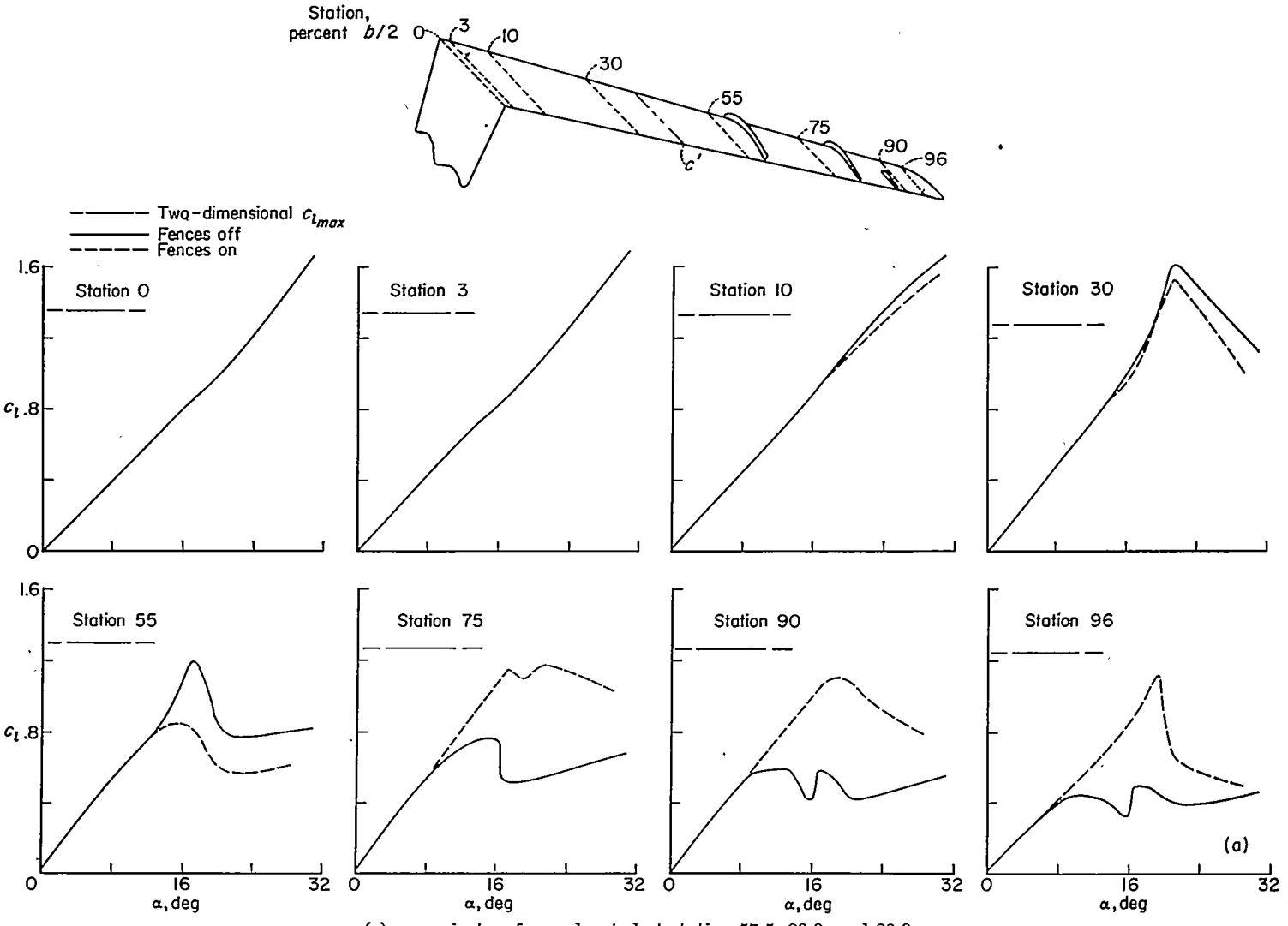

(a) c_l against α; fences located at station 57.5, 80.0, and 89.0.

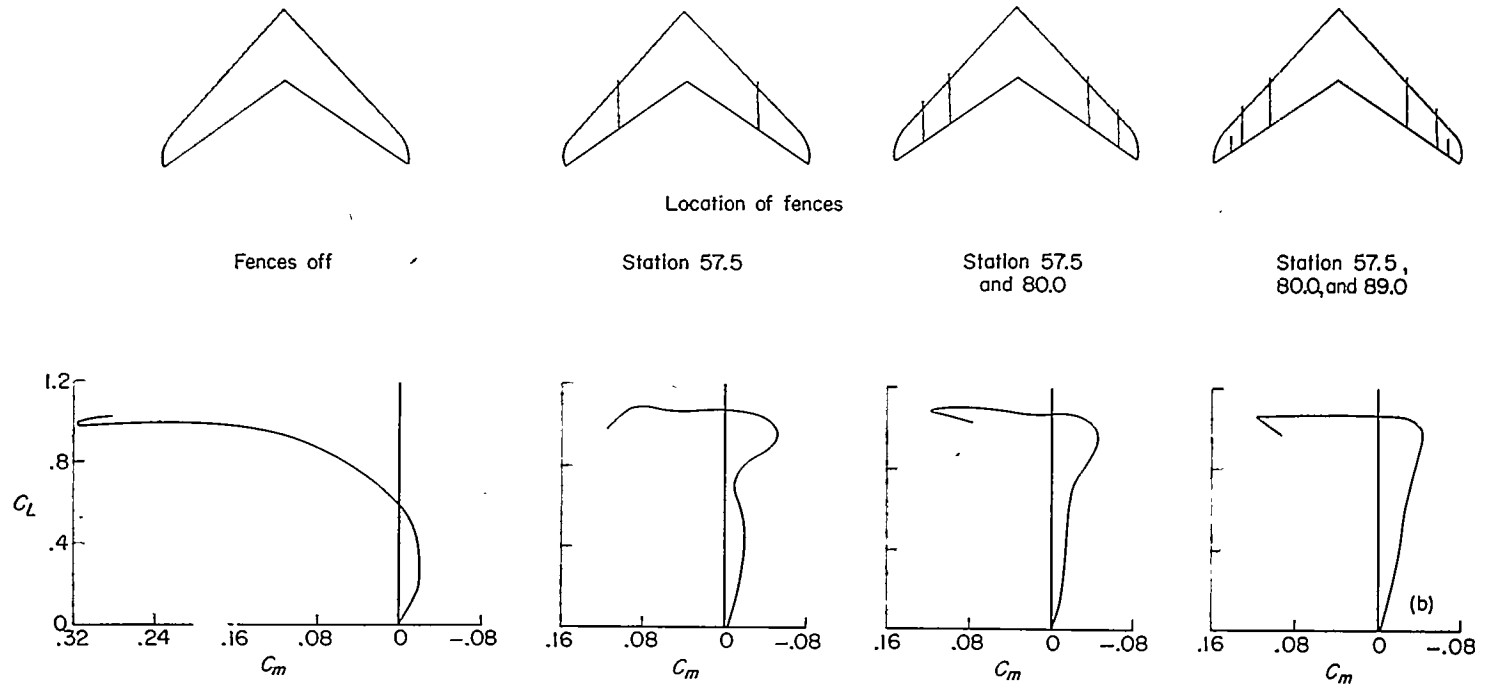

(b) C_m against C_L.

FIGURE 14.—Effect of fences on the section lift and wing pitching-moment characteristics of a sweptback wing ($\Lambda_{c/4}=45°$) having an aspect ratio of 8.02, a taper ratio of 0.45, and NACA 63_1A012 airfoil section. (Data obtained from ref. 70.)

For illustrative purpose, the effects of fences on the pitching-moment characteristics of several sweptback wings of various configurations have been shown in figure 15.

The information available is not sufficient to allow for adequate prediction of the optimum number, size, and location of fences for any given wing. In general, it appears that in each case an exploratory investigation is required to determine the optimum arrangement. The skill and understanding of the investigator will undoubtedly be reflected in the adequacy of the arrangement thus obtained.

Nacelles and stores.—When the airplane design is such that either the power plant, fuel, or cargo must be located outside of the wing and fuselage, the basic requirement is that the location selected will provide the minimum interference drag at high speeds. It is interesting, however, to consider the possibility of positioning these external bodies so that they contribute an improvement to the low-speed longitudinal stability of sweptback wings.

The literature on externally mounted bodies (for example, ref. 100) is largely concerned with specific configurations from the drag considerations.

In the development work on the Boeing B–47 airplane, some low-speed tests were made with the outboard and inboard nacelles in various positions, and a summary of the results appears in reference 77. The improved pitching-moment characteristics obtained in this investigation are shown in figure 16.

The low-speed considerations appear to indicate that the stabilizing advantage to be derived from suitable placement of external bodies could and should receive the attention of the designer.

Extensible leading-edge flaps.—Data on extensible leading-edge flaps are presented in tables 6, 7, 9, 19 to 22, 25, 26, 30, 34, 38, 39, 44 to 46 from references 13, 18, 19, 21, 27, 29, 31, 32, 33, 34, 35, 36, 37, 38, 39, 41, 44, 45, 46, 48, 49, 50, 52, 54, 55, 60, 64, and 65. Additional information is contained in references 101 to 103.

One device which has been used successfully to delay flow separation at the tip sections until lift has been lost further inboard is the extensible leading-edge flap. This flap is patterned after the type suggested by Krüger (ref. 101) to improve the maximum-lift characteristics of high-speed profiles. The difficulties of fabricating and installing an extensible leading-edge flap on an airplane have never been

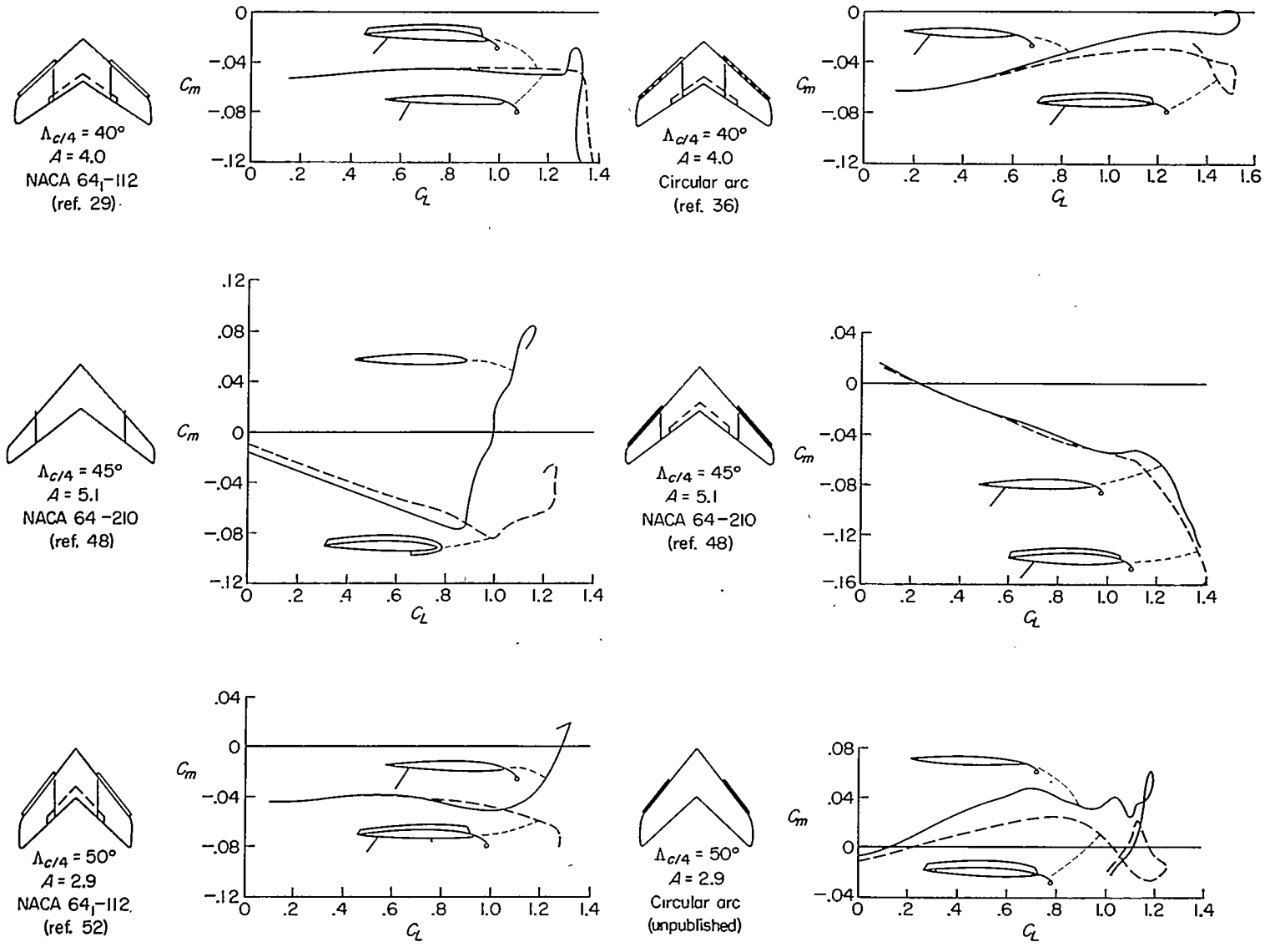

FIGURE 15.—The effect of fences on the pitching-moment characteristics of several sweptback wings.

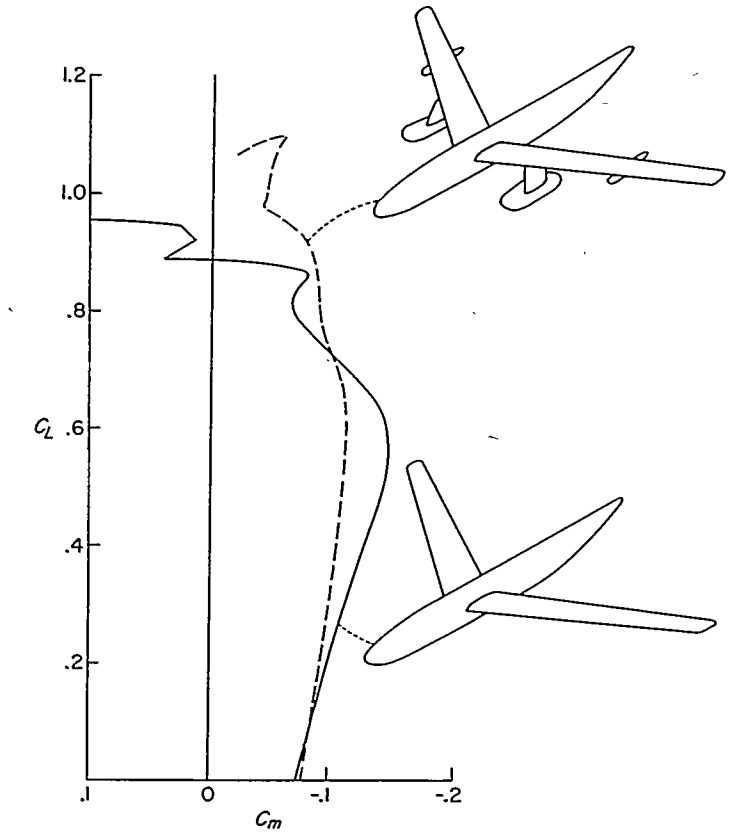

FIGURE 16.—The effect of nacelles on the pitching-moment characteristics of a sweptback wing-fuselage combination ($\Lambda_{c/4}=35°$) having an aspect ratio of 9.43 and a taper ratio of 0.42. (Data obtained from ref. 77.)

surmounted so that slats are generally employed, and the extensible leading-edge flap remains a wind-tunnel tool. Inasmuch as the slat and flap may be considered to provide essentially similar relief to tip stalling (see fig. 17), the ability to circumvent detailed slat-positioning studies by using flaps has allowed a greater scope to be covered in wind-tunnel work on sweptback wings than would have been possible employing slats. The extensible leading-edge flap is generally a partial-span device with the outboard end located in the vicinity of the wing tip. The extension in chord reduces the spanwise flow tendency by partially unstaggering the pressure distributions at the inboard end of the leading-edge flap. A vortex also is shed from the inboard end of the flap that is of such a rotation as to oppose the outflow of the boundary-layer air. The pressure discontinuity at the inboard end of the flap assists in promoting the initial separation inboard of the tip. The camber introduced by the leading-edge flap allows the tip sections to reach higher angles of attack before separation occurs.

In general, in order to obtain the greatest improvement in the maximum lift characteristics while providing longitudinal stability at the stall, the inboard end of the leading-edge flap should be between $0.4b/2$ and $0.6b/2$ so that the initial separation occurs just forward of the moment center. If the wing is initially stable, then greater gains in maximum lift may be obtained with greater spans of leading-edge flaps. Two factors which can cause appreciable changes in the optimum span just described are leading-edge vortex flow

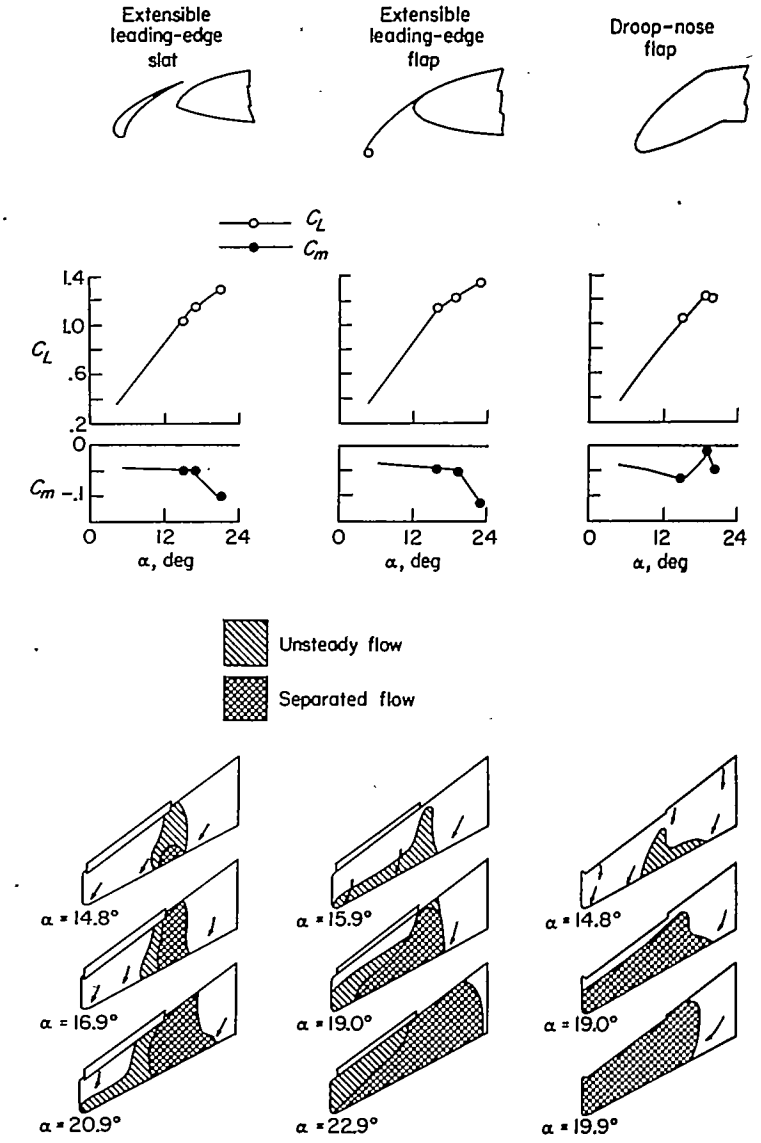

FIGURE 17.—Stall patterns on a sweptback wing ($\Lambda_{c/4}=35°$) having an aspect ratio of 6.0, a taper ratio of 0.5, and NACA 64_1-212 airfoil sections equipped with an extensible leading-edge slat, an extensible leading-edge flap, and a droop-nose flap. (Data obtained from ref. 27.)

and the proximity of the wing geometric characteristics to the stability boundary of figure 12. In the case of leading-edge vortex flow, the optimum span is generally smaller than would otherwise be indicated for a wing exhibiting trailing-edge separation and having similar geometric characteristics (see, for example, ref. 13), and this reduction will be considered in greater detail in a subsequent section entitled "Chord-Extensions." For wings with aspect ratio and sweep angle that approach the boundary of figure 12, longer spans of leading-edge flaps may be used (see, for example, ref. 31).

The influence of a fuselage on the longitudinal stability characteristics of a swept wing equipped with extensible leading-edge flaps has, for the most part, been negligible; however, a series of tests on a 42° sweptback wing of aspect ratio 4 (ref. 31) did show a reduction in the optimum span of extensible leading-edge flap when a fuselage was present.

It has been found that trailing-edge flaps may affect the

optimum span of the leading-edge flap, but of more significance is the fact that they can alter the successful application of extensible leading-edge flaps. For example, the results obtained in an investigation of a 45° sweptback wing of aspect ratio 5.1 have been summarized in figure 18 to show the influence of both type and span of trailing-edge flaps on the longitudinal stability obtained with extensible leading-edge flaps. Trailing-edge flaps having spans in excess of $0.57b/2$ for the split type and $0.45b/2$ for the double-slotted type nullified the stabilizing effectiveness of the extensible leading-edge flap. It is interesting that a greater improvement in stability was obtained when double-slotted flaps of $0.40b/2$ and leading-edge flaps were used in combination than when just the leading-edge flaps were used. Again, the conditions just described perhaps depend on the relative position of the geometric characteristics of the wing to the stability boundary of figure 12. For example, on a 42° sweptback wing of aspect ratio 4.0 (ref. 35), full-span split flaps did not produce any detrimental effect on the longitudinal stability characteristics obtained with extensible leading-edge flaps.

One modification to extensible leading-edge flaps that is suggested from time to time is to taper the flap so that the maximum chord is at the tip. The results that have been obtained (ref. 31) show the tapered leading-edge flap to be ineffective. It is believed that the main reason for the ineffectiveness of the tapered leading-edge flap is that it does not provide the discontinuity in plan form with the associated pressure discontinuity and flap-tip vortex necessary to promote initial separation inboard and ahead of the moment center.

The available experimental data appear to indicate that the extensible leading-edge flap can provide an appreciable but definitely limited shift in the stability boundary of figure 12. Figure 19 has been prepared from experimental data to show the manner in which stall controls displace the

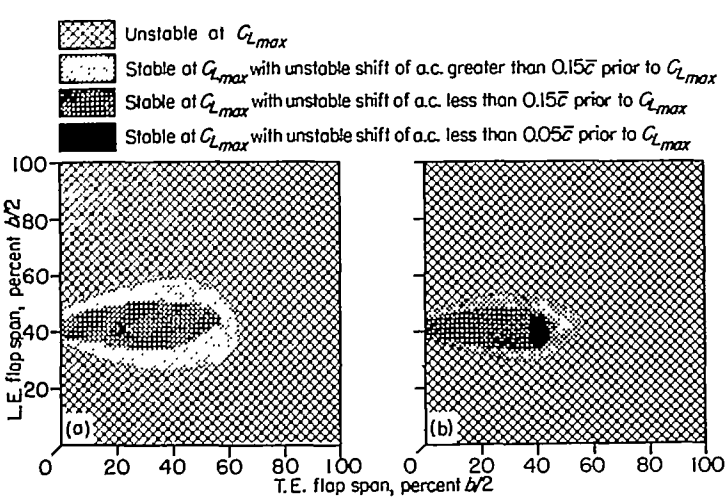

(a) Split flaps. (b) Double-slotted flaps.

FIGURE 18.—General summary of the effects of leading-edge and trailing-edge flaps on the longitudinal stability characteristics of a sweptback wing ($\Lambda_{c/4}=45°$) having an aspect ratio of 5.1, a taper ratio of 0.383, and NACA 64–210 airfoil sections. (Data obtained from ref. 48.)

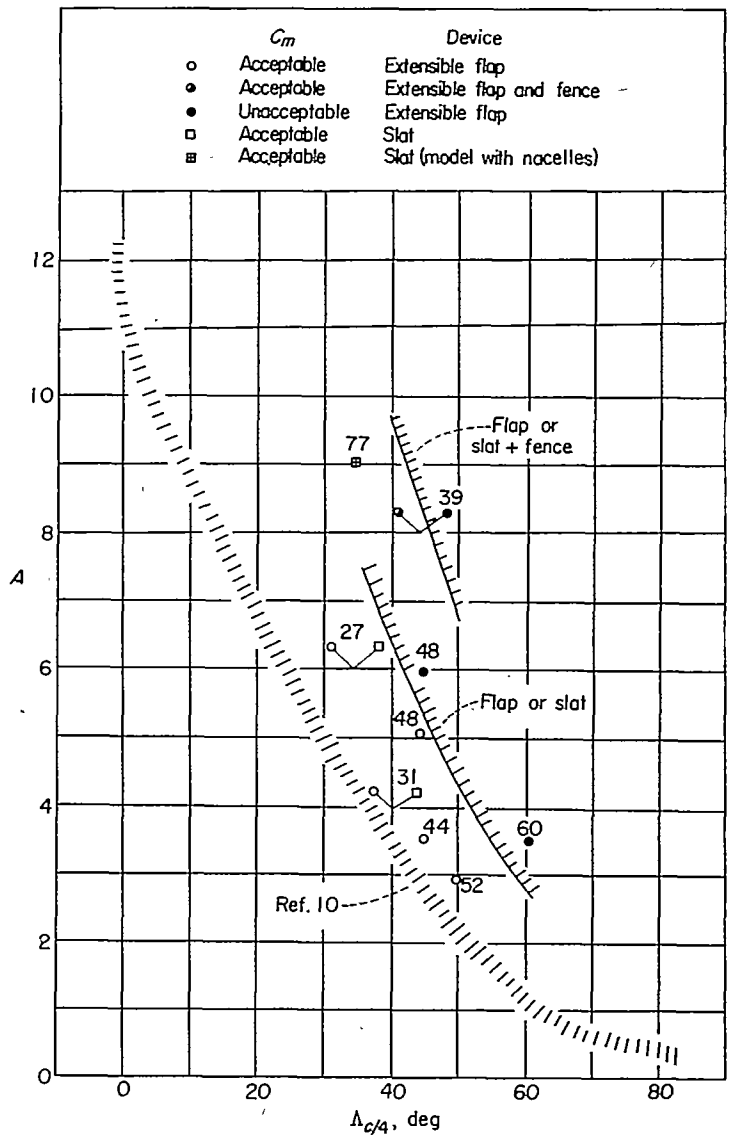

FIGURE 19.—Influence of several types of stall control devices on the longitudinal stability boundary of reference 10 for wings having taper ratios greater than 0.4. (Numbers adjoining symbols denote references.)

stability boundary of figure 12. Also included in figure 19 is an indication of the additional displacement of the stability boundary when fences are used in conjunction with extensible leading-edge flaps. Actually no differentiation is made in this figure for the types of flow separation on swept wings, inasmuch as it appears that only the span of the device will be affected by the type of flow separation.

Limitations must be attached to the boundaries shown in figure 19 which arise from the fact that sweep and aspect ratio are not the only variables. The data indicated by the symbols (fig. 19) are for wings which have taper ratios greater than 0.4, and a comparison of the boundary established with these data with that indicated in figure 12 for wings which have taper ratios of 0 indicates that extreme taper has accomplished the same shift in stability boundary. Thus, generalization of the effectiveness of extensible leading-edge flaps in displacing the boundary shown in figure 19 with the data presently available is still very much conjecture but probably on the conservative side.

There are only limited low-speed data available on the air loads on extensible leading-edge flaps (refs. 34 and 104).

Extensible leading-edge slats.—Data on extensible leading-edge slats are presented in tables 7, 19, and 22 from references 19, 27, 29, and 38. Additional information is contained in references 95 and 105 to 107.

As previously stated, the slat provides essentially the same relief or alleviation of flow separation over the outer part of the wing as does the leading-edge flap (see, for example, fig. 17). It is rational to believe that the effects of span and spanwise position are very similar to corresponding effects noted for leading-edge flaps. The shift in stability boundary due to leading-edge flaps presented in figure 19 is then presumed to apply equally well to slats.

The available positioning studies of slats on sweptback wings are limited (German work reported in ref. 108 and the work reported in refs. 109 and 110). It appears from the specific investigations available that slats were designed and positioned on the basis of two-dimensional data with a few "rules of thumb" considered. If the results obtained in an investigation correlating two-dimensional with three-dimensional single-slotted flap positions (ref. 111) can be considered indicative of the correlation to be obtained by the use of slats, it appears that current design practices need not be assisted by detailed positioning studies. This is somewhat substantiated by the fact that the slat designed from two-dimensional data for a wing of $\Lambda_{c/4}=35°$ and aspect ratio of 6.0 was considered to have fulfilled its design purpose (ref. 27).

Droop nose.—Data on droop-nose flaps are presented in tables 7, 9, 10, 13, 14, 19, 21, 29, 34, 39, 41, and 44 from references 14, 15, 19, 21, 22, 23, 25, 27, 36, 47, 48, 54, 57, and 60. Additional information is contained in reference 112.

The droop nose differs in one very important aspect from either the extensible leading-edge flap or slat. There is no extension in chord; hence the vortex shed from the inboard end of the droop nose is weaker and less effective (for example, the vortex may have a rotation such as to promote outflow) in providing a barrier to the outflow of boundary-layer air over the rearward portions of the wing. For this reason, it would not be expected that the droop nose would be as effective a stabilizing device on sweptback wings as either the flap or slat. The experimental results presented in figure 17 show that such is the case. It should be pointed out, however, that these results merely imply that the shift in the stability boundary would be less for the droop nose than either the flap or slat, and, therefore, for wings only marginally unstable, the droop nose may be as effective as the leading-edge flap. Indications are that in some cases the use of fences with droop nose may provide adequate control.

Boundary-layer control.—Data on boundary-layer control are presented in tables 4, 31, and 32 from references 45, 46, and 16. Additional information is contained in references 92 and 113 to 116.

It has been known for a considerable time that flow separation can be delayed by either adding energy to the low-energy boundary-layer air or removing the boundary layer. Numerous two-dimensional tests have shown that the power expenditure is less when the boundary layer is removed (suction) than when energy is added (blowing). In the case of boundary-layer removal, the air is drawn off through either a slot or permeable surface.

Most experimental data have been obtained on wings which exhibit leading-edge separation. These experimental data have shown the most favorable slot location from flow-separation considerations to be very close to the leading edge, in fact, just rearward of the pressure peak on the wing. Experimentally, this location is difficult to obtain; therefore the slot is usually located so as to include the minimum pressure. With the slot located in the immediate vicinity of the minimum pressure on the wing a very low pressure is required in the plenum chamber in order to induce an inflow into the slot. Actually, a rather large chordwise pressure gradient exists across the slot such that when the minimum pressure is held an excess in differential pressure occurs over the rear part of the slot. The power requirements and rates of flow therefore are relatively high. The results presented in reference 45 (fig. 20) indicate that, as in the case of slats or flaps, desirable longitudinal stability characteristics are dependent on the span over which control is exercised; that is, the initial separation should occur at the inboard end of the slot just forward of the moment center. Some attempt has been made to control leading-edge separation by means of several short chordwise suction slots located along the leading edge, outboard of the 0.56-semispan station (ref. 113). The wing had 63° sweepback of the leading edge, an aspect ratio of 3.5, a taper ratio of 0.25, an NACA 64A006 airfoil section in a streamwise direction, no twist, no camber, no dihedral, and zero wing-fuselage incidence. The separation was delayed to some extent, as indicated by the fact that the lift coefficient at which the pitching moment broke in the unstable direction increased from 0.41 to 0.68. Reference 113 mentions that control inboard could probably have caused a further delay. Although this may be true, it should be pointed out that experimental data with extensible leading-edge flaps would indicate that the increased linear moment range would be accompanied by an increase in the severity of the unstable pitching-moment break. This result is confirmed by the porous area suction investigation of reference 114.

Because the wings on which boundary-layer control has been tried have exhibited leading-edge separation, the effectiveness of suction slots located more rearward on the chord in order to control trailing-edge separation may not be defined clearly by the data presented in reference 46. It is still to be shown whether spanwise or chordwise slots would be more effective in delaying the build-up of low-energy air over the rear portions of the tip sections. Low-scale data for a swept wing ($\Lambda_{c/4}=36.4°$) of aspect ratio 5.85 and incorporating approximately 16.5-percent-thick airfoil sections indicated that a chordwise gap is very effective in the control of flow separation over the tip sections. The improvement in longitudinal stability obtained with the chordwise gap was remarkable inasmuch as the spanwise location seems to have been arbitrarily chosen.

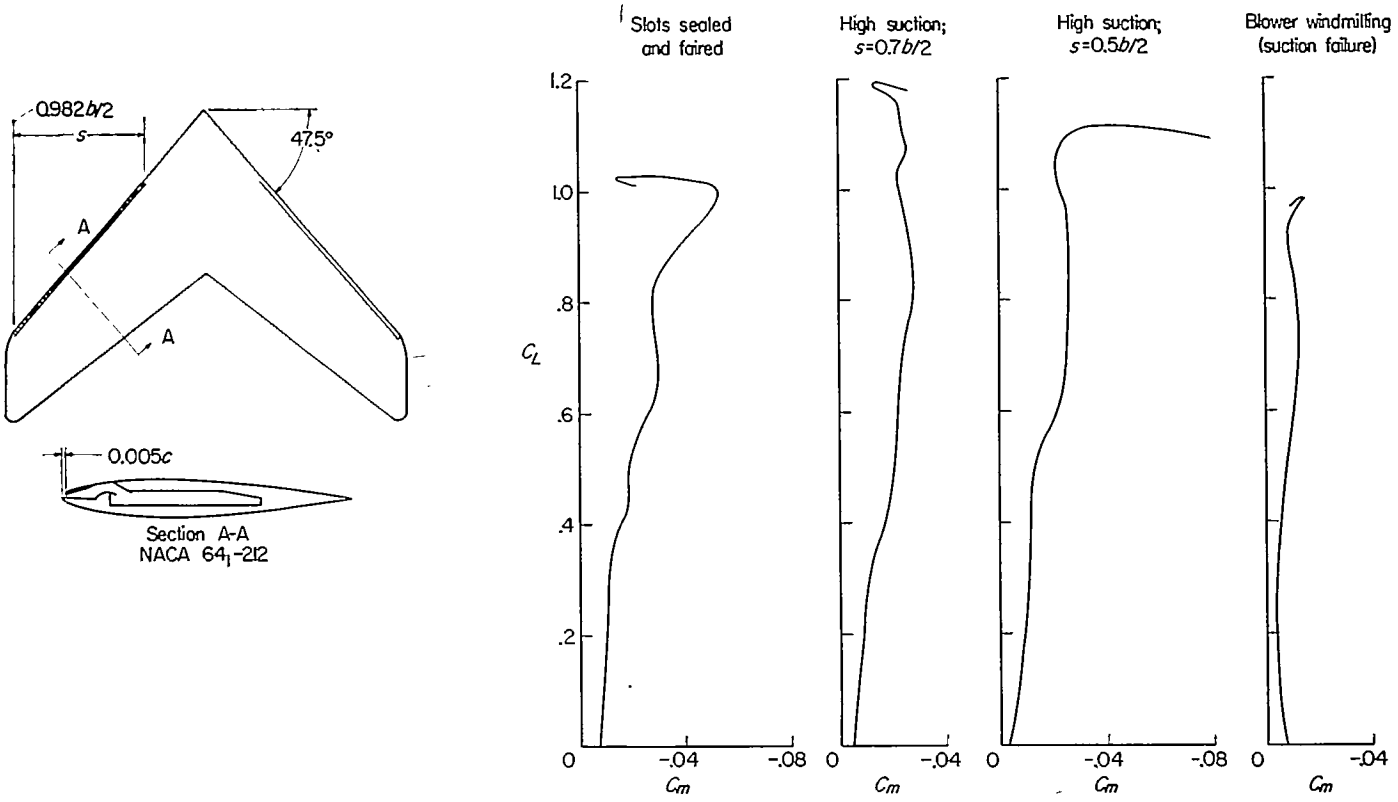

FIGURE 20.—Effect of boundary-layer control by suction at the leading edge on the pitching-moment characteristics of a sweptback wing ($\Lambda_{c/4}=45°$). $A=3.4$; $\lambda=0.51$. (Data obtained from ref. 45.)

As in the case of suction slots, the leading-edge separation has dictated that area suction (porous material) be applied very close to the leading edge. The work described in reference 92 was done with the idea of delaying separation over the entire wing, and hence the configuration does not represent an optimum one from stability considerations if it is assumed that the span of porous suction is as critical a stability factor as leading-edge slats or flaps. The sweep angle ($\Lambda_{c/4}=61°$) and aspect ratio (3.5) of the test wing of reference 92 are such that desirable longitudinal stability would not be expected from the use of the stall-control devices considered so far (fig. 19), although a combination of stall-control devices such as extensible leading-edge flaps and fences may provide the desired results. Data obtained on the wing described in reference 115 indicated that of the chordwise extent of porous suction considered (1, 2, and 3 percent of the chord), the results obtained with a chordwise extent of 1 percent were most favorable from longitudinal-stability considerations. These results, it should be emphasized, were obtained in an attempt to control leading-edge separation and hence are not too applicable to the control of trailing-edge separation. Additional work on the effect of varying chordwise porous area suction is reported in reference 116.

It is not possible at present to compare experimentally the suction slot with the porous area suction of equal coverage because the drag and power evaluations of both are not available; however, theory indicates that porous area suction should require less power than slot suction. From low-speed considerations it appears that, for acceptable pitching-moment characteristics, the advantages of one over the other will be decided more from power and structural considerations than from aerodynamic considerations.

From the material available at this time, it appears that the boundary-layer control may be as effective aerodynamically in providing desirable pitching-moment characteristics as the extensible leading-edge slat and flap and may also be subject to somewhat the same limitations.

Chord-extensions.—Data on chord-extensions from reference 53 are presented in tables 38 and 39.

As previously discussed under the section entitled "Fences" the problem of obtaining satisfactory longitudinal stability when the leading-edge vortex flow is present may not necessarily require a change in the effective camber of the tip sections of the wing but may rather be a matter of diffusing the vortex flow. In this regard, the results obtained by a mere extension of the local chord over the outer portion of two highly sweptback wings are very promising (ref. 53). In figure 21 are presented the pitching-moment variations with lift for two wings with $\Lambda_{c/4}=50°$ equipped with extensible leading-edge flaps and chord-extensions. In the case of the wing which incorporates circular-arc airfoil sections, both the extensible leading-edge flap and the chord-extension improved the longitudinal stability characteristics of the wing alone to about the same degree. In the case of the wing incorporating NACA 64-series airfoil sections, the extensible leading-edge flap was somewhat more effective than either a sharp-nose or round-nose chord-extension. The differences in pitching moment between the round and sharp leading-edge chord-extensions indicate that nose shape of the chord-extension is a significant geometric factor in the the design of this device.

The following discussion of the effects of chord-extensions on the flow over swept wings and on the longitudinal stability of such wings is based on force-test results and on visual

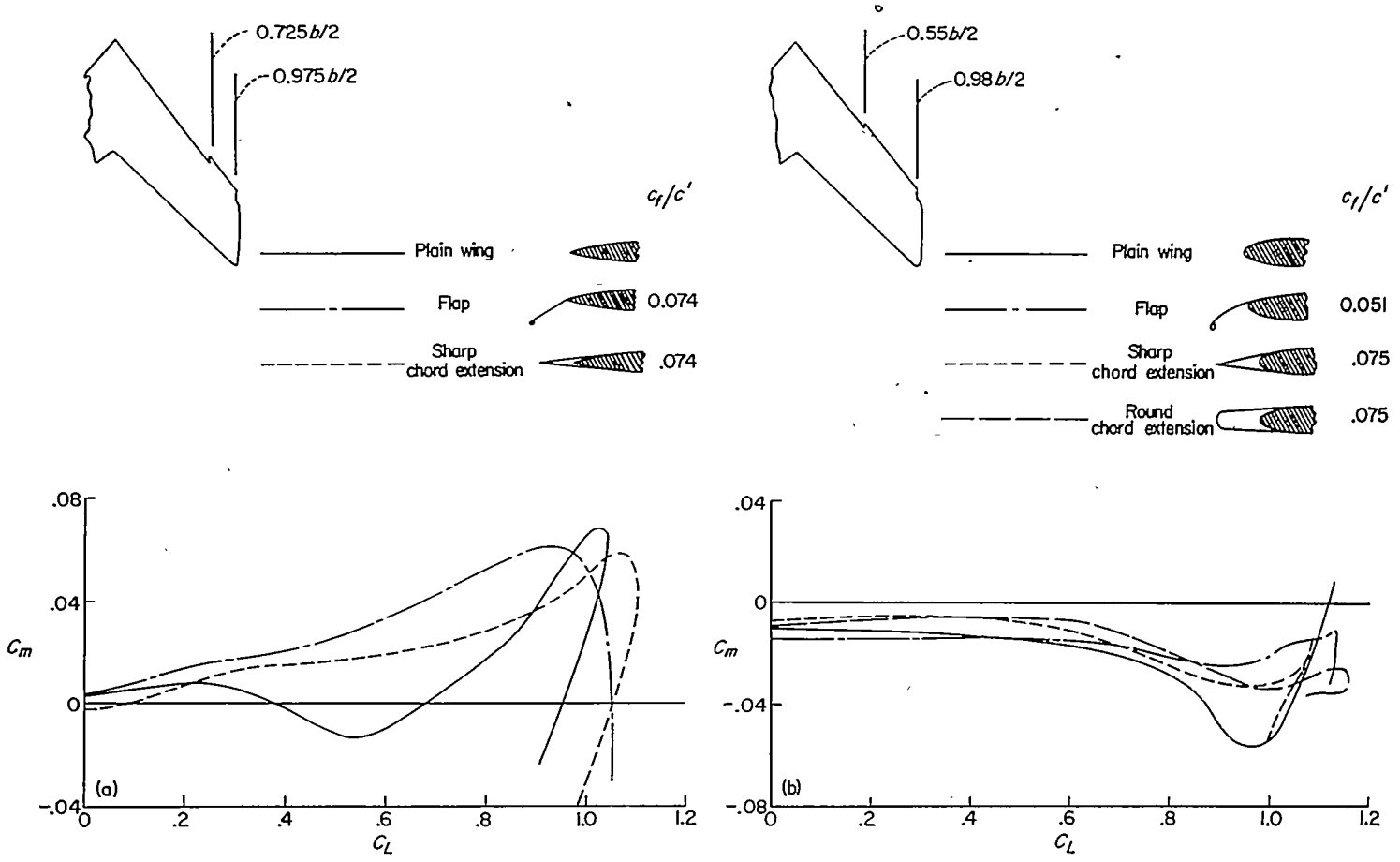

(a) Circular-arc airfoil sections.

(b) NACA 64-series airfoil sections.

FIGURE 21.—Comparison of the effects of extensible leading-edge flaps and chord-extensions on the pitching-moment characteristics of two sweptback wings ($\Lambda_{c/4}=50°$) having different airfoil sections. (Data obtained from ref. 53.)

probe and surface tuft observations of the flow over the wings described in reference 53, and on similar results from another wing of different sweep angle and airfoil section that has been investigated in the Langley 300 MPH 7- by 10-foot tunnel. More precise development of these concepts will probably require pressure-distribution studies.

Chord-extensions would be expected to have a beneficial effect on the pitching-moment characteristics of any sweptback wing because of the fact that, like an extensible leading-edge flap, the plan-form discontinuity at the inboard end of the chord-extension gives rise to a vortex in the stream direction which tends to prevent the low-energy air from the inboard sections from influencing the boundary layer at the outboard sections. The angle-of-attack range through which this improvement in flow over the outboard sections is realized and the manner in which the pitching-moment characteristics are improved seems to depend on the airfoil section employed in the wing and to some extent on the wing plan form. In the following discussion the flow phenomenon is discussed relative to airfoil section although the influence of wing plan form is such that it may increase or decrease the relative importance of airfoil section for any given swept wing.

In the case of a swept wing with a sharp leading edge, leading-edge separation occurs at very low lift coefficients. In fact the leading-edge separation vortex arising from leading-edge separation is quite strong at lift coefficients very much lower than those at which trailing-edge separation would be expected on a wing of the same plan form but incorporating airfoil sections of large leading-edge radius. The action of the chord-extension vortex is such as to alter the direction of the leading-edge vortex emanating from the inboard sections of the wing and its direction of rotation is such as to oppose the rotation of the inboard vortex. Although the diffusion of the two opposing vortices causes them to lose their identity, probe studies indicate that, in contrast to the case of the wing without chord-extension where the spanwise drain of the low-energy boundary-layer air trails off at the wing tips, the chord-extension vortex causes the low-energy air from the inboard sections to trail off the wing at a spanwise station slightly outboard of the inboard end of the chord-extension. The restriction of the inboard leading-edge vortex from the tip sections prevents them from experiencing the increase in lift and the attendant increase in stability between points A and B of sketch 1.

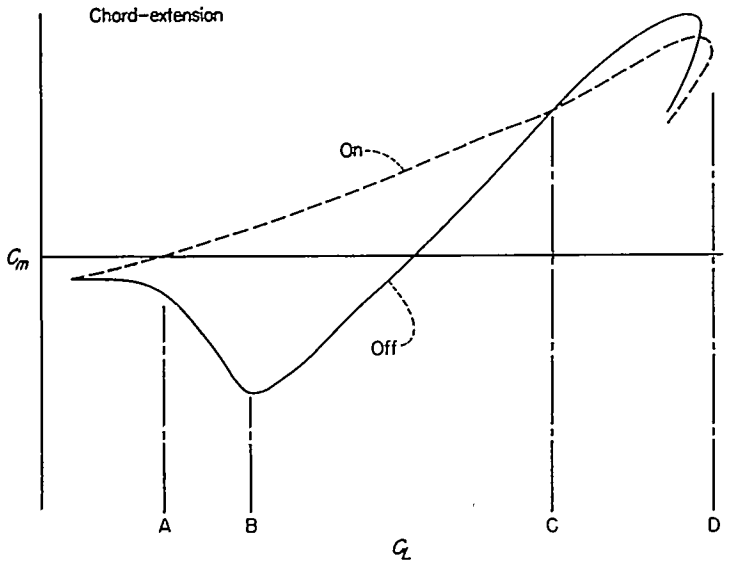

Sketch 1.

Observations of tufts attached to the airfoil surface have indicated an improvement in flow over the tip sections spanned by the chord-extension through the lift-coefficient range from A to B. It should be pointed out that this improvement in flow results in a decrease in lift rather than the increase that is customarily obtained when flow conditions are improved. At lift coefficients only slightly greater than point B, surface tufts do not indicate any substantial differences in flow between the chord-extension on-and-off conditions. This result may arise either from the fact that the inboard leading-edge vortex is strong enough to break through the chord-extension vortex or that the secondary vortex observed to be present on the chord-extension contributes to the general breakdown of flow at the outboard sections or from the combination of both effects. The secondary vortex on the chord-extension has been observed to occur at approximately the same angle of attack as that at which the leading-edge vortex occurred on the basic wing. The strength and growth of the secondary vortex is probably similar to that occurring over a corresponding length of span at the inboard end of the wing. It has a measurable influence on the pitching-moment characteristics in the lift range between D and C. (See sketch 1.) This was indicated by the data of figure 21 where the $0.25b/2$ chord-extensions provided slightly more negative pitching moments near maximum lift than when the outboard $0.19b/2$ of the chord-extension was removed. (In some installations chord-extensions having spans greater than $0.25b/2$ may be required and in such cases the secondary vortex may have an even stronger influence on the pitching-moment characteristics.) Inasmuch as there is an improvement in flow over the outboard sections through only a small lift range and the most positive pitching moment measured on the plain wing is almost attained with the chord-extension on, it can only be concluded that the linearity in the variation of pitching-moment coefficient with lift coefficient arises from balancing areas experiencing increases and decreases in lift. The stable break in the pitching-moment curve at maximum lift (see, for example, fig. 21) is explained by the fact that, in the stalled condition both with and without chord-extensions, the wing has the pitching moment of a stalled flat plate of corresponding plan form.

When chord-extensions are used on a swept wing the airfoil sections and sweep angle of which are such as to place the wing near the boundary for leading-edge separation (see, for example, fig. 5) the basic flow phenomenon appears to be somewhat different from that on the sharp leading-edge wing. The round leading edge of the wing delays leading-edge separation to lift coefficients very much higher than on sharp leading-edge wings with the result that the leading-edge vortex occurs at or only slightly prior to trailing-edge separation. Consequently, such wings do not exhibit a very marked stable dip in the pitching-moment curve prior to the unstable break that results from tip stalling. (See sketch 2.) It is not unlikely that, because the formation of the leading-edge separation bubble would tend to move the adverse pressure gradient rearward, trailing-edge separation and consequent breakdown of flow over the entire chord occurs at lower lift coefficients than it would on a similar wing having a larger leading-edge radius with no tendency for leading-edge separation. Thus, the chord-extension diffuses and directs the inboard leading-edge vortex as in the case of the sharp leading-edge wing but, of equal importance, it also prevents the low-energy air that is flowing outboard along the trailing edge from influencing the flow over the tip sections and thereby delays trailing-edge separation on those sections. Thus, surface-tuft studies have indicated a marked improvement in flow over those sections spanned by the chord-extension through the lift range denoted A to B in sketch 2. The improvement in pitching-moment characteristics on such wings results primarily from the delay in separation over the tip part of the wings to higher angles of attack as would be deduced from

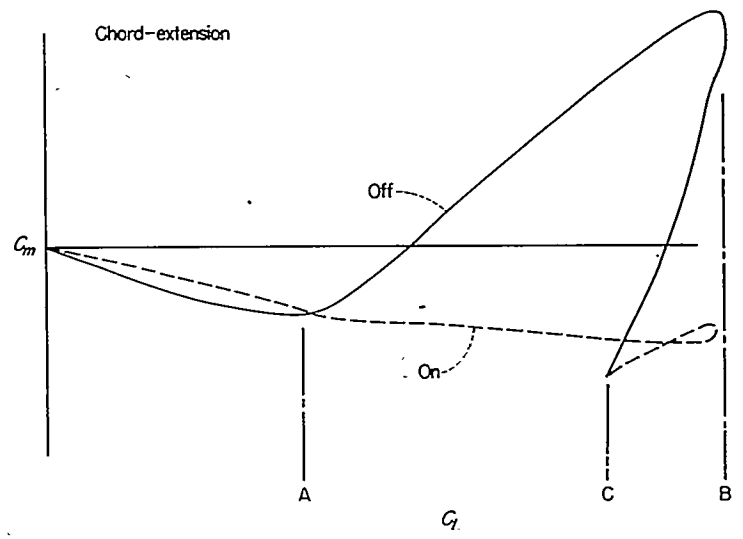

Sketch 2.

available data which indicate only a slight forward shift in aerodynamic center from that obtained in the low-lift range. (See sketch 2.) At maximum lift the pitching-moment break for these experimental data was in the stable direction inasmuch as the pitching moment in the stalled condition was more negative than in the stall-controlled condition. In other cases, however, the pitching-moment break may be in an unstable direction, inasmuch as the induced angle-of-attack distribution and airfoil section characteristics are not greatly influenced by the addition of the chord-extensions. A further improvement in the pitching-moment characteristics may be expected by providing droop in the chord-extension in order to combine the beneficial effects of the chord-extension vortex and leading-edge camber in the same manner as does an extensible leading-edge flap.

When a chord-extension is applied to a wing which exhibits only trailing-edge separation, improvements in flow over the tip sections would still be expected, inasmuch as the chord-extension vortex would tend to divert the outflow over the rear part of the wing that is emanating from the inboard sections.

It should be realized that the most effective span of chord-extensions is as critical as the most effective span of extensible leading-edge flap was shown to be.

Variable sweep.—The information thus far presented emphasizes the problems encountered on an airplane using highly swept wings. A possible method of avoiding these problems is to provide an airplane with wings the sweep angle of which can be changed in flight so that a low sweep angle can be used when it is desired to fly at high lift coefficients and low speed. Some points of interest in connection with the design of such an airplane are illustrated by the results of an investigation at low Reynolds number and Mach number of a variable-sweep airplane model (refs. 78 and 117). Figure 22 illustrates schematically the model used and the longitudinal stability characteristics. As the sweep angle is increased by rotating the wing panels about a pivot point in the fuselage, the wing center of pressure moves rearward and causes a large increase in longitudinal stability. In order to overcome this, the wing-panel pivot point must be allowed to translate forward as the wings are rotated rearward.

The data of figure 22 are, in all likelihood, subject to Reynolds number effects. It would be expected that at $\Lambda_{LE}=23°$ the maximum lift of the wing would increase with an increase in Reynolds number and, because the strength of the leading-edge vortex flow (as indicated by the pitching-moment data) would diminish with an increase in Reynolds number, the maximum lift of the wing at $\Lambda_{LE}=63°$ may be less than the values shown. Thus, the variations in wing aerodynamic center due to variable sweep may also be different at flight values of Reynolds number.

Contra flaps.—Data on contra flaps obtained from references 31 and 32 are presented in table 20. The contra flap is a flap located on the outer part of the wing span in order to provide negative camber in the tip sections. The negative induced camber results in a download at the tip sections in the low angle-of-attack range. The nose-up tendency due to the download at the tip sections decreases with

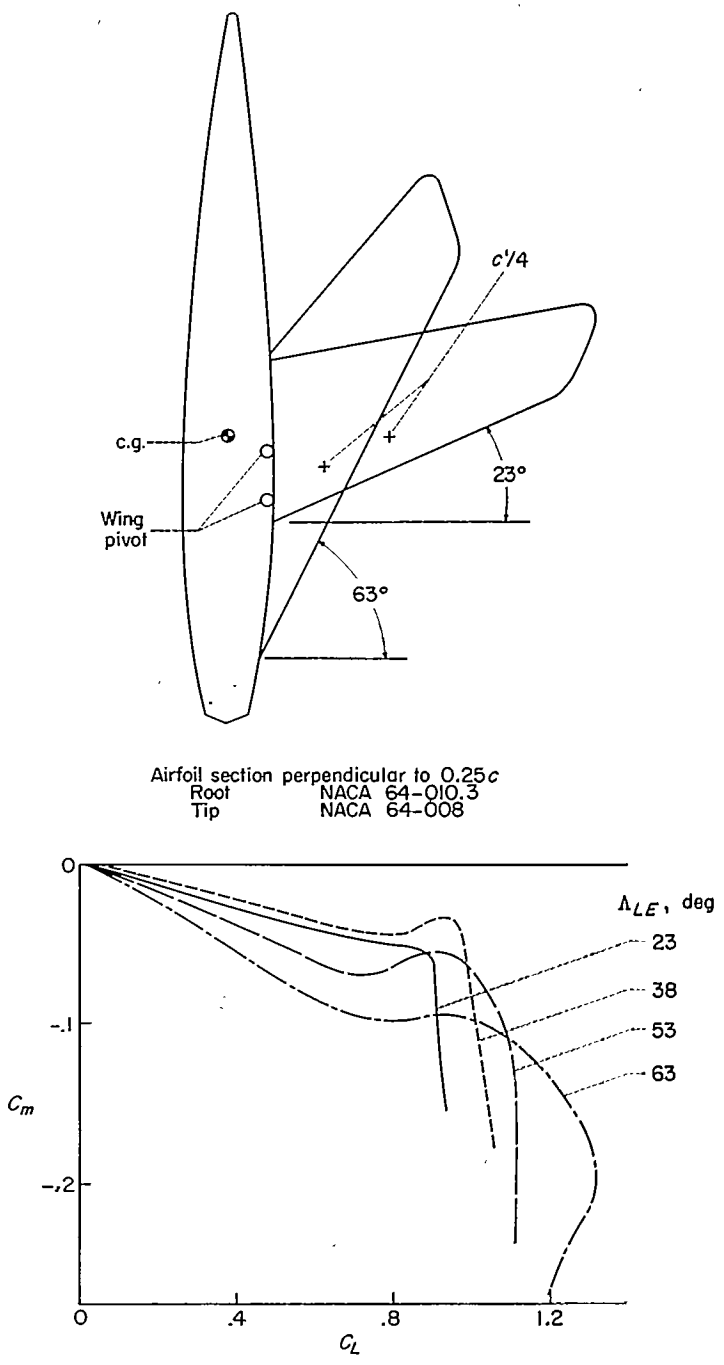

FIGURE 22.—Longitudinal stability characteristics of a model of a variable-sweep airplane. $R=2\times10^6$ (based on c' for $\Lambda_{c/4}=50°$). (Data obtained from ref. 78.)

increases in angle of attack and thereby provides a pitching-moment variation with lift coefficient that has a stable slope. At maximum lift, however, there must remain a nose-up tendency of such a magnitude that when wing stalling occurs the pitching-moment break will be in the stable direction.

The results presented in references 31 and 32 were obtained by using upper-surface split flaps on the outer part of the wing as the contra flaps. The stability characteristics were quite satisfactory through the entire lift range; however, in these particular tests large losses in lift and increases in drag accompanied the improvement in stability. Inasmuch as no attempt was made in these investigations to see if the

adverse lift and drag effects could be minimized while maintaining the beneficial stability effects, the usefulness of the contra-flap principle has not been fully evaluated.

WING GEOMETRY

Camber and twist.—Data on camber and twist are presented in tables 17, 18, and 28 from references 26, 42, and 43. Additional information is contained in references 79, 80, 81, and 96. Although most of the swept wings have incorporated some degree of camber or twist or both camber and twist, the references listed are only those that provide comparisons with the uncambered and untwisted wings.

Combinations of camber and twist have been commonly incorporated in unswept wings designed for relatively low-speed flight in order to obtain, among other things, satisfactory stalling characteristics. Recently, there have been advantages found in the use of camber and twist at transonic flight speeds. Although the introduction of camber and twist in the amount required to provide the desired load distribution at high speed is also in the direction to improve the low-speed longitudinal stability characteristics, it must be remembered that from low-speed longitudinal stability considerations the optimum camber and twist will be that derived from low-speed design consideration. Hence, the data which have been obtained with wings designed to meet a given high-speed requirement are not necessarily indicative of optimum low-speed benefits to be derived from camber and twist.

A study which involved only the effects of camber (constant camber changes over the span) indicated that except for the trim changes to be expected, the pitching-moment characteristics were not materially affected by camber (ref. 26). Somewhat comparable results were obtained in an investigation where the effects of increasing the leading-edge radius and adding forward camber were studied on a $\Lambda_{c/4}=35°$ wing (ref. 85). In each of the previous references (refs. 26 and 85) there was no spanwise variation in camber, and the full low-speed advantages of camber may not have been utilized.

The effects of camber and twist on the pitching-moment characteristics of two wings (refs. 79 and 80) are presented in figure 23. In both cases, the twist and camber were calculated to provide uniform loading at supersonic speeds and at design lift coefficients of 0.4 and 0.5 for the $\Lambda_{c/4}=45°$ and $\Lambda_{c/4}=60.8°$ wings, respectively. Actually, a compromise twist was used in the $\Lambda_{c/4}=45°$ wing such that little resemblance remained between that desired for uniform loading and that tested. The compromise twist was in the direction

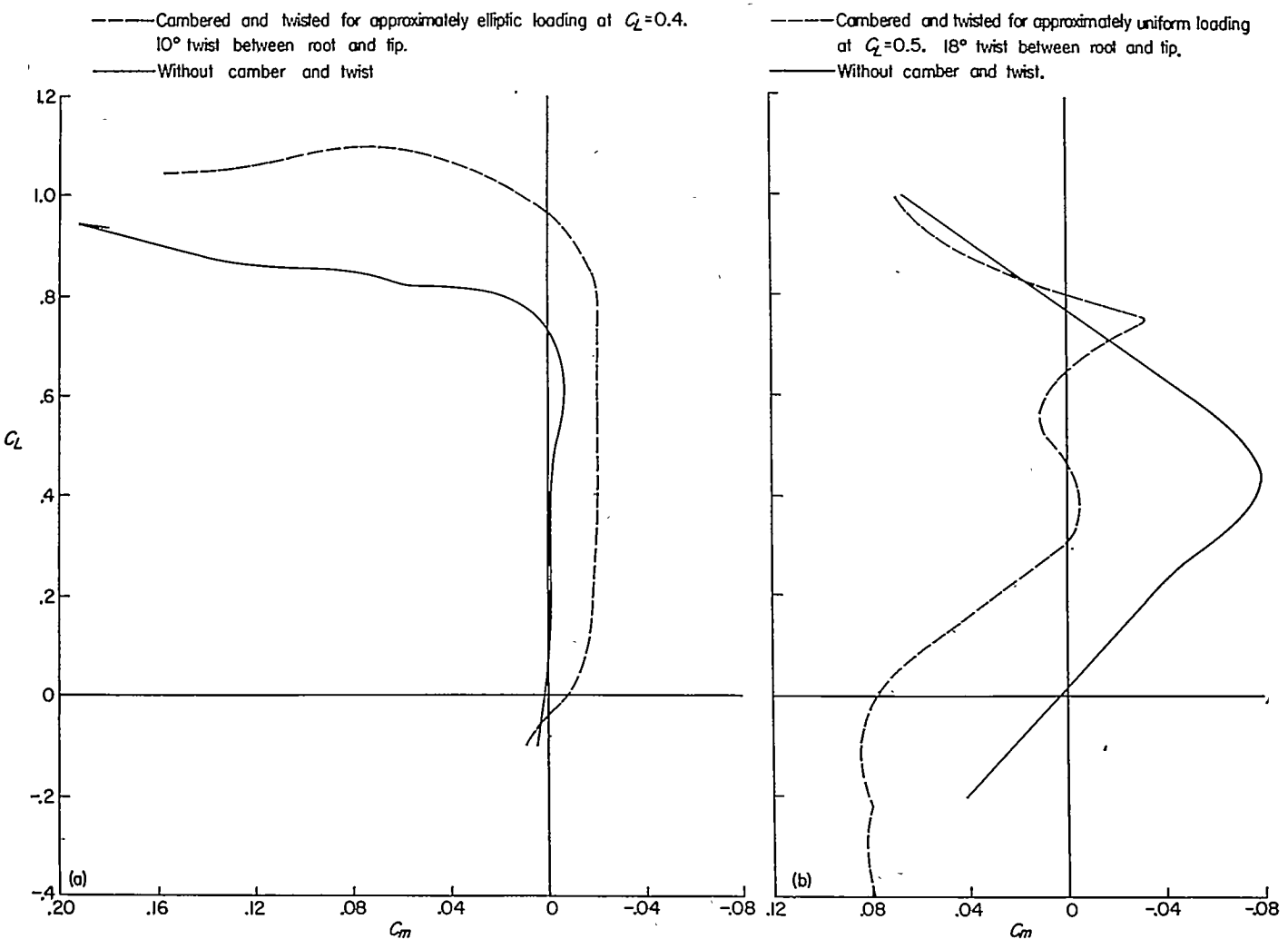

(a) $\Lambda_{c/4}=45°$; $A=6.0$; reference 79.

(b) $\Lambda_{c/4}=60.8°$; $A=3.5$; reference 80.

FIGURE 23.—Effects of combined twist and camber on the variations of pitching-moment coefficient with lift coefficient for two sweptback wings.

to alleviate tip stall, and, as can be seen in figure 23, a small gain in the linear pitching-moment range was obtained. The pitching-moment characteristics of the $\Lambda_{c/4}=60.8°$ wing are more irregular when twist and camber are introduced. It appears from the data available that additional work is required before camber and twist introduced to satisfy high-speed considerations can be evaluated in terms of improvements that will be produced in the low-speed stability characteristics of sweptback wings.

Although camber and twist have not in the limited number of cases available solved the low-speed stability problems, they may result in the need for fewer and less complicated stall-control devices. A comparison is shown in figure 24 of the pitching-moment characteristics of wings with and without camber and twist and both with and without fences. The combination of fences and camber and twist provided rather acceptable pitching-moment characteristics whereas with either the fences or camber and twist a very large destabilizing shift in aerodynamic center occurred at or prior to maximum lift. In the case of the $\Lambda_{c/4}=60.8°$ wing of reference 80, leading-edge flaps and fences were used in order to improve the characteristics. The greatest improvement obtained by using these mechanical devices is illustrated by the results of figure 25. Unfortunately, these data are limited in lift range, and it is not possible to tell whether or not a stable break in pitching moment at maximum lift would be obtained for this configuration.

Inverse taper.—The adverse effects of tip stall on sweptback wings can be avoided by causing the initial stall to occur over the inboard sections. Theoretical considerations would seem to indicate that inboard stall could be accomplished by means of inverse taper (ref. 118). If it were not for the effects of boundary-layer outflow, inverse taper would provide sweptback wings that were longitudinally stable well above the stability boundary of figure 12. Because of the boundary-layer outflow, however, there is a possibility that premature tip stall would limit the usefulness of inverse taper as a means of alleviating the low-speed problems associated with sweptback wings of normal taper ratio. It should be mentioned, however, that fences should be more effective on wings having inverse taper than on wings of normal taper. The low-speed and low Reynolds number tests of a model which incorporated inverse taper (ref. 119) have indicated very satisfactory longitudinal stability characteristics. The sweep angle ($\Lambda_{c/4}=37.5°$) and aspect ratio (3.0), however, were such that satisfactory stability would be expected for wings without inverse taper.

Cranked wings.—Data on cranked wings are presented in table 22 from reference 38. Additional information is contained in references 120 and 121.

It has been suggested (ref. 121) that the low-speed longitudinal stability problems of sweptback wings can be reduced by using a wing plan form in which the sweep angle decreases toward the tip. The reduction can either be continuous

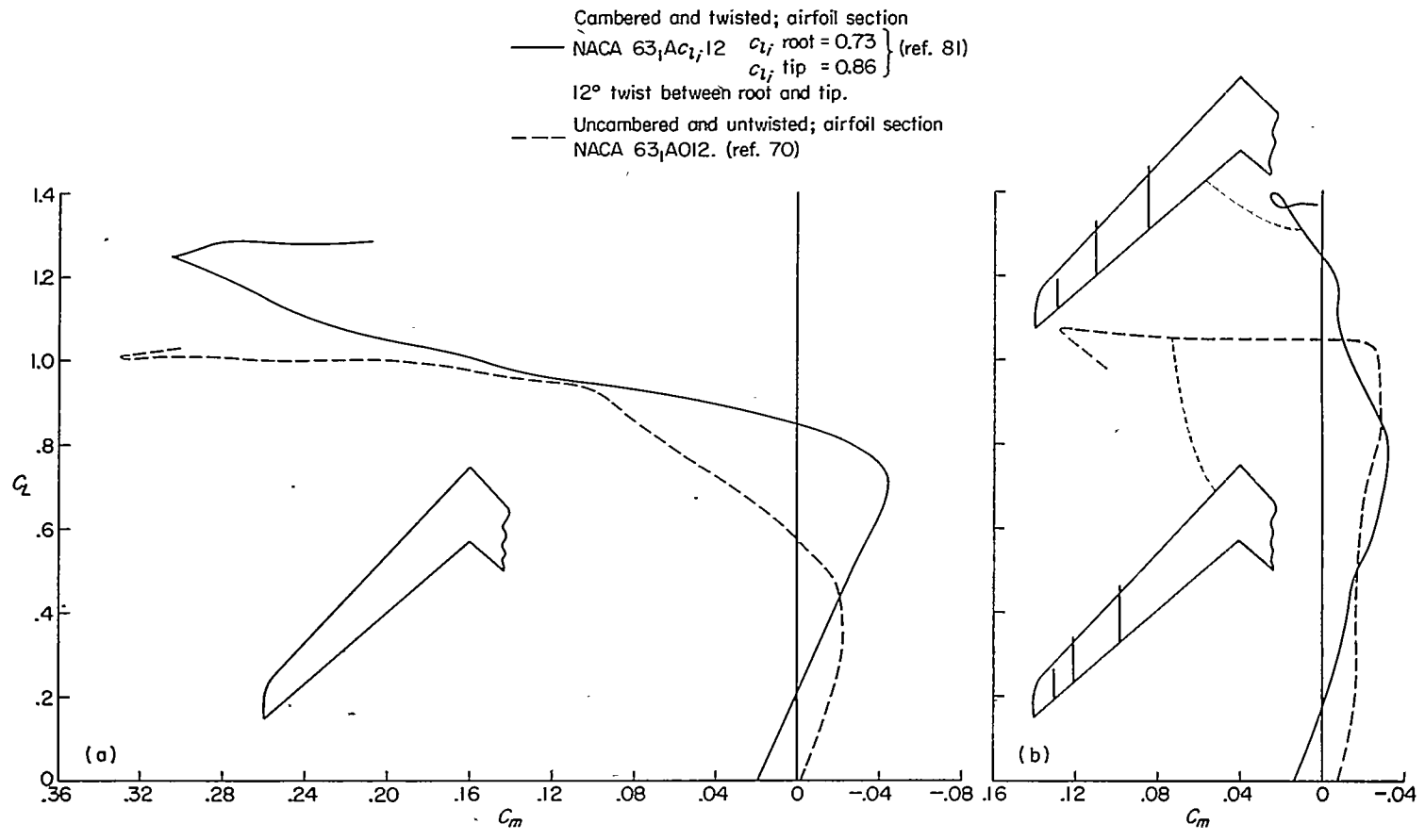

(a) Fences off. (b) Fences on.

FIGURE 24.—Variation of pitching-moment coefficients with lift coefficients for a wing with and without camber and twist, both with and without chordwise fences. $\Lambda_{c/4}=45°$; $A=8.0$; $\lambda=0.45$; $R=4.0\times10^6$.

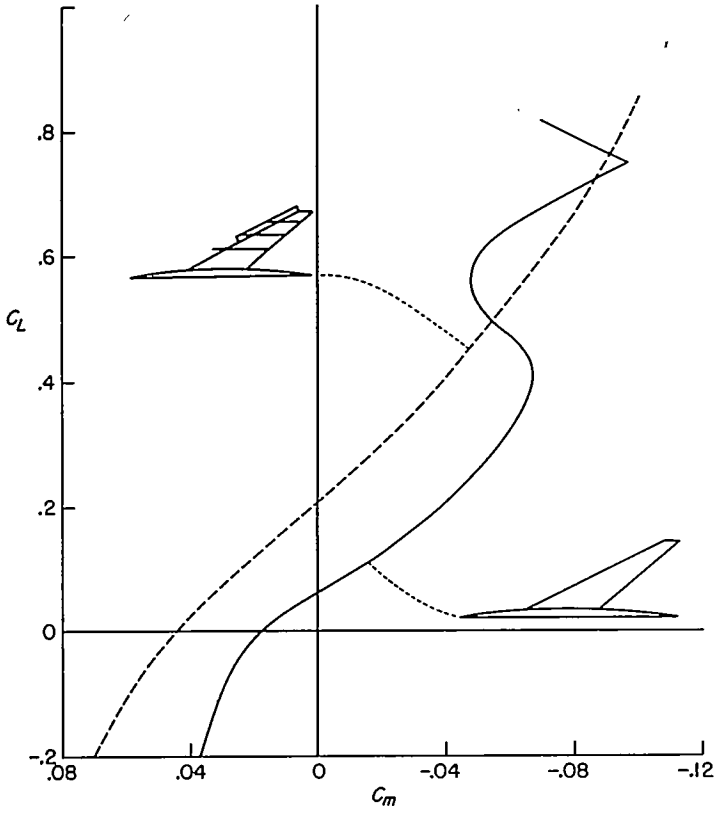

FIGURE 25.—The effect of extensible leading-edge flaps and fences on the pitching-moment characteristics of a twisted and cambered sweptback wing ($\Lambda_{c/4}=60.8°$) having an aspect ratio of 3.5, and a taper ratio of 0.25. (Data obtained from reference 80.)

(crescent-shaped plan form) or consist of several steps (cranked-shape plan form). There have been arguments that the plan-form discontinuities may have adverse effects on the maximum lift characteristics; however, the low-speed data available (see, for example, ref. 38) indicate that good or acceptable lift and pitching-moment characteristics can be obtained. The high-speed drag characteristics therefore dictate its usefulness. The proponents of the cranked-wing concept contend that the equivalent sweptback wing has a leading-edge sweep angle equal to that of the inboard sections of the cranked wing on the basis that the detrimental compressibility effects tend to occur first near the root sections. That the root sections are the more important in determining the critical Mach number is in agreement with the "crest line" concept defined in reference 124. A consideration in the comparison of a cranked wing with a sweptback wing is the effect a body may have on the critical nature of the inboard sections. From low-speed pressure-distribution data, it appears that, with a body on, the "crest line" concept of reference 122 would indicate that the inboard sections are no longer as critical.

Composite (A, M, and W) wings.—In the search for a wing plan form which would incorporate the benefits to be derived from sweep and yet possess acceptable low-speed characteristics, the Germans investigated both the M and W plan forms (ref. 123). Recently work has been done on swept wings with the center sections filled in to form A wings. Substantial improvements have been obtained at low speeds in the longitudinal stability characteristics of these composite wings. Early swept-wing studies in this country (ref. 124) also established the low-speed advantages of the M and W plan forms. There was, however, an implication made in reference 123 that, when split flaps were deflected, there is no advantage in using an M wing instead of a sweptback wing. The high-speed considerations of the juncture drag to be associated with either the M or W plan form were instrumental in shelving these plan forms before any extensive amount of low-speed work had been done. Recently, it has been found that such plan forms may not exhibit the aerodynamic-center shift resulting from twist due to bending, which is an unfavorable characteristic of sweptback wings in the transonic speed range. At present, transonic tests are needed to see if the drag penalties of M and W plan forms are compensated by their structural advantages.

HORIZONTAL TAIL

A horizontal tail is usually employed to obtain damping and control in pitch and a desired static margin. In its conventional location it is subject to the flow field created by the wing-body combination. Whether or not the horizontal tail affects the stability of the combination, other than by the static margin it provides, depends on the manner in which the characteristics of the flow field in which the tail operates vary with angle of attack. In the case of straight wings, the flow separation which could cause nonlinear variations of the flow with angle of attack is restricted to a small angle-of-attack range prior to maximum lift. Inasmuch as straight wings are, in general, quite stable through maximum lift, any nonlinear flow characteristics due to flow separation and of such a nature as to cause the horizontal tail to be destabilizing are not too detrimental. Thus, in straight-wing airplanes the problem is largely to design a tail (geometry and location) that will be capable of trimming the airplane throughout the flight lift range. Body effects may cause the tail location to become a major design problem and this condition has been shown to be particularly true in the case of straight, low-aspect-ratio wings employing sharp leading-edge airfoil sections. In contrast to straight wings, sweptback wings exhibit flow separation at lift coefficients well below maximum lift and, in many cases, sweptback wings are either unstable or possess only marginal stability through maximum lift. In such cases any destabilizing tendencies of the tail resulting from nonlinearities in the flow characteristics may not be tolerable.

As early as 1946 (for example, ref. 10) it had been illustrated that a horizontal tail located behind a stable sweptback wing could result in a wing-tail combination that was unstable through maximum lift. A considerable amount of low-speed work has been done, therefore, in order to determine the most suitable location for a horizontal tail behind a sweptback wing. Data on such work are presented in the tables from references 13, 19, 23, 25, 29, 36, 50, 52, and 55. Additional information is contained in references 28, 82, 95, 98, 99, 112, and 125.

The results of the low-speed tests indicate that, whereas in certain locations the horizontal tail may be detrimental,

there are locations at which the horizontal tail may measurably improve the longitudinal stability characteristics over those of the wing alone. In order to avoid the adverse effects and to obtain the beneficial effects that a horizontal tail is capable of providing, the following general rule can be stated: The location of the horizontal tail should be such that it is emerging from the wake through the nonlinear lift range of the wing (to be discussed later). This rule means that for very short tail lengths the tail will lie below the chord plane extended, and for very long tail lengths the tail will lie somewhat above the chord plane extended.

In cases where the airplane configuration exhibits a high degree of stability in the maximum lift range, it may be desirable from trim and control considerations to locate the tail so that it will have a slight destabilizing influence. Other factors such as ground clearance, high-speed wake buffeting, and structural considerations may dictate a compromise location for the tail. It is necessary, then, to consider separately the effectiveness of the horizontal tail operating in the flow field behind sweptback wings and the over-all stability characteristics of the sweptback wing-tail combinations.

EFFECTIVENESS

The variations of horizontal-tail effectiveness with angle of attack for several sweptback wing-tail combinations are presented in figure 26. The horizontal-tail effectiveness parameter τ is a measure of the influence of the tail and includes the influence of both the wing and fuselage on the downwash and dynamic pressure at the tail plane. A derivation of the formula for τ can be found in reference 55 and the resulting expression is given as

$$\tau=-\eta\left[\frac{q_t}{q}\left(1-\frac{\partial\epsilon}{\partial\alpha}\right)+\alpha_t\frac{\partial\left(\frac{q_t}{q}\right)}{\partial\alpha}\right] \tag{1}$$

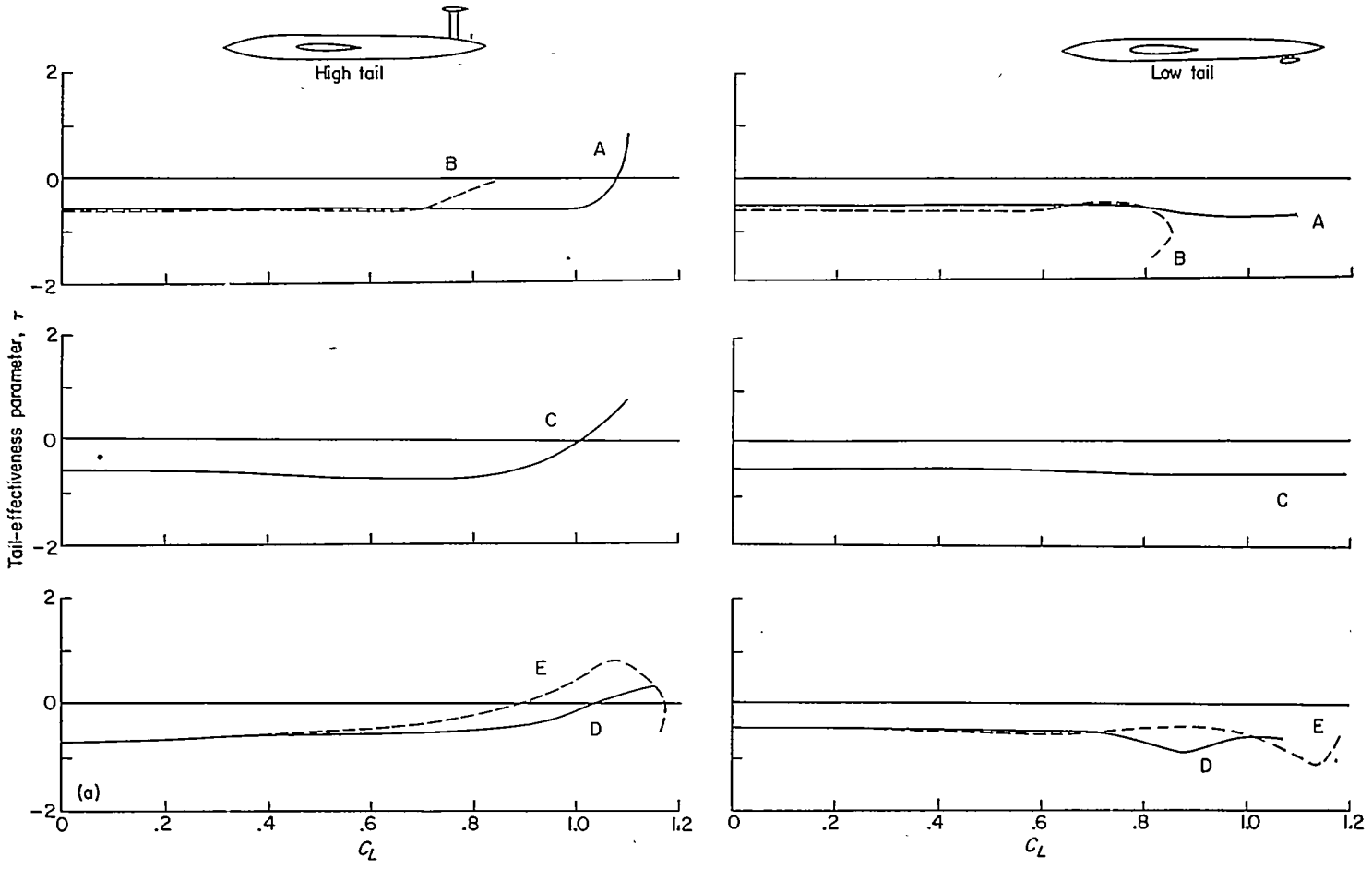

Model	$\Lambda_{c/4}$, deg	A	Airfoil section	Approx. streamwise t/c		Tail position		Tail length, percent c	Ref.
				Root	Tip	High	Low		
A	40	4	64_1-112	0.096	0.096	0.41 $b/2$	−0.06 $b/2$	2.0	29
B	40	4	Circular arc	.079	.052	.46	−.01	2.2	36
C	45	6	64-210	.075	.075	.38	−.05	2.2	50
D	50	2.88	64_1-112	.082	.082	.50	−.07	1.7	52
E	50	2.84	Circular arc	.065	.041	.44	−.13	1.7	55

(a) Flaps off.

FIGURE 26.—Influence of high and low tails on the variation of tail-effectiveness parameter τ with lift coefficient for several sweptback-wing configurations. Tail positions are given with respect to the extended root chord line.

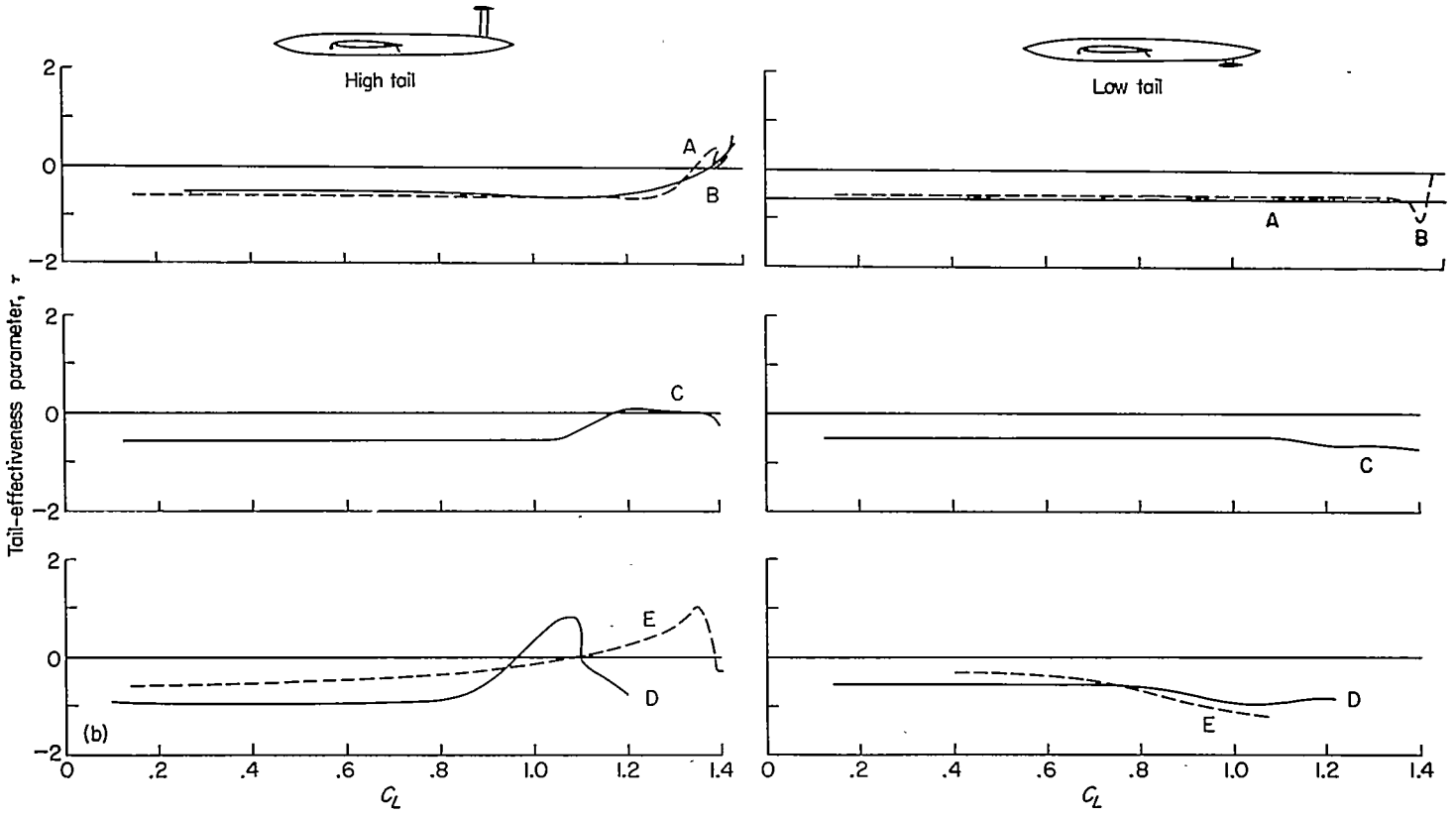

Model	Tail position		Flaps	
	High	Low	Leading edge	Trailing edge
A	0.41 $b/2$	−0.06 $b/2$	0.57 $b/2$	0.5 $b/2$ split
B	.46	−.01	.70	.5 $b/2$ split
C	.38	−.05	.48	.5 $b/2$ split
D	.50	−.07	.40	.4 $b/2$ split
E	.44	−.13	.25	.5 $b/2$ extended

(b) Flaps on.

FIGURE 26.—Concluded.

so that

$$\frac{dC_{m_t}}{d\alpha}=V\tau\left(C_{L_{\alpha_t}}\right)_{isolated} \tag{2}$$

Inasmuch as $\left(C_{L_{\alpha_t}}\right)_{isolated}$ and V (tail volume) are constant for any particular tail and tail location, the variations of τ with angle of attack reflect any changes in the linearity of C_{m_t} with angle of attack. A minus value of τ signifies that the tail is providing a stabilizing contribution.

Data which are representative of the tail effectiveness to be obtained behind sweptback wings are presented in figure 26. Sufficient systematic data to permit the construction of comprehensive design charts however were not available. The influence of tail location on the effectiveness of the tail can be seen by the manner in which τ varies in the high-lift range for the two tail locations considered (fig. 26). Whereas τ for the tail in the high position decreases and actually becomes destabilizing in the high-lift range, τ for the tail in the low position remains essentially constant and in certain cases becomes increasingly negative. A comparison of the data on parts (a) and (b) of figure 26 indicates that the relative tail effectiveness is somewhat improved when flow separation is prevented by extensible leading-edge flaps although the effect is rather slight. In some other available data (ref. 95) the effect is somewhat more pronounced.

The survey data available behind sweptback wings have been used to illustrate in figure 27 the rate of change of wake location with angle of attack as a function of sweep angle. These data indicate that the wake moves up at a greater rate with respect to the chord plane extended as the sweep angle is increased. It should be pointed out that the data presented in figure 27 represent, in general, slopes obtained through an angle-of-attack range from 0° to 16°; however, the trends illustrated in figure 26 appear to continue to even high angles of attack. The significance of these wake movements with relation to the downwash field through which a particular tail will pass is illustrated in figure 28. The tail located in the high position lies well above the wake center through the entire angle-of-attack range and, as can be seen in the accompanying plot of downwash against angle of attack, experiences an increasing rate of change of downwash with angle of attack throughout the greater portion of the angle-of-attack range. The tail located in the medium position lies above, but relatively close, to the wake center in the high angle-of-attack range. The increasing rate of change of downwash with angle of attack is less pronounced than that obtained in the high position. When the tail is

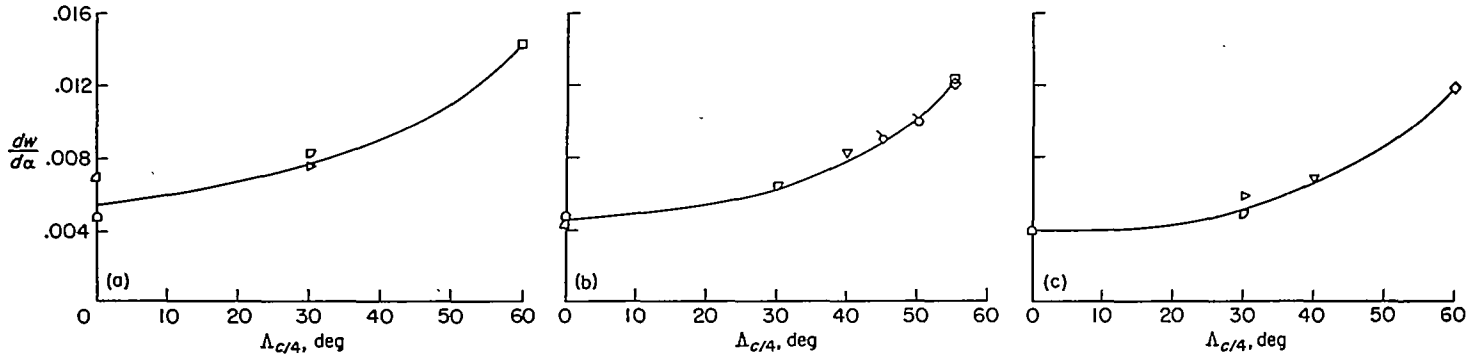

Symbol	Wing				Longitudinal location behind $c'/4$, percent c'	Ref.
	$\Lambda_{c/4}$, deg	A	Airfoil section	c', in.		
◻	0	3.00	NACA 0015	10.00	172.5	82
◻	0	6.00	NACA 0015	10.00	172.5	82
▽	30	5.20	NACA 0015	11.50	172.5	82
▽	30	4.50	NACA 0015	11.50	172.5	82
▽	40	4.01	NACA 64_1-112	34.70	200.0	28
◇	45	5.10	NACA 64-210	31.22	210.0	50
○	50	2.88	NACA 64_1-112	39.97	165.0	13
◻	60	3.00	NACA 0015	20.00	160.0	82
◇	60	1.50	NACA 0015	20.00	172.5	82

(a) Plane of symmetry. (b) 33.3-percent semispan from plane of symmetry. (c) 66.6-percent semispan from plane of symmetry.

FIGURE 27.—The rate of change of wake-center location (from extended root chord line) with angle of attack at several lateral stations, in the region of a horizontal tail behind wings of various plan forms. Flagged symbols indicate midwing fuselage combination; plain symbols indicate fuselage off.

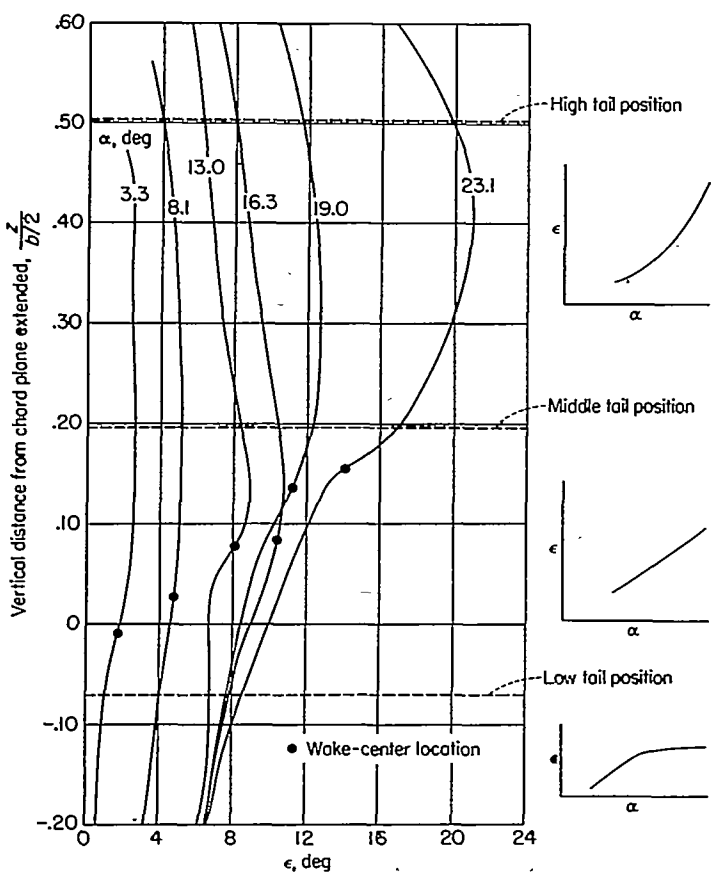

FIGURE 28.—Downwash profiles behind a sweptback wing ($\Lambda_{c/4}=50°$) having an aspect ratio of 2.9, a taper ratio of 0.625, and NACA 64_1-112 airfoil section. Profiles located at a tail length of approximately two mean aerodynamic chords and at a station 0.313 semispan outboard of the plane of symmetry. (Data obtained from ref. 13.)

located in the low position, it lies below the wake center and experiences a decreasing rate of change of downwash with angle of attack as the angle of attack is increased. For any fixed tail location, the movement of the wake seems to define the rolling up of the vortex sheet with respect to the variations of $d\epsilon/d\alpha$ obtained; however, another very significant effect for the present discussion should be noted. An inspection of figure 28 shows that the downwash becomes progressively more unsymmetrical about the wake center as the angle of attack is increased. The unsymmetrical nature of the downwash field arises from the rolling up of the vortex sheet and, to some extent, from the inflow tendencies in the vicinity of the wake. Both of these phenomena are described in reference 126 as they pertain to straight wings. An additional effect which might be expected to contribute to the nonlinearity of the downwash characteristics in the high-lift range is the inward displacement of the tip vortices as stalling occurs at the tip sections of the sweptback wing. Actually the experimental data available seem to indicate that the effect of the inward displacement of the tip vortices is at least partially compensated for by the accompanying reduction in wing lift. This result is somewhat verified by the fact that, when extensible leading-edge flaps are used to prevent flow separation over the tip sections of a sweptback wing, the variations of downwash with angle of attack obtained are strikingly similar to those obtained on the plain wing.

The effects just described can be recapitulated as follows: the rolling up of the vortex sheet (as indicated by the upward movement of the wake) and the inflow tendencies into the wake are both factors contributing to an increasing value of $d\epsilon/d\alpha$ for tails located above the wake center and to a decreasing value of $d\epsilon/d\alpha$ for tails located below the wake center. It has been shown that the effect of the displaced downwash

field (indicated by wake movement) is accentuated by sweep. The influence of sweep on the rolling up of the vortex sheet has not been extensively studied experimentally. Inflow tendencies into the wake would not be expected to be affected greatly by sweep, but even this fact has not been established experimentally. It should be pointed out that the influence of the wake on the downwash and not the absolute values of dynamic-pressure ratios in the wake is the significant factor to consider in low-speed tail design considerations.

WING-FUSELAGE-TAIL COMBINATIONS

A rational tail location is inherently dependent on the stability requirements imposed on the tail by the wing-fuselage combination. Thus, for a wing-fuselage combination exhibiting neutral stability throughout the lift range, a tail located in a field of constant $d\epsilon/d\alpha$ can provide an adequate and constant static margin (see case I, fig. 29). For a wing-fuselage combination exhibiting an abrupt decrease in stability through some part of the lift range, it would be advantageous to have the tail so located that $d\epsilon/d\alpha$ decreased abruptly at the same lift coefficient at which the decrease in stability occurred for the wing-fuselage combination (see case II, fig. 29). The linearity in the stability characteristics of the complete configuration would, of course, be dependent on the degree of instability compensated for by the decrease in $d\epsilon/d\alpha$. A third condition can be considered in which the wing-fuselage combination exhibits an abrupt increase in stability through the lift range of such a magnitude as to be undesirable. A tail located so as to experience an abrupt increase in $d\epsilon/d\alpha$ at the corresponding lift coefficient could conceivably provide linear stability characteristics for the complete configuration (see case III, fig. 29). Although the term "abrupt" has been used in these illustrations, any gradual changes in the stability characteristics of the wing-fuselage combination would necessitate gradual changes in $d\epsilon/d\alpha$ at the tail. Further, the absolute values of dynamic-pressure ratios occurring in the wake have been ignored in the preceding discussion inasmuch as they only affect the effectiveness of the tail and are, therefore, only of secondary importance with respect to $d\epsilon/d\alpha$. Also ignored is

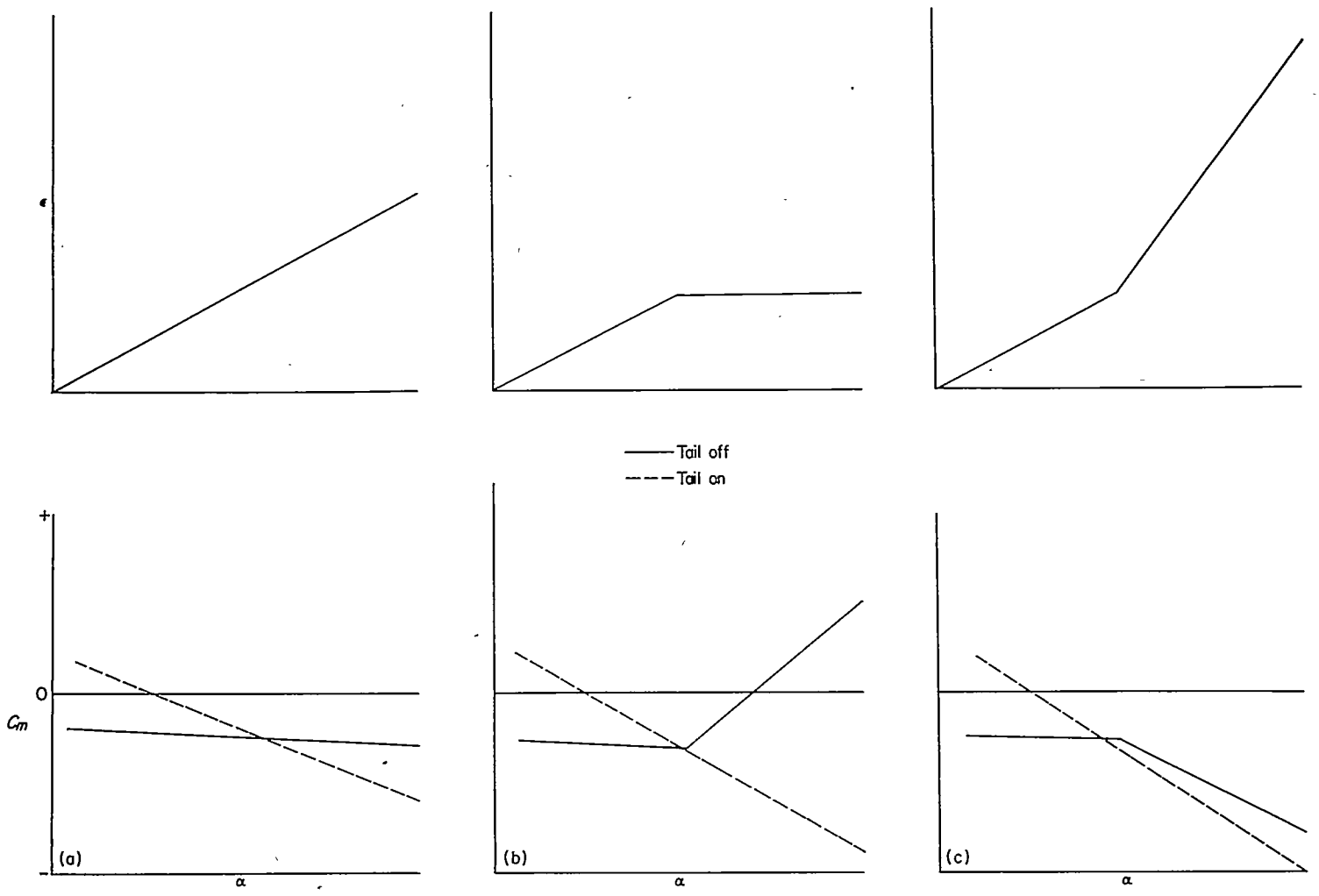

(a) Case I. Constant tail-off stability plus linear downwash characteristics result in constant tail-on stability. (Centrally located tail.)

(b) Case II. Destabilizing shift in tail-off stability plus reduction in $\frac{d\epsilon}{d\alpha}$ results in increased tail effectiveness and constant tail-on stability. (Generally low tail position.)

(c) Case III. Stabilizing shift in tail-off stability plus increase in $\frac{d\epsilon}{d\alpha}$ results in decreased tail effectiveness and constant tail-on stability. (Generally high tail position.)

FIGURE 29.—An idealized illustration of the improvement made in the pitching-moment characteristics of typical wing-fuselage combinations by the use of a horizontal tail operating in the downwash field behind a sweptback wing.

the term $\alpha_t \frac{\partial \frac{q_t}{q}}{\partial \alpha}$ (in equation (1)), which under certain conditions can have a measurable effect on the tail contribution to the over-all stability. For the tail-on tests available at this time, however, conditions of large α_t have not been encountered on tail surfaces entering or leaving the wake.

Condition I of figure 29 represents straight wings and those swept wings on the stable side of the stability boundary of figure 12. Case II of figure 29 is the typical condition encountered with swept wings, and the unstable break in pitching moment may occur at or prior to maximum lift, depending on the combination of sweep and aspect ratio employed. The experimental data available indicated (see fig. 28) that a tail located so as to emerge from the wake in the high-lift range will provide the greatest improvement in the nonlinear pitching-moment characteristics of the wing-fuselage combination. In general, it is hardly to be expected that a tail position can be found such that the nonlinearities of the tail will exactly compensate for the nonlinearities of the wing-fuselage combination. In this regard, air-stream surveys of the downwash and wake characteristics are extemely useful in locating the tail position at which the maximum improvement in the nonlinearities of the wing-fuselage combination can be obtained. For example, air-stream surveys were utilized in reference 33 to show that an inverted vee tail could be used to obtain linear pitching-moment characteristics for a wing-fuselage-tail combination in which the wing had $\Lambda_{c/4}=40°$, an aspect ratio of 4.0, and a taper ratio of 0.625.

In many sweptback-wing cases, the degree of instability is so great that even if the full lift capabilities of the tail could be used, an undesirable amount of instability would remain. Also, if nearly the full lift capabilities of the tail are employed in overcoming the undesirable pitching moment characteristics of the wing-fuselage combination the problem of adequate control becomes paramount. These two conditions necessitate the use of stall-control devices on sweptback wings. When such devices are effective in correcting the deficiencies of the wing-fuselage combination, the use of the maximum effectiveness of the horizontal tail may result in a complete configuration that has such a large degree of static margin as to be undesirable (case III, fig. 29). Because of configurations such as these an optimum tail location cannot be defined without attaching numerous qualifying statements, for it is quite obvious that the use of stall-control devices reduces the tail requirements for satisfactory stability and hence allows a wide range of useful tail locations.

LIFT

PLAIN WING

LIFT-CURVE SLOPE

There are available at present a number of rapid methods for predicting the lift-curve slopes of swept wings (refs. 11, 76, 83, and 84) which do not require extensive calculations of the load distribution in order to obtain the required parameters. Figure 30 has been prepared to show the relationship between the various methods when they are applied to the same set of wings. Considerable scatter around the line of perfect correlation exists, except perhaps for the method of reference 11. The amount of data presented does not suffice, however, to indicate a definite conclusion.

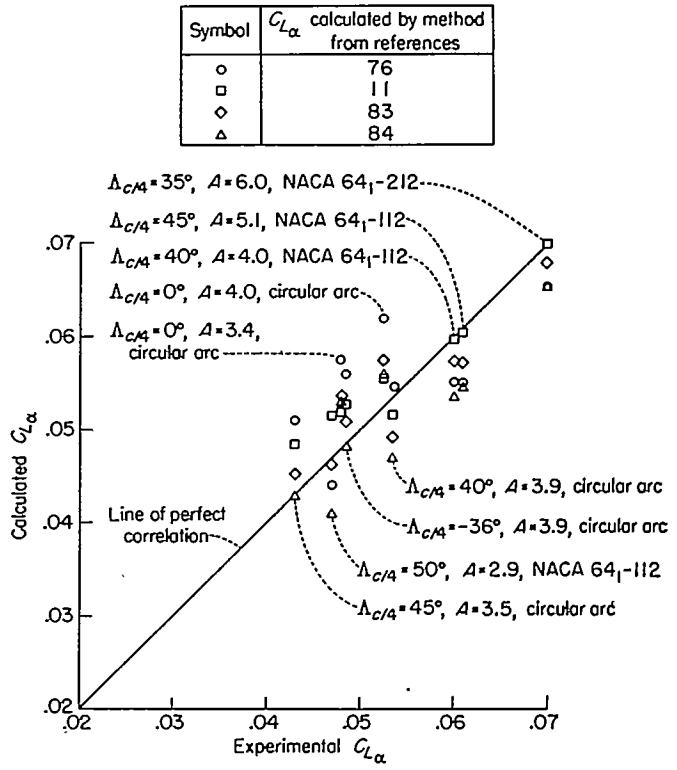

FIGURE 30.—Comparisons of the experimental lift-curve slopes for several wings with those calculated by several methods available for rapidly making such estimates.

The methods available for calculating the span-load distributions of sweptback wings (refs. 69 and 127 to 129) provide values of lift-curve slopes from induced angle-of-attack distributions that have been more rigorously obtained than in the preceding rapid methods. The simplest method of reference 127 has been used to provide the tabulated results presented in reference 76. Although all the methods effectively converge below aspect ratio of 3.0, above this value of aspect ratio the differences among the solutions obtained by the different methods become progressively greater. It is argued that the differences arise to a large extent from the manner in which the plan-form discontinuity at the plane of symmetry is handled in the calculations. Reference 69 proposes means for the special handling of the root discontinuity; however, experimental verification is not yet available. Calculations have been made and compared with experimental data for a wing of aspect ratio 8 and $\Lambda_{c/4}=45°$ and these results indicate that the special handling of the root discontinuity is of minor significance (ref. 130); however, it is necessary to point out that the root discontinuity may be significant for wings of lower aspect ratio. In this particular comparison (ref. 130) even those methods which most closely predicted the load distributions underestimated the experimental lift-curve slope. The reason advanced for this underprediction, however, was that the effect of wing thickness on the section lift-curve slope had not been accounted for rather than that the method of calculation was inadequate.

MAXIMUM LIFT

Simple sweep theory (ref. 3) would indicate that the lift

coefficient for separation, and hence the maximum lift coefficient of an infinite wing, will vary approximately as $\cos^2\Lambda$. This simple rule, as it is generally known, has not been found to be consistent with the experimental maximum lift coefficients of finite-span wings (ref. 131). The maximum lift coefficient is not only a function of sweep but, as will be shown in the following discussion, it is also dependent on the type of flow separation involved. As shown in figure 5, the type of flow separation is in turn dependent on the sweep angle, the leading-edge radius, and the Reynolds number.

Type of flow separation.—The manner in which flow separation may occur on sweptback wings has been previously discussed under the section on "Flow Considerations" and was shown to exert a controlling influence on the longitudinal stability characteristics. As in the case of the longitudinal stability characteristics, the type of flow separation that prevails also plays a significant role in the maximum lift characteristics. Hence, any attempt to establish an empirical rule to predict the maximum lift coefficient that is based on a correlation of experimental data must necessarily take into account the type of flow separation. Figure 31 has been prepared to show the variations of $\frac{C_{L_{max}}}{(C_{L_{max}})_{\Lambda=0}}$ with sweep angle for the cases of wings with and without leading-edge separation. In the case of trailing-edge separation (no leading-edge vortex present) there is a reduction in maximum lift coefficient throughout the sweep range; however, the reduction is somewhat less than that predicted by the $\cos^2\Lambda$ curve. This variance with simple sweep theory has been explained by the phenomena which occur at the tips and at the plane of symmetry on a finite-span wing. Experimental investigations on swept wings (for example, ref. 70) have shown that the root sections do not exhibit leading-edge pressure peaks. In addition, the spanwise pressure gradients are such as to cause an outward drain of the boundary layer from the root sections. The combined influence of these two effects is such as to make the root sections of swept wings highly resistant to flow separation and therefore capable of developing local lift coefficients of such large magnitude as to more than compensate for the lift losses that occur when the tip sections of the wing stall. The high lift potential of the root sections combined with the secondary rise in lift of the tip sections that often occurs after they have initially experienced flow separation generally allows the sweptback wing to experience a maximum lift coefficient in excess of the value to be expected on the basis of simple sweep theory. The upper curve in figure 31 applies to wings having circular-arc airfoil sections. Wings of this section represent an extreme case of leading-edge vortex flow and are quite unaffected by Reynolds number variations up to approximately 10×10^6. The appreciable increases in maximum lift coefficient with an increase in sweep angle indicate that the strength of the vortex is increased by an increase in sweep angle.

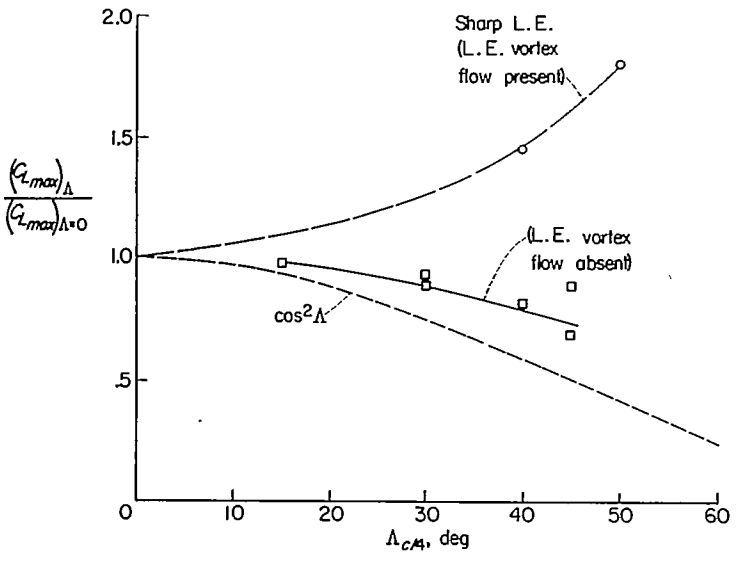

FIGURE 31.—Variations with sweepback angle of the ratio of maximum lift coefficient of the swept wing to the maximum lift coefficient of the equivalent unswept wing for several families of wings as defined by their leading-edge radii.

The experimental curves shown in figure 31 define the band in which the maximum lift coefficient of any particular wing may fall. Experimental data were available to determine the maximum lift at zero sweep for the sharp-leading-edge airfoils, but estimates in the case of the round-leading-edge airfoils had to be used. It is recognized, of course, that at a given Reynolds number any particular airfoil section may not develop leading-edge vortex flow until moderate angles of sweep are reached; hence, the variation of maximum lift coefficient with sweep angle for such a wing may follow the lower curve and then gradually bend upward and approach the upper curve.

The ratios shown in figure 31 do not in themselves completely illustrate the effects of sweep (as defined by flow separation) on the maximum lift coefficient. An attempt was made in figure 32 to collect the values of maximum lift

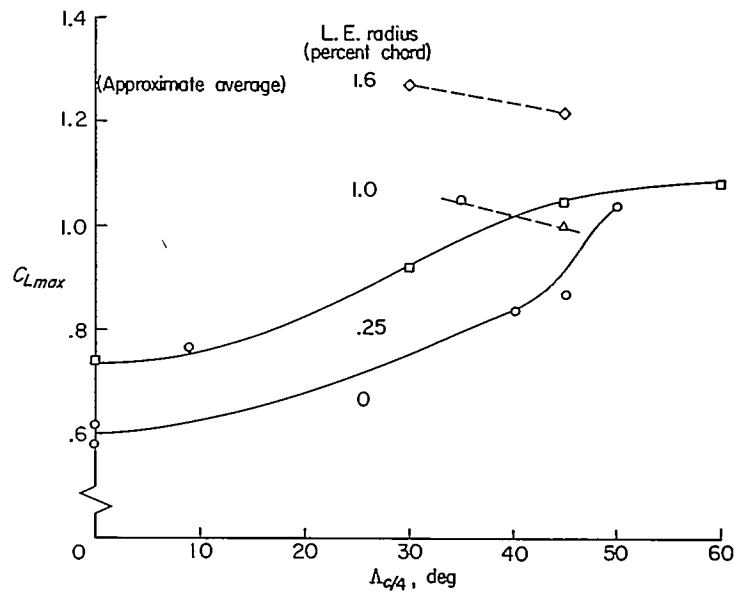

Symbol	Airfoil	Range of aspect ratio	Ref.
○	Circular-arc	2.8 to 4.0	21, 22, 23, 37, 47, 54
□	NACA 65A006	4.0	14
⌂	NACA 65_1A012	10.0	26
△	NACA 63_1A012	8.0	39
◇	NACA 0015 root NACA 23009 tip	3.6 to 4.8	17

FIGURE 32.—Variations of maximum lift coefficient with sweepback angle for several families of uncambered wings as defined by their leading-edge radii.

coefficient that have been obtained on uncambered and untwisted wings. As can be seen, there is a scarcity of data for wing thicknesses much in excess of 6 percent. Actually, most sweptback wings on which data are available have incorporated various degrees of camber and would not, if presented on this figure, correlate. At best, figure 32 illustrates that, although the ratios of maximum lift coefficient of figure 31 are diverging with increasing sweep angle, the corresponding absolute values are converging.

Influence of camber.—Although it was found when figure 32 was prepared that the available maximum-lift-coefficient data were, in most cases, obtained with wings incorporating airfoil sections of some degree of camber, very little information was found which could be used to isolate the effects of camber on the maximum lift of sweptback wings.

Figure 33 has been prepared to present data on wings with either camber or twist or wings with both camber and twist, as well as comparable data on wings either uncambered or untwisted or both uncambered and untwisted. It is significant that camber measurably improved the maximum lift coefficient over that of the comparable uncambered wings. Results presented in reference 26 have indicated that the improvements due to camber on the $\Lambda_{c/4}=35°$, $A=5.14$ and 10.07 wings can be estimated from two-dimensional data.

Reynolds number and Mach number effects.—An important consideration in any discussion of maximum lift coefficients on straight wings (see, for example, ref. 132) is the interrelated effects of Mach number (as low as 0.15) and Reynolds number on maximum lift coefficients at very low speeds. Methods for the quantitative prediction of these interrelated effects have not been developed so that data such as that presented in reference 132 can serve only as a guide in estimating the maximum lift coefficient of straight wings. As far as sweptback wings are concerned, the literature is very meager, even qualitatively. In figure 33 are given two values of maximum lift coefficient for the $\Lambda_{c/4}=35°$, $A=10$ wing incorporating NACA 65_1A012 airfoil sections at a Reynolds number of 6.0×10^6. The Mach numbers were 0.14 and 0.25 for the higher and lower values of maximum lift coefficient, respectively. The difference illustrates that, although simple sweep theory indicates a reduction in the local Mach numbers at the leading edge and thus minimizes the Mach number effect shown to exist at low speeds on straight wings, significant differences in the experimental value of maximum lift coefficient can be obtained when the relationships of Mach number with Reynolds number are changed, as would result from a change in the wing size or the flight altitude. Thus, the data presented in figure 33 for the first three wings were obtained at a constant Mach number and therefore show the effects of Reynolds number at this value of Mach number. For any other value of Mach number or for the condition where the Mach number increases as the Reynolds number is increased, the comparison between the cambered and uncambered wings may be different. It appears, therefore, that any correlation of the maximum lift coefficient of swept wings that is founded only on the basis of comparable Reynolds number may be fortuitous.

Effect of aspect ratio.—The effect of aspect ratio, as determined from tests of a family of wings having $\Lambda_{c/4}=45°$ and 6-percent-thick airfoil sections and three families of wings of $\Lambda_{c/4}=35°$ and 12-percent-thick airfoil sections, are shown in figure 34. The 6-percent-thick wings are representative of those wings that experience leading-edge separation. Over the range covered, the effects of variation in aspect ratio are small, as would be expected from knowledge of straight-wing characteristics. It is interesting, however, that the rate of change of maximum lift coefficient with aspect ratio is opposite in sign to that for straight wings. Presumably, with increasing aspect ratio, it approaches the value for the infinite swept wing, which is of the order of $\cos^2\Lambda$ times the two-dimensional value. (The cosine rule is theoretically exact only if the phenomenon considered involves purely laminar flow, and it is not exact when applied to maximum lift, which is extensively involved with turbulent boundary-layer flows.)

INFLECTION OR USABLE LIFT COEFFICIENT

The terms "inflection" or "usable" lift coefficient have been commonly used to define the lift coefficient of sweptback wings at which large undesirable shifts in aerodynamic center occur. Although the terms inflection C_L and usable C_L were previously introduced as synonymous, it is desirable to put slightly different interpretations on the two terms. The term "inflection lift coefficient" has been used in the present discussion to define the lift coefficient at which there is a break in the pitching-moment curve without any consideration being given to the uncontrollability or undesirability of the shift, whereas "usable lift" connotes a shift in aerodynamic center which could cause serious control design problems. In view of the fact that a horizontal tail can overcome a considerable amount of instability contributed by the wing-fuselage combination, the term usable lift coefficient in the present report is still somewhat arbitrary. This lift coefficient is probably of more significance with regard to the maximum flight lift coefficient than the absolute value of the maximum lift coefficient in that it represents the lift coefficient beyond which stall control is required.

Available data have been compiled and used to indicate the variations of the ratio of inflection lift to maximum lift coefficient with sweep angle for various aspect ratios (fig. 35). It has again been necessary to differentiate between wings which exhibit trailing-edge separation and wings which exhibit leading-edge separation (leading-edge vortex flow present). The data presented in figure 35 (a) for wings having well-rounded leading edges (above vortex formation line of fig. 5) appeared to arrange themselves systematically. In figure 35 (b), however, some difficulty was encountered in systematizing the data for wings having sharp leading edges (wings incorporating circular-arc airfoils for the most part). It was found that on low-aspect-ratio wings subject to leading-edge vortex flow (for example, $A=2$, $\Lambda_{c/4}=45°$, fig. 35 (b)), a stable shift in aerodynamic center occurred at a relatively low value of lift coefficient which remained until the maximum lift coefficient was reached. For wings of somewhat greater aspect ratio (for example, $A=4$, $\Lambda_{c/4}=45°$, fig. 35 (b)), the stable shift occurred at higher values of lift coefficient and was more pronounced than that observed at the lower aspect ratios. The stable shift also was closely followed by a pronounced unstable shift in aerodynamic center.

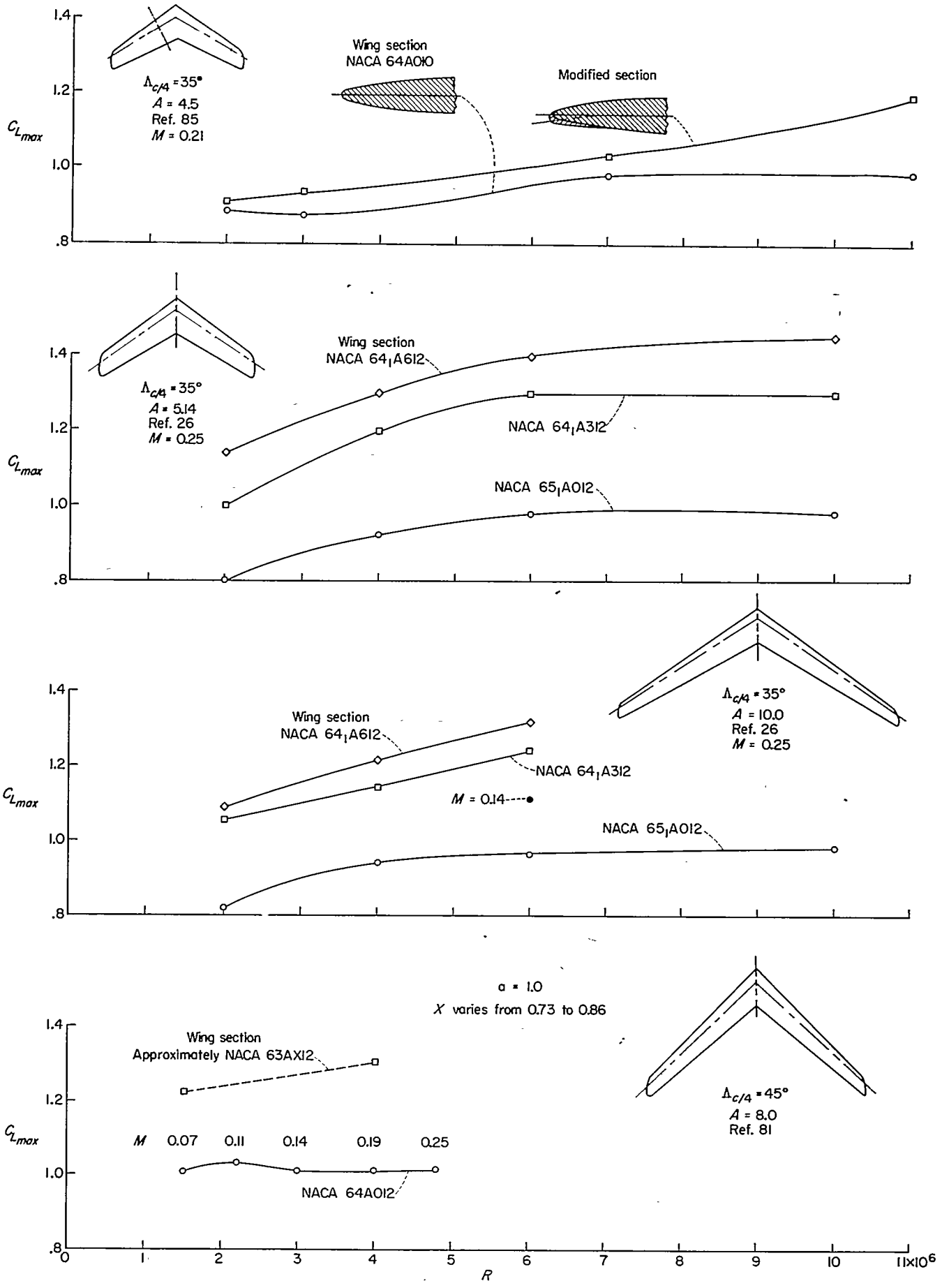

FIGURE 33.—Variation of maximum lift coefficient with Reynolds number for several sweptback wings with various amounts of camber. Effect of Mach number on the low-speed maximum lift coefficient is indicated for one wing.

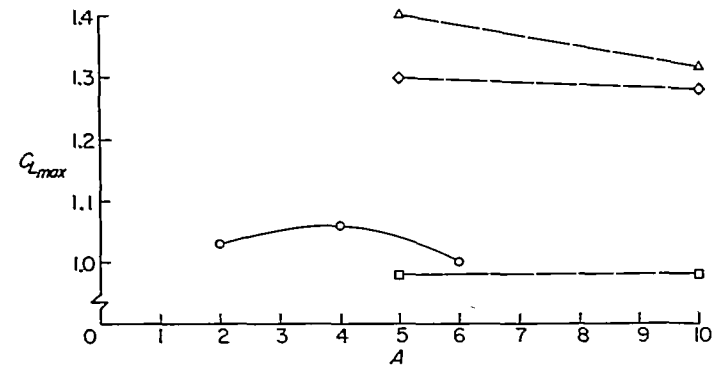

Symbol	$\Lambda_{c/4}$, deg	Airfoil section	λ	Ref.
□	35	NACA 65_1A012	0.500 to 0.713	26
◇	35	NACA 64_1A312	.500 to .713	26
△	35	NACA 64_1A612	.500 to .713	26
○	45	NACA 65A006	.600	14

FIGURE 34.—Variation of maximum lift coefficient with aspect ratio for several sweptback wings. Airfoil sections listed are parallel to the plane of symmetry.

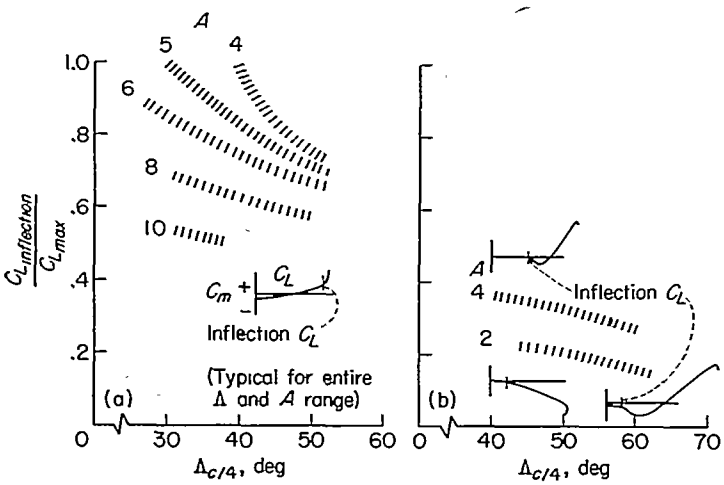

A	$\Lambda_{c/4}$, deg	Ref.
3.6	45	17
4.0	40	28
4.8	30	17
5.0	45	43
5.1	45	45
6.0	35	27
8.0	45	70
10.0	35	26

(a) Tip separation.

A	$\Lambda_{c/4}$, deg	Ref.
2.0	45	14
2.8	50	54
2.5	60	86
2.0	60	87
4.0	40	36
3.5	45	47
4.0	45	14
3.5	60	59
4.0	60	14

(b) Leading-edge separation on wings having sharp leading edges.

FIGURE 35.—Variation of the ratio of inflection lift coefficient to maximum lift coefficient with sweepback angle for wings which exhibit either trailing-edge separation or leading-edge separation.

The preceding discussion has considered representative moment curves in the immediate vicinity of 45° of sweep; and as both the vortex strength and the relative area ratios (previously discussed in section entitled "Longitudinal Stability") change with increasing sweep angle, the discussion is not representative for wings having sweepback angles greater or less than 45°. A $\Lambda_{c/4}=60°$ wing of aspect ratio 2.0 (ref. 87) therefore exhibits an unstable shift in aerodynamic center at a lift coefficient between the inflection and maximum lift coefficients that was not previously noted for a $\Lambda_{c/4}=45°$ wing of the same aspect ratio.

The data presented in figure 35 (a) represent not only the inflection lift coefficient but also the usable lift coefficient. The same cannot be said for figure 35 (b). The stable inflection obtained for an aspect ratio 2.0 wing of $\Lambda_{c/4}=45°$ cannot be considered as seriously limiting the usable range of lift coefficient at all. At $\Lambda_{c/4}=60°$ and aspect ratio 2.0, the stable inflection is again tolerable, but, as previously mentioned, an unstable shift occurs at a somewhat higher value of lift coefficient, which is of such a magnitude as to be very undesirable, and hence defines a usable-lift-coefficient range. It is quite interesting that the ratio of this lift coefficient to the maximum lift coefficient is approximately the same as the inflection lift ratio for the aspect-ratio-4.0 wing having the same sweep angle. The inflection lift coefficient for the aspect-ratio-4.0 wing is also characterized by a stable shift in aerodynamic center but, in this case, is of sufficient magnitude (say in excess of an 8-percent shift) to define also the usable-lift-coefficient range. For the case considered, the usable-lift-coefficient range is the same for wings of aspect ratio 2.0 and aspect ratio 4.0, although it is not defined by the inflection lift coefficient in both cases.

The curves presented in figure 35 were obtained with wings having taper ratios somewhat greater than 0.5. More data would be needed to make a similar analysis for delta or pointed wings. In general, delta wings that do not experience leading-edge vortex flow are subject to a gradual rearward shift in aerodynamic center that adds up to a very large shift between zero and maximum lift. The gradual nature of this rearward movement precludes the use of the term "inflection lift coefficient." When the leading edge is sharp and the consequent leading-edge vortex forms, the rearward movement of the aerodynamic center is arrested in the vicinity of a maximum lift coefficient of 0.5, and a zero or slightly forward shift in aerodynamic center is obtained at a maximum lift coefficient between 0.5 and 1.0. The point at which the rearward movement is arrested can be considered as an inflection lift coefficient. As the aspect ratio for other wings having zero taper ratio approaches the stability boundary defined for such wings in figure 12, the forward shift in aerodynamic center becomes more pronounced but still occurs in the vicinity of a maximum lift coefficient of 0.5. It was found possible to obtain, by a process of interpolation in figures 34 and 35, the inflection lift coefficients of those wings having round-nose airfoils and moderate taper ratios but still subject to the formation of the leading-edge vortex flow. In order to estimate the inflection lift coefficient of such wings, a first-order approximation can be made as follows. Estimate the percentage of the radius defined by the boundary of figure 5 and then use this percentage to interpolate between parts (a) and (b) of figure 35. For example, the $\Lambda_{c/4}=50°$ wing of reference 44 incorporates NACA 64_1-112 airfoil sections perpendicular to the 0.272-chord line and is one of several for which such estimates were made. From figure 5 the effective leading-edge radius can be estimated as approximately 80 percent of the boundary radius. For the aspect ratio of 2.9, the ratios

of inflection lift coefficient for the sharp-nose and round-nose conditions are estimated to be 0.25 and 0.80, respectively (fig. 35). If 80 percent of the difference between 0.25 and 0.80 is added to the value of 0.25, the resulting ratio of inflection lift coefficient to maximum lift coefficient is 0.69. The experimental value as determined from reference 30 is 0.67. The excellent agreement obtained is typical for the several cases tried; however, additional data are considered necessary for a more complete quantitative treatment. It must be emphasized that the boundary presented in figure 5 and the curves presented in figure 35 (a) are subject to Reynolds number effects which must be considered in interpreting the present results. The analysis presented, however, does have general application at both lower and higher values of Reynolds number. For example, the boundary of figure 5 would be displaced upward with a reduction in Reynolds number and hence, in the case of the $\Lambda_{c/4}=50°$ wing, its percentage of the boundary radius would be reduced. Also, somewhat lower values would be obtained in figure 35 (a) so that the combination of the two changes would indicate a lower value of the ratio of inflection lift to maximum lift coefficient. Actually, the experimental data presented in reference 52 show such a reduction.

The data so far presented and discussed concerning the inflection lift on swept wings were obtained on uncambered and untwisted wings. An empirical study of cambered and twisted wings would, however, require considerably more data than are presently available. As previously discussed, there are indications that the effects due to camber are a function of sweep and can be estimated from two-dimensional data (ref. 26). If such is the case, the effects of camber may possibly be additive to the results presented for the uncambered wings.

Another approach to the general problem of predicting the inflection-lift coefficient of swept wings would be to develop a procedure for using two-dimensional airfoil data to predict the three-dimensional characteristics of the wing. Reference 131 presents a first attempt at utilizing two-dimensional data to predict the inflection lift on swept wings. The comparisons presented in reference 131 show almost a consistent underprediction of the pitching-moment breaks obtained experimentally in three-dimensional flow.

HIGH-LIFT AND STALL-CONTROL DEVICES

An inspection of the data contained in the compiled tables shows that a considerable number of rather detailed investigations which involved the use of high-lift and stall-control devices have been reported. The data have not been systematic enough to provide a basis for generalized design charts. Such a conclusion may appear to be restating the same one brought forward in reference 133 in 1947. Actually, however, these specific investigations, which were unavailable at the time reference 133 was written, now permit qualitative generalizations which can be judiciously used in design work.

LINEAR LIFT RANGE

Experience has shown that through the linear lift range, stall-control devices do not greatly influence the lift increments produced by a trailing-edge high-lift device. In an evaluation of the linear-lift effectiveness of trailing-edge flaps therefore data obtained both with and without leading-edge devices can be used.

Figure 36 has been prepared to show the variations of linear lift effectiveness with sweep angle from the systematic data that are available for wings equipped with split flaps. The linear lift effectiveness of the half-span split flaps decreases markedly as the sweep angle is increased. In the case of the wings that exhibit either leading-edge or trailing-edge separation, the linear lift increment is closely predicted by applying simple sweep concepts (fig. 36). In order to indicate the influence sweep has on the linear lift increment when the flap span is other than 0.5 span or the type is a double-slotted flap, the data of references 27 and 48 have been presented in figure 37. Both of the wings used for illustration in figure 37 exhibited trailing-edge separation. The comparison between the experimental and calculated curves indicates that in the case of split flaps the agreement is good, at least up to flap spans of 0.5 span. In either of the examples, however, the linear lift increments obtained experimentally with double-slotted flaps exceed the calculated values for any span of

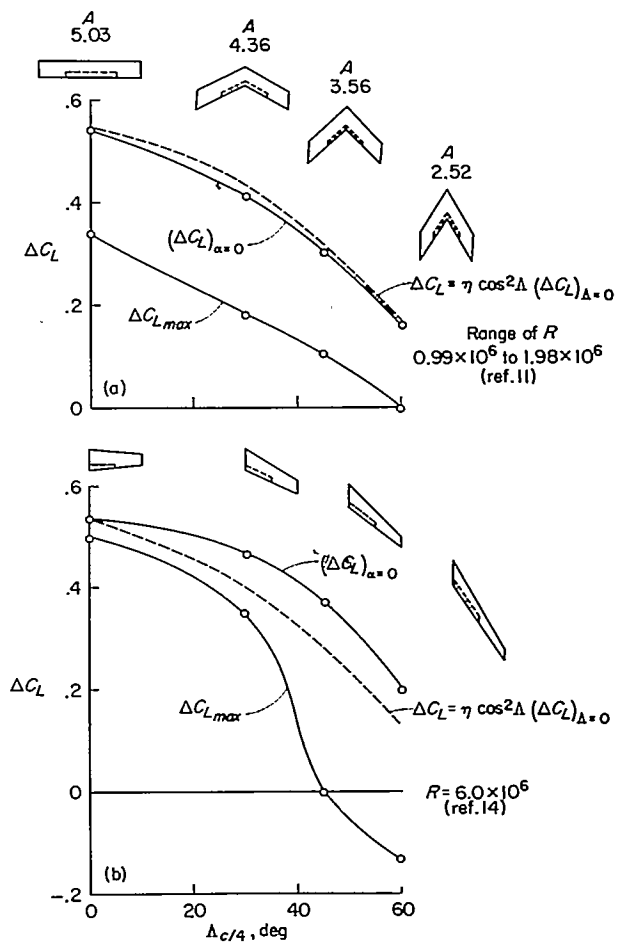

(a) Wings of varying aspect ratio but having a constant taper ratio of 1.0 and NACA 23012 airfoil sections, which were perpendicular to the leading edge.

(b) Wings have an aspect ratio of 4, a taper ratio of 0.6, and NACA 65A006 airfoil sections parallel to the plane of symmetry.

FIGURE 36.—Variation with sweep angle of maximum lift increment and lift increment at an angle of attack of 0° due to semispan split flaps for two families of wings. Flaps deflected 60°.

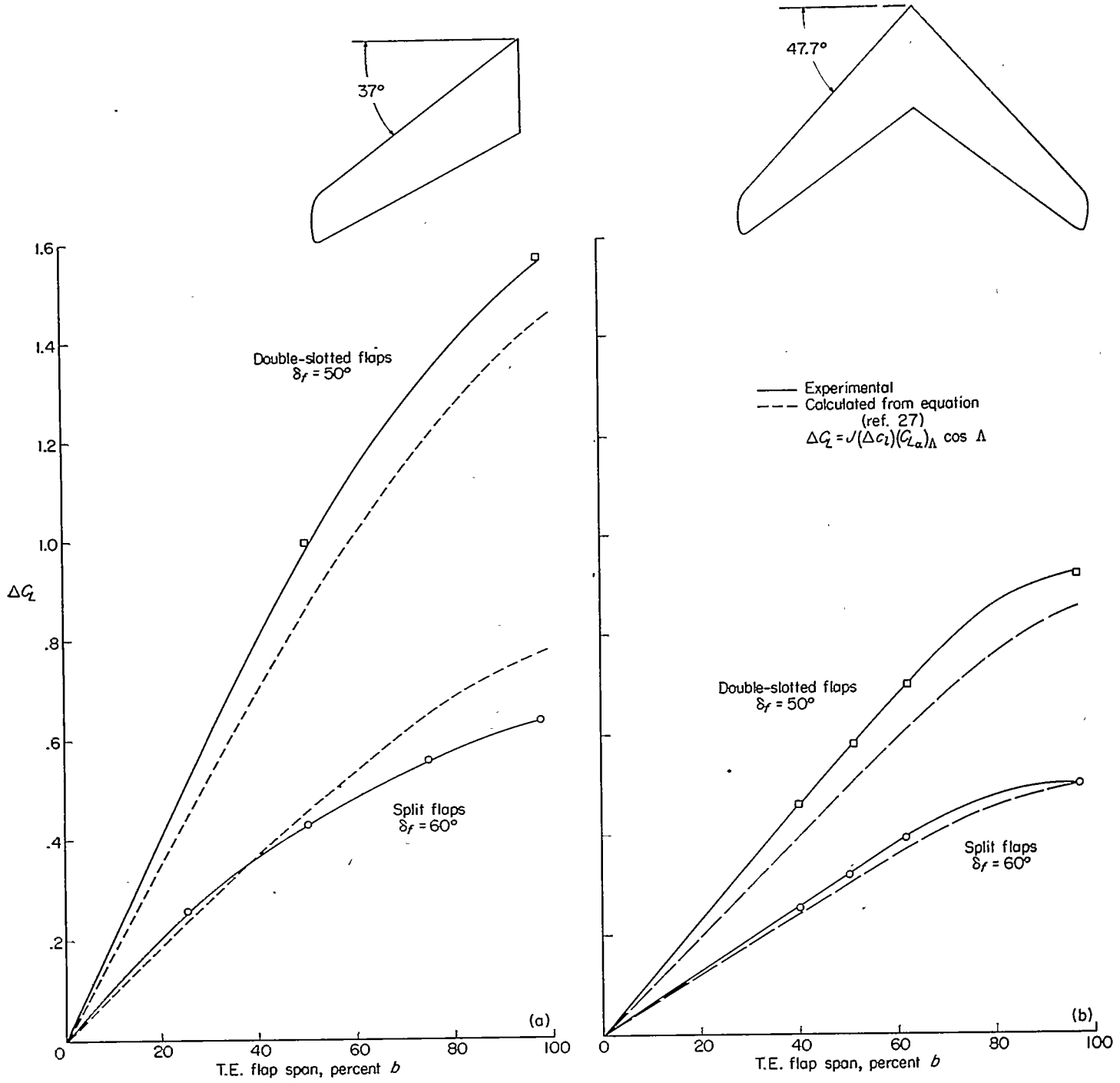

(a) $\Lambda_{c/4}=35°$, $A=6.0$, $\lambda=0.5$, NACA 64_1-212 airfoil section. $R=6.8\times10^6$. (Ref. 27.)

(b) $\Lambda_{c/4}=45°$, $A=5.1$, $\lambda=0.4$, NACA 64-210 airfoil section. $R=6.0\times10^6$. (Ref. 48.)

FIGURE 37.—Comparison of experimental with calculated lift increment at an angle of attack of 0° due to double-slotted and split flaps on two sweptback wings.

flap. It should be pointed out that the calculated lift increments due to flaps can be readily obtained by the method of reference 134 which has become available since the publication of references 27 and 48.

In any case, the loss in linear lift effectiveness in the moderate to high sweep-angle range is rather severe, and it is of interest to consider the effectiveness of area-increasing flaps. The data of references 13, 32, 39, 49, 54, and 60 indicate that increases in linear lift effectiveness approximately of the same order of magnitude as the percent of area increase can be obtained with partial-span extended split flaps (Zap). The comparison made in reference 49 between an extended flap having a rectangular plan form and one of the same area but having a triangular plan form indicates that the increased effectiveness of the extended flaps is somewhat independent of the manner in which the flap area is added.

Figure 38 has been prepared to summarize the available data on the lift effectiveness of trailing-edge flaps measured at an angle of attack of 0°. The data are presented for the

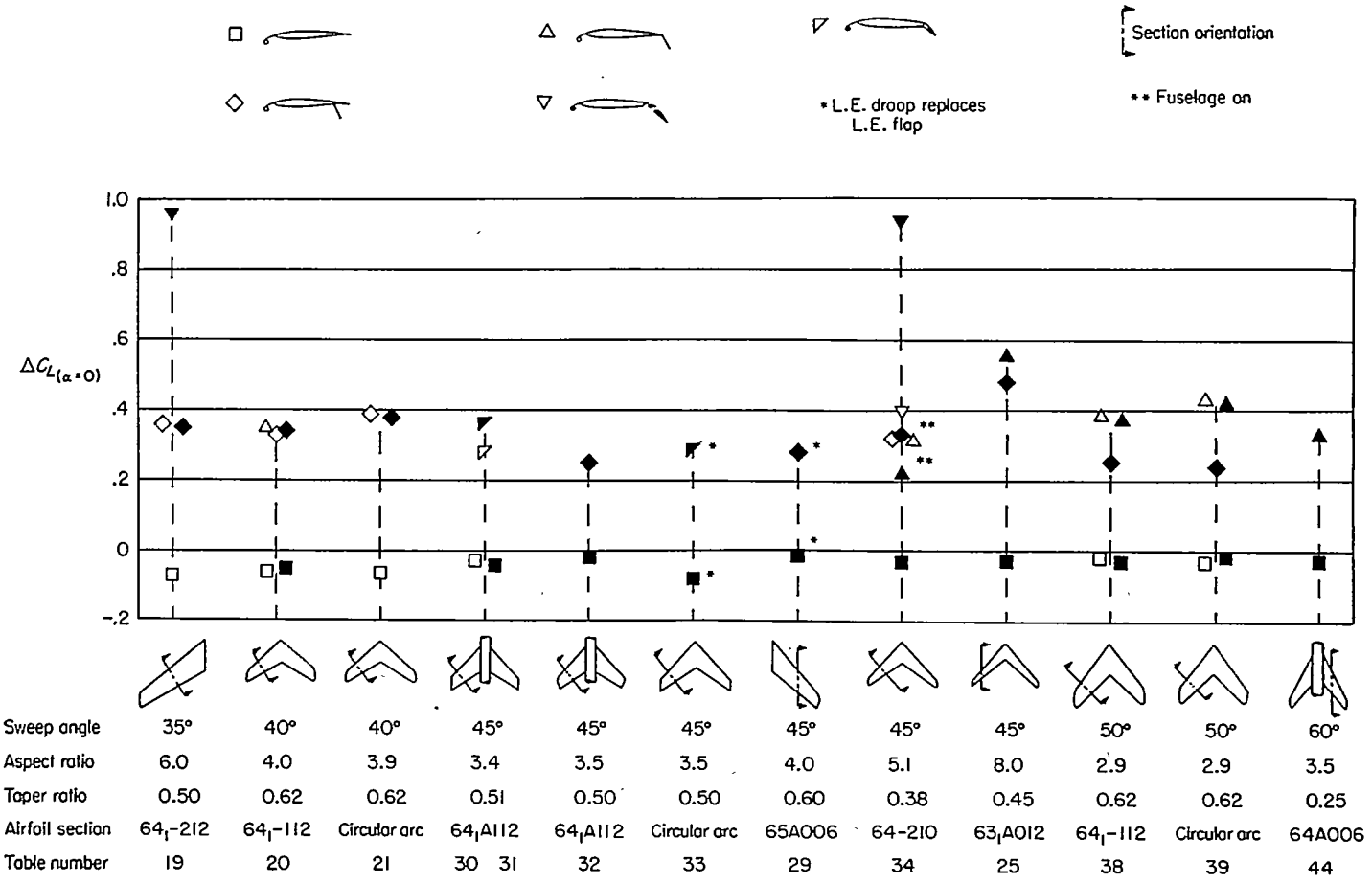

FIGURE 38.—Summary chart of lift increments at an angle of attack of 0° due to various types of trailing-edge flaps. (Solid symbols correspond to flap spans which produce unsatisfactory pitching-moment characteristics; open symbols correspond to flap spans which produce satisfactory pitching-moment characteristics.)

configurations which provided acceptable pitching-moment characteristics through the lift range and also for the configurations which produced the greatest increments in maximum lift coefficient but did not possess acceptable pitching-moment characteristics through the lift range. The flap spans were greater for the configurations possessing undesirable pitching-moment characteristics but they are not actually full-span devices. Where comparisons are available, it appears that the lift effectiveness at an angle of attack of 0° is not appreciably increased by sacrificing acceptable pitching-moment characteristics through the lift range.

MAXIMUM LIFT

Trailing-edge flaps.—The influence of sweep on the maximum lift effectiveness of trailing-edge flaps is illustrated in figure 36. The data were obtained on two families of wings equipped with partial-span split flaps deflected 60°. It can be seen that at moderate sweep angles the flaps on the wings incorporating NACA 65A006 airfoil sections (pronounced leading-edge vortex flow) cause a negative increment of maximum lift coefficient. An attempt was made to analyze the data presented in figure 36 and other available data, either in terms of the maximum lift increment at $\Lambda_{c/4}=0°$ or the linear lift increment previously discussed. No clear correlation could be found. For the two examples presented (fig. 36) the difference between the linear and maximum-lift increments for $\Lambda_{c/4}=0°$ is approximately constant through the sweep range for the wings having NACA 230-series airfoil sections, whereas the corresponding difference is materially increased with an increase in sweep angle for the wings of NACA 65-series airfoil sections.

The influence of a variation in flap span on the increment of maximum lift coefficient for two sweptback wings having both split and double-slotted flaps is shown in figure 39. The results shown are representative, although the reduced effectiveness of the full-span split flaps on the $\Lambda_{c/4}=35°$ wing is quite extreme.

The data available for sweptback wings equipped with slotted or extended flaps seem to indicate that these types of flaps maintain at maximum lift a superiority over split flaps of approximately the same magnitude previously indicated in the linear lift range.

An investigation (ref. 111) on $\Lambda_{LE}=47°$ wing-fuselage combination shows the increments of maximum lift coefficient contributed by a partial-span single-slotted flap to be relatively insensitive to precise flap slot geometry. If the increments, which are admittedly small, are compared, however, on a percentage basis, they are found to be as sensitive to flap position as in the case of two-dimensional flow.

Leading-edge stall-control devices.—Grouped under the heading of leading-edge stall-control devices are such things as leading-edge slats, extensible leading-edge flaps, droop-nose flaps, chord-extensions, and boundary-layer control. Although the primary purpose of these devices is to control

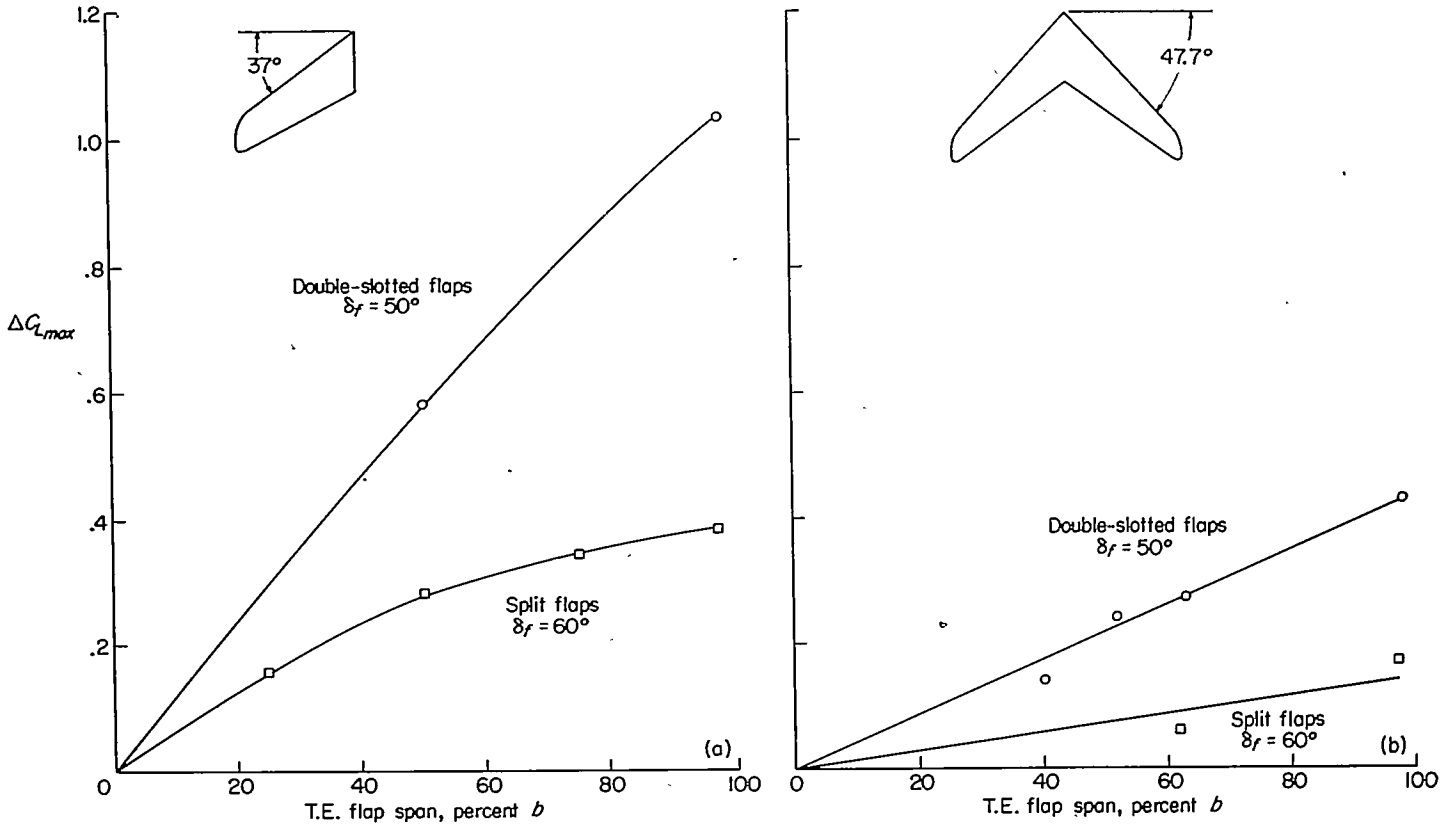

(a) $\Lambda_{c/4}=35°$, $A=6.0$, $\lambda=0.5$, NACA 64_1-212 airfoil section. $R=6.8\times10^6$. (Ref. 27.)

(b) $\Lambda_{c/4}=45°$, $A=5.1$, $\lambda=0.4$, NACA 64-210 airfoil section. $R=6.0\times10^6$. (Ref. 48.)

FIGURE 39.—Variation of increment in maximum lift coefficient with span of double-slotted and split flaps on two sweptback wings.

flow separation and hence to provide acceptable pitching-moment characteristics, it might also be expected that if flow separation were controlled, increases in maximum lift coefficient would be obtained. The gains in maximum lift coefficient obtained with the use of such devices are not large; however, in comparison to the effectiveness of trailing-edge split flaps on moderately to highly swept wings, they are significant.

It has been shown in reference 48 that the optimum span for an extensible leading-edge flap from stability considerations is essentially the optimum with regard to the effectiveness at maximum lift. Such a generalization is not, however, rigorously substantiated by the data of references 27 and 39. The data presented in reference 44 indicate further that the smallest-chord, smallest-span, extensible leading-edge flaps which will provide longitudinal stability over the entire lift range will also provide increases (small) in maximum lift coefficient of the same order of magnitude as those obtained with larger-chord and larger-span extensible leading-edge flaps.

Trailing-edge flaps in combination with leading-edge stall-control devices.—The individual effectiveness of both leading- and trailing-edge devices at maximum lift has been discussed. When these devices are used in combination, the increments of maximum lift coefficient are not additive except in a few isolated cases as can be seen from an inspection of the data presented in the tables.

Figure 40 has been prepared to show in a more graphic manner the incremental values of maximum lift coefficient that have been obtained through the use of both leading- and trailing-edge flaps on sweptback wings. Again as in figure 37, the configurations which possessed acceptable pitching-moment characteristics and those that did not but gave the greatest improvement in maximum lift coefficient have been included. It is interesting to note that the extended split flaps compare favorably with the double-slotted flaps for the several cases available.

DRAG

PLAIN WING

INDUCED DRAG

The changes in spanwise lift distribution attributable to sweep necessarily produce corresponding changes in the drag due to lift (induced drag). Inasmuch as experimental data are unavailable, recourse has been made to calculations in order to show the influence of sweep on the induced drag (fig. 41). The calculations were made by the Weissinger method in which 15 spanwise control points were used in preference to the more commonly used seven spanwise control points. (The loadings computed by the Weissinger method utilizing 15 spanwise control points which correspond to the drag values presented in fig. 41 are unpublished.) For wings having taper ratios of approximately 0.25, sweep has only a small effect on the induced drag for the aspect-ratio range covered. For taper ratios greater than 0.25, sweep has an adverse effect on the induced drag which is accentuated by an increase in either taper ratio or aspect ratio. For taper ratios less than 0.25, sweep has a beneficial effect on the induced drag.

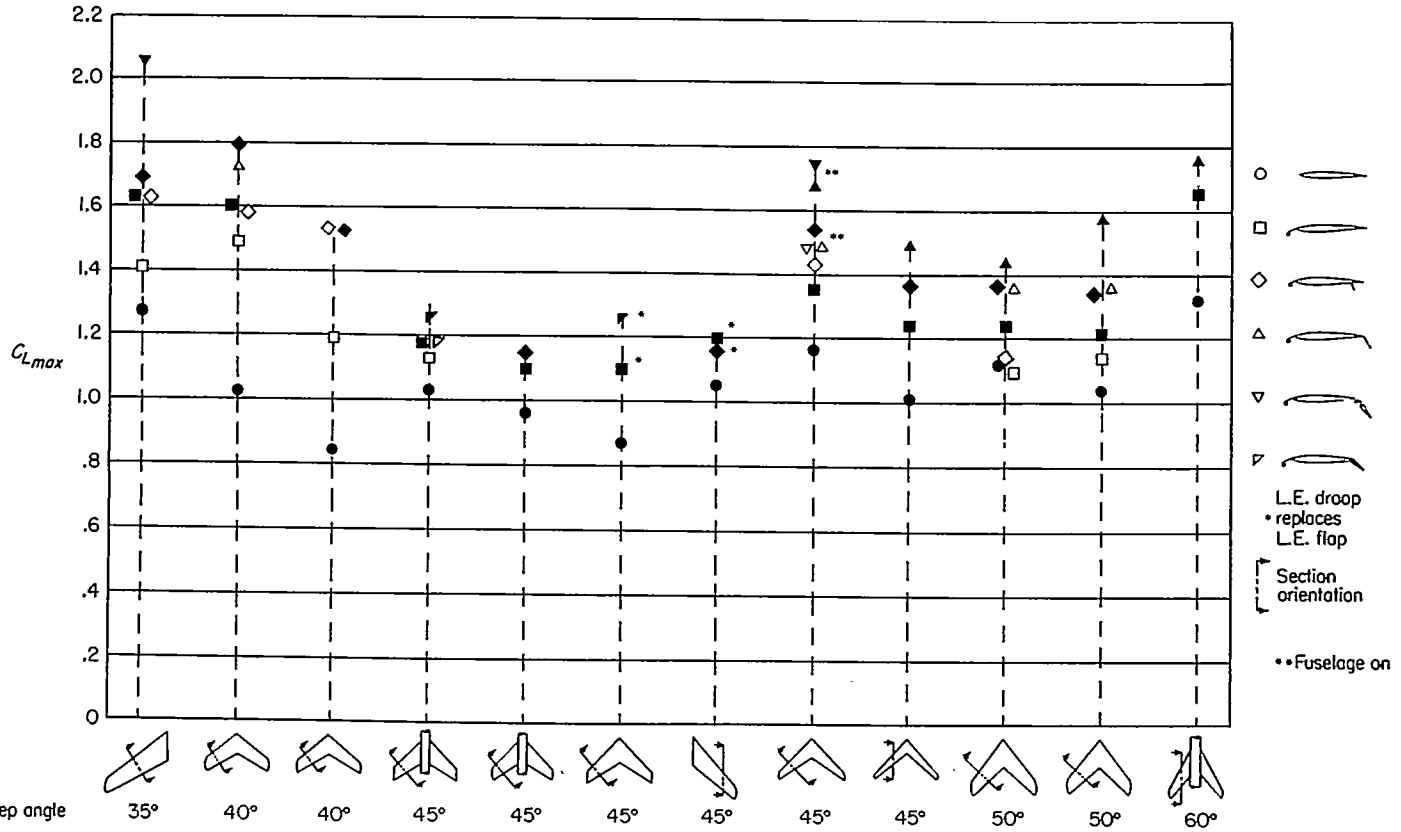

Sweep angle	35°	40°	40°	45°	45°	45°	45°	45°	45°	50°	50°	60°
Aspect ratio	6.0	4.0	3.9	3.4	3.5	3.5	4.0	5.1	8.0	2.9	2.9	3.5
Taper ratio	0.50	0.62	0.62	0.51	0.50	0.50	0.60	0.38	0.45	0.62	0.62	0.25
Airfoil section	64_1-212	64_1-112	Circular arc	64_1A112	64_1A112	Circular arc	65A006	64-210	63_1A012	64_1-112	Circular arc	64A006
Table number	19	20	21	30 31	32	33	29	34	25	38	39	44

FIGURE 40.—Summary chart of maximum lift coefficients obtained with various types of trailing-edge flaps. (Solid symbols correspond to flap spans which produce unsatisfactory pitching-moment characteristics; open symbols correspond to flap spans which produce satisfactory pitching-moment characteristics.)

PROFILE DRAG

The minimum drag data available from a systematic investigation of a family of wings having aspect ratios of 4.0, taper ratios of 0.6, and NACA 65A006 airfoil sections parallel to the plane of symmetry are presented in figure 42. The drag scale has been enlarged from that used in reference 14 in order to show more clearly the effects of sweep. This enlarged scale appears to be consistent with the accuracy of data obtained by semispan testing. As would be expected, these data indicate that sweep has a negligible influence on the minimum drag, although there is a slight increase indicated between 45° and 60° of sweep.

An indication of the effect of sweep on the variation of the profile drag with lift coefficient is given by the wake-drag measurements presented in reference 88. The results of reference 88 are presented in figure 43. It will be noted that the minimum wake drag is unaffected by sweep, as has previously been shown by the data of figure 42. There is, however, a measurably large increase in the wake drag for the swept airfoil as the lift is increased. In this particular comparison, it should be pointed out that the wing thickness and leading-edge radius of the airfoil section taken parallel to the air stream are considerably less for the swept wing than for the unswept wing. These changes in airfoil shape may have had a greater influence than the sweep in increasing the rate of increase in wake drag with lift coefficient for the swept case over that obtained in the unswept case.

With regard to camber, it can be shown from geometrical considerations that the design lift coefficient of a swept wing is considerably less than that corresponding to the camber of the sections normal to a swept reference line and is even less than that corresponding to the camber of the sections taken in the stream direction. Figure 44 has been prepared to show the decrease in lift coefficient for minimum profile drag when the panels of an unswept wing employing airfoil sections having a design lift coefficient of 0.2 are rotated such that the airfoil sections are alined perpendicular to the 0.286 chord line on the swept wing.

SPAN EFFICIENCY

The drag of a wing may be considered to be comprised of three parts: namely, the minimum profile drag, that part of the profile drag which varies with lift coefficient, and the induced drag. Various investigators have compiled and analyzed experimental data on straight wings for the purpose of deriving a generalized drag equation for use in performance calculations. In this country, the commonly applied drag equation in performance calculations contains Oswald's efficiency factor e and the equation is written

$$C_D=(C_{D_0})_{C_L=0}+\frac{C_L^2}{\pi Ae}$$

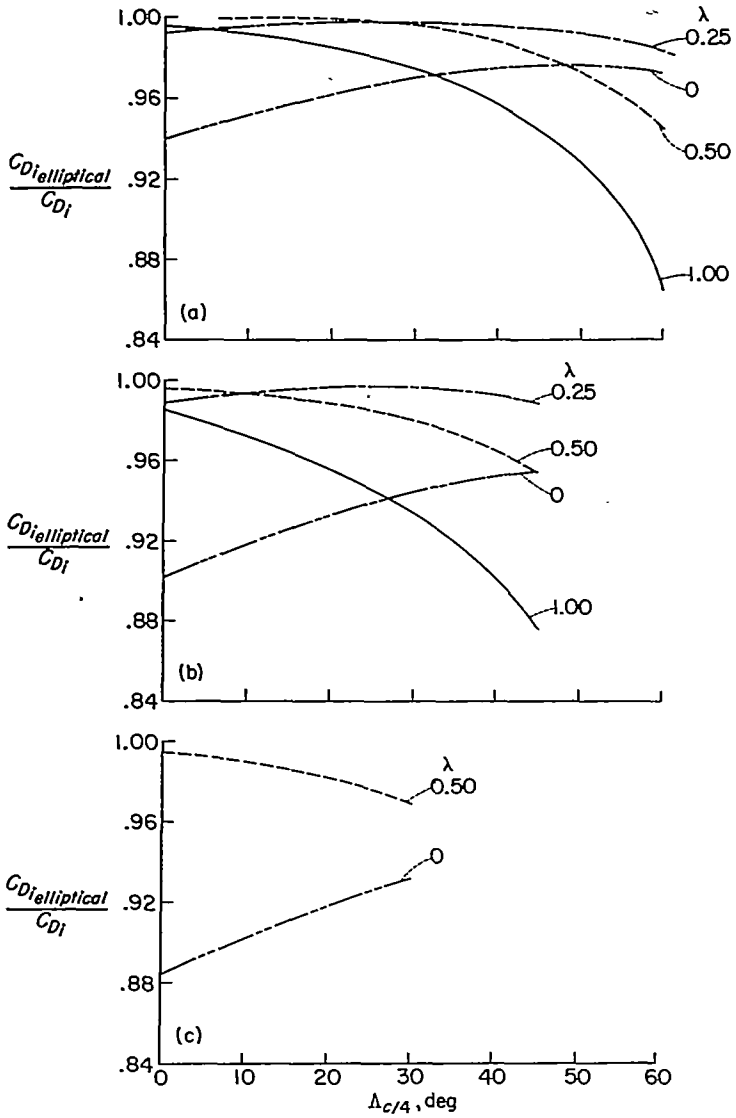

(a) $A=3.5$.
(b) $A=6.0$.
(c) $A=8.0$.

FIGURE 41.—Variations with sweep angle of the ratios of induced drag coefficient for elliptical loading to the calculated induced drag coefficient for wings of various aspect ratios and taper ratios. Calculations made by the Weissinger method using 15 points in the solution.

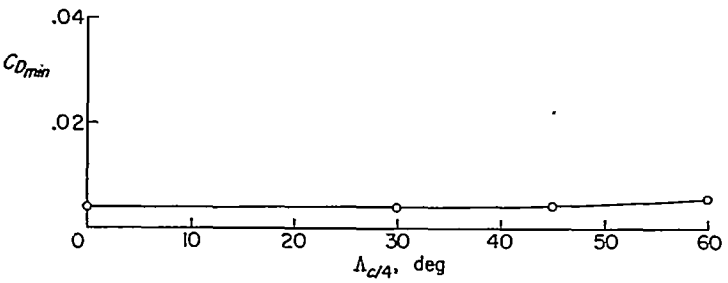

FIGURE 42.—Variation of the minimum drag coefficient with sweep angle for a family of wings having aspect ratios of 4, taper ratios of 0.6, and NACA 65A006 airfoil sections parallel to the plane of symmetry. (Data obtained from ref. 14.)

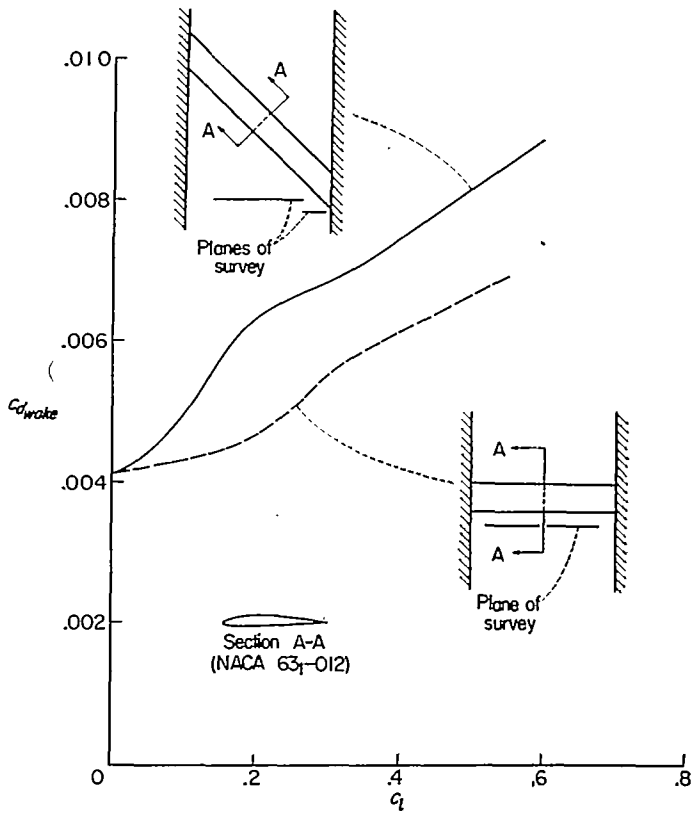

FIGURE 43.—Wake drag characteristics for a swept and unswept airfoil section. (Data obtained from ref. 88.)

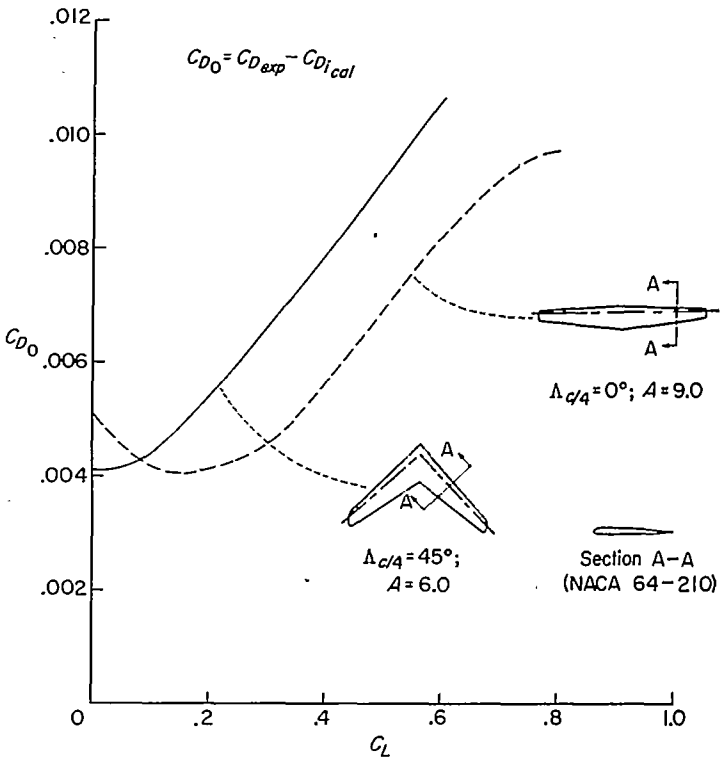

FIGURE 44.—Variations with lift coefficient of the profile drag coefficient for an unswept and sweptback wing.

It can be seen that the factor e is used to lump the variable part of the profile drag and the percent deviation of the induced drag from that of the elliptical wing into a single term. The literature includes attempted correlations of this factor with such parameters as aspect ratio and taper ratio (for example, ref. 135). More recently, attempts have been made to extend the correlations to include the effects of sweep (ref. 136). Unfortunately, the lift range where the parabolic drag variation is applicable is generally small and the scatter obtained in such correlations has been of such magnitude as to limit seriously the usefulness of the factor e. A cursory examination of the scatter seems to indicate that leading-edge radius, thickness, and thickness distribution are factors affecting e to the same degree as aspect ratio, taper ratio, and sweep angle.

In the event that sufficient similarities may be found between one of the wings in the present report and a particular design of interest, values of e and the lift coefficient to which they are applicable are presented in the following table:

Λ_{LE}, deg	$\Lambda_{c/4}$, deg	A	λ	Airfoil section	R	e	Up to C_L of
9.9	5	2.5	0.63	Modified double wedge	7.6×10^6	0.55	0.2
37.0	35	6.0	.50	NACA 64_1-112	6.8	.78	1.0
42.0	40	3.9	.63	Circular-arc	6.9	.37	.2
42.0	40	4.0	.63	NACA 64_1-112	6.8	.82	.8
47.7	45	6.0	.31	NACA 64—210	6.0	.83	.4
47.7	45	5.1	.38	NACA 64-210	6.0	.83	.3
46.3	45	8.0	.45	NACA 63_1A012	4.0	.68	.4
52.0	50	2.9	.63	NACA 64_1-112	6.8	.80	.6
52.0	50	2.9	.63	Circular-arc	6.8	.42	.4

Only drag data which could be reliably read have been used.

HIGH-LIFT AND STALL-CONTROL DEVICES

The drag increment attributable to trailing-edge flaps is, in general, reduced when sweep is incorporated in the wing. This fact is illustrated in figure 45, where the effective parasite drags of two types of trailing-edge flaps on a sweptback wing are compared with those obtained on an unswept wing. When a simple method is used to reduce the straight-wing data to that of the sweptback wing, the reduction due to sweep is approximately a function of the cosine squared of the sweep angle.

The reduction in profile drag and lift effectiveness of trailing-edge flaps that occurs when sweep is employed means that the principal effect of sweep (indicated by applying simple sweep theory) is the change in the effective velocity component ($V \cos \Lambda$). The relative drag-producing qualities are then in the same order on swept wings as on unswept wings in that split, double slotted, and slotted flaps are in a descending order of drag increment.

SUMMARY OF RESULTS

The more significant wind-tunnel data on the low speed, longitudinal, aerodynamic characteristics of swept, delta, and thin unswept wings have been presented in tabular form.

An analysis of these data indicates that two basically different types of flow separation can exist; namely, trailing-edge separation and leading-edge separation. Either or

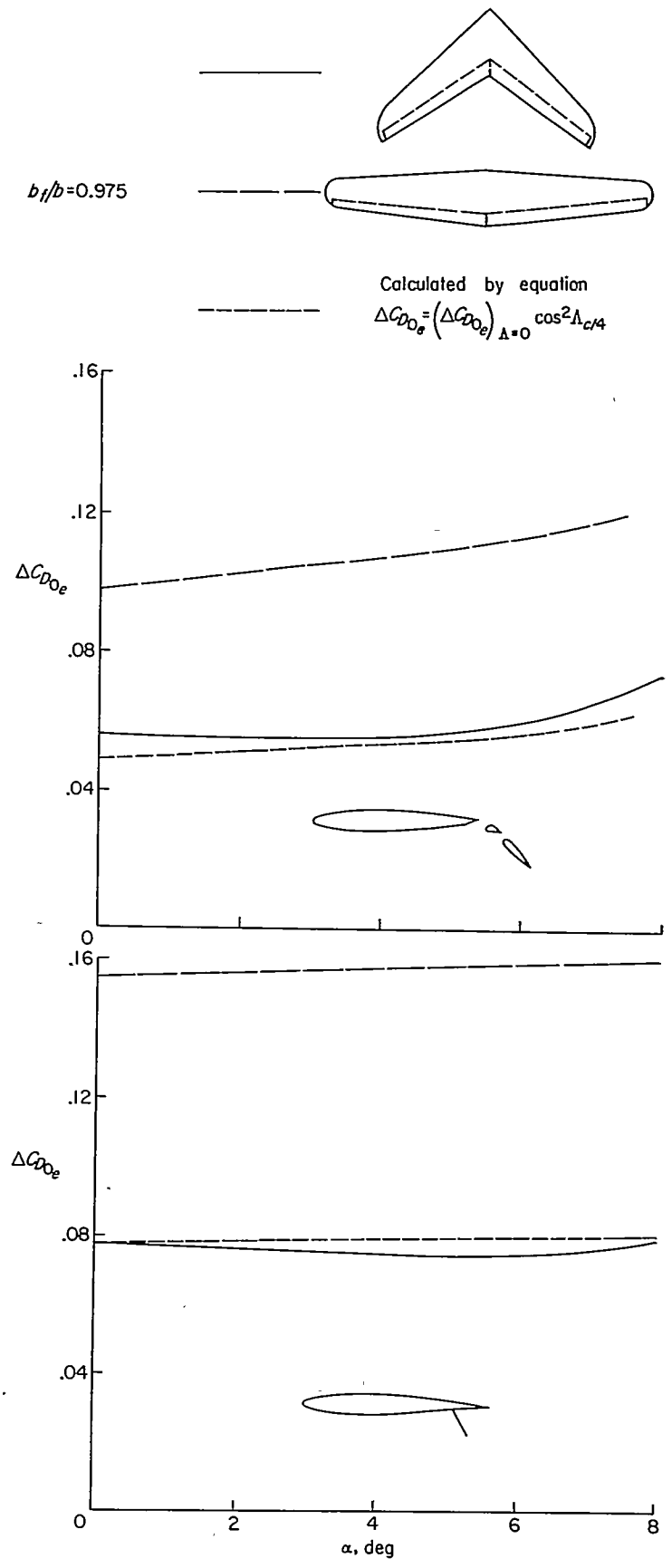

FIGURE 45.—An illustration of the effect of sweep on the estimated and experimental values of effective profile-drag coefficient at low angles of attack for two types of trailing-edge flaps. (Data obtained from refs. 48 and 89.)

both types of separation can occur, depending primarily on leading-edge radius, sweep angle, aspect ratio, and Reynolds number. Criteria for predicting the type of separation are indicated.

For thin, round-nose airfoils, longitudinal stability characteristics through the lift range can be misleading, if the data are obtained at any Reynolds number below the flight value. On sweptback wings exhibiting trailing-edge separation, the addition of roughness eliminates the beneficial effects in stability sometimes obtained by an increase in Reynolds number. An empirical relation based on data for a wide range of wing sweep angles, aspect ratios, and taper ratios indicates that the longitudinal stability characteristics will be good if the wing area rearward of the quarter-chord point of the mean aerodynamic chord exceeds 69 percent of the total wing area.

Effectiveness of various methods of stall control as applicable to each type flow separation are discussed. A detailed discussion is given on the effects of fences (or vanes), extensible leading-edge flaps and slats, droop noses, boundary-layer control, and chord-extensions; limited discussion is given on the effects of nacelles and stores, contra flaps, camber and twist, and unusual plan-form shapes, including variable sweep, inverse taper, cranked wings, and A, M, and W shapes.

Analysis of horizontal-tail data indicates that the influence of wing wake on downwash is the key factor in stability. The wake moves up at an ever greater rate as sweep angle is increased. Addition of the tail can measurably improve or worsen longitudinal stability characteristics. For the best results, the horizontal tail should be so located that it is emerging from the wake through the nonlinear lift range of the wing. In general, this location means that the tail should lie below the chord plane extended for very short tail lengths and somewhat above the chord plane for very long tail lengths.

A compilation is made of various methods for calculating lift-curve slope and, for the four most rapid methods, comparisons made with experiment indicate that no one method is entirely satisfactory. At low sweep angles, wings having trailing-edge separation develop higher maximum lifts than wings having leading-edge separation; these differences tend to disappear as sweepback is increased. Camber can, in general, be used to increase maximum lift. Maximum lift is shown to depend not only on Reynolds number, but also on Mach number even in the low Mach number range. Charts are presented for obtaining the point on the lift curve where large undesirable changes in aerodynamic center occur. The effects on maximum lift of leading- and trailing-edge devices, together with information as to the desirability of the pitching moment characteristics, are summarized in charts.

Calculated induced drag, experimental profile drag, and experimental values of Oswald's efficiency factor are presented for a variety of sweptback wings.

Langley Aeronautical Laboratory,
National Advisory Committee for Aeronautics,
Langley Field, Va., *May 14, 1952.*

REFERENCES

1. Busemann, A.: Aerodynamischer Auftrieb bei Überschallgeschwindigkeit. Luftfahrtforschung, Bd. 12, Nr. 6, Oct. 3, 1935, pp. 210–220.
2. Göthert, B.: Ebene und räumliche Strömung bei hohen Unterschallgeschwindigkeiten (Erweiterung der Prandtlschen Regel). Bericht 127 der Lilienthal-Gesellschaft für Luftfahrtforschung, 1940, pp. 97–101.
3. Göthert, B.: Berechnung des Geschwindigkeitsfeldes von Pfeilflügeln bei hohen Unterschallgeschwindigkeiten. Bericht 127 der Lilienthal-Gesellschaft für Luftfahrtforschung, Sept. 1940, pp. 52–56.
4. Ludwieg, H.: Pfeilflügel bei hohen Geschwindigkeiten. Bericht 127 der Lilienthal-Gesellschaft für Luftfahrtforschung, pp. 44–52.
5. Ludwieg, H.: Improvement of the Critical Mach Number of Aerofoils by Sweep-Back. Reps. and Translations No. 84, British M.A.P. Völkenrode, May 15, 1946.
6. Jones, Robert T.: Properties of Low-Aspect-Ratio Pointed Wings at Speeds Below and Above the Speed of Sound. NACA Rep. 835, 1946. (Supersedes NACA TN 1032.)
7. Jones, Robert T.: Wing Plan Forms for High-Speed Flight. NACA Rep. 863, 1947. (Supersedes NACA TN 1033.)
8. Jones, Robert T.: Effects of Sweep-Back on Boundary Layer and Separation. NACA Rep. 884, 1947. (Supersedes NACA TN 1402.)
9. Soulé, Hartley A.: Influence of Large Amounts of Wing Sweep on Stability and Control Problems of Aircraft. NACA TN 1088, 1946.
10. Shortal, Joseph A., and Maggin, Bernard: Effect of Sweepback and Aspect Ratio on Longitudinal Stability Characteristics of Wings at Low Speeds. NACA TN 1093, 1946.
11. Letko, William, and Goodman, Alex: Preliminary Wind-Tunnel Investigation at Low Speed of Stability and Control Characteristics of Swept-Back Wings. NACA TN 1046, 1946.
12. Pearson, Henry A., and Anderson, Raymond F.: Calculation of the Aerodynamic Characteristics of Tapered Wings With Partial-Span Flaps. NACA Rep. 665, 1939.
13. Griner, Roland F., and Foster, Gerald V.: Low-Speed Longitudinal and Wake Air-Flow Characteristics at a Reynolds Number of 6.0×10^6 of a 52° Sweptback Wing Equipped With Various Spans of Leading-Edge and Trailing-Edge Flaps, a Fuselage, and a Horizontal Tail at Various Vertical Positions. NACA RM L50K29, 1951.
14. Cahill, Jones F., and Gottlieb, Stanley M.: Low-Speed Aerodynamic Characteristics of a Series of Swept Wings Having NACA 65A006 Airfoil Sections (Revised). NACA RM L50F16, 1950.
15. McCormack, Gerald M., and Cook, Woodrow L.: Effects of Several Leading-Edge Modifications on the Stalling Characteristics of a 45° Swept-Forward Wing. NACA RM A9D29, 1949.
16. McCormack, Gerald M., and Cook, Woodrow L.: Effects of Boundary-Layer Control on the Longitudinal Characteristics of a 45° Swept-Forward Wing-Fuselage Combination. NACA RM A9K02a, 1950.
17. McCormack, Gerald M., and Stevens, Victor I., Jr.: An Investigation of the Low-Speed Stability and Control Characteristics of Swept-Forward and Swept-Back Wings in the Ames 40- by 80-Foot Wind Tunnel. NACA RM A6K15, 1947.
18. Conner, D. William, and Cancro, Patrick A.: Low-Speed Characteristics in Pitch of a 34° Sweptforward Wing With Circular-Arc Airfoil Sections. NACA RM L7F04a, 1948.
19. Martina, Albert P., and Deters, Owen J.: Maximum Lift and Longitudinal Stability Characteristics at Reynolds Numbers Up to 7.8×10^6 of a 35° Sweptforward Wing Equipped With High-Lift and Stall-Control Devices, Fuselage, and Horizontal Tail. NACA RM L9H18a, 1950.
20. Graham, Robert R.: Lateral-Control Investigation at a Reynolds Number of 5,300,000 of a Wing of Aspect Ratio 5.8 Sweptforward 32° at the Leading Edge. NACA RM L9H18, 1950.

21. Lange, Roy H., and May, Ralph W., Jr.: Effect of Leading-Edge High-Lift Devices and Split Flaps on the Maximum-Lift and Lateral Characteristics of a Rectangular Wing of Aspect Ratio 3.4 With Circular-Arc Airfoil Sections at Reynolds Numbers From 2.9×10^6 to 8.4×10^6. NACA RM L8D30, 1948.
22. Lange, Roy H.: Langley Full-Scale-Tunnel Investigation of the Maximum-Lift and Stalling Characteristics of a Trapezoidal Wing of Aspect Ratio 4 With Circular-Arc Airfoil Sections. NACA TN 2823, 1952. (Supersedes NACA RM L7H19.)
23. Johnson, Ben H., Jr., and Rollins, Francis W.: Investigation of a Thin Wing of Aspect Ratio 4 in the Ames 12-Foot Pressure Wind Tunnel. V—Static Longitudinal Stability and Control Throughout the Subsonic Speed Range of a Semispan Model of a Supersonic Airplane. NACA RM A9I01, 1949.
24. Johnson, Ben H., Jr., and Reed, Verlin D.: Investigation of a Thin Wing of Aspect Ratio 4 in the Ames 12-Foot Pressure Wind Tunnel. IV—The Effect of a Constant-Chord Leading-Edge Flap at High Subsonic Speeds. NACA RM A8K19, 1949.
25. Foster, Gerald V., Mollenberg, Ernst F., and Woods, Robert L.: Low-Speed Longitudinal Characteristics of an Unswept Hexagonal Wing With and Without a Fuselage and a Horizontal Tail Located at Various Positions at Reynolds Numbers From 2.8×10^6 to 7.6×10^6. NACA RM L52L11b, 1953.
26. Tinling, Bruce E., and Kolk, W. Richard. The Effects of Mach Number and Reynolds Number on the Aerodynamic Characteristics of Several 12-Percent-Thick Wings Having 35° of Sweepback and Various Amounts of Camber. NACA RM A50K27, 1951.
27. Koven, William, and Graham, Robert R.: Wind-Tunnel Investigation of High-Lift and Stall-Control Devices on a 37° Sweptback Wing of Aspect Ratio 6 at High Reynolds Numbers. NACA RM L8D29, 1948.
28. Furlong, G. Chester, and Bollech, Thomas V.: Effect of Ground Interference on the Aerodynamic Characteristics of a 42° Sweptback Wing. NACA RM L8F04, 1948.
29. Spooner, Stanley H., and Martina, Albert P.: Longitudinal Stability Characteristics of a 42° Sweptback Wing and Tail Combination at a Reynolds Number of 6.8×10^6. NACA RM L8E12, 1948.
30. Salmi, Reino J., Conner, D. William, and Graham, Robert R.: Effects of a Fuselage on the Aerodynamic Characteristics of a 42° Sweptback Wing at Reynolds Numbers to 8,000,000. NACA RM L7E13, 1947.
31. Graham, Robert R., and Conner, D. William: Investigation of High-Lift and Stall-Control Devices on an NACA 64-Series 42° Sweptback Wing With and Without Fuselage. NACA RM L7G09, 1947.
32. Conner, D. William, and Neely, Robert H.: Effects of a Fuselage and Various High-Lift and Stall-Control Flaps on Aerodynamic Characteristics in Pitch of an NACA 64-Series 40° Swept-Back Wing. NACA RM L6L27, 1947.
33. Foster, Gerald V., and Griner, Roland F.: A Study of Several Factors Affecting the Stability Contributed by a Horizontal Tail at Various Vertical Positions on a Sweptback-Wing Airplane Model. NACA TN 3848, 1956. (Supersedes NACA RM L9H19.)
34. Salmi, Reino J.: Pressure-Distribution Measurements Over an Extensible Leading-Edge Flap on Two Wings Having Leading-Edge Sweep of 42° and 52°. NACA RM L9A18, 1949.
35. Pratt, George L., and Bollech, Thomas V.: The Effect of Span and Deflection of Split Flaps and Leading-Edge Roughness on the Longitudinal Stability and Gliding Characteristics of a 42° Sweptback Wing Equipped With Leading-Edge Flaps. NACA RM L9E02, 1949.
36. Woods, Robert L., and Spooner, Stanley H.: Effects of High-Lift and Stall-Control Devices, Fuselage, and Horizontal Tail on a Wing Swept Back 42° at the Leading Edge and Having Symmetrical Circular-Arc Airfoil Sections at a Reynolds Number of 6.9×10^6. NACA RM L9B11, 1949.
37. Neely, Robert H., and Koven, William: Low-Speed Characteristics in Pitch of a 42° Sweptback Wing With Aspect Ratio 3.9 and Circular-Arc Airfoil Sections. NACA RM L7E23, 1947.
38. Lange, Roy H.: Maximum-Lift Characteristics of a Wing With the Leading-Edge Sweepback Decreasing From 45° at the Root to 20° at the Tip at Reynolds Numbers From 2.4×10^6 to 6.0×10^6. NACA RM L50A04a, 1950.
39. Pratt, George L., and Shields, E. Rousseau: Low-Speed Longitudinal Characteristics of a 45° Sweptback Wing of Aspect Ratio 8 With High-Lift and Stall-Control Devices at Reynolds Numbers From 1,500,000 to 4,800,000. NACA RM L51J04, 1952.
40. Salmi, Reino J., and Jacques, William A.: Effect of Vertical Location of a Horizontal Tail on the Static Longitudinal Stability Characteristics of a 45° Sweptback-Wing—Fuselage Combination of Aspect Ratio 8 at a Reynolds Number of 4.0×10^6. NACA RM L51J08, 1952.
41. Salmi, Reino J.: Low-Speed Longitudinal Aerodynamic Characteristics of a Twisted and Cambered Wing of 45° Sweepback and Aspect Ratio 8 With and Without High-Lift and Stall-Control Devices and a Fuselage at Reynolds Numbers From 1.5×10^6 to 4.8×10^6. NACA RM L52C11, 1952.
42. Johnson, Ben H., Jr., and Shibata, Harry H.: Characteristics Throughout the Subsonic Speed Range of a Plane Wing and of a Cambered and Twisted Wing, Both Having 45° of Sweepback. NACA RM A51D27, 1951.
43. Hunton, Lynn W.: Effects of Twist and Camber on the Low-Speed Characteristics of a Large-Scale 45° Swept-Back Wing. NACA RM A50A10, 1950.
44. Pasamanick, Jerome, and Sellers, Thomas B.: Low-Speed Investigation of Leading-Edge and Trailing-Edge Flaps on a 47.5° Sweptback Wing of Aspect Ratio 3.4 at a Reynolds Number of 4.4×10^6. NACA RM L50E02, 1950.
45. Pasamanick, Jerome, and Sellers, Thomas B.: Full-Scale Investigation of Boundary-Layer Control by Suction through Leading-Edge Slots on a Wing-Fuselage Configuration Having 47.5° Leading-Edge Sweep With and Without Flaps. NACA RM L50B15, 1950.
46. Pasamanick, Jerome, and Proterra, Anthony J.: The Effect of Boundary-Layer Control by Suction and Several High-Lift Devices on the Longitudinal Aerodynamic Characteristics of a 47.5° Sweptback Wing-Fuselage Combination. NACA RM L8E18, 1948.
47. Guryansky, Eugene R., and Lipson, Stanley: Effect of High-Lift Devices on the Longitudinal and Lateral Characteristics of a 45° Sweptback Wing With Symmetrical Circular-Arc Sections. NACA RM L8D06, 1948.
48. Salmi, Reino J.: Effects of Leading-Edge Devices and Trailing-Edge Flaps on Longitudinal Characteristics of Two 47.7° Sweptback Wings of Aspect Ratios 5.1 and 6.0 at a Reynolds Number of 6.0×10^6. NACA RM L50F20, 1950.
49. Spooner, Stanley H., and Mollenberg, Ernst F.: Low-Speed Investigation of Several Types of Split Flap on a 47.7° Sweptback-Wing—Fuselage Combination of Aspect Ratio 5.1 at a Reynolds Number of 6.0×10^6. NACA RM L51D20, 1951.
50. Salmi, Reino J.: Horizontal-Tail Effectiveness and Downwash Surveys for Two 47.7° Sweptback Wing-Fuselage Combinations With Aspect Ratios of 5.1 and 6.0 at a Reynolds Number of 6.0×10^6. NACA RM L50K06, 1951.
51. Mollenberg, Ernst F., and Spooner, Stanley H.: Low-Speed Investigation of the Effects of Single Slotted and Double Slotted Flaps on a 47.7° Sweptback-Wing—Fuselage Combination at a Reynolds Number of 6.0×10^6. NACA RM L51E24, 1951.
52. Foster, Gerald V., and Fitzpatrick, James E.: Longitudinal-Stability Investigation of High-Lift and Stall-Control Devices on a 52° Sweptback Wing With and Without Fuselage and Horizontal Tail at a Reynolds Number of 6.8×10^6. NACA RM L8I08, 1948.
53. Furlong, G. Chester: Exploratory Investigation of Leading-Edge Chord-Extensions To Improve the Longitudinal Stability Characteristics of Two 52° Sweptback Wings. NACA RM L50A30, 1950.

54. Foster, Gerald V., and Griner, Roland F.: Low-Speed Longitudinal Characteristics of a Circular-Arc 52° Sweptback Wing of Aspect Ratio 2.84 With and Without Leading-Edge and Trailing-Edge Flaps at Reynolds Numbers From 1.6×10^6 to 9.7×10^6. NACA RM L50F16a, 1950.
55. Foster, Gerald V., and Griner, Roland F.: Low-Speed Longitudinal and Wake Air-Flow Characteristics at a Reynolds Number of 5.5×10^6 of a Circular-Arc 52° Sweptback Wing With a Fuselage and a Horizontal Tail at Various Vertical Positions. NACA RM L51C30, 1951.
56. Lovell, J. Calvin, and Wilson, Herbert A., Jr.: Langley Full-Scale-Tunnel Investigation of Maximum Lift and Stability Characteristics of an Airplane Having Approximately Triangular Plan Form (DM-1 Glider). NACA RM L7F16, 1947.
57. Whittle, Edward F., Jr., and Lovell, J. Calvin: Full-Scale Investigation of an Equilateral Triangular Wing Having 10-Percent-Thick Biconvex Airfoil Sections. NACA RM L8G05, 1948.
58. Anderson, Adrien E.: Chordwise and Spanwise Loadings Measured at Low Speed on Large Triangular Wings. NACA RM A9B17, 1949.
59. McCormack, Gerald M., and Walling, Walter C.: Aerodynamic Study of a Wing-Fuselage Combination Employing a Wing Swept Back 63°.—Investigation of a Large-Scale Model at Low Speed. NACA RM A8D02, 1949.
60. Hopkins, Edward J.: Aerodynamic Study of a Wing-Fuselage Combination Employing a Wing Swept Back 63°.—Effects of Split Flaps, Elevons, and Leading-Edge Devices at Low Speed. NACA RM A9C21, 1949.
61. Anderson, Adrien E.: An Investigation at Low Speed of a Large-Scale Triangular Wing of Aspect Ratio Two. III—Characteristics of Wing With Body and Vertical Tail. NACA RM A9H04, 1949.
62. Kolbe, Carl D., and Tinling, Bruce E.: Tests of a Triangular Wing of Aspect Ratio 2 in the Ames 12-Foot Pressure Wind Tunnel. III—The Effectiveness and Hinge Moments of a Skewed Wing-Tip Flap. NACA RM A8E21, 1948.
63. Stephenson, Jack D., and Ameudo, Arthur R.: Tests of a Triangular Wing of Aspect Ratio 2 in the Ames 12-Foot Pressure Wind Tunnel. II—The Effectiveness and Hinge Moments of a Constant-Chord Plain Flap. NACA RM A8E03, 1948.
64. Wick, Bradford H., and Graham, David: Exploratory Investigation of the Effect of Skewed Plain Nose Flaps on the Low-Speed Characteristics of a Large-Scale Triangular-Wing-Fuselage Model. NACA RM A9K22, 1950.
65. Anderson, Adrien E.: An Investigation at Low Speed of a Large-Scale Triangular Wing of Aspect Ratio Two. I—Characteristics of a Wing Having a Double-Edge Airfoil Section With Maximum Thickness at 20-Percent Chord. NACA RM A7F06, 1947.
66. Anderson, Adrien E.: An Investigation at Low Speed of a Large-Scale Triangular Wing of Aspect Ratio Two. II—The Effect of Airfoil Section Modifications and the Determination of the Wake Downwash. NACA RM A7H28, 1947.
67. Graham, David: Chordwise and Spanwise Loadings Measured at Low Speeds on a Large Triangular Wing Having an Aspect Ratio of 2 and a Thin, Subsonic-Type Airfoil Section. NACA RM A50A04a, 1950.
68. Sivells, James C., and Neely, Robert H.: Method for Calculating Wing Characteristics by Lifting-Line Theory Using Nonlinear Section Lift Data. NACA Rep. 865, 1947. (Supersedes NACA TN 1269.)
69. Multhopp, H.: Methods for Calculating the Lift Distribution of Wings (Subsonic Lifting Surface Theory). Rep. No. Aero. 2353, British R.A.E., Jan. 1950.
70. Graham, Robert R.: Low-Speed Characteristics of a 45° Sweptback Wing of Aspect Ratio 8 From Pressure Distributions and Force Tests at Reynolds Numbers From 1,500,000 to 4,800,000. NACA RM L51H13, 1951.
71. Anderson, Raymond F.: Determination of the Characteristics of Tapered Wings. NACA Rep. 572, 1936.
72. Lange, Roy H., Whittle, Edward F., Jr., and Fink, Marvin E.: Investigation at Large Scale of the Pressure Distribution and Flow Phenomena Over a Wing With the Leading Edge Swept Back 47.5° Having Circular-Arc Airfoil Sections and Equipped With Drooped-Nose and Plain Flaps. NACA RM L9G15, 1949.
73. Salmi, Reino J., and Carros, Robert J.: Longitudinal Characteristics of Two 47.7° Sweptback Wings With Aspect Ratios of 5.1 and 6.0 at Reynolds Numbers up to 10×10^6. NACA RM L50A04, 1950.
74. Fitzpatrick, James E., and Foster, Gerald V.: Static Longitudinal Aerodynamic Characteristics of a 52° Sweptback Wing of Aspect Ratio 2.88 at Reynolds Numbers From 2,000,000 to 11,000,000. NACA RM L8H25, 1948.
75. May, Ralph W., Jr., and Hawes, John G.: Low-Speed Pressure Distribution and Flow Investigation for a Large Pitch and Yaw Range of Three Low-Aspect-Ratio Pointed Wings Having Leading Edge Swept Back 60° and Biconvex Sections. NACA RM L9J07, 1949.
76. DeYoung, John: Theoretical Additional Span Loading Characteristics of Wings With Arbitrary Sweep, Aspect Ratio, and Taper Ratio. NACA TN 1491, 1947.
77. Ganzer, Victor M.: Aerodynamic Development of the XB-47 Airplane. Pt. II—Development of Model 450 up to June, 1947. Rep. No. D-7824A, Boeing Aircraft Co., Sept. 1947.
78. Kemp, William B., Jr., Becht, Robert E., and Few, Albert G., Jr.: Stability and Control Characteristics at Low Speed of a ¼-Scale Bell X-5 Airplane Model. Longitudinal Stability and Control. NACA RM L9K08, 1950.
79. Hunton, Lynn W., and Dew, Joseph K.: The Effects of Camber and Twist on the Aerodynamic Loading and Stalling Characteristics of a Large-Scale 45° Swept-Back Wing. NACA RM A50J24, 1951.
80. Weiberg, James A., and Carel, Hubert C.: Wind-Tunnel Investigation at Low Speed of a Wing Swept Back 63° and Twisted and Cambered for a Uniform Load at a Lift Coefficient of 0.5. NACA RM A50A23, 1950.
81. Pratt, George L.: Effects of Twist and Camber on the Low-Speed Longitudinal Stability Characteristics of a 45° Sweptback Wing of Aspect Ratio 8 at Reynolds Numbers From 1.5×10^6 to 4.8×10^6 As Determined by Pressure Distributions, Force Tests, and Calculations. NACA RM L52J03a, 1952.
82. Hoggard, H. Page, Jr., and Hagerman, John R.: Downwash and Wake Behind Untapered Wings of Various Aspect Ratios and Angles of Sweep. NACA TN 1703, 1948.
83. Polhamus, Edward C.: A Simple Method of Estimating the Subsonic Lift and Damping in Roll of Sweptback Wings. NACA TN 1862, 1949.
84. Toll, Thomas A., and Queijo, M. J.: Approximate Relations and Charts for Low-Speed Stability Derivatives of Swept Wings. NACA TN 1581, 1948.
85. Demele, Fred A., and Sutton, Fred B.: The Effects of Increasing the Leading-Edge Radius and Adding Forward Camber on the Aerodynamic Characteristics of a Wing With 35° of Sweepback. NACA RM A50K28a, 1951.
86. Rose, Leonard M.: Low-Speed Investigation of a Small Triangular Wing of Aspect Ratio 2.0. II—Flaps. NACA RM A7L11, 1948.
87. Lowry, John G., and Schneiter, Leslie E.: Investigation at Low Speed of the Longitudinal Stability Characteristics of a 60° Swept-Back Tapered Low-Drag Wing. NACA TN 1284, 1947.
88. Dannenberg, Robert E.: Measurements of Section Characteristics of a 45° Swept Wing Spanning a Rectangular Low-Speed Wind Tunnel as Affected by the Tunnel Walls. NACA TN 2160, 1950.
89. Sivells, James C., and Spooner, Stanley H.: Investigation in the Langley 19-Foot Pressure Tunnel of Two Wings of NACA 65-210 and 64-210 Airfoil Sections With Various Type Flaps. NACA Rep. 942, 1949. (Supersedes NACA TN 1579.)
90. Kuethe, A. M.: Velocity Distribution in the Boundary Layer of a Swept-Back Wing. Project No. M404, NACA, Dept. Engineering Res., Univ. Mich., April 1944.

91. Wilson, Herbert A., Jr., and Lovell, J. Calvin: Full-Scale Investigation of the Maximum Lift and Flow Characteristics of an Airplane Having Approximately Triangular Plan Form. NACA RM L6K20, 1947.

92. Cook, Woodrow L., Griffin, Roy N., Jr., and McCormack, Gerald M.: The Use of Area Suction for the Purpose of Delaying Separation of Air Flow at the Leading Edge of a 63° Swept-Back Wing. NACA RM A50H09, 1950.

93. Von Doenhoff, Albert E., and Tetervin, Neal: Investigation of the Variation of Lift Coefficient With Reynolds Number at a Moderate Angle of Attack on a Low-Drag Airfoil. NACA WR L-661, 1942. (Formerly NACA CB, Nov. 1942.)

94. Neely, Robert H., and Conner, D. William: Aerodynamic Characteristics of a 42° Swept-Back Wing With Aspect Ratio 4 and NACA 64_1-112 Airfoil Sections at Reynolds Numbers From 1,700,000 to 9,500,000. NACA RM L7D14, 1947.

95. Queijo, M. J., Jaquet, Byron M., and Wolhart, Walter D.: Wind-Tunnel Investigation at Low Speed of the Effects of Chordwise Wing Fences and Horizontal-Tail Position on the Static Longitudinal Stability Characteristics of an Airplane Model With a 35° Sweptback Wing. NACA Rep. 1203, 1954. (Supersedes NACA RM L50K07 by Queijo and Jaquet and RM L51H17 by Queijo and Wolhart.)

96. Weiberg, James A., and Carel, Hubert C.: Wind-Tunnel Investigation at Low Speed of a Wing Swept Back 63° and Twisted and Cambered for Uniform Load at a Lift Coefficient of 0.5 and With a Thickened Tip Section. NACA RM A50I14, 1950.

97. Naeseth, Rodger L., and MacLeod, Richard G.: Aerodynamic Characteristics of an Airfoil-Forebody Swept Flying-Boat Hull With a Wing and Tail Swept Back 51.3° at the Leading Edge. NACA RM L9F08, 1949.

98. Foster, Gerald V.: Effects of Twist and Camber, Fences, and Horizontal-Tail Height on the Low-Speed Longitudinal Stability Characteristics of a Wing-Fuselage Combination With a 45° Sweptback Wing of Aspect Ratio 8 at a Reynolds Number of 4.0×10^6. NACA RM L52J03, 1952.

99. Foster, Gerald V.: Longitudinal Stability and Wake-Flow Characteristics of a Twisted and Cambered Wing-Fuselage Combination of 45° Sweepback and Aspect Ratio 8 With a Horizontal Tail and Stall-Control Devices at a Reynolds Number of 4.0×10^6. NACA RM L53D08, 1953.

100. Tinling, Bruce E., and Kolk, W. Richard: The Effects of Centrally Mounted Wing-Tip Tanks on the Subsonic Aerodynamic Characteristics of a Wing of Aspect Ratio 10 With 35° of Sweepback. NACA RM A50K15, 1951.

101. Krüger, W.: Systematic Wind-Tunnel Measurements on a Laminar Wing With Nose Flap. NACA TM 1119, 1947.

102. Spence, A.: Low-Speed Wind-Tunnel Tests of Fowler Flaps, Slats and Nose Flaps on a Model of a Jet Aircraft With a 40 Deg Swept-Back Wing. R. & M. No. 2752, British A.R.C., Nov. 1948.

103. Krüger, W.: Wind Tunnel Investigations on a 35° Swept-Back Wing With Different High-Lift Devices. Part I—Six-Component Measurements. Reps. and Translations No. 311, British M.A.P. Völkenrode, Oct. 1, 1946.

104. Conner, D. William, and Foster, Gerald V.: Investigation of Pressure Distribution Over an Extended Leading-Edge Flap on a 42° Swept-back Wing. NACA RM L7J03, 1947.

105. Cahill, Jones F., and Oberndorfer, Gale C.: Pressure Distributions Over a Retracted Leading-Edge Slat on a 40° Sweptback Wing at Mach Numbers up to 0.9. NACA RM L50L04a, 1951.

106. Queijo, M. J., and Lichtenstein, Jacob H.: The Effects of High-Lift Devices on the Low-Speed Stability Characteristics of a Tapered 37.5° Sweptback Wing of Aspect Ratio 3 in Straight and Rolling Flow. NACA RM L8I03, 1948.

107. Trouncer, J.: A Comparison of the Effects of Slats, Nose Flaps and Double Split Flaps on a Model of a 40° Sweptback Tailless Aircraft. Rep. No. Aero 2141, British R.A.E., June 1946.

108. Recknagel, Paul W.: The Aerodynamics of Wings Having Sweep. NAVAER DR Rep. No. 1001, Bur. Aero., April 1946.

109. Turner, W. N., and Katkov, R. B.: Wind Tunnel Tests of a ⅓-Scale Semispan Model of the XP-86 Airplane To Determine the Effect of a Revised Slat Position on Stability Slat-Opening Tendencies and Slat Pressures. Rep. No. NA-48-375, North American Aviation, Inc., Mar. 24, 1948.

110. Kelly, John A., and Hayter, Nora-Lee F.: Aerodynamic Characteristics of a Leading-Edge Slat on a 35° Swept-Back Wing for Mach Numbers From 0.30 to 0.88. NACA RM A51H23, 1951.

111. Spooner, Stanley H., and Mollenberg, Ernst F.: Positioning Investigation of Single Slotted Flaps on a 47.7° Sweptback Wing at Reynolds Numbers of 4.0×10^6 and 6.0×10^6. NACA RM L50H29, 1950.

112. Hadaway, William M., and Cancro, Patrick A.: Low-Speed Longitudinal Characteristics of Two Unswept Wings of Hexagonal Airfoil Sections Having Aspect Ratios of 2.5 and 4.0 With Fuselage and Horizontal Tail Located at Various Vertical Positions. NACA RM L53H14a, 1953.

113. McCormack, Gerald M., and Tolhurst, William H., Jr.: The Effects of Boundary-Layer Control on the Longitudinal Characteristics of a Swept-Back Wing Using Suction Through Streamwise Slots in the Outboard Portion of the Wing. NACA RM A50K06, 1951.

114. Graham, Robert R., and Jacques, William A.: Wind-Tunnel Investigation of Stall Control by Suction Through a Porous Leading Edge on a 37° Sweptback Wing of Aspect Ratio 6 at Reynolds Numbers From 2.5×10^6 to 8.10×10^6. NACA RM L52L05, 1953.

115. Pasamanick, Jerome, and Scallion, William I.: The Effects of Suction Through Porous Leading-Edge Surfaces on the Aerodynamic Characteristics of a 47.5° Sweptback Wing-Fuselage Combination at a Reynolds Number of 4.4×10^6. NACA RM L51K15, 1952.

116. Yates, E. Carson, Jr.: Low-Speed Wind-Tunnel Investigation of Leading-Edge Porous Suction on a 4-Percent-Thick 60° Delta Wing. NACA RM L54L21, 1955.

117. Kemp, William B., Jr., Becht, Robert E., and Few, Albert G., Jr.: Investigation of the Low-Speed Aerodynamic Characteristics of a Variable-Sweep Airplane Model With a Twisted and Cambered Wing. NACA RM L51K22, 1952.

118. McLarren, Robert: Theory of the Inversely Tapered Wing. Aviation Week, vol. 50, no. 12, March 21, 1949, pp. 30–33.

119. Purser, Paul E., and Bates, William R.: Low-Speed Wind-Tunnel Investigation of a 37.5° Swept-Back Wing Having Inverse Taper With and Without a Horizontal Tail. NACA MR L6G17, 1946.

120. Barnett, U. Reed, Jr., and Lange, Roy H.: Low-Speed Pressure-Distribution Measurements at a Reynolds Number of 3.5×10^6 on a Wing With Leading-Edge Sweepback Decreasing From 45° at the Root to 20° at the Tip. NACA RM L50A23a, 1950.

121. Krüger, W.: Six-Component Measurements on a Cranked Swept-Back Wing for Ar 234. Reps. and Translations No. 816, British M.A.P. Völkenrode, Jan. 15, 1947.

122. Edwards, George G., and Boltz, Frederick W.: An Analysis of the Forces and Pressure Distribution on a Wing With the Leading Edge Swept Back 37.25°. NACA RM A9K01, 1950.

123. Lemme, H. G.: Investigation on a Normal Swept-Back Wing, a Blunted Swept-Back Wing and an M-Wing. Reps. and Translations No. 441, British M.O.S.(A) Völkenrode, 1946.

124. Purser, Paul E., and Spearman, M. Leroy: Wind-Tunnel Tests at Low Speed of Swept and Yawed Wings Having Various Plan Forms. NACA TN 2445, 1951. (Supersedes NACA RM L7D23.)

125. Purser, Paul E., Spearman, M. Leroy, and Bates, William R.: Preliminary Investigation at Low Speed of Downwash Characteristics of Small-Scale Sweptback Wings. NACA TN 1378, 1947.

126. Silverstein, Abe, Katzoff, S., and Bullivant, W. Kenneth: Downwash and Wake Behind Plain and Flapped Airfoils. NACA Rep. 651, 1939.

127. Weissinger, J.: The Lift Distribution of Swept-Back Wings. NACA TM 1120, 1947.

128. Mutterperl, William: The Calculation of Span Load Distributions on Swept-Back Wings. NACA TN 834, 1941.

129. Falkner, V. M.: The Calculation of Aerodynamic Loading on Surfaces of Any Shape. R. & M. No. 1910, British A.R.C., Aug. 1943.

130. Schneider, William C.: A Comparison of the Spanwise Loading Calculated by Various Methods With Experimental Loadings Obtained on a 45° Sweptback Wing of Aspect Ratio 8.02 at a Reynolds Number of 4.0×10^6. NACA Rep. 1208, 1954. (Supersedes NACA RM L51G30.)

131. Maki, Ralph L.: The Use of Two-Dimensional Section Data To Estimate the Low-Speed Wing Lift Coefficient at Which Section Stall First Appears on a Swept Wing. NACA RM A51E15, 1951.

132. Furlong, G. Chester, and Fitzpatrick, James E.: Effects of Mach Number up to 0.34 and Reynolds Number up to 8×10^6 on the Maximum Lift Coefficient of a Wing of NACA 66-Series Airfoil Sections. NACA TN 2251, 1950.

133. Young, A. D.: The Aerodynamic Characteristics of Flaps. Rep. No. Aero 2185, British R.A.E., Feb. 1947.

134. DeYoung, John: Theoretical Symmetric Span Loading. Due to Flap Deflection for Wings of Arbitrary Plan Form at Subsonic Speeds. NACA TN 2278, 1951.

135. Wood, K. D.: Aspect Ratio Corrections. Jour. Aero. Sci., vol. 10, no. 8, Oct. 1943, pp. 270–272.

136. Driggs, Ivan H.: Aircraft Design Analysis Methods as Employed by the Research Division of the Bureau of Aeronautics, U. S. Navy Department. NAVAER DR Rep. No. 1139, Bur. Aero., Oct. 6, 1949.

TABLE 1.—INDEX TO TABULATED DATA

Table	Λ_{LE}, deg	$\Lambda_{c/4}$, deg	A	λ	Airfoil section	Trailing-edge device	Stall-control device	Fuselage	Horizontal tail
2	−43.2	−45.0	4.00	0.600	NACA 65A006	Split flap	------	------	------
3	−41.3	−45.0	3.55	0.500	NACA 64_1A112	------	L. E. droop	------	------
4	−41.3	−45.0	3.55	0.500	NACA 64_1A112	Split flap	Boundary-layer control	On	------
5	−40.6	−45.0	3.12	0.380	Root: NACA 0015 Tip: NACA 23009	Split flap	------	------	------
6	−34.0	−36.2	3.94	0.625	Circular arc	Split flap	L. E. flap	On	------
7	−32.3	−35.3	5.79	0.389	NACA 64-210	Split flap Single-slotted flap Double-slotted flap	L. E. flap L. E. slat L. E. droop Fence	On	On
8	−25.9	−30.0	4.69	0.400	Root: NACA 0015 Tip: NACA 23009	Split flap	------	------	------
9	0	0	3.40	1.00	Circular arc	Split flap	L. E. flap L. E. droop Round L. E.	------	------
10	0	0	4.00	1.00	Circular arc	Plain flap	L. E. droop	------	------
11	3.58	0	4.00	0.600	NACA 65A006	Split flap	------	------	------
12	3.6	0	4.62	0.550	Root: NACA 0015 Tip: NACA 23009	Split flap	------	------	------
13	9.46	9.0	4.00	0.500	Double wedge	Plain flap	L. E. droop	On	On
14	10.46	5.28	2.50	0.625	Hexagonal $\frac{t}{c}=0.06$	Plain flap	L. E. droop	On	On
15	32.6	30.0	4.00	0.600	NACA 65A006	Split flap	------	------	------
16	33.4	30.0	4.84	0.440	Root: NACA 0015 Tip: NACA 23009	Split flap	------	------	------
17	36.25	35.0	5.14	0.713	NACA 65_1A012 NACA 64_1A312 NACA 64_1A612	------	------	------	------
18	36.25	35.0	10.07	0.500	NACA 65_1A012 NACA 64_1A312 NACA 64_1A612	------	------	------	------
19	37.25	35.0	6.00	0.500	NACA 64_1-212	Split flap Double-slotted flap	L. E. flap L. E. slat L. E. droop Fence	------	------
20	42.0	40.0	4.01	0.625	NACA 64_1-112	Split flap	L. E. flap L. E. slat Fence	On	On
21	42.0	40.0	3.94	0.625	Circular arc	Split flap	L. E. flap L. E. droop Fence	On	On
22	45–20	Variable	4.12	0.360	NACA 64A009	Split flap	L. E. flap L. E. slat	------	------
23	45.0	45.0	4.00	1.00	NACA 65A006	Split flap	------	------	------

TABLE 1.—INDEX TO TABULATED DATA—Concluded

Table	Λ_{LE}, deg	$\Lambda_{c/4}$, deg	A	λ	Airfoil section	Trailing-edge device	Stall-control device	Fuselage	Horizontal tail
24	46.2	45.0	6.00	0.600	NACA 65A006	Split flap	----------	------	------
25	46.33	45.0	8.02	0.450	NACA 63_1A012	Split flap	L. E. flap Fences	On	On
26	46.33	45.0	8.00	0.450	Cambered 63-012	Split flap	L. E. flap Fence	------	------
27	46.55	45.0	5.00	0.565	NACA 64A010 NACA 64A810	----------	----------	On	------
28	46.6	45.0	6.00	0.500	NACA 64A010 NACA 64A810	----------	----------	------	------
29	46.7	45.0	4.00	0.600	NACA 65A006	Split flap	L. E. droop Fence	------	------
30	47.5	45.0	3.40	0.510	NACA 64_1A112	Plain flap	L. E. flap	On	------
31	47.5	45.0	3.40	0.510	NACA 64_1A112	Split flap	Boundary-layer control	On	------
32	47.5	45.0	3.50	0.500	NACA 64_1A112	Split flap	Boundary-layer control	On	------
33	47.5	45.0	3.50	0.500	Circular arc	Plain flap	L. E. droop Round L. E. Fence	------	------
34	47.7	45.0	5.10	0.383	NACA 64-210	Split flap Single-slotted flap Double-slotted flap Triangular flap	L. E. flap L. E. droop Fence	On	On
35	48.1	45.0	3.64	0.420	Root: NACA 0015 Tip: NACA 23009	Split flap	----------	------	------
36	48.4	45.0	2.00	0.600	NACA 65A006	Split flap	----------	------	------
37	48.6	45.0	4.00	0.300	NACA 65A006	Split flap	----------	------	------
38	52.0	50.0	2.88	0.625	NACA 64_1-112	Split flap	L. E. flap L. E. chord-extension Fence	On	On
39	52.0	50.2	2.84	0.616	Circular arc	Split flap	L. E. flap L. E. droop L. E. chord-extension	On	On
40	60.0	50.6	1.80	0	NACA 0015-64	Plain flap	Sharp L. E.	On	------
41	60.0	52.4	2.31	0	Circular arc	Plain flap	L. E. droop	------	------
42	60.0	52.4	2.31	0	NACA 65-006.5	Plain flap	----------	On	------
43	60.9	60.0	4.00	0.600	NACA 65A006	Split flap	----------	------	------
44	63.0	60.8	3.50	0.250	NACA 64A006	Split flap Triangular flap	L. E. flap L. E. droop Sharp L. E.	On	------
45	63.03	55.7	2.04	0	Double wedge	Skewed flap Plain flap	L. E. flap	On	------
46	63.43	56.3	2.00	0	Double wedge	Split flap	L. E. flap Round L. E.	------	------
47	63.43	56.3	2.00	0	NACA 0005	Plain flap	----------	------	------

TABLE 2.—SUMMARY OF LONGITUDINAL STABILITY CHARACTERISTICS OF A WING WITH 43.2° OF LEADING-EDGE SWEEPFORWARD

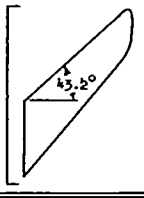

$\Lambda_{c/4} = -45°$ $A = 4.0$ $R_{max} = 6.0 \times 10^6$

$\lambda = 0.600$ $M_{max} = 0.20$

Airfoil sections (parallel to plane of symmetry)

Root: NACA 65A006

Tip: NACA 65A006

Span of L.E. device (b/2)	Span of T.E. device (b/2)	Configuration	$C_{L_{max}}$	$\alpha_{C_{L_{max}}}$	L/D at 0.85 $C_{L_{max}}$	C_m characteristics	Reference
None	None	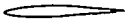	0.99	26.0	3.41	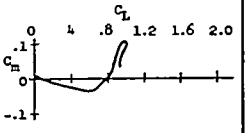	14
	.500 split flap	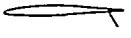	1.17	29.0	2.87	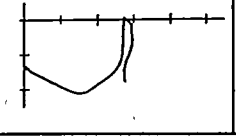	14

TABLE 3.—SUMMARY OF LONGITUDINAL STABILITY CHARACTERISTICS OF A WING WITH 41.3° OF LEADING-EDGE SWEEPFORWARD

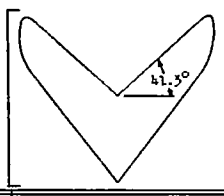

$\Lambda_{c/4} = 45°$ $A = 3.55$ $R_{max} = 10.6 \times 10^6$

$\lambda = 0.500$ $M_{max} = 0.14$

Airfoil sections (perpendicular to 0.25 chord line)

Root: NACA 64_1A112

Tip: NACA 64_1A112

Span of L.E. device (b/2)	Span of T.E. device (b/2)	Configuration	$C_{L_{max}}$	$\alpha_{C_{L_{max}}}$	L/D at 0.85 $C_{L_{max}}$	C_m characteristics	Reference
None	None	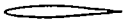	1.04	28.0	4.32	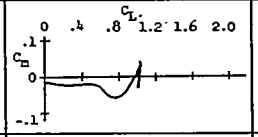	15
.500 L.E. droop	None	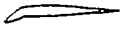	1.18	33.0	4.04	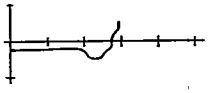	15
.750 L.E. droop	None	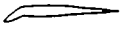	1.21	31.0	4.68	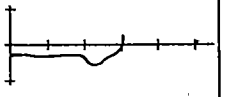	15
1.000 L.E. droop	None	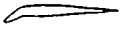	1.26	30.0	4.70	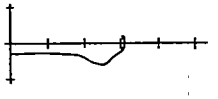	15
		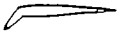	1.24	31.0	4.39	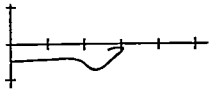	15
.500 outboard up .500 inboard down	None	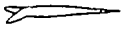	1.14	31.0	3.26	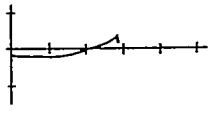	15
.500 cambered nose	None	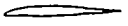	1.07	29.0	4.60	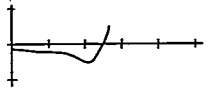	15
1.000 cambered nose	None	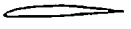	1.05	28.0	5.00	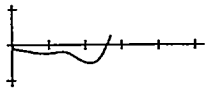	15

TABLE 4.—SUMMARY OF LONGITUDINAL STABILITY CHARACTERISTICS OF A WING WITH 41.3° OF LEADING-EDGE SWEEPFORWARD

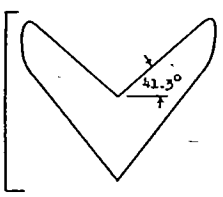

$\Lambda_{c/4} = -45°$ $A = 3.55$ $R_{max} = 10.6 \times 10^6$

$\lambda = 0.500$ $M_{max} = 0.14$

Airfoil sections (perpendicular to 0.25 chord line)

Root: NACA 64_1A112

Tip: NACA 64_1A112

Span of L.E. device (b/2)	Span of T.E. device (b/2)	Configuration	Moment-center location ($\bar{c}$)	$C_{L_{max}}$	$\alpha_{C_{L_{max}}}$	C_Q	C_m characteristics	Reference
None	None	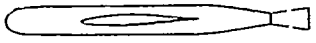	.140	1.10	33.0	—	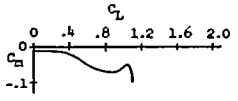	16
		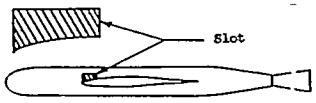	.128	1.18	29.0	0.0121	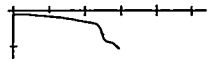	16
	.558 split flap	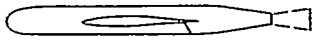	.204	1.24	29.0	—	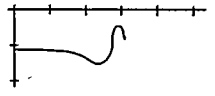	16
		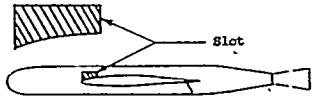	.198	1.29	29.0	0.0118	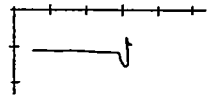	16
1.000 L.E. droop	None	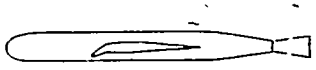	.152	1.31	29.0	—	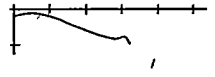	16
			.150	1.40	29.0	0.0125	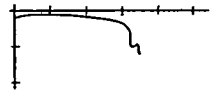	16
	.558 split flap	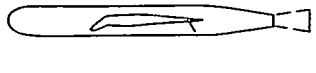	.215	1.39	29.0	—	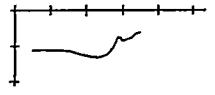	16
		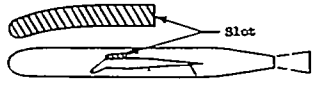	.204	1.51	29.0	0.0121	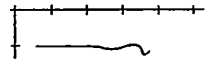	16

TABLE 5.—SUMMARY OF LONGITUDINAL STABILITY CHARACTERICTICS OF A WING WITH 40.6° OF LEADING-EDGE SWEEPFORWARD

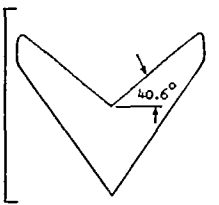

$\Lambda_{c/4} = -45°$ $A = 3.12$ $R_{max} = 18.0 \times 10^6$

$\lambda = 0.380$

Airfoil sections (variable)

Root: NACA 0015 (approximate)

Tip: NACA 23009 (approximate)

Span of L.E. device (b/2)	Span of T.E. device (b/2)	Configuration	$C_{L_{max}}$	$\alpha_{C_{L_{max}}}$	L/D at 0.85 $C_{L_{max}}$	C_m characteristics	Reference
None	None	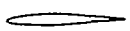	1.08	31.5	4.40	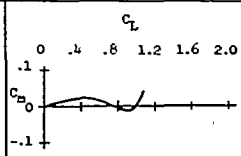	17
	.623 split flap	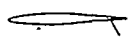	1.22	27.0	4.50	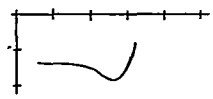	17
	.970 split flap	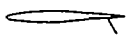	1.31	26.0	5.40	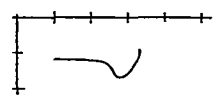	17

TABLE 6.—SUMMARY OF LONGITUDINAL STABILITY CHARACTERISTICS OF A WING WITH 34° OF LEADING-EDGE SWEEPFORWARD

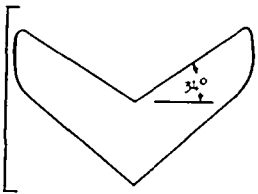

$\Lambda_{c/4} = -36.2°$ $A = 3.94$ $R_{max} = 9.6 \times 10^6$

$\lambda = 0.625$ $M_{max} = 0.22$

Airfoil sections (normal to line of maximum thickness)

Root: 10-percent-thick circular arc

Tip: 6.4-percent-thick circular arc

Span of L.E. device (b/2)	Span of T.E. device (b/2)	Configuration	$C_{L_{max}}$	$\alpha_{C_{L_{max}}}$	L/D at 0.85 $C_{L_{max}}$	C_m characteristics	Reference
None	None		0.77	21.0	3.85	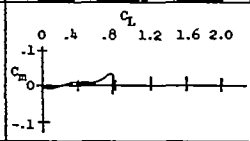	18
		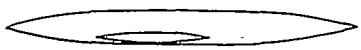	0.96	26.0	3.13	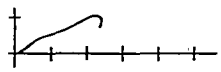	18
		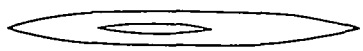	0.97	27.0	3.11	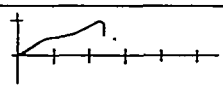	18
		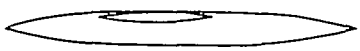	0.92	26.0	3.22	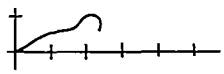	18

TABLE 6.—SUMMARY OF LONGITUDINAL STABILITY CHARACTERISTICS OF A WING WITH 34° OF LEADING-EDGE SWEEPFORWARD—Concluded

Span of L.E. device (b/2)	Span of T.E. device (b/2)	Configuration	$C_{L_{max}}$	$\alpha_{C_{L_{max}}}$	L/D at 0.85 $C_{L_{max}}$	C_m characteristics	Reference
None	.500 split flap	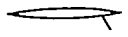	1.06	21.0	2.99	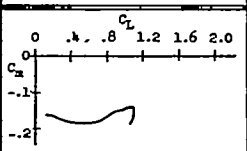	18
		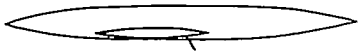	1.13	26.5	2.91	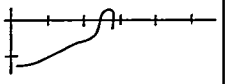	18
			1.17	28.2	2.74	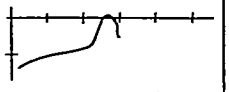	18
		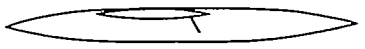	1.13	27.0	3.00	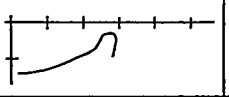	18
.800 L.E. flap	None	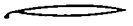	1.20	26.5	4.86	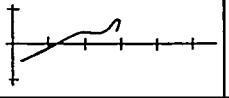	18
	.500 split flap	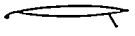	1.34	27.0	4.78	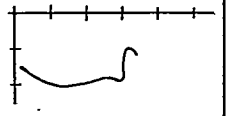	18
.975 L.E. flap	None	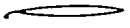	1.21	26.0	5.55	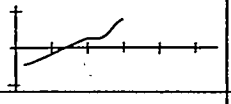	18
		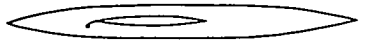	1.31	26.0	5.19	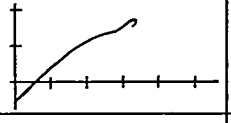	18
	.500 split flap	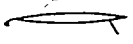	1.40	28.0	4.96	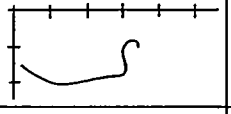	18
		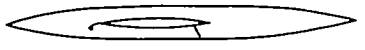	1.52	25.6	4.48	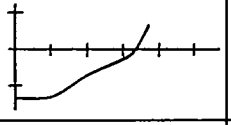	18
	.500 upper surface flap	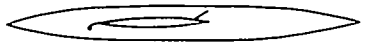	1.31	26.0	5.25	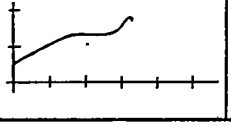	18

TABLE 7.—SUMMARY OF LONGITUDINAL STABILITY CHARACTERISTICS OF A WING WITH 32.3° OF LEADING-EDGE SWEEPFORWARD

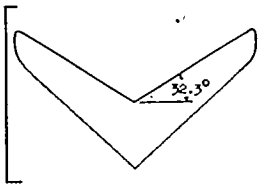

$\Lambda_{c/4} = -35.3°$ $A = 5.79$ $R_{max} = 7.80 \times 10^6$

$\lambda = 0.389$ $M_{max} = 0.24$

Airfoil sections (perpendicular to 0.225 chord line)

Root: NACA 64-210

Tip: NACA 64-210

Span of L.E. device (b/2)	Span of T.E. device (b/2)	Configuration	$C_{L_{max}}$	$\alpha_{C_{L_{max}}}$	L/D at 0.85 $C_{L_{max}}$	C_m characteristics	Reference
None	None		0.96	18.7	8.15	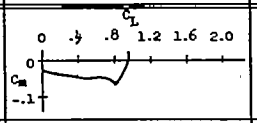	19
			1.21	26.0	3.86	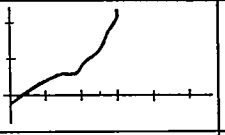	19
		$i_t = -1.6°$ $\frac{2x}{b} = .361$	1.20*	25.0	—	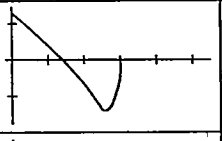	19
		$i_t = -1.3°$ $\frac{2x}{b} = .252$	1.21*	25.0	—	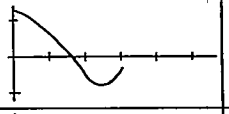	19
		$i_t = -1.1°$ $\frac{2x}{b} = .114$	1.28*	25.0	—	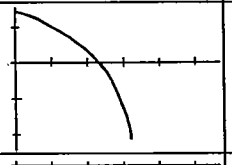	19
		$i_t = -2.2°$ $\frac{2x}{b} = -.107$	1.38*	25.0	—	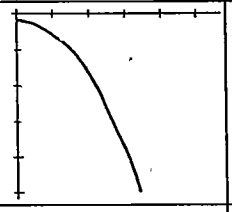	19
	.425 split flap		1.10	17.0	7.78	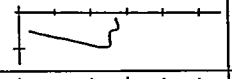	19
	.500 split flap		1.20	18.0	5.10		19
	.600 split flap		1.12	16.0	8.65	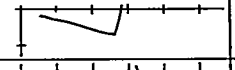	19
	.867 split flap		1.31	18.0	6.20	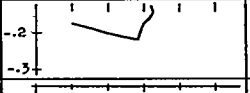	19
	.425 single slotted flap		1.13	11.0	10.10	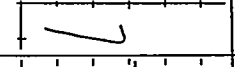	19
	.500 single slotted flap		1.24	18.0	8.45		19

*$C_{L_{max}}$ not reached.

TABLE 7.—SUMMARY OF LONGITUDINAL STABILITY CHARACTERISTICS OF A WING WITH 32.3° OF LEADING-EDGE SWEEPFORWARD—Continued

Span of L.E. device (b/2)	Span of T.E. device (b/2)	Configuration	$C_{L_{max}}$	$\alpha_{C_{L_{max}}}$	L/D at 0.85 $C_{L_{max}}$	C_m characteristics	Reference
None	.600 single slotted flap	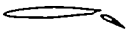	1.19	9.0	10.60	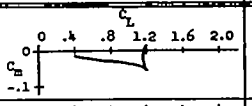	19
	.867 single slotted flap	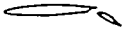	1.38	9.0	10.20		19
	.425 double slotted flap	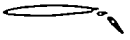	1.20	10.0	8.51	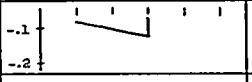	19
	.500 double slotted flap	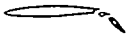	1.35	18.0	6.75	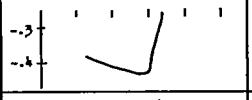	19
	.600 double slotted flap	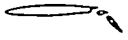	1.32	8.0	8.77	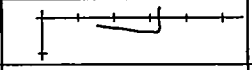	19
	.867 double slotted flap	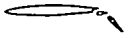	1.56	7.0	8.84		19
.410 L.E. flap	None	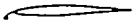	1.20	25.0	5.67	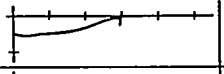	19
		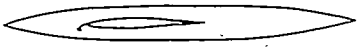	1.35*	26.0	3.66	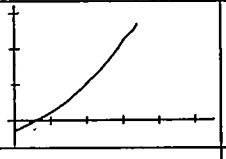	19
			1.20	24.0	6.38	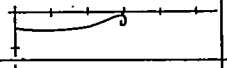	19
		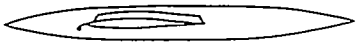	1.35	26.0	3.66	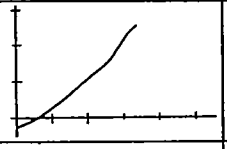	19
		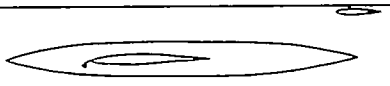 $i_t = -1.6°$ $\frac{2x}{b} = .361$	1.30*	25.0	—	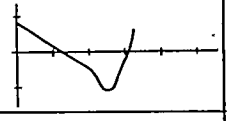	19
		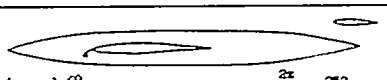 $i_t = -1.6°$ $\frac{2x}{b} = .252$	1.32*	25.0	—	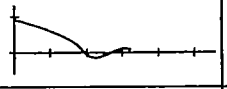	19
		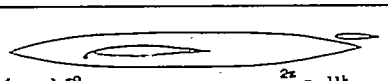 $i_t = -1.5°$ $\frac{2x}{b} = .114$	1.33*	25.0	—	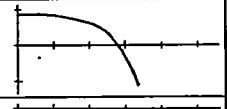	19
		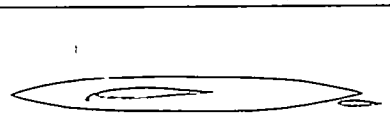 $i_t = -2.1°$ $\frac{2x}{b} = -.107$	1.42*	25.0	—	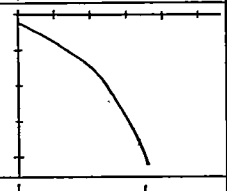	19
	.425 split flap	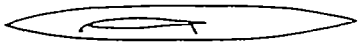	1.39*	20.0	5.37	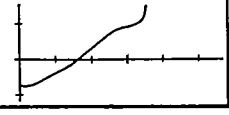	19

*$C_{L_{max}}$ not reached.

TABLE 7.—SUMMARY OF LONGITUDINAL STABILITY CHARACTERISTICS OF A WING WITH 32.3° OF LEADING-EDGE SWEEPFORWARD—Continued

Span of L.E. device (b/2)	Span of T.E. device (b/2)	Configuration	$C_{L_{max}}$	$\alpha_{C_{L_{max}}}$	L/D at 0.85 $C_{L_{max}}$	C_m characteristics	Reference
.410 L.E. flap	.500 split flap	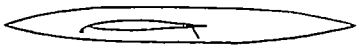	1.55	23.0	4.54	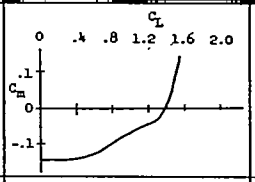	19
	.600 split flap	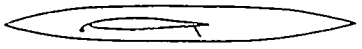	1.46	21.0	5.39	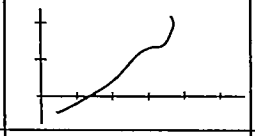	19
	.867 split flap	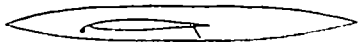	1.61	18.0	5.26	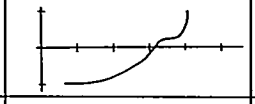	19
	.867 single slotted flap	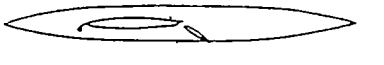	1.68	18.0	7.93	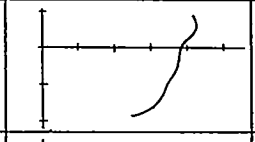	19
		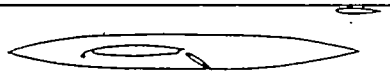 $i_t = -1.3°$ $\frac{2z}{b} = .361$	1.78	21.5	—	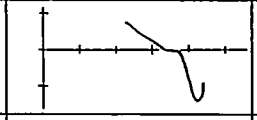	19
		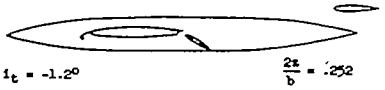 $i_t = -1.2°$ $\frac{2z}{b} = .252$	1.69	17.0	—	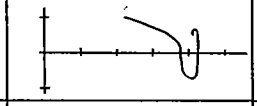	19
		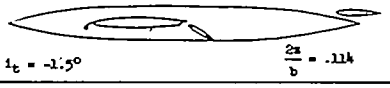 $i_t = -1.5°$ $\frac{2z}{b} = .114$	1.68	19.0	—	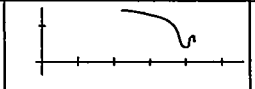	19
		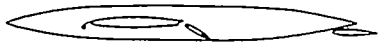 $i_t = -2.2°$ $\frac{2z}{b} = -.107$	1.82*	23.2	—	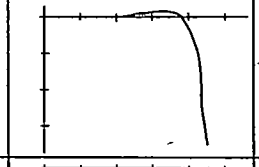	19
	.500 double slotted flap		1.76	21.2	5.77	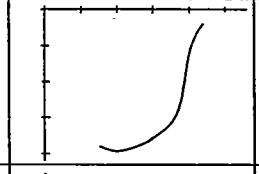	19
		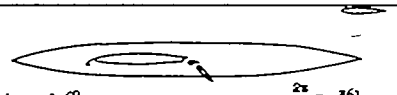 $i_t = -1.6°$ $\frac{2z}{b} = .361$	1.80	23.2	—	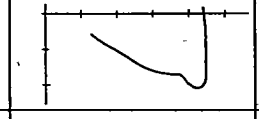	19
		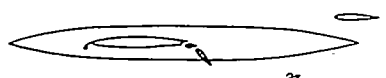 $i_t = -1.6°$ $\frac{2z}{b} = .252$	1.76	23.2	—	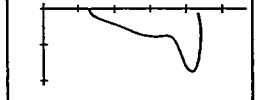	19
		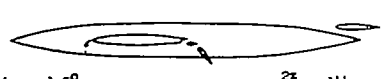 $i_t = -1.5°$ $\frac{2z}{b} = .144$	1.76	23.2	—	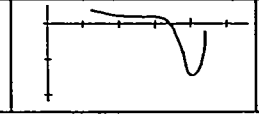	19

*$C_{L_{max}}$ not reached.

TABLE 7.—SUMMARY OF LONGITUDINAL STABILITY CHARACTERISTICS OF A WING WITH 32.3° OF LEADING-EDGE SWEEPFORWARD—Continued

Span of L.E. device (b/2)	Span of T.E. device (b/2)	Configuration	$C_{L_{max}}$	$\alpha_{C_{L_{max}}}$	L/D at 0.85 $C_{L_{max}}$	C_m characteristics	Reference
.410 L.E. flap	.500 double slotted flap	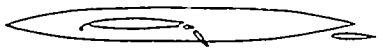 $i_t = -2.1°$ $\frac{2x}{b} = -.107$	1.88	25.5	—	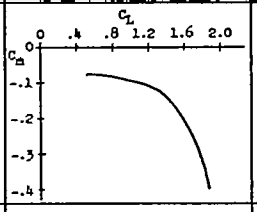	19
	.600 double slotted flap	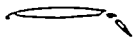	1.78	21.3	—		20
	.867 double slotted flap	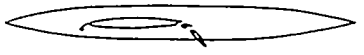	1.85	17.2	8.07	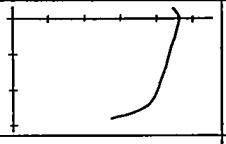	19
		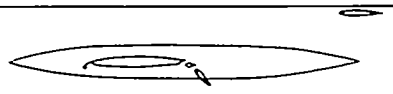 $i_t = -1.1°$ $\frac{2x}{b} = .361$	1.88	17.2	—	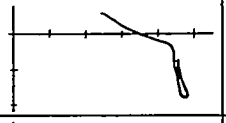	19
		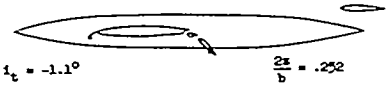 $i_t = -1.1°$ $\frac{2x}{b} = .252$	1.85	17.2	—	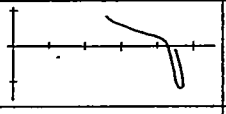	19
		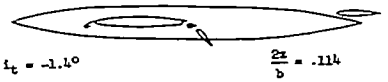 $i_t = -1.4°$ $\frac{2x}{b} = .114$	1.83	16.0	—	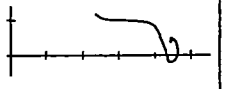	19
		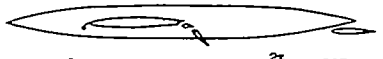 $i_t = -2.3°$ $\frac{2x}{b} = -.107$	1.86	19.0	—	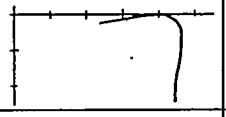	19
.575 L.E. flap	None	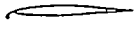	1.28*	29.0	7.27	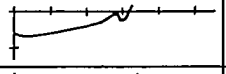	19
.750 L.E. flap	None		1.40*	29.0	8.80	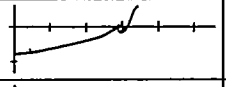	19
	.425 split flap	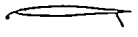	1.48	23.0	8.85	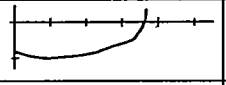	19
	.500 split flap	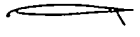	1.46*	25.0	7.53	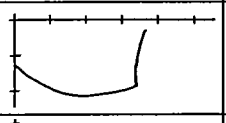	19
	.600 split flap	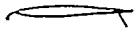	1.48*	25.0	8.38	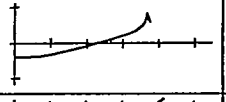	19
	.867 split flap	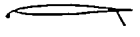	1.62	23.0	7.35	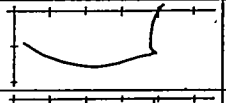	19
	.425 single slotted flap		1.62	23.0	9.19	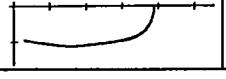	19

*$C_{L_{max}}$ not reached.

TABLE 7.—SUMMARY OF LONGITUDINAL STABILITY CHARACTERISTICS OF A WING WITH 32.3° OF LEADING-EDGE SWEEPFORWARD—Concluded

Span of L.E. device (b/2)	Span of T.E. device (b/2)	Configuration	$C_{L_{max}}$	$\alpha_{C_{L_{max}}}$	L/D at 0.85 $C_{L_{max}}$	C_m characteristics	Reference
.750 L.E. flap	.425 double slotted flap	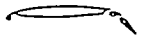	1.68	22.0	7.94	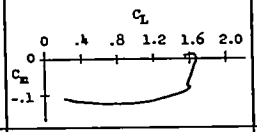	19
.410 L.E. slat	None		1.20	25.0	6.00	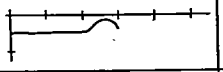	19
		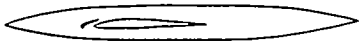	1.36	25.0	3.99	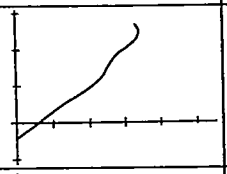	19
	.425 split flap	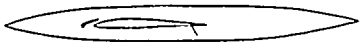	1.42	21.0	5.25	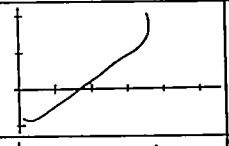	19
	.500 split flap	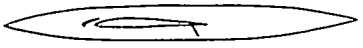	1.51*	23.0	5.35	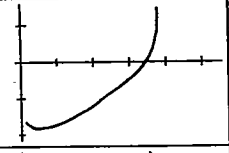	19
	.600 split flap	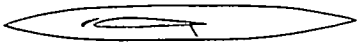	1.46	19.0	5.17	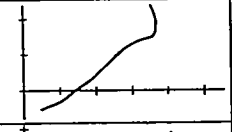	19
	.867 split flap	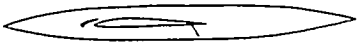	1.60	19.0	5.67	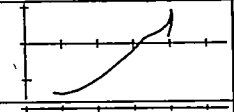	19
	None	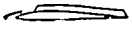	1.20*	26.0	6.37	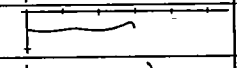	19
		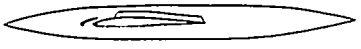	1.36	25.0	4.28	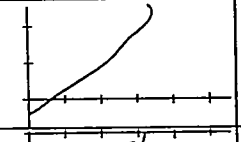	19
.575 L.E. slat	None		1.26*	26.0	6.90	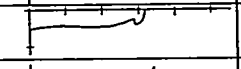	19
.750 L.E. slat	None		1.33*	26.0	8.37	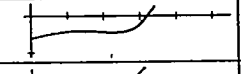	19
.410 L.E. droop	None	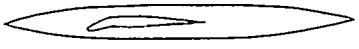	1.28*	26.0	3.70	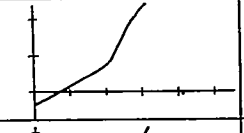	19
	None	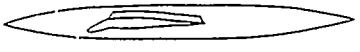	1.28	26.0	3.75	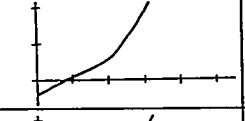	19
.575 L.E. droop	None		1.37	26.0	3.94	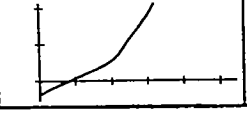	19

*$C_{L_{max}}$ not reached.

TABLE 8.—SUMMARY OF LONGITUDINAL STABILITY CHARACTERISTICS OF A WING WITH 25.9° OF LEADING-EDGE SWEEPFORWARD

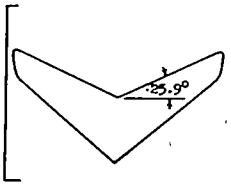

$\Lambda_{c/4} = -30°$ $A = 4.69$ $R_{max} = 18.0 \times 10^6$

$\lambda = 0.400$

Airfoil sections (variable)

Root: NACA 0015 (approximate)

Tip: NACA 23009 (approximate)

Span of L.E. device (b/2)	Span of T.E. device (b/2)	Configuration	$C_{L_{max}}$	$\alpha_{C_{L_{max}}}$	L/D at 0.85 $C_{L_{max}}$	C_m characteristics	Reference
None	None		1.18	22.5	7.70	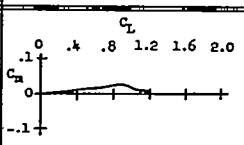	17
	.623 split flap	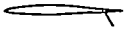	1.47	21.0	6.02	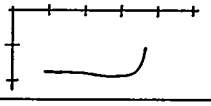	17
	.932 split flap	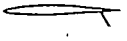	1.60	19.5	5.92	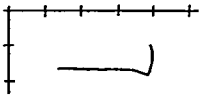	17

TABLE 9.—SUMMARY OF LONGITUDINAL STABILITY CHARACTERISTICS OF A WING WITH 0° OF LEADING-EDGE SWEEPBACK

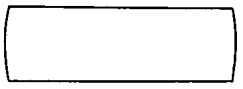

$\Lambda_{c/4} = 0°$ $A = 3.4$ $R_{max} = 8.4 \times 10^6$

$\lambda = 1.00$ $M_{max} = 0.14$

Airfoil sections (normal to line of maximum thickness)

Root: 10-percent-thick circular arc

Tip: 10-percent-thick circular arc

Span of L.E. device (b/2)	Span of T.E. device (b/2)	Configuration	$C_{L_{max}}$	$\alpha_{C_{L_{max}}}$	L/D at 0.85 $C_{L_{max}}$	C_m characteristics	Reference
None	None		0.58	15.9	6.58	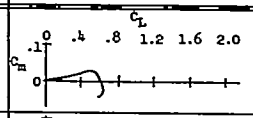	21
		0.032c round leading edge	0.80	15.5	9.06	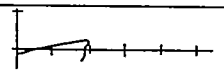	21
	.480 split flap		1.00	10.0	4.25	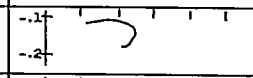	21
		0.032c round leading edge	1.25	15.5	5.33	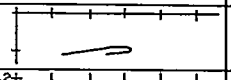	21
	.975 split flap		1.24	8.00	3.40	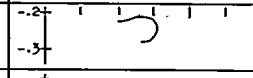	21
1.000 L.E. flap	None		1.20	22.8	7.84	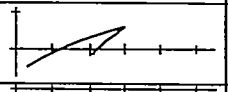	21
	.480 split flap		1.58	20.0	4.64		21
	.975 split flap		1.68	17.5	3.37	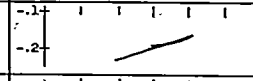	21
1.000 L.E. droop	None	$\delta_n = 30°$	0.78	18.5	8.29	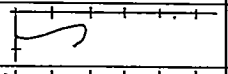	21
	.480 split flap	$\delta_n = 10°$	1.15	14.0	4.66	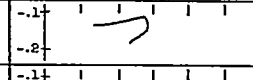	21
		$\delta_n = 20°$	1.23	16.5	4.74	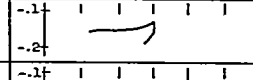	21
		$\delta_n = 30°$	1.27	18.0	4.90	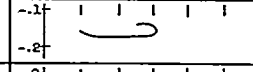	21
	.975 split flap	$\delta_n = 10°$	1.35	12.5	3.37	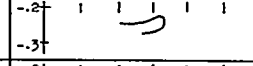	21
		$\delta_n = 20°$	1.46	16.0	3.45	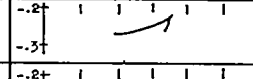	21
		$\delta_n = 30°$	1.48	16.0	3.38		21
	None	$\delta_n = 10°$ 0.032 round leading edge	1.21	23.5	7.92	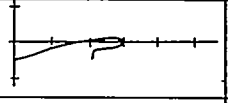	21
	.480 split flap	$\delta_n = 10°$ 0.032 round leading edge	1.45	20.0	5.14	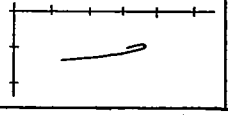	21

TABLE 10.—SUMMARY OF LONGITUDINAL STABILITY CHARACTERISTICS OF A WING WITH 0° OF LEADING-EDGE SWEEPBACK

$\Lambda_{c/4} = 0°$ $A = 4.00$ $R_{max} = 7.67 \times 10^6$

$\lambda = 1.000$ $M_{max} = 0.13$

Airfoil sections (normal to line of maximum thickness)

Root: 10-percent-thick circular arc

Tip: 10-percent-thick circular arc

Span of L.E. device (b/2)	Span of T.E. device (b/2)	Configuration	$C_{L_{max}}$	$\alpha_{C_{L_{max}}}$	L/D at 0.85 $C_{L_{max}}$	C_m characteristics	Reference
None	None	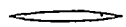	0.62	14.8	6.58	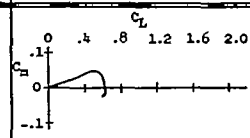	22
	.450 plain flap	$\delta_f = 30°$ 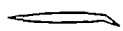	0.82	13.4	6.23	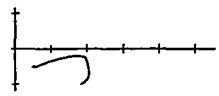	22
		$\delta_f = 45°$ 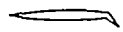	0.88	11.5	5.62	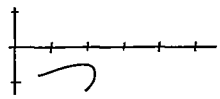	22
		$\delta_f = 60°$	0.94	10.5	5.09	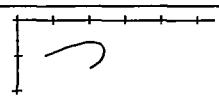	22
	1.000 plain flap	$\delta_f = 15°$ 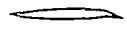	0.84	12.0	7.00	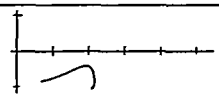	22
		$\delta_f = 30°$ 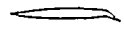	1.00	11.0	5.59	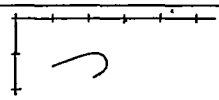	22
		$\delta_f = 45°$ 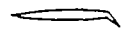	1.11	9.8	4.97	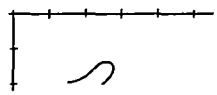	22
		$\delta_f = 60°$ 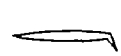	1.16	9.3	4.34	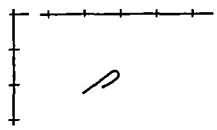	22
1.000 L.E. droop	None	$\delta_n = 10°$	0.82	18.0	8.50	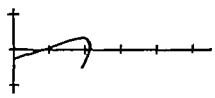	22
		$\delta_n = 20°$ 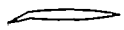	0.95	23.0	8.06	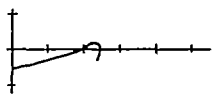	22

TABLE 10.—SUMMARY OF LONGITUDINAL STABILITY CHARACTERISTICS OF A WING WITH 0° OF LEADING-EDGE SWEEPBACK—Concluded

Span of L.E. device (b/2)	Span of T.E. device (b/2)	Configuration	$C_{L_{max}}$	$\alpha_{C_{L_{max}}}$	L/D at 0.85 $C_{L_{max}}$	C_m characteristics	Reference
1.000 L.E. droop	None	$\delta_n = 30°$ 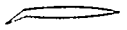	0.85	26.0	4.32	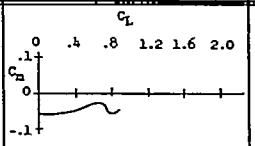	22
		$\delta_n = 36°$ 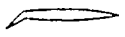	0.76	18.6	7.43	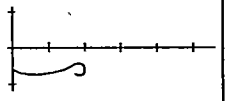	22
		$\delta_n = 40°$ 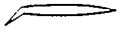	0.70	25.5	3.72	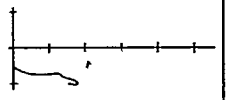	22
	.450 plain flap	$\delta_n = 20°$ $\delta_f = 60°$ 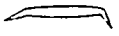	1.20	19.7	6.00	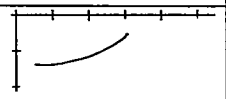	22
		$\delta_n = 30°$ $\delta_f = 60°$ 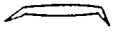	1.09	16.9	5.00	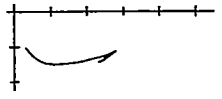	22
		$\delta_n = 36°$ $\delta_f = 60°$	1.10	17.9	5.00	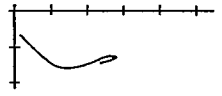	22
		$\delta_n = 40°$ $\delta_f = 60°$ 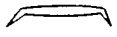	0.98	16.0	4.02	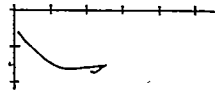	22
	1.000 plain flap	$\delta_n = 20°$ $\delta_f = 60°$ 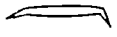	1.39	17.0	4.34	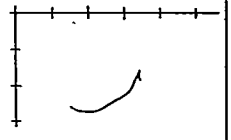	22
		$\delta_n = 30°$ $\delta_f = 60°$ 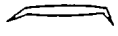	1.32	16.4	4.12	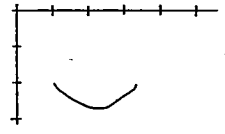	22
		$\delta_n = 36°$ $\delta_f = 60°$ 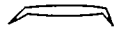	1.32	15.5	3.80	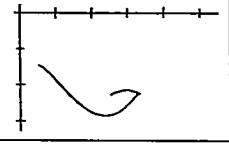	22
		$\delta_n = 40°$ $\delta_f = 60°$ 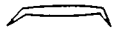	1.22	14.8	3.39	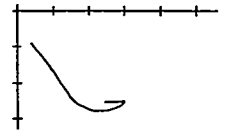	22

TABLE 11.—SUMMARY OF LONGITUDINAL STABILITY CHARACTERISTICS OF A WING WITH 3.58° OF LEADING-EDGE SWEEPBACK

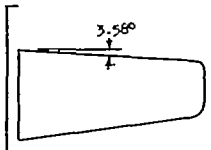

$\Lambda_{c/4} = 0°$ $A = 4.0$ $R_{max} = 12.3 \times 10^6$

$\lambda = 0.600$ $M_{max} = 0.20$

Airfoil sections (parallel to plane of symmetry)

Root: NACA 65A006

Tip: NACA 65A006

Span of L.E. device (b/2)	Span of T.E. device (b/2)	Configuration	$C_{L_{max}}$	$\alpha_{C_{L_{max}}}$	L/D at 0.85 $C_{L_{max}}$	C_m characteristics	Reference
None	None	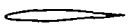	0.73	13.4	6.54	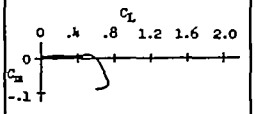	14
	.500 split flap	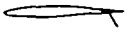	1.23	11.8	4.93	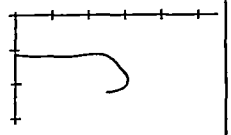	14

TABLE 12.—SUMMARY OF LONGITUDINAL STABILITY CHARACTERISTICS OF A WING WITH 3.6° OF LEADING-EDGE SWEEPBACK

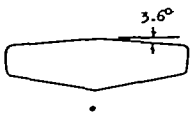

$\Lambda_{c/4} = 0°$ $A = 4.62$ $R_{max} = 18.0 \times 10^6$

$\lambda = 0.550$

Airfoil sections (variable)

Root: NACA 0015

Tip: NACA 23009

Span of L.E. device (b/2)	Span of T.E. device (b/2)	Configuration	$C_{L_{max}}$	$\alpha_{C_{L_{max}}}$	L/D at 0.85 $C_{L_{max}}$	C_m characteristics	Reference
None	None	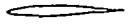	1.37	21.0	8.97	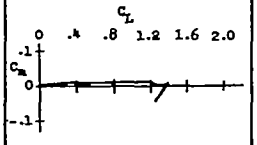	17
	.625 split flap	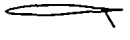	1.98	20.2	5.43	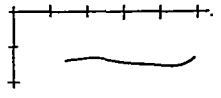	17
	.925 split flap	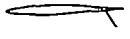	2.21	20.8	4.57	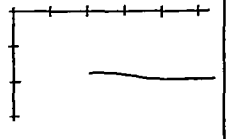	17

TABLE 13.—SUMMARY OF LONGITUDINAL STABILITY CHARACTERISTICS OF A WING WITH 9.46° OF LEADING-EDGE SWEEPBACK

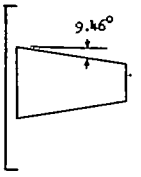

$\Lambda_{c/4} = 4.8°$ $A = 4.0$ $R_{max} = 10.0 \times 10^6$

$\lambda = 0.500$ $M_{max} = 0.20$

Airfoil sections (parallel to plane of symmetry)

Root: 4.2-percent-thick hexagonal

Tip: 4.2-percent-thick hexagonal

Span of L.E. device (b/2)	Span of T.E. device (b/2)	Configuration	$C_{L_{max}}$	$\alpha_{C_{L_{max}}}$	L/D at 0.85 $C_{L_{max}}$	C_m characteristics	Reference
None	None		0.77	13.0	5.94	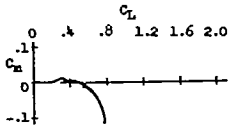	23
		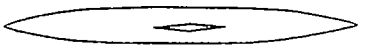	0.72	13.0	6.12	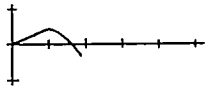	23
		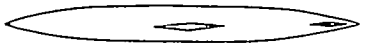 $i_t = -4°$ $\frac{2x}{b} = 0$	0.80*	15.0	5.24	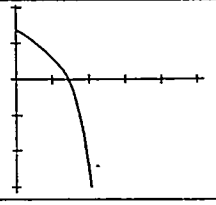	23
		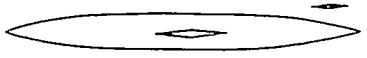 $i_t = -4°$ $\frac{2x}{b} = .361$	0.82*	18.0	4.98	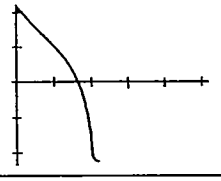	23
1.000 L.E. droop	None	$\delta_n = 20°$	0.97	18.0	9.70	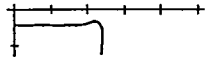	24
	.609 plain flap	$\delta_n = 30°$ $\delta_f = 50°$	1.40	16.5	5.73	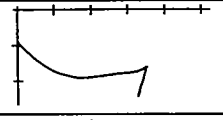	23
		$\delta_n = 30°$ $\delta_f = 50°$ 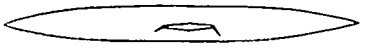	1.33	16.5	6.42	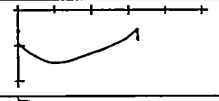	23
		$\delta_n = 30°$ $\delta_f = 50°$ 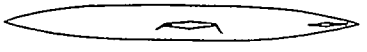 $i_t = -4°$ $\frac{2x}{b} = 0$	1.33*	15.0	6.02	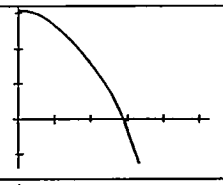	23
		$\delta_n = 30°$ $\delta_f = 50°$ 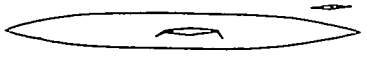 $i_t = 0°$ $\frac{2x}{b} = .361$	1.33	15.0	5.98	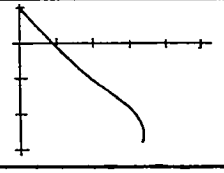	23

*$C_{L_{max}}$ not reached.

TABLE 14.—SUMMARY OF LONGITUDINAL STABILITY CHARACTERISTICS OF A WING WITH 10.46° OF LEADING-EDGE SWEEPBACK

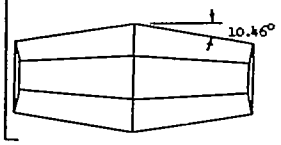

$\Lambda_{c/4} = 5.28°$ $A = 2.5$ $R_{max} = 7.6 \times 10^6$

$\lambda = 0.625$ $M_{max} = .16$

Airfoil sections (normal to line of maximum thickness)

Root: Hexagonal $t/c = .06$

Tip: Hexagonal $t/c = .06$

Span of L.E. device (b/2)	Span of T.E. device (b/2)	Configuration	$C_{L_{max}}$	$\alpha_{C_{L_{max}}}$	L/D at 0.85 $C_{L_{max}}$	C_m characteristics	Reference
None	None		.725	14.7°	5.32	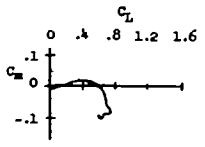	25
			—	—	—	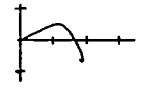	25
		$l/\bar{c} = 2$ $\frac{2z}{b} = .40$ $i_t = -2.00°$	—	—	—	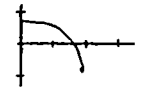	25
		$l/\bar{c} = 2$ $\frac{2z}{b} = .177$ $i_t = -1.75°$	—	—	—	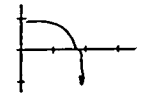	25
		$l/\bar{c} = 2$ $\frac{2z}{b} = -.177$ $i_t = -2.14°$	—	—	—	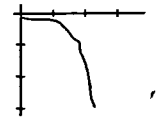	25
			—	—	—	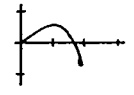	25
		$l/\bar{c} = 3$ $\frac{2z}{b} = .40$ $i_t = -1.99°$	—	—	—	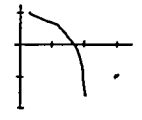	25
		$l/\bar{c} = 3$ $\frac{2z}{b} = .177$ $i_t = -1.73°$	—	—	—	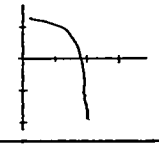	25
		$l/\bar{c} = 3$ $\frac{2z}{b} = .177$ $i_t = 2.15°$	—	—	—	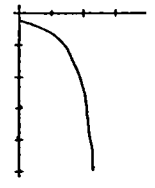	25
	.35 T.E. flaps	$\delta_f = 30°$	.955	12.9°	6.98	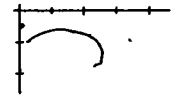	25

TABLE 14.—SUMMARY OF LONGITUDINAL STABILITY CHARACTERISTICS OF A WING WITH 10.46° OF LEADING-EDGE SWEEPBACK—Continued

Span of L.E. device (b/2)	Span of T.E. device (b/2)	Configuration	$C_{L_{max}}$	$\alpha_{C_{L_{max}}}$	L/D at 0.85 $C_{L_{max}}$	C_m characteristics	Reference
None	.35 T.E. flaps	$\delta_f = 40°$	1.025	12.9°	4.85	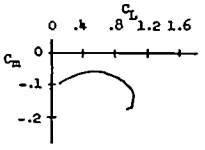	25
		$\delta_f = 50°$	1.070	13.0°	4.29	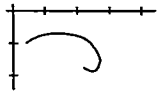	25
	.75 T.E. flaps	$\delta_f = 30°$	1.16	12.0°	4.58	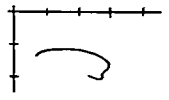	25
		$\delta_f = 40°$	1.26	12.1°	3.96	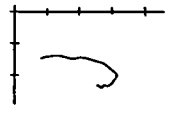	25
		$\delta_f = 50°$	1.34	12.2°	3.59	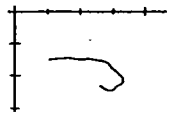	25
		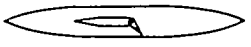 $\delta_f = 50°$	—	—	—	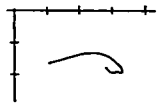	25
.775 L.E. droop	None	$\delta_n = 10°$	0.84*	21.8	5.25	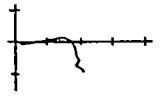	25
		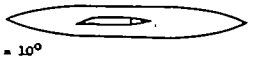 $\delta_n = 10°$	—	—	—	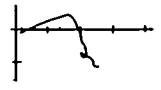	25
	.35 T.E. flaps	$\delta_n = 10°$ $\delta_f = 50°$	1.09	14.2	4.41	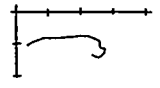	25
		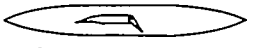 $\delta_n = 10°$ $\delta_f = 50°$	—	—	—	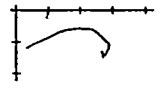	25
	.75 T.E. flaps	$\delta_n = 10°$ $\delta_f = 50°$	1.38	14.2	3.44	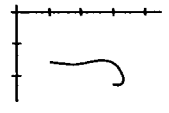	25

*$C_{L_{max}}$ not reached.

TABLE 14.—SUMMARY OF LONGITUDINAL STABILITY CHARACTERISTICS OF A WING WITH 10.46° OF LEADING-EDGE SWEEPBACK—Continued

Span of L.E. device (b/2)	Span of T.E. device (b/2)	Configuration	$C_{L_{max}}$	$\alpha_{C_{L_{max}}}$	L/D at 0.85 $C_{L_{max}}$	C_m characteristics	Reference
.775 L.E. droop	.75 T.E. flaps	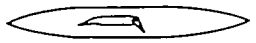 $\delta_n = 10°$ $\delta_f = 50°$	—	—	—	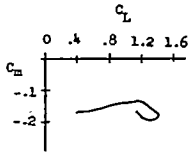	25
	None	$\delta_n = 20°$	.81	15.3	7.10	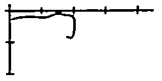	25
		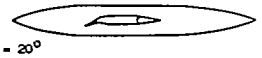 $\delta_n = 20°$	—	—	—	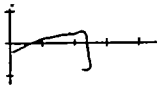	25
	.35 T.E. flaps	$\delta_n = 20°$ $\delta_f = 50°$	1.10	14.9	4.82	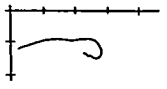	25
		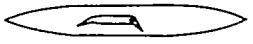 $\delta_n = 20°$ $\delta_f = 50°$	—	—	—	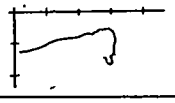	25
	.75 T.E. flaps	$\delta_n = 20°$ $\delta_f = 50°$	1.36	15.1	3.50	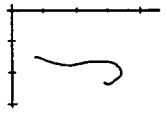	25
		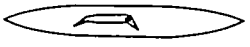 $\delta_n = 20°$ $\delta_f = 50°$	—	—	—	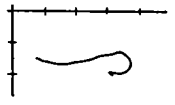	25
	None	$\delta_n = 30°$	.87	16.6	6.84	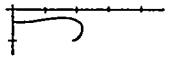	25
		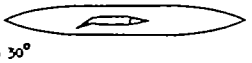 $\delta_n = 30°$	—	—	—	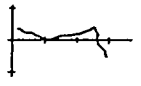	25
		$l/\bar{c} = 2$ $i_t = -1.96°$ 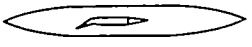 $\delta_n = 30°$ $\frac{2z}{b} = .40$	—	—	—	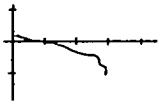	25
		$l/\bar{c} = 2$ $i_t = -1.75°$ 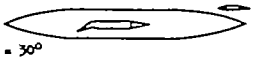 $\delta_n = 30°$ $\frac{2z}{b} = .177$	—	—	—	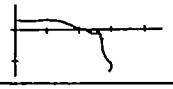	25
		$l/\bar{c} = 2$ $i_t = -2.16°$ 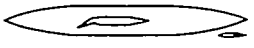 $\delta_n = 30°$ $\frac{2z}{b} = -.177$	—	—	—		25

TABLE 14.—SUMMARY OF LONGITUDINAL STABILITY CHARACTERISTICS OF A WING WITH 10.46° OF LEADING-EDGE SWEEPBACK—Continued

Span of L.E. device (b/2)	Span of T.E. device (b/2)	Configuration	$C_{L_{max}}$	$\alpha_{C_{L_{max}}}$	L/D at 0.85 $C_{L_{max}}$	C_m characteristics	Reference
.775 L.E. droop	.35 T.E. flaps	$\delta_n = 30°$ $\delta_f = 50°$	1.17	16.2	4.52	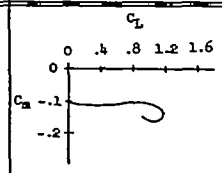	25
		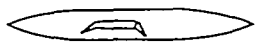 $\delta_n = 30°$ $\delta_f = 50°$	—	—	—	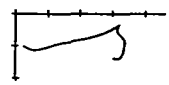	25
		$l/\bar{c} = 2$ $\frac{2x}{b} = .40$ $i_t = -1.96°$ $\delta_n = 30°$ $\delta_f = 50°$	—	—	—	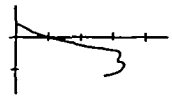	25
		$l/\bar{c} = 2$ $\frac{2x}{b} = .177$ $i_t = -1.75°$ 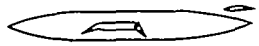 $\delta_n = 30°$ $\delta_f = 50°$	—	—	—	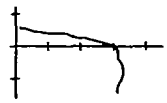	25
		$l/\bar{c} = 2$ $\frac{2x}{b} = -.177$ $i_t = -2.14°$ 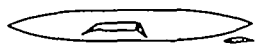 $\delta_n = 30°$ $\delta_f = 50°$	—	—	—	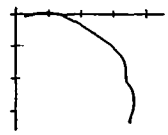	25
.775 L.E. droop	.35 T.E. flaps	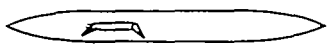 $\delta_n = 30°$ $\delta_f = 50°$	—	—	—	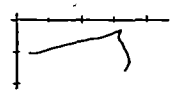	25
		$l/\bar{c} = 3$ $\frac{2x}{b} = .40$ 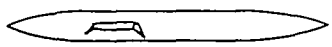 $i_t = -1.98°$ $\delta_n = 30°$ $\delta_f = 50°$	—	—	—		25
		$l/\bar{c} = 3$ $\frac{2x}{b} = .177$ 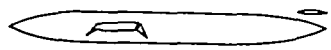 $i_t = -1.70°$ $\delta_n = 30°$ $\delta_f = 50°$	—	—	—	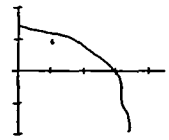	25
		$l/\bar{c} = 3$ $\frac{2x}{b} = -.177$ 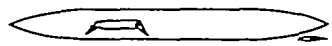 $i_t = -2.10°$ $\delta_n = 30°$ $\delta_f = 50°$	—	—	—	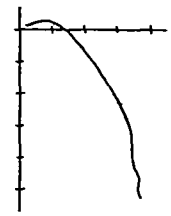	25
.775 L.E. droop	.75 T.E. flaps	$\delta_n = 30°$ $\delta_f = 50°$	1.39	16.3	3.81	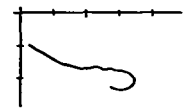	25

TABLE 14.—SUMMARY OF LONGITUDINAL STABILITY CHARACTERISTICS OF A WING WITH 10.46° OF LEADING-EDGE SWEEPBACK—Concluded

Span of L.E. device (b/2)	Span of T.E. device (b/2)	Configuration	$C_{L_{max}}$	$\alpha_{C_{L_{max}}}$	L/D at 0.85 $C_{L_{max}}$	C_m characteristics	Reference
.775 L.E. droop	.75 T.E. flaps	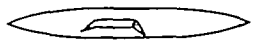 $\delta_n = 30°$ $\delta_f = 50°$	—	—	—	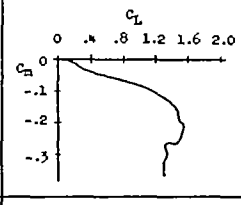	25
		$l/\bar{c} = 2$ $\frac{2z}{b} = .40$ $i_t = -3.96°$ 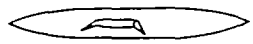 $\delta_n = 30°$ $\delta_f = 50°$	—	—	—	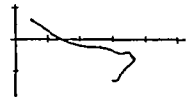	25
		$l/\bar{c} = 2$ $\frac{2z}{b} = .177$ $i_t = -1.70°$ 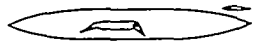 $\delta_n = 30°$ $\delta_f = 50°$	—	—	—		25
		$l/\bar{c} = 2$ $\frac{2z}{b} = -.177$ $i_t = -2.14°$ 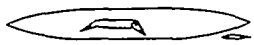 $\delta_n = 30°$ $\delta_f = 50°$	—	—	—		25
		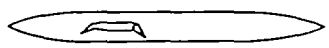 $\delta_n = 30°$ $\delta_f = 50°$	—	—	—	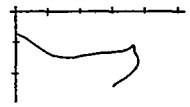	25
		$l/\bar{c} = 3$ $\frac{2z}{b} = .40$ 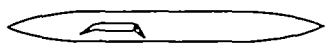 $\delta_n = 30°$ $i_t = -1.89°$ $\delta_f = 50°$	—	—	—	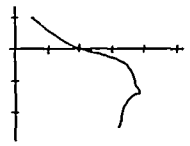	25
		$l/\bar{c} = 3$ $\frac{2z}{b} = .177$ 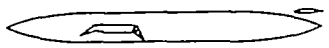 $\delta_n = 30°$ $i_t = -1.68°$ $\delta_f = 50°$	—	—	—	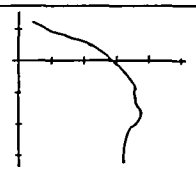	25
		$l/\bar{c} = 3$ $\frac{2z}{b} = -.177$ 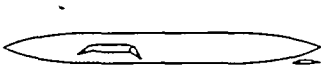 $\delta_n = 30°$ $i_t = -2.12°$ $\delta_f = 50°$	—	—	—	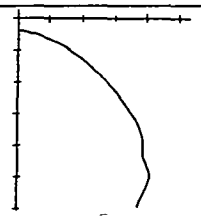	25
None	1.00 T.E. flaps	$\delta_f = 50°$	—	—	—	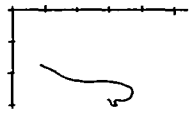	25

TABLE 15.—SUMMARY OF LONGITUDINAL STABILITY CHARACTERISTICS OF A WING WITH 32.6° OF LEADING-EDGE SWEEPBACK

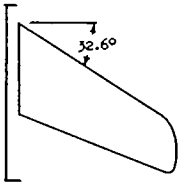

$\Lambda_{c/4} = 30°$ $A = 4.0$ $R_{max} = 12.0 \times 10^6$

$\lambda = 0.600$ $M_{max} = 0.20$

Airfoil sections (parallel to plane of symmetry)

Root: NACA 65A006

Tip: NACA 65A006

Span of L.E. device (b/2)	Span of T.E. device (b/2)	Configuration	$C_{L_{max}}$	$\alpha_{C_{L_{max}}}$	L/D at 0.85 $C_{L_{max}}$	C_m characteristics	Reference
None	None	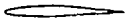	0.92	19.5	4.89	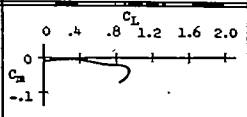	14
	.500 split flap	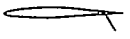	1.18	14.0	4.37	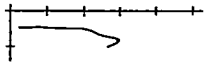	14

TABLE 16.—SUMMARY OF LONGITUDINAL STABILITY CHARACTERISTICS OF A WING WITH 33.4° OF LEADING-EDGE SWEEPBACK

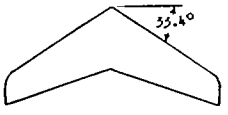

$\Lambda_{c/4} = 30°$ $A = 4.84$ $R_{max} = 18.0 \times 10^6$

$\lambda = 0.440$

Airfoil sections (variable)

Root: NACA 0015 (approximate)
Tip: NACA 23009 (approximate)

Span of L.E. device (b/2)	Span of T.E. device (b/2)	Configuration	$C_{L_{max}}$	$\alpha_{C_{L_{max}}}$	L/D at 0.85 $C_{L_{max}}$	C_m characteristics	Reference
None	None	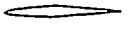	1.28	20.0	9.87	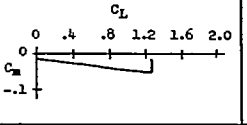	17
	.625 split flap	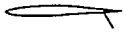	1.77	18.5	5.83	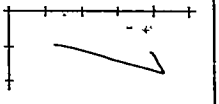	17
	.970 split flap	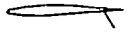	1.70	15.5	4.67	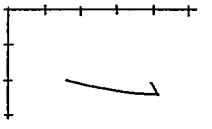	17

TABLE 17.—SUMMARY OF LONGITUDINAL STABILITY CHARACTERISTICS OF A WING WITH 36.25° OF LEADING-EDGE SWEEPBACK

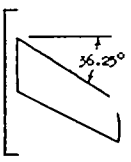

$\Lambda_{c/4} = 35°$ $A = 5.14$ $R_{max} = 10.0 \times 10^6$

$\lambda = 0.713$ $M_{max} = 0.25$

Airfoil sections (parallel to plane of symmetry)

Span of L.E. device (b/2)	Span of T.E. device (b/2)	Configuration	NACA airfoil section	$C_{L_{max}}$	$\alpha_{C_{L_{max}}}$	L/D at 0.85 $C_{L_{max}}$	C_m characteristics	Reference
None	None		65_1A012	0.98	17.0	13.6	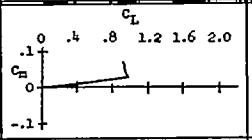	26
			64_1A312	1.30	21.0	10.5	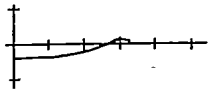	26
			64_1A612	1.43	22.0	9.85	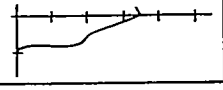	26

TABLE 18.—SUMMARY OF LONGITUDINAL STABILITY CHARACTERISTICS OF A WING WITH 36.25° OF LEADING-EDGE SWEEPBACK

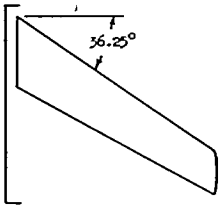

$\Lambda_{c/4} = 35°$ $A = 10.07$ $R_{max} = 10.0 \times 10^6$

$\lambda = 0.500$ $M_{max} = 0.25$

Airfoil sections (parallel to plane of symmetry)

Span of L.E. device (b/2)	Span of T.E. device (b/2)	Configuration	NACA airfoil section	$C_{L_{max}}$	$\alpha_{C_{L_{max}}}$	L/D at 0.85 $C_{L_{max}}$	C_m characteristics	Reference
None	None		65_1A012	0.96	16.0	23.3	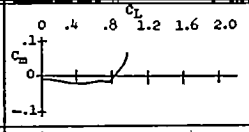	26
			64_1A312	1.24	21.0	17.0	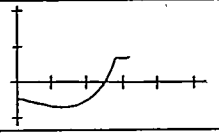	26
			64_1A612	1.32	20.0	16.0	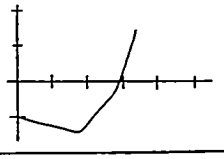	26

TABLE 19.—SUMMARY OF LONGITUDINAL STABILITY CHARACTERISTICS OF A WING WITH 37.25° OF LEADING-EDGE SWEEPBACK

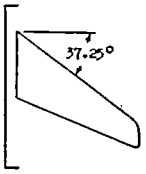

$\Lambda_{c/4} = 35°$ $A = 6.0$ $R_{max} = 9.35 \times 10^6$

$\lambda = 0.5$ $M_{max} = 0.18$

Airfoil sections (perpendicular to 0.270 chord line)

Root: NACA 64_1-212
Tip: NACA 64_1-212

Span of L.E. device (b/2)	Span of T.E. device (b/2)	Configuration	$C_{L_{max}}$	$\alpha_{C_{L_{max}}}$	L/D at 0.85 $C_{L_{max}}$	C_m characteristics	Reference
None	None	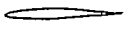	1.27	19.0	12.35	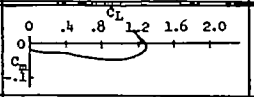	27
	.500 split flap	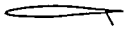	1.55	17.1	7.46	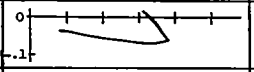	27
	.975 split flap	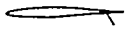	1.65	15.1	6.36		27
	.500 double slotted flap	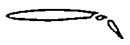	1.92	14.3	7.09	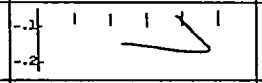	27
	.975 double slotted flap	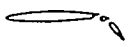	2.32	11.9	6.85	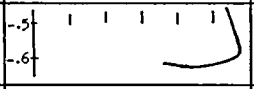	27
.250 L.E. flap	.500 split flap	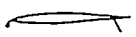	1.36	15.0	13.33	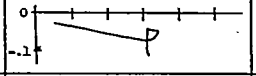	27
	.500 double slotted flap	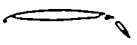	1.76	11.1	7.75	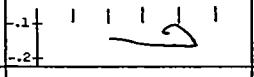	27
.375 L.E. flap	None	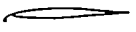	1.25	19.9	11.82	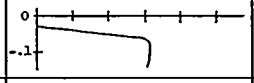	27
	.500 split flap	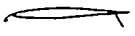	1.37	21.9	12.10	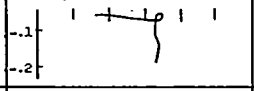	27
	.500 double slotted flap	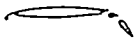	1.81	15.2	7.15		27
.500 L.E. flap	None	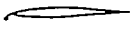	1.39	24.0	9.80		27
	.500 split flap	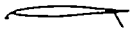	1.46	15.0	8.26	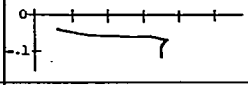	27
	.500 double slotted flap	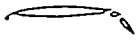	1.87	13.4	7.05	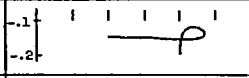	27
.650 L.E. flap	None	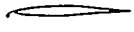	1.40	24.0	10.50	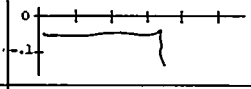	27
	.500 split flap	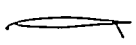	1.63	18.2	7.82	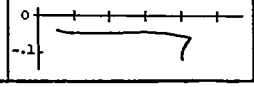	27

TABLE 19.—SUMMARY OF LONGITUDINAL STABILITY CHARACTERISTICS OF A WING WITH 37.25° OF LEADING-EDGE SWEEPBACK—Concluded

Span of L.E. device (b/2)	Span of T.E. device (b/2)	Configuration	$C_{L_{max}}$	$\alpha_{C_{L_{max}}}$	L/D at 0.85 $C_{L_{max}}$	C_m characteristics	Reference
.650 L.E. flap	.500 double slotted flap	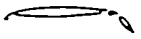	2.06	16.4	6.90	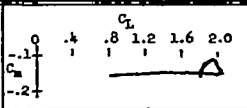	27
.700 L.E. flap	None		1.41	25.0	10.75	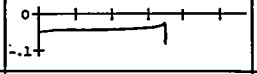	27
	.500 split flap	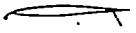	1.69	21.3	7.75	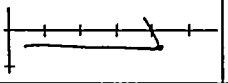	27
.950 L.E. flap	None		1.65	24.3	9.49	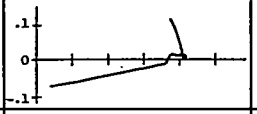	27
.500 L.E. slat	None		1.42	26.0	8.13	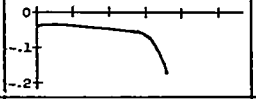	27
	.500 split flap	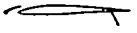	1.43	15.0	8.06	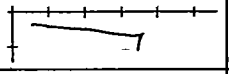	27
	.500 double slotted flap	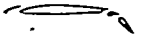	1.85	14.3	7.10	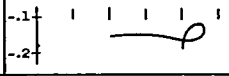	27
.500 L.E. droop	None	$\delta_n = 20°$	1.28	23.0	11.45	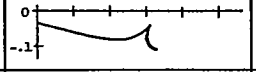	27
		$\delta_n = 30°$ 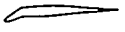	1.28	20.0	11.90	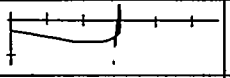	27
		$\delta_n = 30°$ 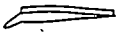	1.28	18.9	11.75	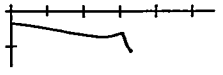	27
		$\delta_n = 40°$ 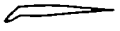	1.26	20.0	11.88	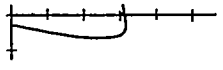	27
	.500 split flap	$\delta_n = 30°$ 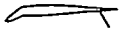	1.55	18.1	8.06	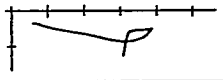	27
		$\delta_n = 30°$ 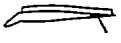	1.49	16.0	8.20	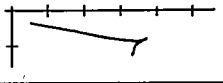	27
	.500 double slotted flap	$\delta_n = 30°$ 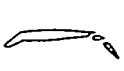	1.94	15.3	7.10	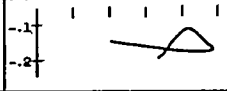	27
		$\delta_n = 30°$	2.02	17.4	6.95	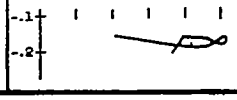	27

TABLE 20.—SUMMARY OF LONGITUDINAL STABILITY CHARACTERISTICS OF A WING WITH 42° OF LEADING-EDGE SWEEPBACK

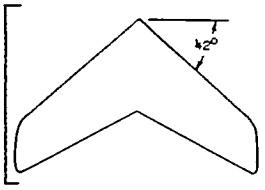

$\Lambda_{c/4} = 40°$ $A = 4.01$ $R_{max} = 9.50 \times 10^6$

$\lambda = 0.625$ $M_{max} = 0.22$

Airfoil sections (perpendicular to 0.273 chord line)

Root: NACA 64_1-112

Tip: NACA 64_1-112

Span of L.E. device (b/2)	Span of T.E. device (b/2)	Configuration	$C_{L_{max}}$	$\alpha_{C_{L_{max}}}$	L/D at 0.85 $C_{L_{max}}$	C_m characteristics (b)	Reference
None	None		1.02	19.0	11.52	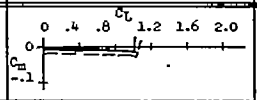	28
			1.06	18.0	—	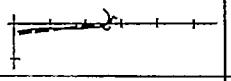	29
		$i_t = -3.7°$ $\frac{2z}{b} = .509$	1.08	17.0	—	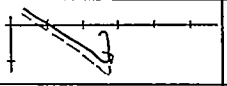	29
		$i_t = -3.1°$ $\frac{2z}{b} = .254$	1.09	17.0	—	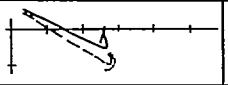	29
		$i_t = -4.1°$ $\frac{2z}{b} = .031$	1.14[a]	22.0	—	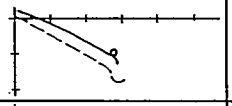	29
			1.05	22.0	—	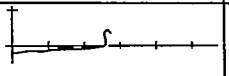	29
		$i_t = -3.6°$ $\frac{2z}{b} = .417$	1.08	18.0	—	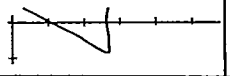	29
		$i_t = -3.6°$ $\frac{2z}{b} = .162$	1.08	22.0	—	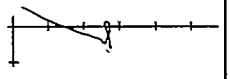	29
		$i_t = -4.2°$ $\frac{2z}{b} = -.061$	1.15[a]	22.0	—	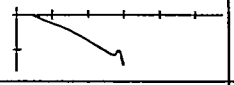	29
			1.05	18.0	—	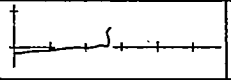	29
		$i_t = -3.5°$ $\frac{2z}{b} = .254$	1.08	18.0	—	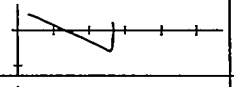	29
		$i_t = -4.1°$ $\frac{2z}{b} = -.146$	1.13	22.0	—	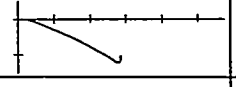	29
	.500 split flap		1.28	17.3	7.26	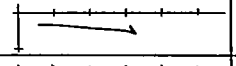	30
			1.26	16.3	7.05	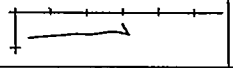	30
			1.26	16.3	7.28	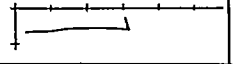	30
			1.28	16.4	7.25	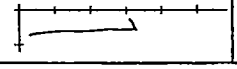	30

[a] $C_{L_{max}}$ not reached.

[b] Dash curves for distance 0.925 from ground.

TABLE 20.—SUMMARY OF LONGITUDINAL STABILITY CHARACTERISTICS OF A WING WITH 42° OF LEADING-EDGE SWEEPBACK—Continued

Span of L.E. device (b/2)	Span of T.E. device (b/2)	Configuration	$C_{L_{max}}$	$\alpha_{C_{L_{max}}}$	L/D at 0.85 $C_{L_{max}}$	C_m characteristics	Reference
None	.500 upper-surface flap .500 split flap	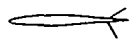	1.15	15.0	6.26	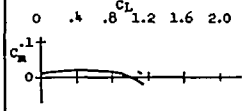	31
	.450 upper-surface flap .500 split flap	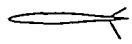	1.14	15.1	6.06	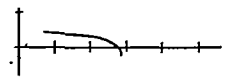	31
	.575 upper-surface flap .500 split flap	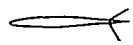	1.13	15.1	5.86	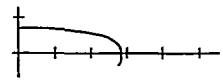	31
	.500 ext. split flap	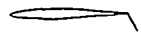	1.40	16.5	7.09	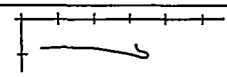	32
	.575 upper-surface flap .500 ext. split flap	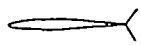	1.29	18.4	5.08	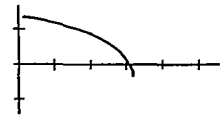	32
.425 L.E. flap	None	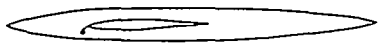	1.10	20.2	—	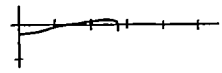	33
		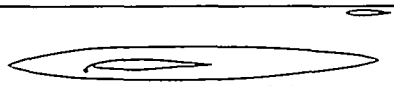 $i_t = -3.4°$ $\frac{2z}{b} = .417$	1.13	20.2	—	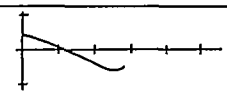	33
		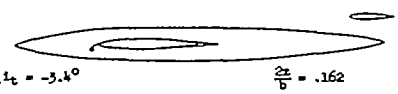 $i_t = -3.4°$ $\frac{2z}{b} = .162$	1.13	20.2	—	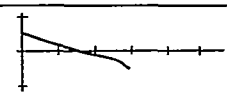	33
		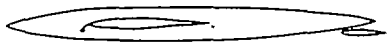 $i_t = -4.2°$ $\frac{2z}{b} = -.061$	1.19	20.2	—	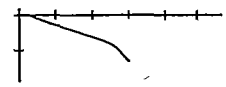	33
	.500 split flap	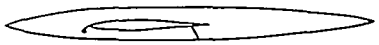	1.23	17.2	—	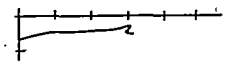	33
		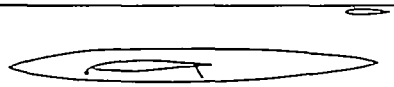 $i_t = -3.4°$ $\frac{2z}{b} = .417$	1.24	18.4	—	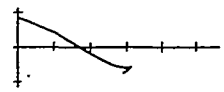	33
		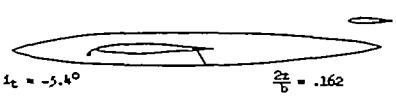 $i_t = -5.4°$ $\frac{2z}{b} = .162$	1.20	16.2	—	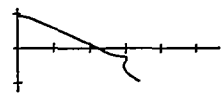	33
		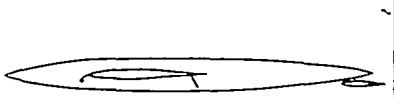 $i_t = -4.3°$ $\frac{2z}{b} = -.061$	1.26	17.5	—	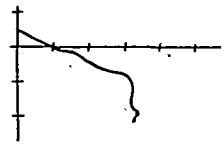	33

TABLE 20.—SUMMARY OF LONGITUDINAL STABILITY CHARACTERISTICS OF A WING WITH 42° OF LEADING-EDGE SWEEPBACK—Continued

Span of L.E. device (b/2)	Span of T.E. device (b/2)	Configuration	$C_{L_{max}}$	$\alpha_{C_{L_{max}}}$	L/D at 0.85 $C_{L_{max}}$	C_m characteristics (a)	Reference
.575 L.E. flap	None		1.24	25.0	7.30		31
	.500 split flap		1.39	18.6	6.77		28
			1.36	20.5	—		29
		$i_t = -3.4°$ $\frac{2x}{b} = .509$	1.41	20.5	—		29
		$i_t = -3.2°$ $\frac{2x}{b} = .254$	1.35	19.4	—		29
		$i_t = -4.1°$ $\frac{2x}{b} = .031$	1.42	20.4	—		29
			1.42	21.5	—		29
		$i_t = -3.8°$ $\frac{2x}{b} = .417$	1.46	21.5	—		29
		$i_t = -3.4°$ $\frac{2x}{b} = .162$	1.44	22.5	—		29
		$i_t = -4.5°$ $\frac{2x}{b} = -.061$	1.51	22.0	—		29
			1.42	22.4	—		33
		$i_t = -3.5°$ $\frac{2x}{b} = .417$	1.43	21.5	—		33
		$i_t = -3.4°$ $\frac{2x}{b} = .162$	1.41	21.5	—		33
		$i_t = -4.0°$ $\frac{2x}{b} = -.061$	1.49	21.8	—		33

[a]Dash curves are for distance 0.92$\bar{c}$ from ground.

TABLE 20.—SUMMARY OF LONGITUDINAL STABILITY CHARACTERISTICS OF A WING WITH 42° OF LEADING-EDGE SWEEPBACK—Continued

Span of L.E. device (b/2)	Span of T.E. device (b/2)	Configuration	$C_{L_{max}}$	$\alpha_{C_{L_{max}}}$	L/D at 0.85 $C_{L_{max}}$	C_m characteristics (b)	Reference
.575 L.E. flap	.500 split flap	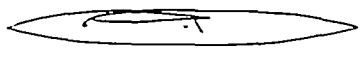	1.52	23.5	5.62	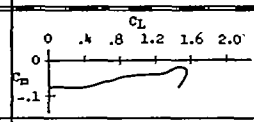	34
		$i_t = -3.5°$ $\frac{2z}{b} = .254$	1.45[a]	21.6	—	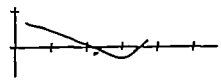	29
		$i_t = -4.0°$ $\frac{2z}{b} = -.146$	1.56[a]	21.6	—	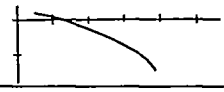	29
		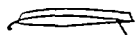	1.32	18.0	—	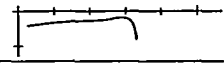	29
		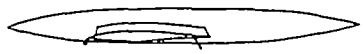	1.31	19.1	—	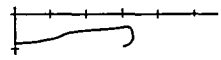	29
		$i_t = -5.4°$ $\frac{2z}{b} = .509$	1.38	19.1	—	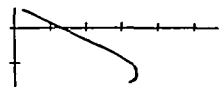	29
		$i_t = -3.2°$ $\frac{2z}{b} = .254$	1.31[a]	19.1	—	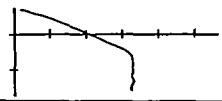	29
		$i_t = -4.1°$ $\frac{2z}{b} = .031$	1.38	19.1	—	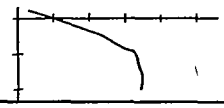	29
		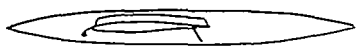	1.41	20.5	—	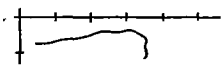	29
		$i_t = -3.4°$ $\frac{2z}{b} = .417$	1.44	20.5	—	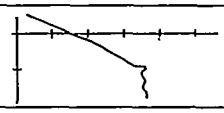	29
		$i_t = -3.4°$ $\frac{2z}{b} = .162$	1.41	21.0	—	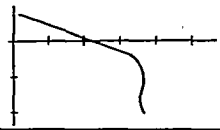	29
.575 L.E. flap	.975 split flap	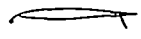	1.53	18.5	—	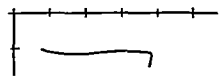	33
	.500 ext. split flap	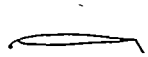	1.52	19.1	6.40	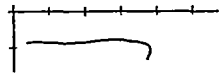	32
.725 L.E. flap	None	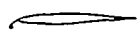	1.29[a]	27.4	7.82	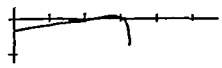	32
	.500 split flap	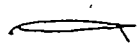	1.58	24.0	6.25	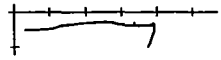	31
		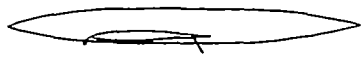	1.50[a]	25.8	—	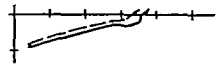	29

[a] $C_{L_{max}}$ not reached.

[b] Dash curves are for distance 0.92$\bar{c}$ from ground.

TABLE 20.—SUMMARY OF LONGITUDINAL STABILITY CHARACTERISTICS OF A WING WITH 42° OF LEADING-EDGE SWEEPBACK—Continued

Span of L.E. device (b/2)	Span of T.E. device (b/2)	Configuration	$C_{L_{max}}$	$\alpha_{C_{L_{max}}}$	L/D at 0.85 $C_{L_{max}}$	C_m characteristics (b)	Reference
.725 L.E. flap	.500 split flap	$i_t = -3.4°$ $\frac{2x}{b} = .509$	1.52	23.8	—		29
		$i_t = -3.2°$ $\frac{2x}{b} = .254$	1.51[a]	23.8	—		29
		$i_t = -4.1°$ $\frac{2x}{b} = .031$	1.59[a]	23.8	—		29
			1.52	24.0	—		29
		$i_t = -3.3°$ $\frac{2x}{b} = .417$	1.58	24.0	—		29
		$i_t = -3.5°$ $\frac{2x}{b} = .162$	1.56[a]	24.0	—		29
		$i_t = -4.2°$ $\frac{2x}{b} = -.061$	1.65[a]	24.0	—		29
			1.57[a]	21.8	—		29
		$i_t = -3.5°$ $\frac{2x}{b} = .254$	1.56[a]	22.0	—		29
		$i_t = -4.0°$ $\frac{2x}{b} = -.146$	1.62[a]	21.8	—		29
			1.43[a]	22.5	—		29
		$i_t = -3.2°$ $\frac{2x}{b} = .254$	1.53[a]	23.8	—		29
		$i_t = -4.1°$ $\frac{2x}{b} = .031$	1.60[a]	23.8	—		29
			1.68	23.8	—		29
		$i_t = -3.4°$ $\frac{2x}{b} = .417$	1.68	26.5	—		29
		$i_t = -3.5°$ $\frac{2x}{b} = .162$	1.68	26.5	—		29

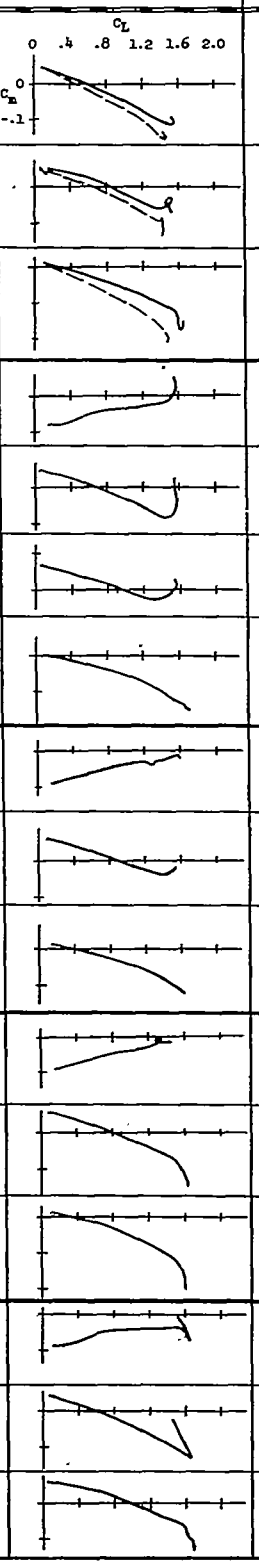

[a] $C_{L_{max}}$ not reached.

[b] Dash curves for distance 0.92$\bar{c}$ from ground.

TABLE 20.—SUMMARY OF LONGITUDINAL STABILITY CHARACTERISTICS OF A WING WITH 42° OF LEADING-EDGE SWEEPBACK—Continued

Span of L.E. device (b/2)	Span of T.E. device (b/2)	Configuration	$C_{L_{max}}$	$\alpha_{C_{L_{max}}}$	L/D at 0.85 $C_{L_{max}}$	C_m characteristics	Reference
.725 L.E. flap	.500 ext. split flap	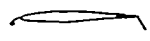	1.73	23.8	5.88	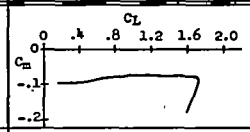	32
.975 L.E. flap	None		1.60	27.0	7.46	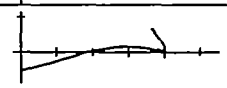	31
	.500 split flap	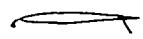	1.79	25.0	6.14	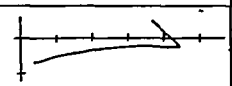	31
.575 L.E. slat	None	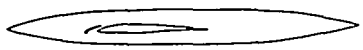	1.43	31.0	3.57	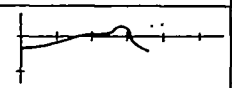	31
		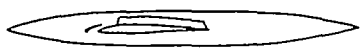	1.48	31.0	3.76	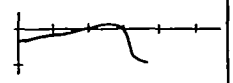	31
	.500 split flap	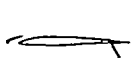	1.33	19.0	6.50	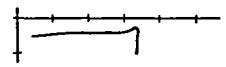	31
		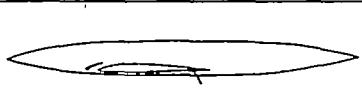	1.40	22.0	—	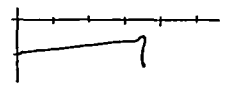	29
		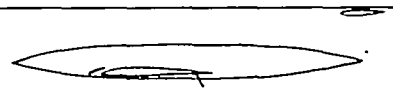 $i_t = -3.3°$ $\frac{2x}{b} = .509$	1.43	21.5	—		29
		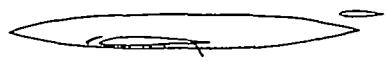 $i_t = -5.2°$ $\frac{2x}{b} = .254$	1.41	24.0	—	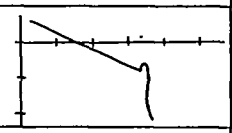	29
		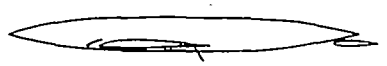 $i_t = -4.4°$ $\frac{2x}{b} = .031$	1.48*	24.0	—	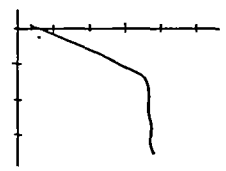	29
		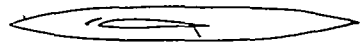	1.48	31.0	5.92	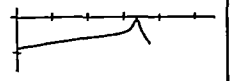	31
		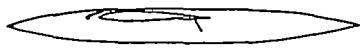	1.48	28.0	5.72	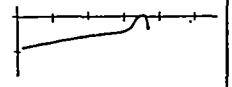	31
		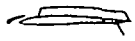	1.41	25.0	6.37	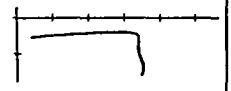	31

*$C_{L_{max}}$ not reached.

TABLE 20.—SUMMARY OF LONGITUDINAL STABILITY CHARACTERISTICS OF A WING WITH 42° OF LEADING-EDGE SWEEPBACK—Concluded

Span of L.E. device (b/2)	Span of T.E. device (b/2)	Configuration	$C_{L_{max}}$	$\alpha_{C_{L_{max}}}$	L/D at 0.85 $C_{L_{max}}$	C_m characteristics	Reference
.575 L.E. slat	.500 split flap	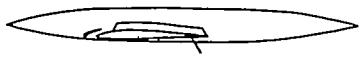	1.39	22.5	—	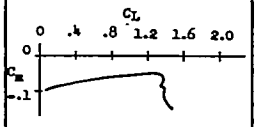	29
		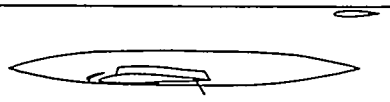 $i_t = -3.5°$ $\frac{2z}{b} = .509$	1.42	20.5	—	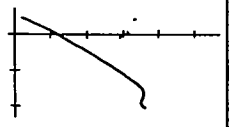	29
		$i_t = -3.6°$ $\frac{2z}{b} = .254$	1.38	20.5	—	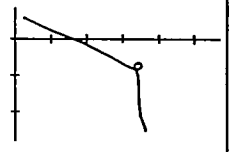	29
		$i_t = -4.0°$ $\frac{2z}{b} = .031$	1.46	21.5	—	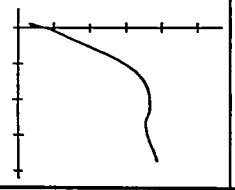	29
		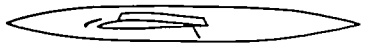	1.52	31.0	5.19	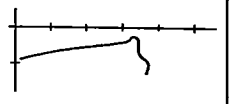	31
			1.55	26.0	5.19	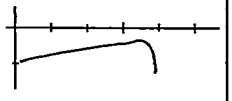	31
.725 L.E. slat	None	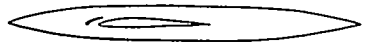	1.48	29.0	5.00	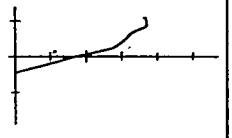	31
	.500 split flap	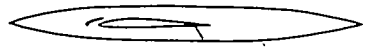	1.54	28.0	5.82	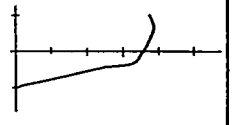	31
			1.68	28.0	5.05	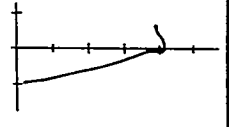	31

TABLE 21.—SUMMARY OF LONGITUDINAL STABILITY CHARACTERISTICS OF A WING WITH 42° OF LEADING-EDGE SWEEPBACK

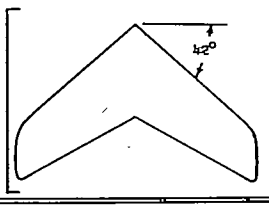

$\Lambda_{c/4} = 40°$ $A = 3.94$ $R_{max} = 9.60 \times 10^6$

$\lambda = 0.625$ $M_{max} = 0.22$

Airfoil sections (normal to line of maximum thickness)

Root: 10-percent-thick circular arc

Tip: 6.4-percent-thick circular arc

Span of L.E. device (b/2)	Span of T.E. device (b/2)	Configuration	$C_{L_{max}}$	$\alpha_{C_{L_{max}}}$	L/D at 0.85 $C_{L_{max}}$	C_m characteristics	Reference
None	None		0.84	21.0	4.82		36
			0.85	19.0	—		36
		$i_t = -1.1°$ $\frac{2x}{b} = .466$	0.88	19.0	—		36
		$i_t = -1.4°$ $\frac{2x}{b} = .339$	0.85	19.0	—		36
		$i_t = -1.2°$ $\frac{2x}{b} = .211$	0.85	19.0	—		36
		$i_t = -2.1°$ $\frac{2x}{b} = -.011$	0.95	20.0	—		36
			0.89	20.0	4.43		37
			0.89	21.0	4.34		37
	.500 split flap		0.95	14.0	5.18		37
	.500 split flap		0.97	17.0	4.34		37
	.500 split flap		1.00	17.0	4.42		37
	.500 split flap		1.00	17.0	4.60		37
	None		0.87	17.0	4.27		36
	.500 split flap		1.02	11.5	5.26		36
.550 L.E. flap (flat)	.500 split flap		1.35	20.4	4.42		36

TABLE 21.—SUMMARY OF LONGITUDINAL STABILITY CHARACTERISTICS OF A WING WITH 42° OF LEADING-EDGE SWEEPBACK—Continued

Span of L.E. device (b/2)	Span of T.E. device (b/2)	Configuration	$C_{L_{max}}$	$\alpha_{C_{L_{max}}}$	L/D at 0.85 $C_{L_{max}}$	C_m characteristics	Reference
.550 L.E. flap (flat)	.500 split flap	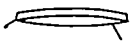	1.34	21.4	5.07	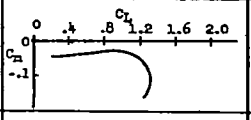	36
			1.35	26.4	4.59	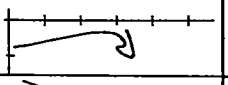	36
		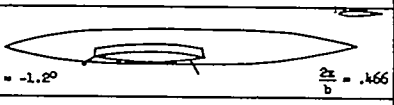 $i_t = -1.2°$ $\frac{2x}{b} = .466$	1.31	17.2	—	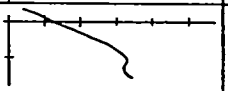	36
		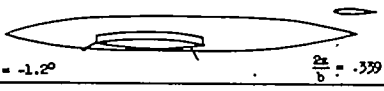 $i_t = -1.2°$ $\frac{2x}{b} = .339$	1.30	17.2	—	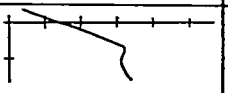	36
		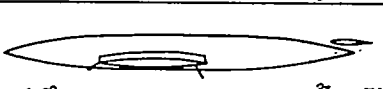 $i_t = -1.2°$ $\frac{2x}{b} = .211$	1.30	17.2	—	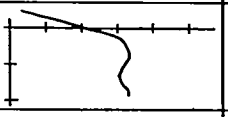	36
		$i_t = -2.1°$ $\frac{2x}{b} = -.011$	1.35	17.2	—	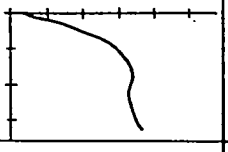	36
		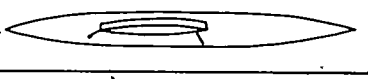	1.44	24.5	4.90	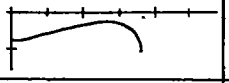	36
		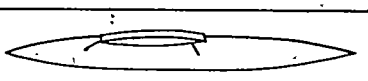	1.32	22.6	4.17	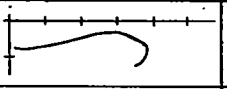	36
.695 L.E. flap (flat)	None	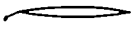	1.19	24.4	5.26	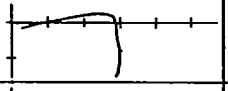	37
	None	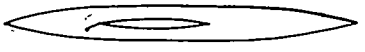	1.40	24.5	4.95	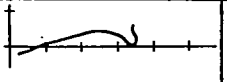	37
	.500 split flap	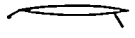	1.33	21.5	4.63	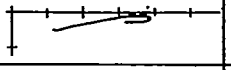	37
	.500 split flap	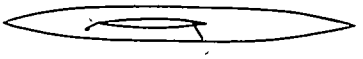	1.50	21.5	5.27	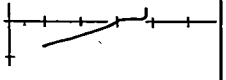	37
.700 L.E. flap (flat)	.500 split flap	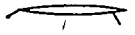	1.32	21.2	5.01	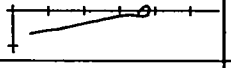	36
		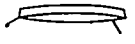	1.32	20.6	5.17	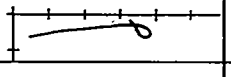	36
		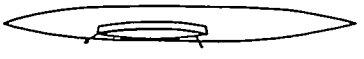	1.42	22.6	5.48	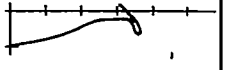	36
		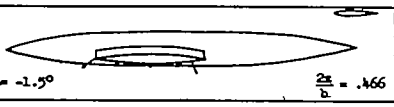 $i_t = -1.5°$ $\frac{2x}{b} = .466$	1.43	18.7	—	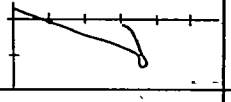	36
		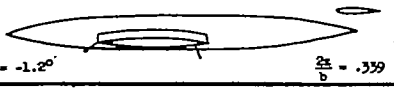 $i_t = -1.2°$ $\frac{2x}{b} = .339$	1.43	18.7	—	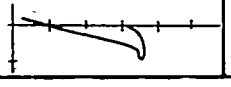	36

TABLE 21.—SUMMARY OF LONGITUDINAL STABILITY CHARACTERISTICS OF A WING WITH 42° OF LEADING-EDGE SWEEPBACK—Concluded

Span of L.E. device (b/2)	Span of T.E. device (b/2)	Configuration	$C_{L_{max}}$	$\alpha_{C_{L_{max}}}$	L/D at 0.85 $C_{L_{max}}$	C_m characteristics	Reference
.700 L.E. flap (flat)	.500 split flap	$i_t = -1.0°$ $\frac{2x}{b} = .211$	1.40	18.7	—		36
		$i_t = -2.1°$ $\frac{2x}{b} = -.011$	1.55	22.6	—		36
			1.54	20.6	5.38		36
			1.53	20.2	5.37		36
.695 L.E. flap (curved)	None		1.17	22.4	6.02		37
	.500 split flap		1.52	20.5	5.04		37
.600 L.E. droop	None		1.16	23.0	3.58		36
			1.13	25.0	4.67		36
			1.28	24.5	4.27		36
			1.23	24.5	4.11		36
	.500 split flap		1.28	20.5	4.21		36
			1.26	19.3	4.68		36
			1.25	19.0	4.43		36
		$i_t = -1.2°$ $\frac{2x}{b} = .466$	1.29	18.5	—		36
		$i_t = -1.0°$ $\frac{2x}{b} = .339$	1.28	18.5	—		36
		$i_t = -1.3°$ $\frac{2x}{b} = .211$	1.26	18.5	—		36
		$i_t = -1.9°$ $\frac{2x}{b} = -.011$	1.32	18.5	—		36
			1.35	20.7	5.22		36
			1.35	20.4	4.87		36
.750 L.E. droop	None		1.12	22.0	5.01		36
	.500 split flap		1.29	19.0	4.97		36
	.500 split flap		1.28	19.4	5.58		36

TABLE 22.—SUMMARY OF LONGITUDINAL STABILITY CHARACTERISTICS OF A WING WITH 45°–20° OF LEADING-EDGE SWEEPBACK

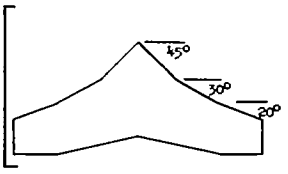

$\lambda = 0.36$ $A = 4.12$ $R_{max} = 6.0 \times 10^6$

$M_{max} = 0.13$

Airfoil sections (parallel to plane of symmetry)

Root: NACA 64A009

Tip: NACA 64A009

Span of L.E. device (b/2)	Span of T.E. device (b/2)	Configuration	$C_{L_{max}}$	$\alpha_{C_{L_{max}}}$	L/D at 0.85 $C_{L_{max}}$	C_m characteristics	Reference
None	None		0.88	17.5	12.06	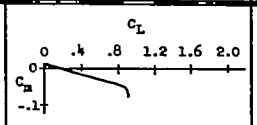	38
	.650 split flap	$\delta_f = 30°$	1.17	14.5	6.42	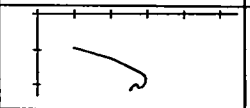	38
		$\delta_f = 45°$	1.26	13.1	5.36	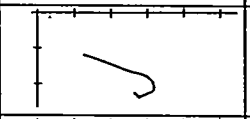	38
			1.25	12.8	4.94		38
.350 L.E. flap	None		0.90	16.5	11.10	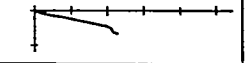	38
	.650 split flap		1.33	13.0	4.77	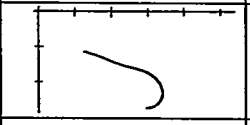	38
.700 L.E. flap	None		1.17	20.4	9.05	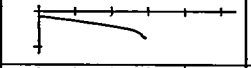	38
	.650 split flap		1.60	16.8	4.95	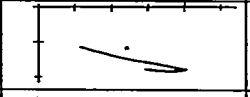	38
1.000 L.E. flap	None		1.25	20.0	9.15	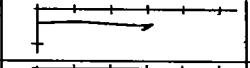	38
	.650 split flap		1.66	17.8	5.10	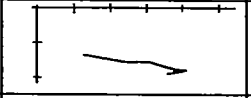	38
.350 L.E. slat	None		0.92	19.5	10.30	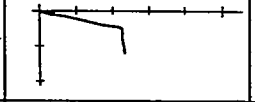	38
	.650 split flap		1.33	13.0	4.92	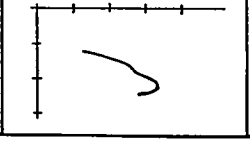	38

TABLE 23.—SUMMARY OF LONGITUDINAL STABILITY CHARACTERISTICS OF A WING WITH 45° OF LEADING-EDGE SWEEPBACK

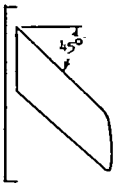

$\Lambda_{c/4} = 45°$ $A = 4.0$ $R_{max} = 9.0 \times 10^6$

$\lambda = 1.000$ $M_{max} = 0.20$

Airfoil sections (parallel to plane of symmetry)

Root: NACA 65A006

Tip: NACA 65A006

Span of L.E. device (b/2)	Span of T.E. device (b/2)	Configuration	$C_{L_{max}}$	$\alpha_{C_{L_{max}}}$	L/D at 0.85 $C_{L_{max}}$	C_m characteristics	Reference
None	None		1.01	25.0	3.73	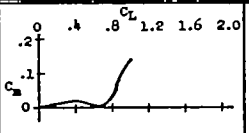	14
	.500 split flap		1.04	22.0	4.21	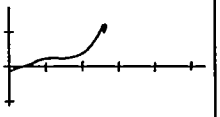	14

TABLE 24.—SUMMARY OF LONGITUDINAL STABILITY CHARACTERISTICS OF A WING WITH 46.2° OF LEADING-EDGE SWEEPBACK

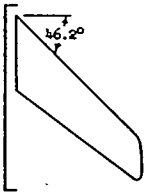

$\Lambda_{c/4} = 45°$ $A = 6.0$ $R_{max} = 6.0 \times 10^6$

$\lambda = 0.600$ $M_{max} = 0.20$

Airfoil sections (parallel to plane of symmetry)

Root: NACA 65A006

Tip: NACA 65A006

Span of L.E. device (b/2)	Span of T.E. device (b/2)	Configuration	$C_{L_{max}}$	$\alpha_{C_{L_{max}}}$	L/D at 0.85 $C_{L_{max}}$	C_m characteristics	Reference
None	None		1.03	28.5	3.31	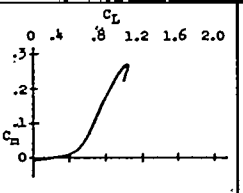	14
	.500 split flap	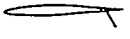	1.00	22.8	4.26	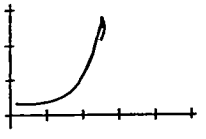	14

TABLE 25.—SUMMARY OF LONGITUDINAL STABILITY CHARACTERISTICS OF A WING WITH 46.33° OF LEADING-EDGE SWEEPBACK

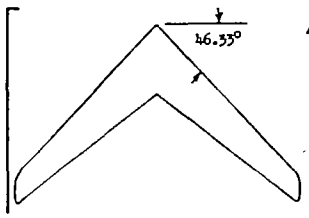

$\Lambda_{c/4} = 45°$
$\lambda = 0.450$

$A = 8.02$

$R_{max} = 4.8 \times 10^6$
$M_{max} = 0.23$

Airfoil sections (parallel to plane of symmetry)
Root: NACA 63_1A012
Tip: NACA 63_1A012

Span of L.E. device (b/2)	Span of T.E. device (b/2)	Fence location (b/2)	Configuration	$C_{L_{max}}$	$\alpha_{C_{L_{max}}}$	L/D at 0.85 $C_{L_{max}}$	C_m characteristics	Reference
None	None	None	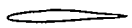	1.01	21.0	8.40	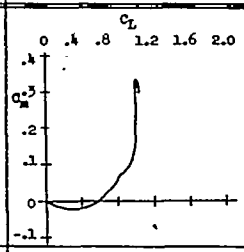	39
			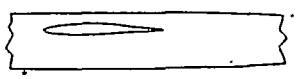 $i_w = 0°$	1.14	31.0	6.05	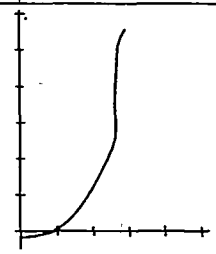	39
			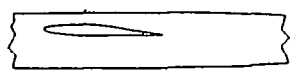 $i_w = 4°$	1.15	31.0	6.30	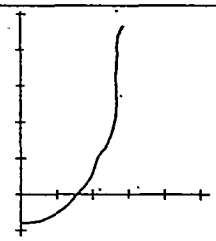	39
		.575	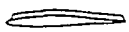	1.07	25.0	—	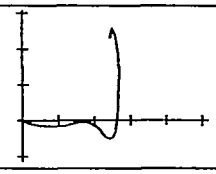	39
		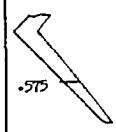 .575	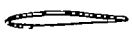	1.10	27.0	—	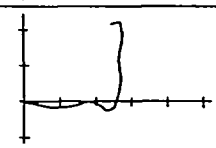	39
		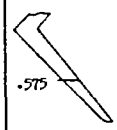 .575	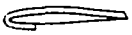	1.30	27.0	9.60	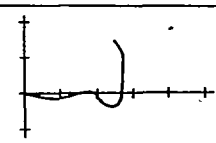	39

TABLE 25.—SUMMARY OF LONGITUDINAL STABILITY CHARACTERISTICS OF A WING WITH 46.33° OF LEADING-EDGE SWEEPBACK—Continued

Span of L.E. device (b/2)	Span of T.E. device (b/2)	Fence location (b/2)	Configuration	$C_{L_{max}}$	$\alpha_{C_{L_{max}}}$	L/D at 0.85 $C_{L_{max}}$	C_m characteristics	Reference
None	None	.575 .80 .89	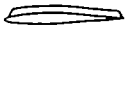	1.05	19.0	——	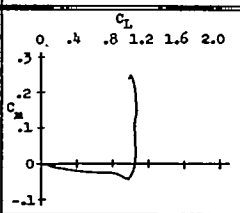	39
		.575 .80 .89		1.09	27.0	8.95	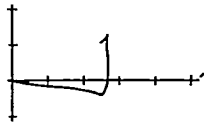	39
		.575 .80 .89	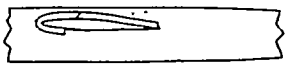 $i_v = 4°$	1.19	31.0	——	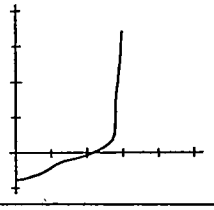	39
	.350 split flap	None	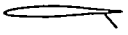	1.22	16.6	10.58	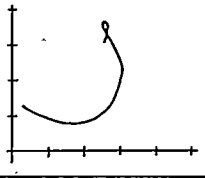	39
	.500 split flap	None	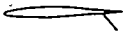	1.29	15.6	10.25	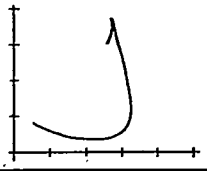	39
	.600 split flap	None	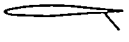	1.34	15.6	10.25	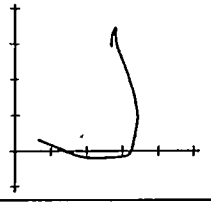	39
	.350 ext. split flap	None		1.30	15.6	11.05	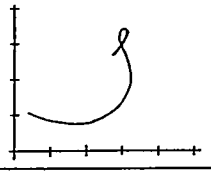	39
	.500 ext. split flap	None		1.40	15.6	10.72	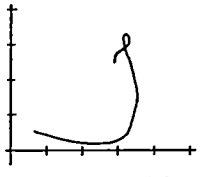	39
		.575 .80		1.37	14.7	——	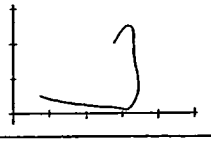	39

TABLE 25.—SUMMARY OF LONGITUDINAL STABILITY CHARACTERISTICS OF A WING WITH 46.33° OF LEADING-EDGE SWEEPBACK—Continued

Span of L.E. device (b/2)	Span of T.E. device (b/2)	Fence location (b/2)	Configuration	$C_{L_{max}}$	$\alpha_{C_{L_{max}}}$	L/D at 0.85 $C_{L_{max}}$	C_m characteristics	Reference
None	None	.575		1.13	27.0	——	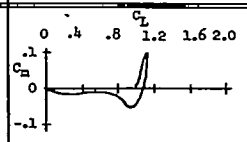	39
		.80		1.05	27.0	——	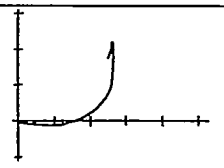	39
		.575 .80		1.06	19.0	——	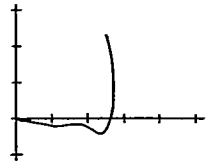	39
		.575 .80	$i_v = 4°$	1.13	22.0	——	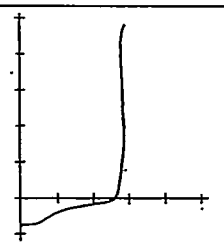	39
		.575 .89	$i_v = 4°$	1.19	29.0	——	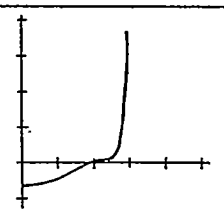	39
		.575 .80		1.08	27.0	——	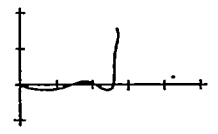	39
		.575 .80		1.09	25.0	——	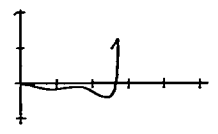	39
		.575 .80	$i_v = 4°$	1.21	31.0	——	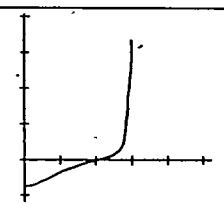	39

TABLE 25.—SUMMARY OF LONGITUDINAL STABILITY CHARACTERISTICS OF A WING WITH 46.33° OF LEADING-EDGE SWEEPBACK—Continued

Span of L.E. device (b/2)	Span of T.E. device (b/2)	Fence location (b/2)	Configuration	$C_{L_{max}}$	$\alpha_{C_{L_{max}}}$	L/D at 0.85 $C_{L_{max}}$	C_m characteristics	Reference
None	.600 ext. split flap	None	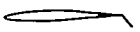	1.46	15.7	11.08	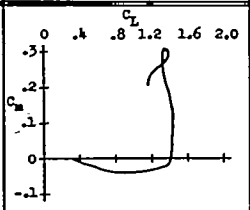	39
		.575 .80		1.44	14.8	10.46	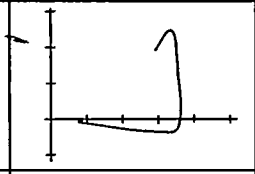	39
.350 L.E. flap	None	None	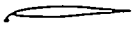	1.18	28.6	9.52	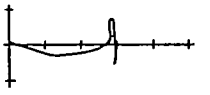	39
		.575 .80		1.19	26.6	—	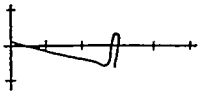	39
	.350 split flap	None	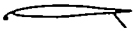	1.26	15.6	—		39
		.575 .80		1.26	15.6	—	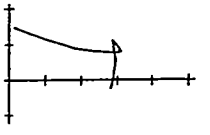	39
	.500 split flap	None		1.29	14.6	—	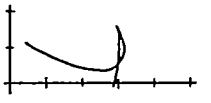	39
	.600 split flap	None	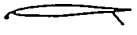	1.34	14.6	—	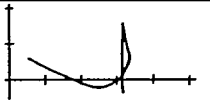	39
		.575 .80		1.30	15.0	—	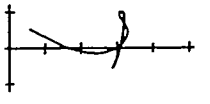	39
	.600 ext. split flap	.575 .80		1.45	27.7	—	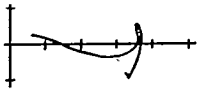	39

TABLE 25.—SUMMARY OF LONGITUDINAL STABILITY CHARACTERISTICS OF A WING WITH 46.33° OF LEADING-EDGE SWEEPBACK—Continued

Span of L.E. device (b/2)	Span of T.E. device (b/2)	Fence location (b/2)	Configuration	$C_{L_{max}}$	$\alpha_{C_{L_{max}}}$	L/D at 0.85 $C_{L_{max}}$	C_m characteristics	Reference
.400 L.E. flap	None	None	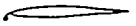	1.21	28.6	——	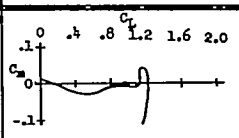	39
	.350 split flap	None		1.23	15.6	——	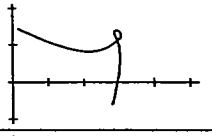	39
	.500 split flap	None	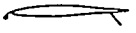	1.26	15.0	——	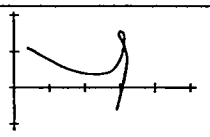	39
	.600 split flap	None	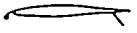	1.34	15.4	——	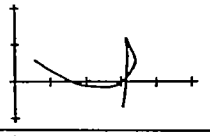	39
.450 L.E. flap	None	None		1.22	27.0	8.95	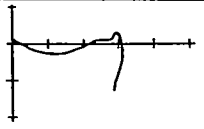	39
		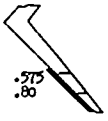	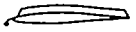	1.25	27.0	9.00	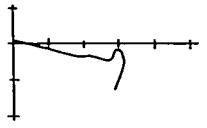	39
		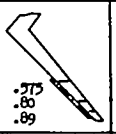	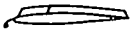	1.28	27.0	——	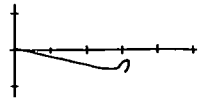	39
		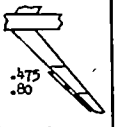	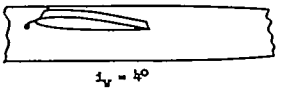	1.31	31.0	——	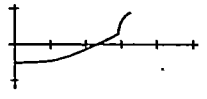	39
	.350 split flap	None	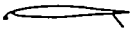	1.22	16.6	11.58	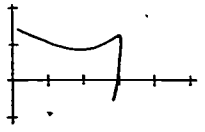	39
			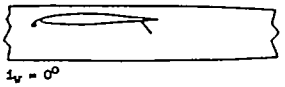	1.39	30.7	——	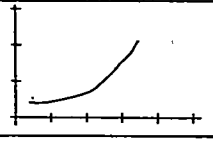	39
			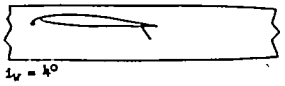	1.34	30.7	——	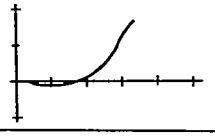	39
			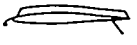	1.23	24.6	——	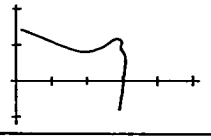	39
			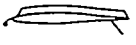	1.24	24.0	——	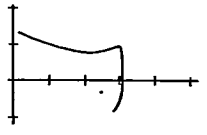	39

TABLE 25.—SUMMARY OF LONGITUDINAL STABILITY CHARACTERISTICS OF A WING WITH 46.33° OF LEADING-EDGE SWEEPBACK—Continued

Span of L.E. device (b/2)	Span of T.E. device (b/2)	Fence location (b/2)	Configuration	$C_{L_{max}}$	$\alpha_{C_{L_{max}}}$	L/D at 0.85 $C_{L_{max}}$	C_m characteristics	Reference
.450 L.E flap				1.27	24.6	10.87	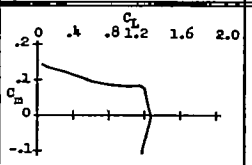	39
	.350 split flap	.575 .80	$i_v = 0°$	1.40	28.7	—	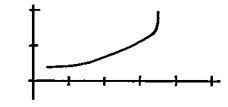	39
		.575 .80	$i_v = 4°$	1.35	30.7	—	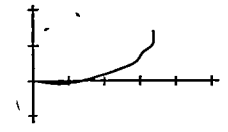	39
		.575 .89	$i_v = 4°$	1.36	30.7	—	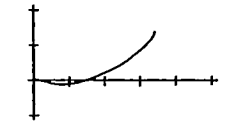	39
	.500 split flap	None		1.26	15.6	10.40	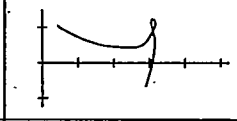	39
			$i_v = 4°$	1.35	30.7	—	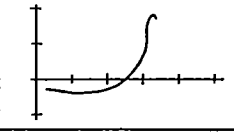	39
		.575 .80		1.28	16.0	10.52	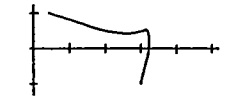	39
		.575 .80	$i_v = 4°$	1.38	28.7	—	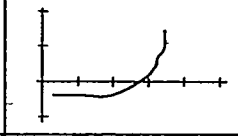	39
		.575 .89	$i_v = 4°$	1.38	28.7	—	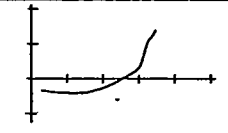	39
	.600 split flap	None		1.33	15.5	10.27	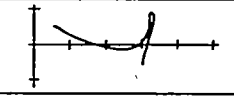	39
		.575 .80		1.33	15.5	9.92	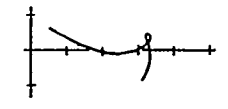	39

TABLE 25.—SUMMARY OF LONGITUDINAL STABILITY CHARACTERISTICS OF A WING WITH 46.33° OF LEADING-EDGE SWEEPBACK—Continued

Span of L.E. device (b/2)	Span of T.E. device (b/2)	Fence location (b/2)	Configuration	$C_{L_{max}}$	$\alpha_{C_{L_{max}}}$	L/D at 0.85 $C_{L_{max}}$	C_m characteristics	Reference
.450 L.E. flap	.350 ext. split flap	None	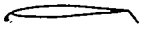	1.37	17.6	11.64	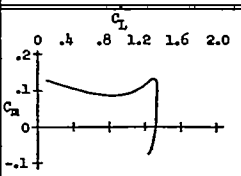	39
		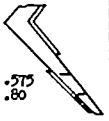 .575 .80		1.36	16.6	—	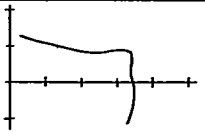	39
	.500 ext. split flap	None	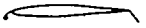	1.42	15.6	11.39	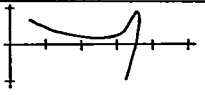	39
			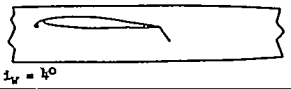 $i_w = 4°$	1.52	28.8	—	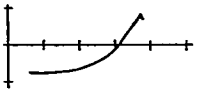	39
		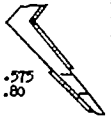 .575 .80		1.43	16.6	—	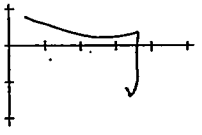	39
		.575 .80	$i_w = 0°$	1.58	27.0	—	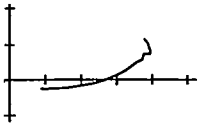	39
		.575 .80	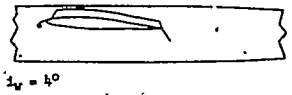 $i_w = 4°$	1.53	26.8	—	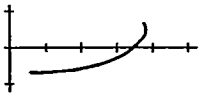	39
	.600 ext. split flap	None	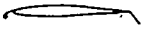	1.49	22.7	11.08	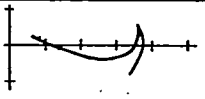	39
		.575 .80	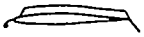	1.54	24.7	—	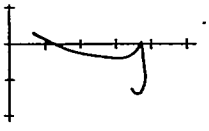	39
.500 L.E. flap	None	None	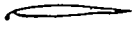	1.24	26.8	—	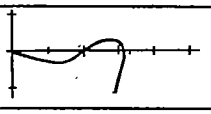	39
		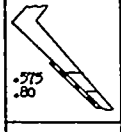 .575 .80	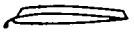	1.30	26.8	—	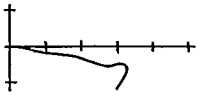	39
		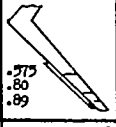 .575 .80 .89	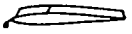	1.29	26.8	—	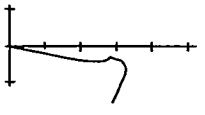	39
	.350 split flap	None	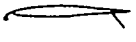	1.21	16.6	—	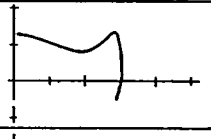	39
	.500 split flap	None	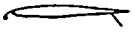	1.29	16.0	—	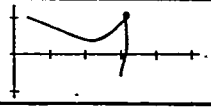	39

TABLE 25.—SUMMARY OF LONGITUDINAL STABILITY CHARACTERISTICS OF A WING WITH 46.33° OF LEADING-EDGE SWEEPBACK—Continued

Span of L.E. device (b/2)	Span of T.E. device (b/2)	Fence location (b/2)	Configuration	$C_{L_{max}}$	$\alpha_{C_{L_{max}}}$	L/D at 0.85 $C_{L_{max}}$	C_m characteristics	Reference
.500 L.E. flap	.500 split flap	.80	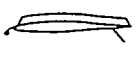	1.27	20.7	——	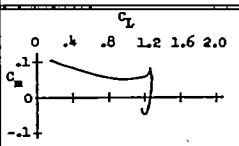	39
		.575 .80		1.32	16.6	——	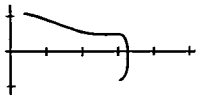	39
		.575 .80 .89		1.32	15.8	——	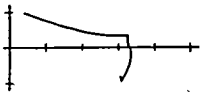	39
	.600 split flap	None		1.32	15.0	——	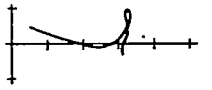	39
		.575 .80	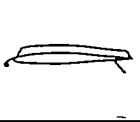	1.38	16.2	——	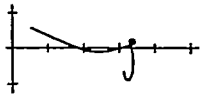	39
	.500 ext. split flap	None	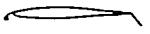	1.45	24.0	——	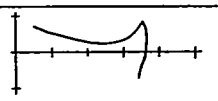	39
		.575 .80		1.50	24.7	——	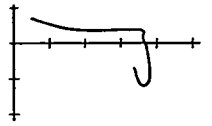	39
	.600 ext. split flap	None	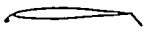	1.52	24.7	——	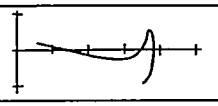	39
		.575 .80		1.55	24.0	——	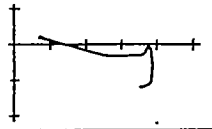	39
.575 L.E. flap	None	None		1.24	27.0	7.32	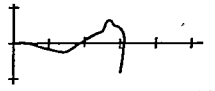	39
		.575 .80		1.29	26.2	——	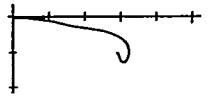	39
	.350 split flap	None	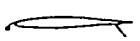	1.25	24.0	——	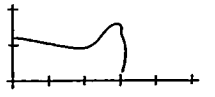	39
		.575	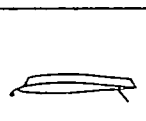	1.31	24.6	——	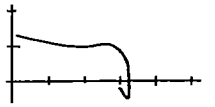	39

TABLE 25.—SUMMARY OF LONGITUDINAL STABILITY CHARACTERISTICS OF A WING WITH 46.33° OF LEADING-EDGE SWEEPBACK—Continued

Span of L.E. device (b/2)	Span of T.E. device (b/2)	Fence location (b/2)	Configuration	$C_{L_{max}}$	$\alpha_{C_{L_{max}}}$	L/D at 0.85 $C_{L_{max}}$	C_m characteristics	Reference
.575 L.E. flap	.500 split flap	None	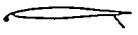	1.34	24.6	——	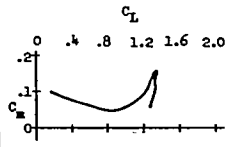	39
		.575 .80	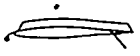	1.40	24.6	——	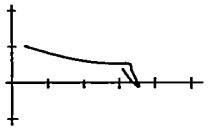	39
	.600 split flap	None	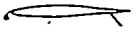	1.37	23.6	——	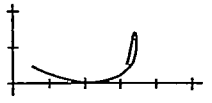	39
		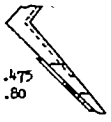 .475 .80	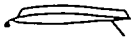	1.42	24.7	——	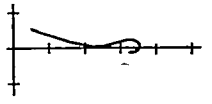	39
		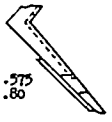 .575 .80	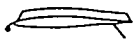	1.43	24.7	——	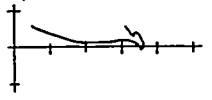	39
	.500 ext. split flap	None	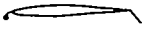	1.56	24.0	——	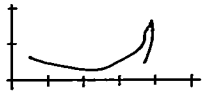	39
		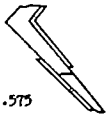 .575		1.59	22.8	——	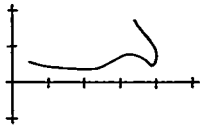	39
		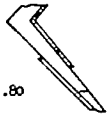 .80	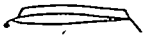	1.57	23.0	——	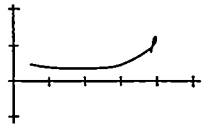	39
		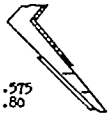 .575 .80	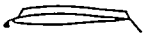	1.62	22.7	——	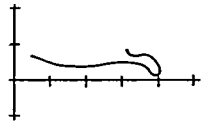	39
	.600 ext. split flap	.575 .80	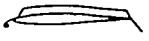	1.66	22.7	——	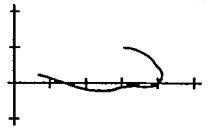	39

TABLE 25.—SUMMARY OF LONGITUDINAL STABILITY CHARACTERISTICS OF A WING WITH 46.33° OF LEADING-EDGE SWEEPBACK—Continued

Span of L.E. device (b/2)	Span of T.E. device (b/2)	Fence location (b/2)	Configuration	$C_{L_{max}}$	$\alpha_{C_{L_{max}}}$	L/D at 0.85 $C_{L_{max}}$	C_m characteristics	Reference
None	None	None	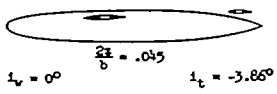 $\frac{2z}{b} = .045$ $i_w = 0°$ $i_t = -3.86°$	1.26*	31.1	—	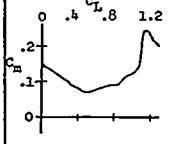	40
			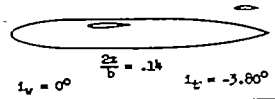 $\frac{2z}{b} = .14$ $i_w = 0°$ $i_t = -3.80°$	1.24*	31.1	—	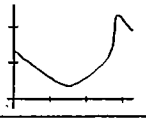	40
			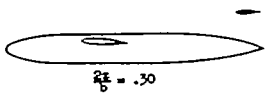 $\frac{2z}{b} = .30$ $i_w = 4°$ $i_t = -3.76°$	1.18*	31.1	—	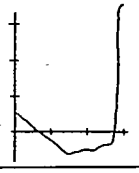	40
			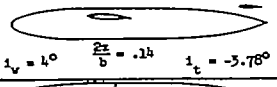 $i_w = 4°$ $\frac{2z}{b} = .14$ $i_t = -3.78°$	1.26*	31.1	—		40
			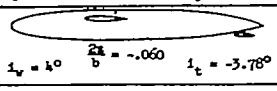 $i_w = 4°$ $\frac{2z}{b} = -.060$ $i_t = -3.78°$	1.31*	31.1	—	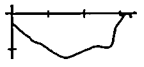	40
		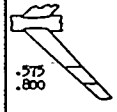 .575 .800	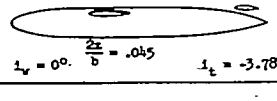 $i_w = 0°$ $\frac{2z}{b} = .045$ $i_t = -3.78°$	1.27*	31.1	—	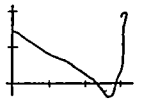	40
			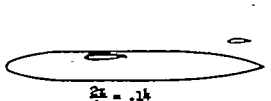 $\frac{2z}{b} = .14$ $i_w = 0°$ $i_t = -3.76°$	1.26*	31.1	—	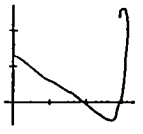	40
			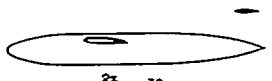 $\frac{2z}{b} = .30$ $i_w = 4°$ $i_t = -3.76°$	1.18*	31.0	—	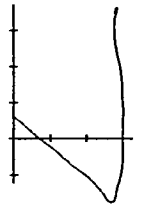	40
			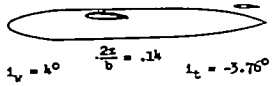 $i_w = 4°$ $\frac{2z}{b} = .14$ $i_t = -3.76°$	1.25*	31.1	—	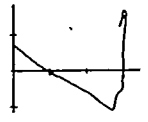	40
			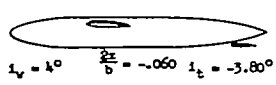 $i_w = 4°$ $\frac{2z}{b} = -.060$ $i_t = -3.80°$	1.31*	31.1	—	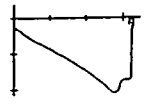	40
.45 L.E. flaps		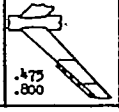 .475 .800	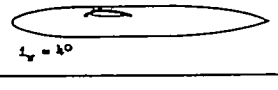 $i_w = 4°$	1.31*	26.8	—	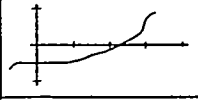	40

*$C_{L_{max}}$ not reached.

TABLE 25.—SUMMARY OF LONGITUDINAL STABILITY CHARACTERISTICS OF A WING WITH 46.33° OF LEADING-EDGE SWEEPBACK—Continued

Span of L.E. device (b/2)	Span of T.E. device (b/2)	Fence location (b/2)	Configuration	$C_{L_{max}}$	$\alpha_{C_{L_{max}}}$	L/D at 0.85 $C_{L_{max}}$	C_m characteristics	Reference
.45 L.E. flaps	None		$\frac{2x}{b} = .30$; $i_w = 4°$; $i_t = -3.80°$	1.40*	28.8	—	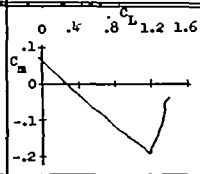	40
		.475 .800	$\frac{2x}{b} = .14$; $i_w = 4°$; $i_t = -3.88°$	1.45*	28.8	—	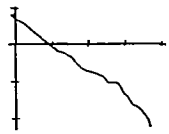	40
			$\frac{2x}{b} = -.060$; $i_w = 4°$; $i_t = -3.88°$	1.52*	28.8	—	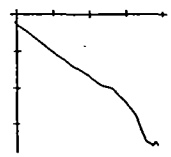	40
	.35 split flaps	None	$\frac{2x}{b} = .14$; $i_w = 0°$; $i_t = -3.73°$	1.46	30.4	—	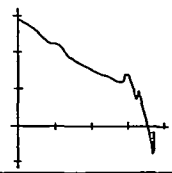	40
			$\frac{2x}{b} = .045$; $i_w = 0°$; $i_t = -3.85°$	1.44	30.5	—	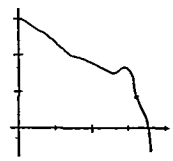	40
			$\frac{2x}{b} = .30$; $i_w = 4°$; $i_t = -3.74°$	1.39*	30.8	—	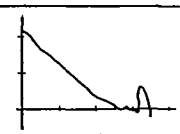	40
			$\frac{2x}{b} = .14$; $i_w = 4°$; $i_t = -3.78°$	1.45	30.8	—	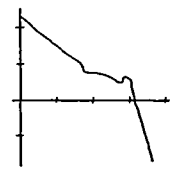	40
			$\frac{2x}{b} = -.060$; $i_w = 4°$; $i_t = -3.78°$	1.52	30.5	—	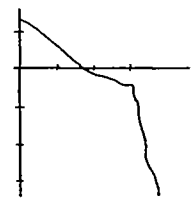	40
		.575 .800	$\frac{2x}{b} = .140$; $i_w = 0°$; $i_t = -3.73°$	1.46	30.4	—	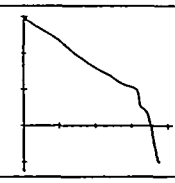	40

*$C_{L_{max}}$ not reached.

TABLE 25.—SUMMARY OF LONGITUDINAL STABILITY CHARACTERISTICS OF A WING WITH 46.33° OF LEADING-EDGE SWEEPBACK—Continued

Span of L.E. device (b/2)	Span of T.E. device (b/2)	Fence location (b/2)	Configuration	$C_{L_{max}}$	$\alpha_{C_{L_{max}}}$	L/D at 0.85 $C_{L_{max}}$	C_m characteristics	Reference
.45 L.E. flaps	.35 split flaps	.575 .800	$\frac{2z}{b}$ = .045; i_w = 0°; i_t = -3.92°	1.50	29.8	—	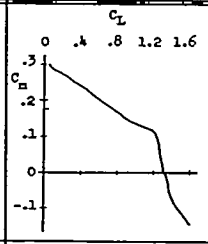	40
			$\frac{2z}{b}$ = .30; i_w = 4°; i_t = -3.68°	1.40	30.0	—	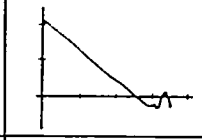	40
			$\frac{2z}{b}$ = .14; i_w = 4°; i_t = -3.78°	1.45	29.9	—	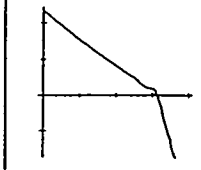	40
			$\frac{2z}{b}$ = -.060; i_w = 4°; i_t = -3.82°	1.50	29.7	—	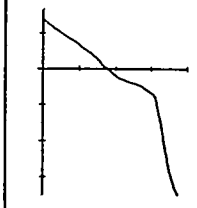	40
	.50 ext. split flaps	.575 .800	$\frac{2z}{b}$ = .14; i_w = 0°; i_t = -3.77°	1.63	28.0	—		40
			$\frac{2z}{b}$ = .045; i_w = 0°; i_t = -3.81°	1.66	28.0	—	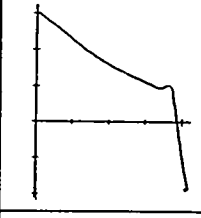	40
			$\frac{2z}{b}$ = .30; i_w = 4°; i_t = -3.72°	1.54	27.5	—	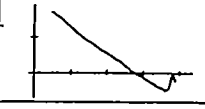	40
			$\frac{2z}{b}$ = .14; i_w = 4°; i_t = -3.81°	1.61	28.8	—	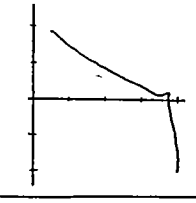	40

TABLE 25.—SUMMARY OF LONGITUDINAL STABILITY CHARACTERISTICS OF A WING WITH 46.33° OF LEADING-EDGE SWEEPBACK—Concluded

Span of L.E. device (b/2)	Span of T.E. device (b/2)	Fence location (b/2)	Configuration	$C_{L_{max}}$	$\alpha_{C_{L_{max}}}$	L/D at 0.85 $C_{L_{max}}$	C_m characteristics	Reference
.45 L.E. flaps	.50 ext. split flaps	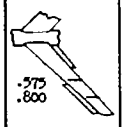 .575 .800	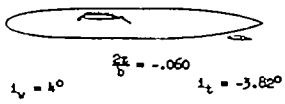 $\frac{z_t}{b} = -.060$ $i_w = 4°$ $i_t = -3.82°$	1.70	28.6	—	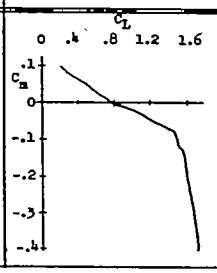	40

TABLE 26.—SUMMARY OF LONGITUDINAL STABILITY CHARACTERISTICS OF A WING WITH 46.33° OF LEADING-EDGE SWEEPBACK

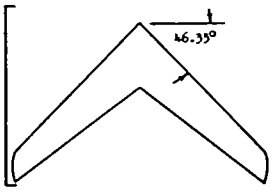

$\Lambda_{c/4} = 45°$ $A = 8.0$ $R_{max} = 4.2 \times 10^6$

$\lambda = 0.45$ $M_{max} = 0.19$

Airfoil sections (parallel to plane of symmetry)

Root: } NACA 63A series, 12 percent thick, camber varies from 0.73 at root
Tip: } to 0.86 at the tip

Span of L.E. device (b/2)	Span of T.E. device (b/2)	Fence location (b/2)	Configuration	$C_{L_{max}}$	$\alpha_{C_{L_{max}}}$	L/D at 0.85 $C_{L_{max}}$	C_m characteristics	Reference
None	None	None	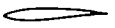	1.30	27.0	7.5	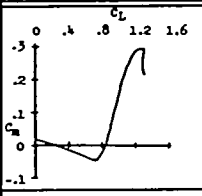	41
		.35	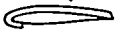	1.35	28.2	—	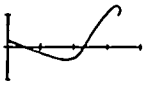	41
		.575		1.38	26.8	—	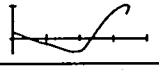	41
		.80	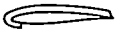	1.36	29.0	—	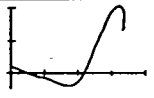	41
		.35 .575	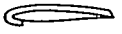	1.37	27.6	—	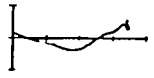	41
		.575 .80		1.40	27.1	8.2	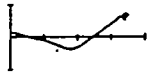	41
		.35 .575 .80	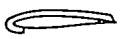	1.38	27.5	—	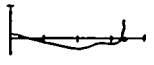	41
		.575 .80 .89	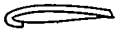	1.38	27.0	—	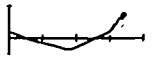	41
		.35 .575 .80 .89	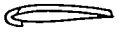	1.37	27.8	—	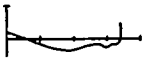	41
		.575 .80 .89	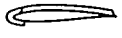	1.34	27.0	—	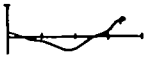	41
		.575 .70 .80	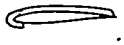	1.40	28.0	—	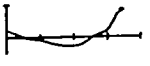	41
		.575 .70 .80 .89	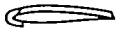	1.40	26.8	—	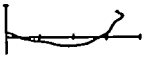	41
		.575 .80	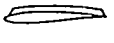	1.42	27.0	—	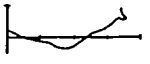	41
		.45 .70 .89	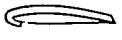	1.40	26.2	—	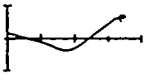	41

TABLE 26.—SUMMARY OF LONGITUDINAL STABILITY CHARACTERISTICS OF A WING WITH 46.33° OF LEADING-EDGE SWEEPBACK—Continued

Span of L.E. device (b/2)	Span of T.E. device (b/2)	Fence location (b/2)	Configuration	$C_{L_{max}}$	$\alpha_{C_{L_{max}}}$	L/D at 0.85 $C_{L_{max}}$	C_m characteristics	Reference
None	None	.35 .575 .80		1.39	26.5	——		41
		.35 .575 .80 .89		1.39	26.5	——		41
		.35 .575 .70 .80 .89		1.39	27.0	——		41
	.35 split flaps	None	$\delta_f = 60°$	1.30	24.2	——		41
		.575 .80	$\delta_f = 60°$	1.41	22.5	——		41
	.50 split flaps	None	$\delta_f = 60°$	1.34	24.2	——		41
		.575 .80	$\delta_f = 60°$	1.44	22.2	——		41
		.35 .575 .80 .89	$\delta_f = 30°$	1.44	27.0	——		41
	.60 split flaps	None	$\delta_f = 60°$	1.35	24.2	——		41
		.575 .80	$\delta_f = 60°$	1.48	23.0	——		41
	.50 ext. split flaps	None.	$\delta_f = 30°$	1.61*	31.2	——		41

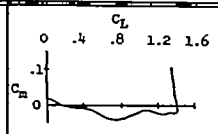

* $C_{L_{max}}$ not reached.

TABLE 26.—SUMMARY OF LONGITUDINAL STABILITY CHARACTERISTICS OF A WING WITH 46.33° OF LEADING-EDGE SWEEPBACK—Continued

Span of L.E. device (b/2)	Span of T.E. device (b/2)	Fence location (b/2)	Configuration	$C_{L_{max}}$	$\alpha_{C_{L_{max}}}$	L/D at 0.85 $C_{L_{max}}$	C_m characteristics	Reference
None	.50 ext. split flaps	.575 .80	$\delta_f = 30°$	1.61*	31.2	—		41
		.575 .80	$\delta_f = 30°$	1.64*	31.2	—		41
		.35 .575 .80	$\delta_f = 30°$	1.58	25.4	—		41
		.35 .575 .80 .89	$\delta_f = 30°$	1.59	25.4	—		41
.45 L.E. flaps	None	None		1.44	27.0	9.4		41
	.50 split flaps	None	$\delta_f = 60°$	1.45	21.0	—		41
		.575 .80	$\delta_f = 30°$	1.49	31.2	11.0		41
	.50 ext. split flaps	None	$\delta_f = 60°$	1.61	20.2	—		41
		.575 .80	$\delta_f = 30°$	1.68	24.4	10.3		41
	None	.575 .80		1.47	26.5	9.0		41
.50 L.E. flaps	None	None		1.44*	31.2	—		41
	.35 split flaps	None	$\delta_f = 60°$	1.42	21.2	—		41

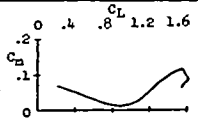

* $C_{L_{max}}$ not reached.

TABLE 26.—SUMMARY OF LONGITUDINAL STABILITY CHARACTERISTICS OF A WING WITH 46.33° OF LEADING-EDGE SWEEPBACK—Continued

Span of L.E. device (b/2)	Span of T.E. device (b/2)	Fence location (b/2)	Configuration	$C_{L_{max}}$	$\alpha_{C_{L_{max}}}$	L/D at 0.85 $C_{L_{max}}$	C_m characteristics	Reference
.50 L.E. flaps	.50 split flaps	None	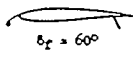 $\delta_f = 60°$	1.49	21.2	—	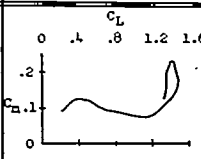	41
	.60 split flaps	None	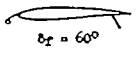 $\delta_f = 60°$	1.49	20.0	—	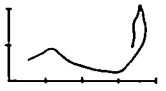	41
	.35 split flaps	.80	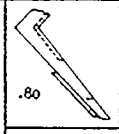 $\delta_f = 60°$	1.44	20.4	—	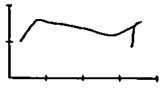	41
		.575 .80	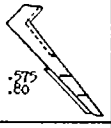 $\delta_f = 60°$	1.46	21.2	10.5	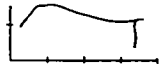	41
	.50 split flaps	.575 .80	$\delta_f = 60°$	1.51	21.0	—	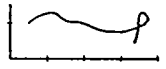	41
	.60 split flaps	.575 .80	$\delta_f = 60°$	1.55	21.2	—	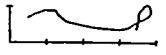	41
	.35 split flaps	.575 .80	$\delta_f = 30°$	1.47	24.2	11.5	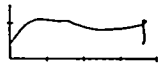	41
	.50 split flaps	.575 .80	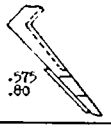 $\delta_f = 30°$	1.49	22.4	—	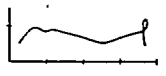	41
	.60 split flaps	.575 .80	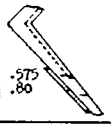 $\delta_f = 30°$	1.54	25.0	—	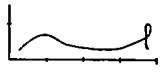	41
	.35 ext. split flaps	.575 .80	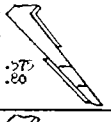 $\delta_f = 60°$	1.57	20.4	—	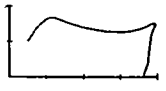	41
	.50 ext. split flaps	.575 .80	$\delta_f = 60°$	1.66	20.4	—	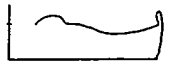	41
	.60 ext. split flaps	.575 .80	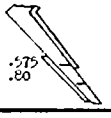 $\delta_f = 60°$	1.72	30.0	—	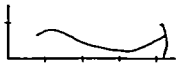	41

TABLE 26.—SUMMARY OF LONGITUDINAL STABILITY CHARACTERISTICS OF A WING WITH 46.33° OF LEADING-EDGE SWEEPBACK—Continued

Span of L.E. device (b/2)	Span of T.E. device (b/2)	Fence location (b/2)	Configuration	$C_{L_{max}}$	$\alpha_{C_{L_{max}}}$	L/D at 0.85 $C_{L_{max}}$	C_m characteristics	Reference
.50 L.E. flaps	.35 ext. split flaps	.575 .80	$\delta_f = 30°$	1.61	28.0	10.8	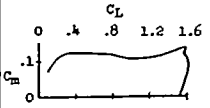	41
	.50 ext. split flaps	.575 .80	$\delta_f = 30°$	1.74	28.0	—		41
	.60 ext. split flaps	.575 .80	$\delta_f = 30°$	1.78*	30.2	—	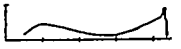	41
	None	.575 .80		1.50	31.2	—	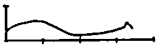	41
		.35 .575 .80		1.47	30.4	—	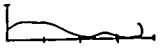	41
		.35 .575 .80 .89		1.48	30.0	—	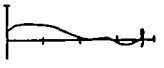	41
.575 L.E. flaps	None	None		1.40	30.0	—	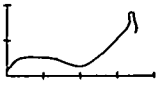	41
		.575 .80		1.51*	31.2	—	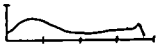	41
.32 L.E. flaps	None	None	Inboard end of L.E. flap at .40b/2	1.39	30.0	11.0	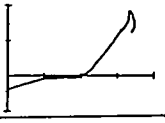	41
		.575 .80	Inboard end of L.E. flap at .40b/2	1.43	29.0	—	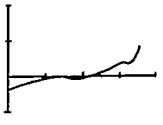	41
.195 L.E. flaps	None	.575 .80	Inboard end of L.E. flap at .525b/2	1.43	26.5	—	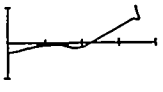	41

*$C_{L_{max}}$ not reached.

TABLE 26.—SUMMARY OF LONGITUDINAL STABILITY CHARACTERISTICS OF A WING WITH 46.33° OF LEADING-EDGE SWEEPBACK—Concluded

Span of L.E. device (b/2)	Span of T.E. device (b/2)	Fence location (b/2)	Configuration	$C_{L_{max}}$	$\alpha_{C_{L_{max}}}$	L/D at 0.85 $C_{L_{max}}$	C_m characteristics	Reference
None	None	.575 .80	Fence height = $0.15t_{max}$	1.39	26.2	—	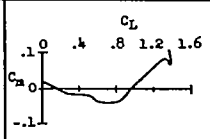	41
		.575 .80	Fence height = $0.15t_{max}$ → $0.30t_{max}$	1.41	26.5	—	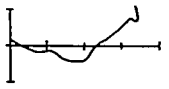	41
		None	$i_w = 0°$	1.31	27.2	7.5	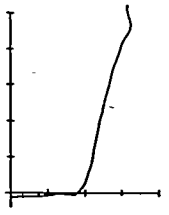	41
			$i_w = 4°$	1.32	27.2	—	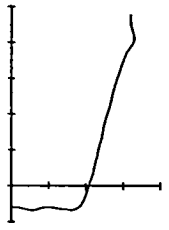	41
		.575 .80	$i_w = 0°$	1.43	28.2	8.5		41
		.575 .80	$i_w = 4°$	1.45	27.4	—	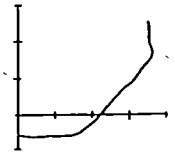	41
.45 L.E. flaps	.50 ext. split flaps	.275 .80	$i_w = 4°$ $\delta_f = 30°$	1.68*	31.2	—	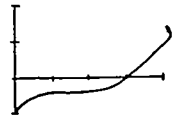	41

*$C_{L_{max}}$ not reached.

TABLE 27.—SUMMARY OF LONGITUDINAL STABILITY CHARACTERISTICS OF A WING WITH 46.55° OF LEADING-EDGE SWEEPBACK

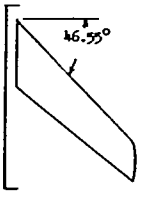

$\Lambda_{c/4} = 45°$ $A = 5.00$ $R_{max} = 10.0 \times 10^6$

$\lambda = 0.565$ $M_{max} = 0.23$

Airfoil sections (perpendicular to 0.250 chord line)

Span of L.E. device (b/2)	Span of T.E. device (b/2)	Configuration	NACA airfoil section	$C_{L_{max}}$	$\alpha_{C_{L_{max}}}$	L/D at 0.85 $C_{L_{max}}$	C_m characteristics	Reference
None	None	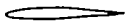	64A010	0.95	23.0	4.37	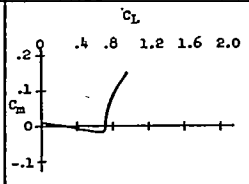	42
		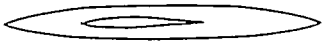	64A010	0.95	23.0	6.82	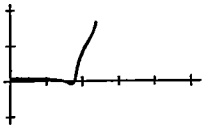	42
		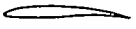	64A810	1.06	23.0	12.02	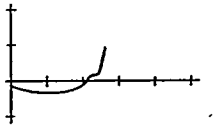	42
		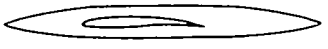	64A810	1.06	24.0	12.00	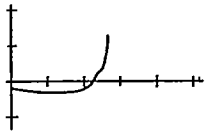	42

TABLE 28.—SUMMARY OF LONGITUDINAL STABILITY CHARACTERISTICS OF A WING WITH 46.6° OF LEADING-EDGE SWEEPBACK

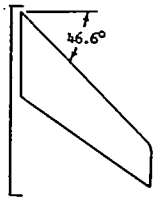

$\Lambda_{c/4} = 45°$ $A = 6.0$ $R_{max} = 8.0 \times 10^6$

$\lambda = 0.500$

Airfoil sections (perpendicular to 0.250 chord line)

Span of L.E. device (b/2)	Span of T.E. device (b/2)	Configuration	NACA airfoil section	$C_{L_{max}}$	$\alpha_{C_{L_{max}}}$	L/D at 0.85 $C_{L_{max}}$	C_m characteristics	Reference
None	None	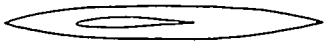	64A010	0.94	24.0	7.60	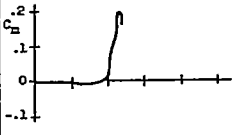	43
		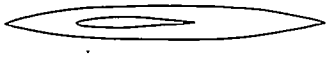	64A810	1.09	21.5	13.50	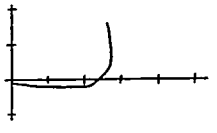	43

TABLE 29.—SUMMARY OF LONGITUDINAL STABILITY CHARACTERISTICS OF A WING WITH 46.7° OF LEADING-EDGE SWEEPBACK

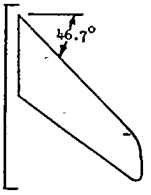

$\Lambda_{c/4} = 45°$ $A = 4.00$ $R_{max} = 11.5 \times 10^6$

$\lambda = 0.600$ $M_{max} = 0.20$

Airfoil sections (parallel to plane of symmetry)

Root: NACA 65A006

Tip: NACA 65A006

Span of L.E. device (b/2)	Span of T.E. device (b/2)	Configuration	$C_{L_{max}}$	$\alpha_{C_{L_{max}}}$	L/D at 0.85 $C_{L_{max}}$	C_m characteristics	Reference
None	None		1.05	25.0	3.72	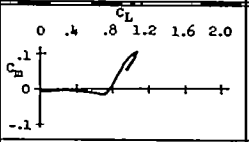	14
	.500 split flap	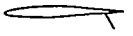	1.04	20.0	4.66	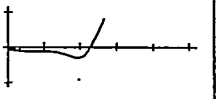	14
.370 L.E. droop	None	$\delta_n = 30°$ 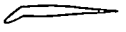	1.01	25.5	3.73	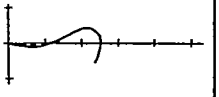	14
	.500 split flap	$\delta_n = 30°$ 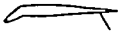	1.05	26.6	4.25	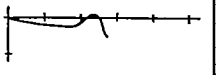	14
.500 L.E. droop	None	$\delta_n = 10°$ 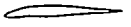	1.02	24.5	3.95	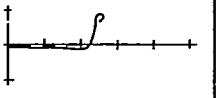	14
		$\delta_n = 20°$ 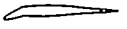	1.06	27.8	3.61	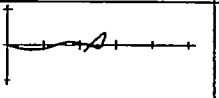	14
		$\delta_n = 30°$ 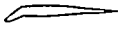	1.20	30.0	2.84	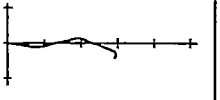	14
		$\delta_n = 40°$ 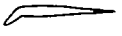	1.14	30.7	3.03	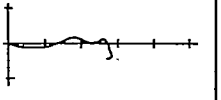	14
	.500 split flap	$\delta_n = 10°$ 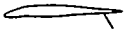	1.04	16.5	5.20	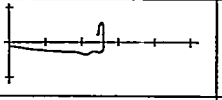	14
		$\delta_n = 20°$	1.11	21.8	4.72	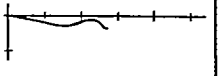	14
		$\delta_n = 30°$	1.12	23.7	3.58	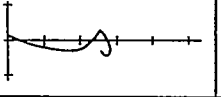	14
		$\delta_n = 40°$	1.05	24.0	4.97	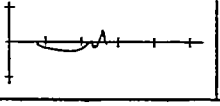	14

TABLE 29.—SUMMARY OF LONGITUDINAL STABILITY CHARACTERISTICS OF A WING WITH 46.7° OF LEADING-EDGE SWEEPBACK—Concluded

Span of L.E. device (b/2)	Span of T.E. device (b/2)	Configuration	$C_{L_{max}}$	$\alpha_{C_{L_{max}}}$	L/D at 0.85 $C_{L_{max}}$	C_m characteristics	Reference
.620 L.E. droop	None	$\delta_n = 20°$	1.06	27.0	4.18	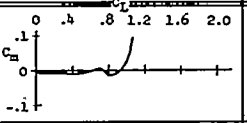	14
		$\delta_n = 30°$ 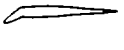	1.09	27.8	4.22	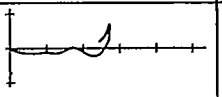	14
	.500 split flap	$\delta_n = 20°$ 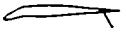	1.12	23.5	5.01	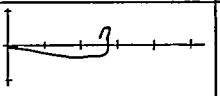	14
		$\delta_n = 30°$	1.14	22.0	4.97	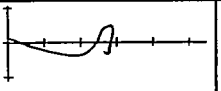	14
.750 L.E. droop	None	$\delta_n = 20°$	1.08	26.5	3.99	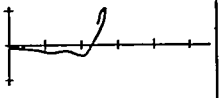	14
		$\delta_n = 30°$ 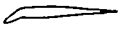	1.09	27.8	4.87	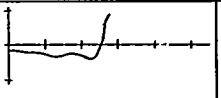	14
		$\delta_n = 30°$ 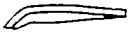	1.12	25.0	6.34	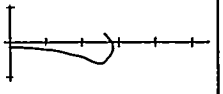	14
	.500 split flap	$\delta_n = 20°$ 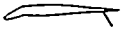	1.14	22.8	5.38	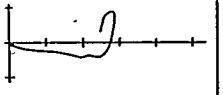	14
		$\delta_n = 30°$ 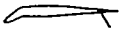	1.16	20.0	5.37	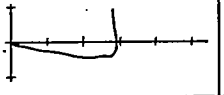	14
		$\delta_n = 30°$ 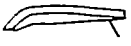	1.22	21.8	6.12	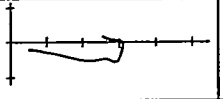	14
1.000 L.E. droop	None	$\delta_n = 20°$ 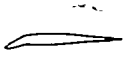	1.08	26.5	5.11	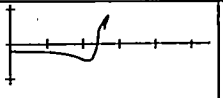	14
		$\delta_n = 30°$ 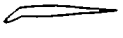	1.15	26.8	6.11	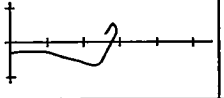	14
	.500 split flap	$\delta_n = 20°$ 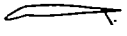	1.10	21.0	6.45	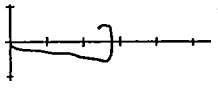	14
		$\delta_n = 30°$ 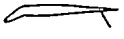	1.16	18.6	7.35	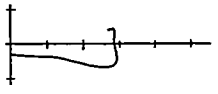	14

TABLE 30.—SUMMARY OF LONGITUDINAL STABILITY CHARACTERISTICS OF A WING WITH 47.5° OF LEADING-EDGE SWEEPBACK

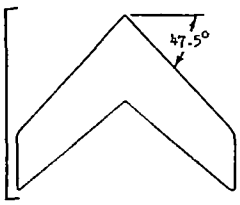

$\Lambda_{c/4} = 45°$ $A = 3.40$ $R_{max} = 4.4 \times 10^6$

$\lambda = 0.510$ $M_{max} = 0.07$

Airfoil sections (perpendicular to 0.250 chord line)

Root: NACA 64_1A112

Tip: NACA 64_1A112

Span of L.E. device (b/2)	Span of T.E. device (b/2)	Configuration	$C_{L_{max}}$	$\alpha_{C_{L_{max}}}$	L/D at 0.85 $C_{L_{max}}$	C_m characteristics	Reference
None	None		0.98	22.0	7.57		44
.300 L.E. flap	None	$\delta_n = 30°$ c" = 0.10	1.04	23.0	6.32		44
		$\delta_n = 30°$ c" = 0.15	1.02	24.0	6.20		44
		$\delta_n = 30°$ c" = 0.20	1.03	23.0	6.04		44
		$\delta_n = 45°$ c" = 0.10	1.03	23.5	6.74		44
		$\delta_n = 45°$ c" = 0.15	1.01	24.0	5.72		44
		$\delta_n = 45°$ c" = 0.20	1.01	22.0	7.15		44
		$\delta_n = 60°$ c" = 0.10	1.04	23.0	6.32		44
		$\delta_n = 60°$ c" = 0.15	1.02	24.0	5.60		44
		$\delta_n = 60°$ c" = 0.20	1.01	24.0	7.79		44
	.430 plain flap	$\delta_n = 30°$ c" = 0.10	1.18	21.5	5.91		44
		$\delta_n = 45°$ c" = 0.10	1.14	20.0	6.68		44

TABLE 30.—SUMMARY OF LONGITUDINAL STABILITY CHARACTERISTICS OF A WING WITH 47.5° OF LEADING-EDGE SWEEPBACK—Continued

Span of L.E. device (b/2)	Span of T.E. device (b/2)	Configuration	$C_{L_{max}}$	$\alpha_{C_{L_{max}}}$	L/D at 0.85 $C_{L_{max}}$	C_m characteristics	Reference
.300 L.E. flap	.655 plain flap	$\delta_n = 30°$ 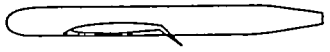 $c'' = 0.10$	1.22	20.5	6.10	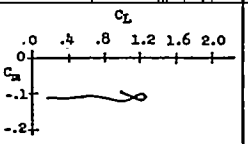	44
		$\delta_n = 45°$ 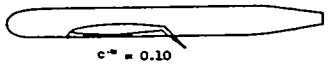 $c'' = 0.10$	1.18	18.0	6.48	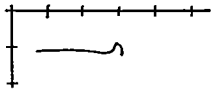	44
	.880 plain flap	$\delta_n = 30°$ 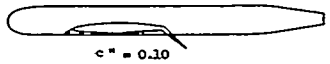 $c'' = 0.10$	1.26	21.0	5.95	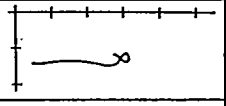	44
		$\delta_n = 45°$ 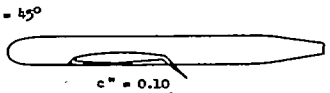 $c'' = 0.10$	1.23	22.5	6.00	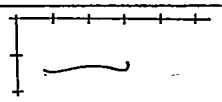	44
.350 L.E. flap	None	$\delta_n = 30°$ 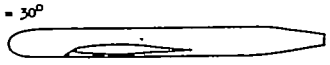 $c'' = 0.10$	1.08	22.5	5.40	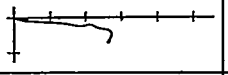	44
		$\delta_n = 30°$ 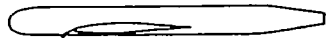 $c'' = 0.15$	1.07	23.0	5.33	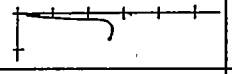	44
		$\delta_n = 30°$ 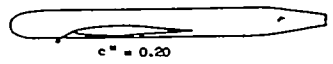 $c'' = 0.20$	1.06	23.5	5.51	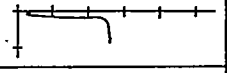	44
		$\delta_n = 45°$ 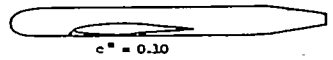 $c'' = 0.10$	1.08	24.0	6.12	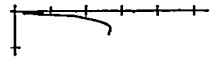	44
		$\delta_n = 45°$ 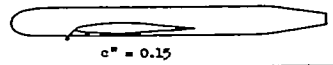 $c'' = 0.15$	1.05	23.5	5.75	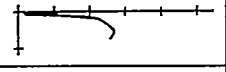	44
		$\delta_n = 45°$ 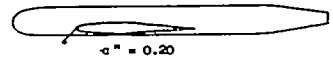 $c'' = 0.20$	1.07	24.0	5.33	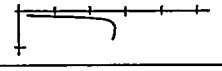	44
		$\delta_n = 60°$ 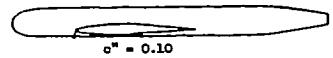 $c'' = 0.10$	1.07	23.5	6.07	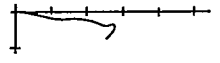	44
		$\delta_n = 60°$ 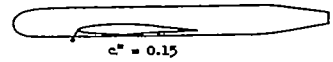 $c'' = 0.15$	1.06	24.0	6.24	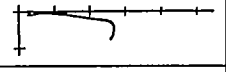	44
		$\delta_n = 60°$ 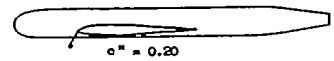 $c'' = 0.20$	1.03	22.5	7.94	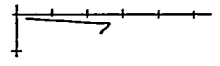	44
	.430 plain flap	$\delta_n = 30°$ 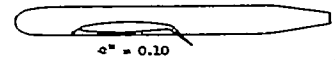 $c'' = 0.10$	1.16	18.5	6.36	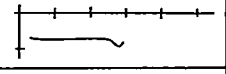	44
	.655 plain flap	$\delta_n = 30°$ 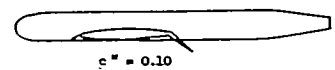 $c'' = 0.10$	1.26	20.5	5.95	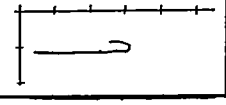	44

TABLE 30.—SUMMARY OF LONGITUDINAL STABILITY CHARACTERISTICS OF A WING WITH 47.5° OF LEADING-EDGE SWEEPBACK—Continued

Span of L.E. device (b/2)	Span of T.E. device (b/2)	Configuration	$C_{L_{max}}$	$\alpha_{C_{L_{max}}}$	L/D at 0.85 $C_{L_{max}}$	C_m characteristics	Reference
.400 L.E. flap	None	$\delta_n = 30°$ 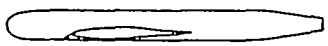 c" = 0.10	1.10	23.0	5.35	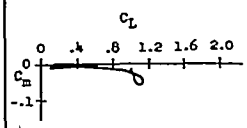	44
		$\delta_n = 30°$ 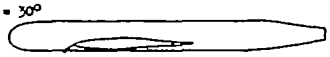 c" = 0.15	1.10	23.0	5.34	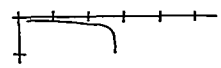	44
		$\delta_n = 30°$ 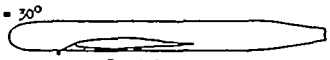 c" = 0.20	1.06	22.0	5.29	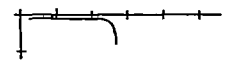	44
		$\delta_n = 45°$ 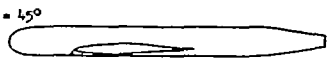 c" = 0.10	1.09	23.0	5.45	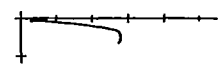	44
		$\delta_n = 45°$ 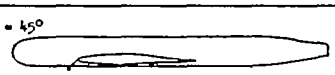 c" = 0.15	1.08	22.0	5.47	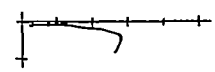	44
		$\delta_n = 45°$ 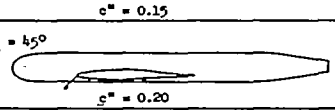 c" = 0.20	1.05	22.0	5.95	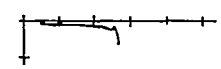	44
		$\delta_n = 60°$ 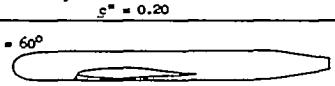 c" = 0.10	1.07	23.0	6.14	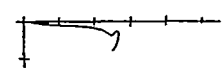	44
		$\delta_n = 60°$ 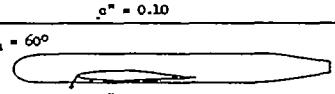 c" = 0.15	1.07	23.0	5.35	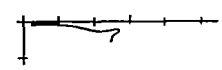	44
		$\delta_n = 60°$ 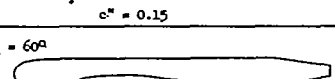 c" = 0.20	1.04	23.0	6.80	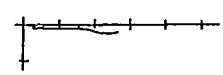	44
	.430 plain flap	$\delta_n = 45°$ 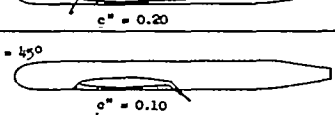 c" = 0.10	1.18	21.0	6.28	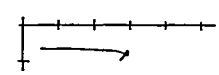	44
	.655 plain flap	$\delta_n = 45°$ 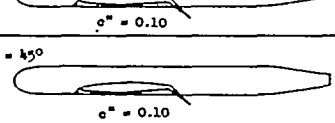 c" = 0.10	1.23	21.5	6.15	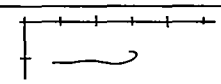	44
.450 L.E. flap	None	$\delta_n = 30°$ 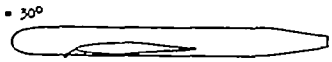 c" = 0.15	1.10	22.0	5.20	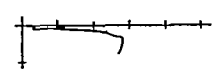	44
		$\delta_n = 30°$ 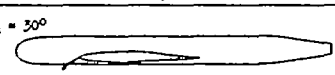 c" = 0.20	1.06	22.0	5.30	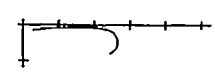	44
		$\delta_n = 45°$ 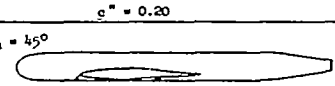 c" = 0.10	1.09	22.0	5.30	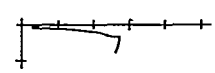	44
		$\delta_n = 45°$ 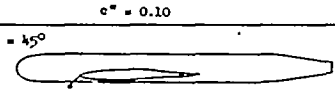 c" = 0.15	1.07	22.0	5.45	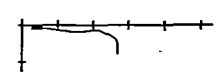	44
		$\delta_n = 45°$ 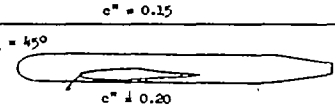 c" = 0.20	1.06	22.0	6.00	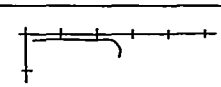	44

TABLE 30.—SUMMARY OF LONGITUDINAL STABILITY CHARACTERISTICS OF A WING WITH 47.5° OF LEADING-EDGE SWEEPBACK—Concluded

Span of L.E. device (b/2)	Span of T.E. device (b/2)	Configuration	$C_{L_{max}}$	$\alpha_{C_{L_{max}}}$	L/D at 0.85 $C_{L_{max}}$	C_m characteristics	Reference
.450 L.E. flap	None	$\delta_n = 60°$ 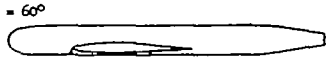 $c'' = 0.10$	1.09	23.5	5.45	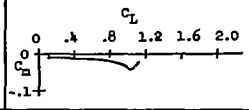	44
		$\delta_n = 60°$ 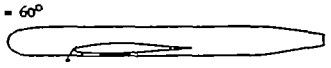 $c'' = 0.15$	1.09	22.5	5.99	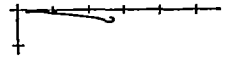	44
		$\delta_n = 60°$ 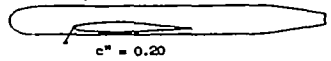 $c'' = 0.20$	1.08	23.0	5.75	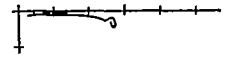	44
.500 L.E. flap	None	$\delta_n = 30°$ 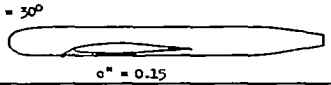 $c'' = 0.15$	1.09	22.0	5.30	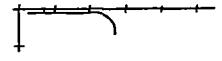	44
		$\delta_n = 30°$ 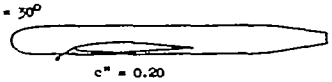 $c'' = 0.20$	1.08	22.0	5.10	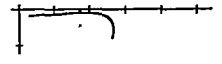	44
		$\delta_n = 45°$ 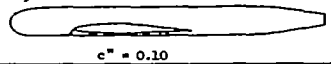 $c'' = 0.10$	1.09	23.0	5.45	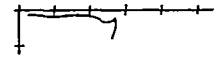	44
		$\delta_n = 45°$ 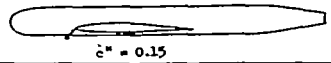 $c'' = 0.15$	1.09	23.0	5.45	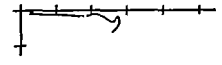	44
		$\delta_n = 45°$ 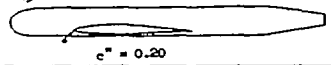 $c'' = 0.20$	1.08	22.0	5.75	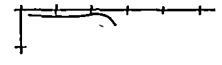	44
		$\delta_n = 60°$ 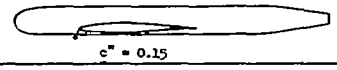 $c'' = 0.15$	1.08	23.5	6.10	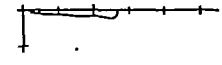	44
.550 L.E. flap	None	$\delta_n = 30°$ 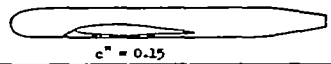 $c'' = 0.15$	1.08	22.0	6.30	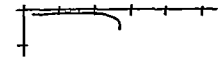	44
		$\delta_n = 30°$ 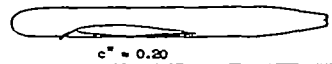 $c'' = 0.20$	1.09	22.0	5.80	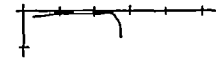	44
		$\delta_n = 45°$ 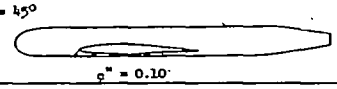 $c'' = 0.10$	1.10	24.0	5.50	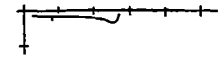	44
		$\delta_n = 45°$ 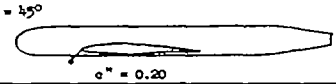 $c'' = 0.20$	1.09	22.0	5.90	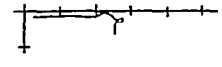	44
.600 L.E. flap	None	$\delta_n = 30°$ 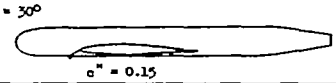 $c'' = 0.15$	1.08	22.0	6.45	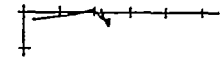	44
		$\delta_n = 30°$ 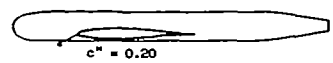 $c'' = 0.20$	1.09	23.0	5.45	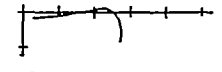	44
		$\delta_n = 45°$ 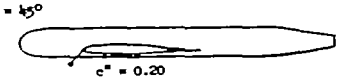 $c'' = 0.20$	1.10	22.5	6.46	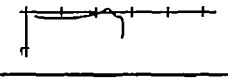	44

TABLE 31.—SUMMARY OF LONGITUDINAL STABILITY CHARACTERISTICS OF A WING WITH 47.5° OF LEADING-EDGE SWEEPBACK

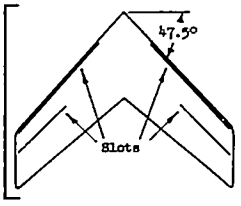

$\Lambda_{c/4} = 45°$ $A = 3.4$ $R_{max} = 6.1 \times 10^6$

$\lambda = 0.510$ $M_{max} = 0.10$

Airfoil sections (perpendicular to 0.250 chord line)

Root: NACA 64_1A112

Tip: NACA 64_1A112

Span of L.E. device (b/2)	Span of T.E. device (b/2)	Configuration	Suction slots	$C_{L_{max}}$	$\Delta C_{L_{max}}$ suction	C_Q	C_m characteristics	Reference
None	None	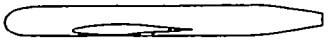	Sealed	1.03	—	—	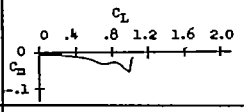	45
			0.005c	1.20	0.17	High	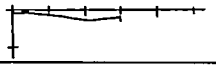	45
			0.005c	1.12	0.09	Moderate	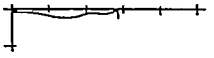	45
			0.005c	0.98	-0.21	Suction power failure	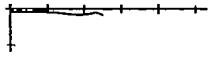	45
			Outboard 0.005c	1.13	0.10	High	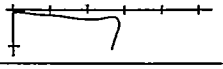	45
			0.005c and 0.40c	1.19	0.16	High	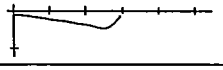	45
			0.005c and 0.40c	1.13	0.10	Moderate	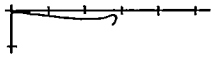	45
			Outboard 0.005c and 0.40c	1.17	0.14	High	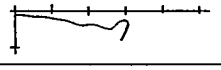	45
			0.025c	1.20	0.17	High	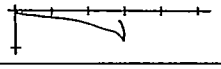	45
			0.025c	1.13	0.10	Moderate	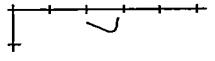	45
			0.025c and 0.40c	1.19	0.16	High	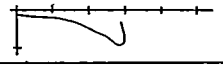	45
			0.025c and 0.40c	1.13	0.13	Moderate	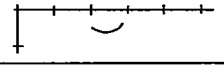	45
	.440 split flap	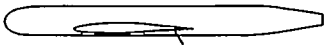	Sealed	1.06	—	—	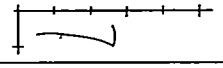	45
			0.005c	1.22	0.16	High	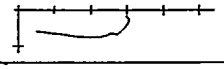	45
			0.005c	1.13	0.07	Moderate	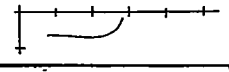	45

TABLE 31.—SUMMARY OF LONGITUDINAL STABILITY CHARACTERISTICS OF A WING WITH 47.5° OF LEADING-EDGE SWEEPBACK—Concluded

Span of L.E. device (b/2)	Span of T.E. device (b/2)	Configuration	Suction slots	$C_{L_{max}}$	$\Delta C_{L_{max}}$ suction	C_Q	C_m characteristics	Reference
None	.440 split flap	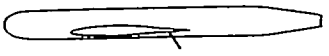	Out-board 0.005c	1.18	0.12	High	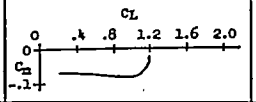	45
			0.005c and 0.40c	1.20	0.14	High	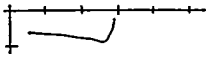	45
			0.005c and 0.40c	1.11	0.05	Moderate	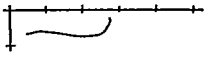	45
			Out-board 0.005c and 0.40c	1.20	0.14	High	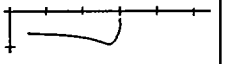	45
.470 L.E. flap	None	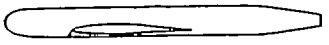	Sealed	1.13	—	—	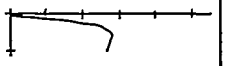	45
			0.025c	1.19	0.06	High	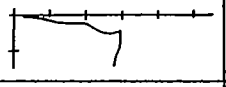	45
			0.025c	1.17	0.04	Moderate	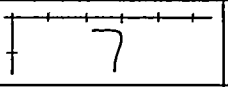	45
.590 L.E. flap	None	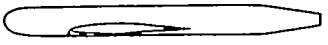	Sealed	1.18	—	—	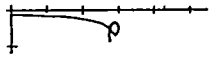	45
			0.025c	1.21	0.03	High	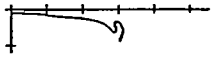	45
			0.025c	1.20	0.02	Moderate	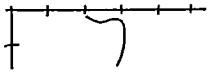	45
.740 L.E. flap	None	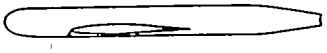	Sealed	1.18	—	—	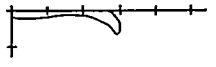	45
			0.025c	1.26	0.08	High	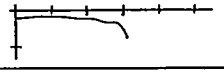	45
			0.025c	1.23	0.05	Moderate	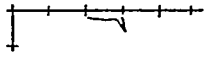	45
			0.025c	1.09	-0.17	Suction power failure	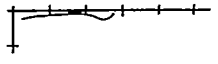	45
			0.025c and 0.40c	1.29	0.11	High	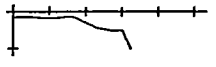	45
			0.025c and 0.40c	1.24	0.06	Moderate	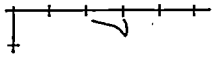	45
	.440 split flap	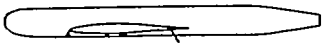	0.025c	1.32	—	High	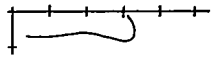	45

TABLE 32.—SUMMARY OF LONGITUDINAL STABILITY CHARACTERISTICS OF A WING WITH 47.5° OF LEADING-EDGE SWEEPBACK

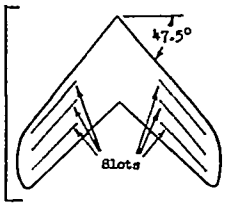

$\Lambda_{c/4} = 45°$ $A = 3.5$ $R_{max} = 7.1 \times 10^6$

$\lambda = 0.500$ $M_{max} = 0.13$

Airfoil sections (perpendicular to 0.250 chord line)

Root: NACA 64_1A112

Tip: NACA 64_1A112

Span of L.E. device (b/2)	Span of T.E. device (b/2)	Configuration	Suction slots	$C_{L_{max}}$	$\alpha_{C_{L_{max}}}$	C_Q	C_m characteristics	Reference
None	None	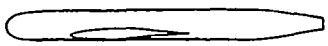	Sealed	0.96	21.0	—	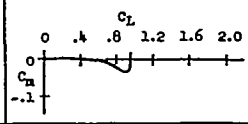	46
			0.20c	1.11	23.0	0.028	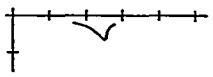	46
			0.40c	1.06	22.0	0.024	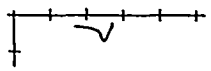	46
			0.70c	1.00	22.0	0.026	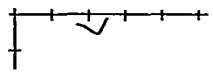	46
			0.20c 0.40c	1.13	22.5	0.034	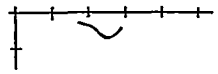	46
			0.20c 0.70c	1.12	24.0	0.033	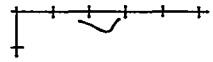	46
			0.40c 0.70c	1.08	24.0	0.035	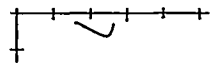	46
			0.20c 0.40c 0.70c	1.11	23.0	0.036	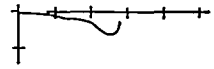	46
	.450 split flap	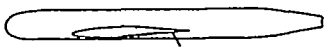	Sealed	1.02	16.0	—	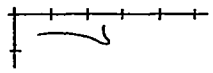	46
			0.20c 0.40c 0.70c	1.14	19.0	0.037	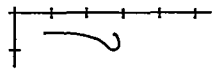	46
	.780 split flap	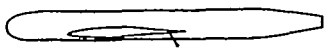	Sealed	1.09	15.5	—	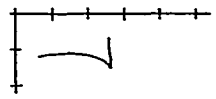	46
			0.20c 0.40c 0.70c	1.23	18.5	0.037	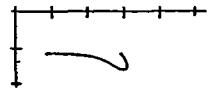	46

TABLE 32.—SUMMARY OF LONGITUDINAL STABILITY CHARACTERISTICS OF A WING WITH 47.5° OF LEADING-EDGE SWEEPBACK—Concluded

Span of L.E. device (b/2)	Span of T.E. device (b/2)	Configuration	Suction slots	$C_{L_{max}}$	$\alpha_{C_{L_{max}}}$	C_Q	C_m characteristics	Reference
.500 L.E. flap	None	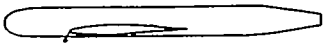	Sealed	1.10	23.5	——	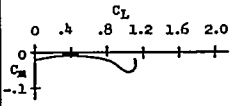	46
			.20c .40c .70c	1.14	22.5	0.037	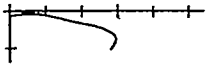	46
	.450 split flap	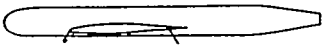	Sealed	1.15	19.6	——	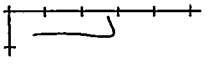	46
			.20c .40c .70c	1.21	21.5	0.037	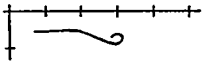	46
.600 L.E. flap	None	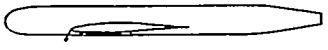	Sealed	1.09	22.8	——	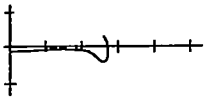	46
			.20c .40c .70c	1.17	24.0	0.037	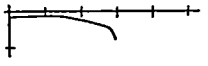	46
	.450 split flap	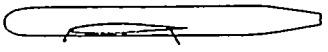	Sealed	1.14	20.0	——	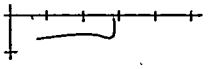	46
			.20c .40c .70c	1.24	21.5	0.037	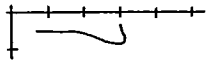	46
.710 L.E. flap	None	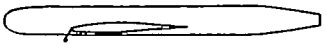	Sealed	1.10	23.0	——	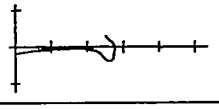	46
			.20c .40c .70c	1.18	24.8	0.037	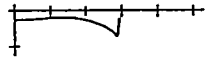	46
	.450 split flap	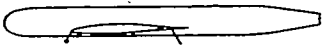	Sealed	1.15	20.3	——	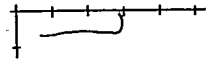	46
			.20c .40c .70c	1.28	21.5	0.037	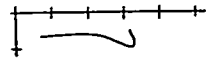	46

TABLE 33.—SUMMARY OF LONGITUDINAL STABILITY CHARACTERISTICS OF A WING WITH 47.5° OF LEADING-EDGE SWEEPBACK

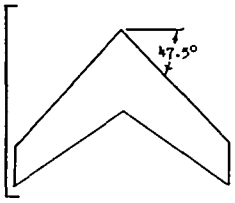

$\Lambda_{c/4} = 45°$ $A = 3.50$ $R_{max} = 6.8 \times 10^6$

$\lambda = 0.500$

Airfoil sections (normal to line of maximum thickness)

Root: 10-percent-thick circular arc

Tip: 10-percent-thick circular arc

Span of L.E. device (b/2)	Span of T.E. device (b/2)	Configuration	$C_{L_{max}}$	$\alpha_{C_{L_{max}}}$	L/D at 0.85 $C_{L_{max}}$	C_m characteristics	Reference
None	None	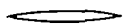	0.87	21.6	3.71	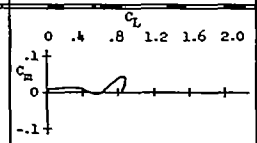	47
		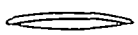	0.84	23.5	4.08	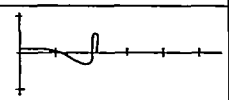	47
.500 rounded L.E.	None	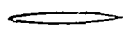	0.88	23.0	3.57	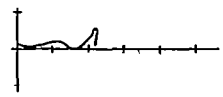	47
		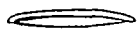	0.87	25.0	3.79	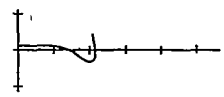	47
None	.500 plain flap	$\delta_f = 20°$ 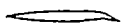	0.95	20.0	4.94	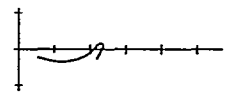	47
		$\delta_f = 40°$ 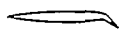	0.94	18.0	5.00	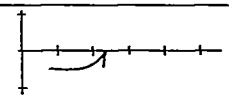	47
		$\delta_f = 60°$ 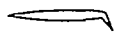	0.92	16.0	4.86	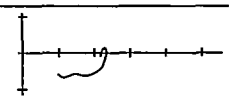	47
	1.000 plain flap	$\delta_f = 20°$	1.01	19.5	5.05	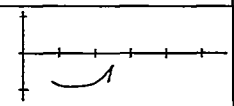	47
		$\delta_f = 40°$ 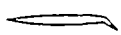	1.05	18.0	4.85	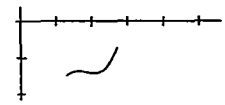	47
		$\delta_f = 60°$ 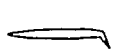	1.05	16.0	4.69	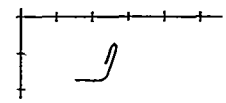	47

TABLE 33.—SUMMARY OF LONGITUDINAL STABILITY CHARACTERISTICS OF A WING WITH 47.5° OF LEADING-EDGE SWEEPBACK—Continued

Span of L.E. device (b/2)	Span of T.E. device (b/2)	Configuration	$C_{L_{max}}$	$\alpha_{C_{L_{max}}}$	L/D at 0.85 $C_{L_{max}}$	C_m characteristics	Reference
.250 L.E. droop	None	$\delta_n = 20°$ 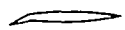	0.88	23.6	3.48	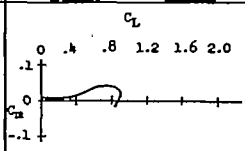	47
		$\delta_n = 30°$ 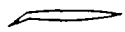	0.86	23.6	3.57	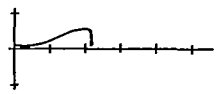	47
	.500 plain flap	$\delta_n = 30°$ 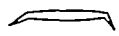	0.91	17.0	4.69	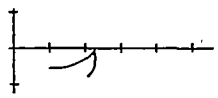	47
.500 L.E. droop	None	$\delta_n = 20°$ 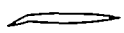	0.92	22.5	3.72	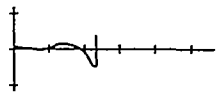	47
		$\delta_n = 30°$ 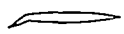	1.02*	26.3	3.21	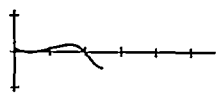	47
	.500 plain flap	$\delta_n = 30°$ $\delta_f = 60°$ 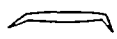	1.06	24.2	3.40	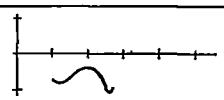	47
.750 L.E. droop	None	$\delta_n = 20°$ 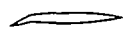	1.00	26.3	4.36	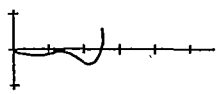	47
		$\delta_n = 30°$ 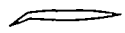	1.10	26.3	3.74	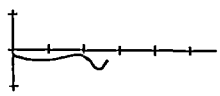	47
	.500 plain flap	$\delta_n = 30°$ $\delta_f = 60°$ 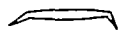	1.16	22.0	4.41	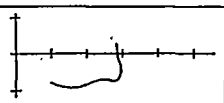	47
1.000 L.E. droop	None	$\delta_n = 10°$	0.94	24.5	4.37	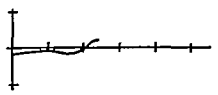	47
		$\delta_n = 20°$ 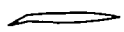	1.00*	26.3	5.49	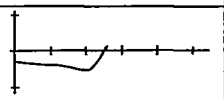	47
		$\delta_n = 30°$ 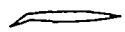	1.05*	26.3	6.61	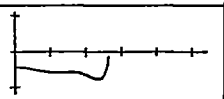	47
		$\delta_n = 40°$ 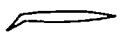	1.07*	26.3	7.28	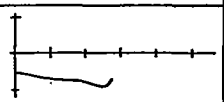	47

*$C_{L_{max}}$ not reached.

TABLE 33.—SUMMARY OF LONGITUDINAL STABILITY CHARACTERISTICS OF A WING WITH 47.5° OF LEADING-EDGE SWEEPBACK—Concluded

Span of L.E. device (b/2)	Span of T.E. device (b/2)	Configuration	$C_{L_{max}}$	$\alpha_{C_{L_{max}}}$	L/D at 0.85 $C_{L_{max}}$	C_m characteristics	Reference
	.500 plain flap	$\delta_n = 30°$ $\delta_f = 60°$ 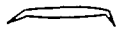	1.11	18.2	6.08	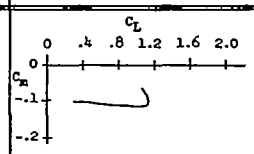	47
		$\delta_n = 40°$ $\delta_f = 60°$ 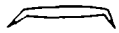	1.15	20.0	6.11	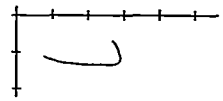	47
	1.000 plain flap	$\delta_n = 10°$ $\delta_f = 20°$ 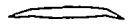	1.06	21.2	5.81	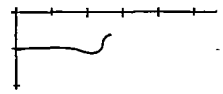	47
		$\delta_n = 10°$ $\delta_f = 40°$ 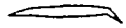	1.10	20.0	5.35	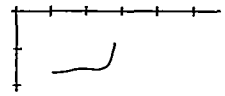	47
		$\delta_n = 10°$ $\delta_f = 60°$ 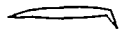	1.10	16.0	4.86	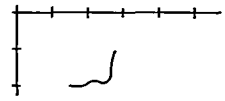	47
		$\delta_n = 20°$ $\delta_f = 20°$ 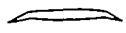	1.12	23.0	6.34	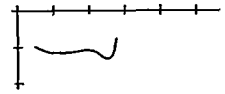	47
1.000 L.E. droop		$\delta_n = 20°$ $\delta_f = 40°$ 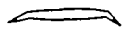	1.16	18.0	5.80	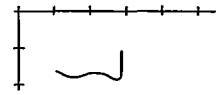	47
		$\delta_n = 20°$ $\delta_f = 60°$ 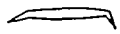	1.17	16.0	5.11	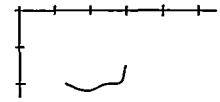	47
		$\delta_n = 30°$ $\delta_f = 20°$ 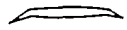	1.20	26.0	6.38	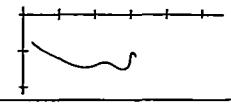	47
		$\delta_n = 30°$ $\delta_f = 40°$ 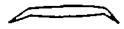	1.23	20.0	5.97	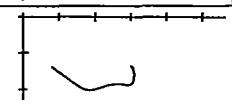	47
		$\delta_n = 30°$ $\delta_f = 60°$ 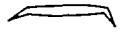	1.23	18.0	5.09	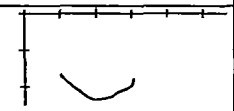	47
		$\delta_n = 40°$ $\delta_f = 40°$ 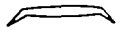	1.25	23.0	6.07	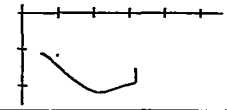	47
		$\delta_n = 40°$ $\delta_f = 60°$ 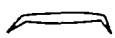	1.26	22.0	5.16	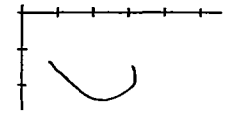	47

TABLE 34.—SUMMARY OF LONGITUDINAL STABILITY CHARACTERISTICS OF A WING WITH 47.7° OF LEADING-EDGE SWEEPBACK

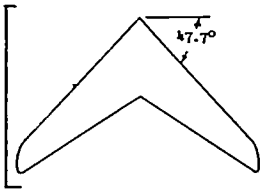

$\Lambda_{c/4} = 45°$ $A = 5.10$ $R_{max} = 6.00 \times 10^6$

$\lambda = 0.383$ $M_{max} = 0.14$

Airfoil sections (perpendicular to 0.286 chord line)

Root: NACA 64-210

Tip: NACA 64-210

Span of L.E. device (b/2)	Span of T.E. device (b/2)	Configuration	$C_{L_{max}}$	$\alpha_{C_{L_{max}}}$	L/D at 0.85 $C_{L_{max}}$	C_m characteristics	Reference
None	None		1.16	26.1	4.52	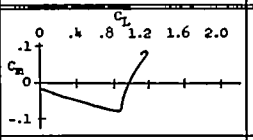	48
			1.16	26.1	7.67	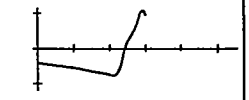	49
		$i_t = -4.1°$ $\frac{2z}{b} = -.053$	1.30*	26.2	—	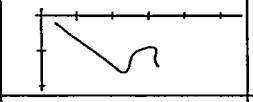	50
		$i_t = -3.1°$ $\frac{2z}{b} = .382$	1.16	22.0	—	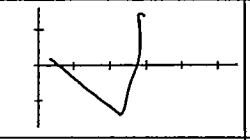	50
	.450 split flap		1.17	21.7	—	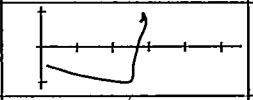	49
	.600 split flap		1.19	21.0	—	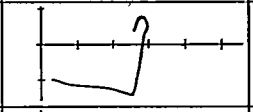	49
	.618 split flap		1.22	24.0	7.41	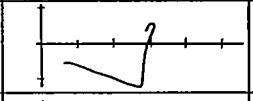	48
	.972 split flap		1.34	24.3	—	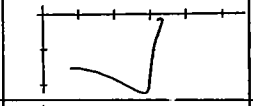	48
	.450 single slotted flap		1.26	25.0	—	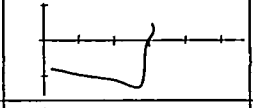	49
	.400 double slotted flap		1.30	23.0	7.27	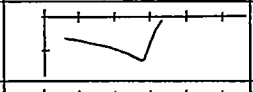	48
	.450 double slotted flap	$\delta_f = 30°$	1.36	25.0	5.82	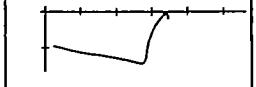	49
	.516 double slotted flap		1.39	23.2	7.62	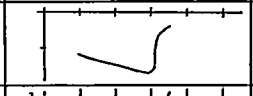	48
	.626 double slotted flap		1.42	23.0	7.54		48

*$C_{L_{max}}$ not reached.

TABLE 34.—SUMMARY OF LONGITUDINAL STABILITY CHARACTERISTICS OF A WING WITH 47.7° OF LEADING-EDGE SWEEPBACK—Continued

Span of L.E. device (b/2)	Span of T.E. device (b/2)	Configuration	$C_{L_{max}}$	$\alpha_{C_{L_{max}}}$	L/D at 0.85 $C_{L_{max}}$	C_m characteristics	Reference
None	.978 double slotted flap	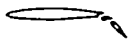	1.61	24.5	——	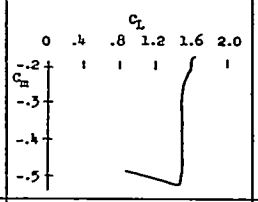	48
	Tri-angular flap	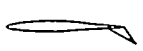 $\delta_f = 30°$	1.30	18.0	——	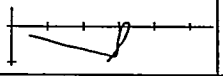	49
	.450 rotated split flap	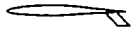	1.25	19.0	——	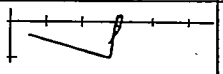	49
	.450 ext. split flap	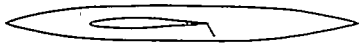	1.34	21.0	——	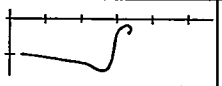	49
	.600 ext. split flap	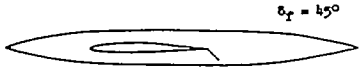 $\delta_f = 45°$	1.39	21.0	——	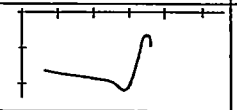	49
.275 L.E. flap	.400 split flap	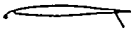	1.20	23.0	7.28	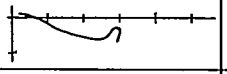	48
	.618 split flap	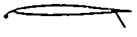	1.21	20.0	7.62	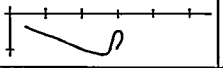	48
.375 L.E. flap	None		1.23	27.2	4.75	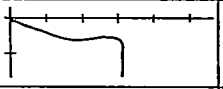	48
		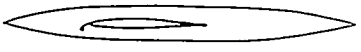	1.36*	29.3	3.94	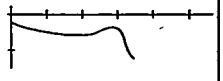	49
	.400 split flap	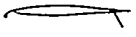	1.26	25.0	6.92	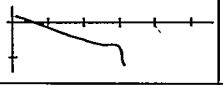	48
	.450 split flap	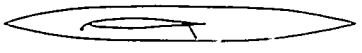	1.32	31.0	——	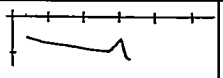	49
	.500 split flap	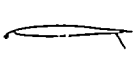	1.31	25.0	6.18	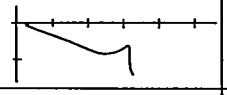	48
	.600 split flap	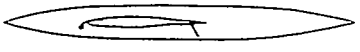	1.34*	16.0	——	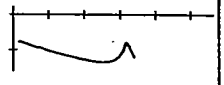	49
	.618 split flap	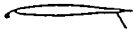	1.35*	23.5	6.72	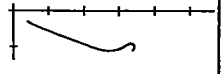	48
	.450 single slotted flap	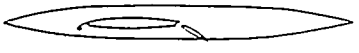	1.45	29.5	4.60	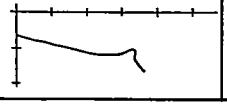	51

*$C_{L_{max}}$ not reached.

TABLE 34.—SUMMARY OF LONGITUDINAL STABILITY CHARACTERISTICS OF A WING WITH 47.7° OF LEADING-EDGE SWEEPBACK—Continued

Span of L.E. device (b/2)	Span of T.E. device (b/2)	Configuration	$C_{L_{max}}$	$\alpha_{C_{L_{max}}}$	L/D at 0.85 $C_{L_{max}}$	C_m characteristics	Reference
.373 L.E. flap	.400 double slotted flap	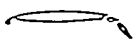	1.36	22.5	6.73	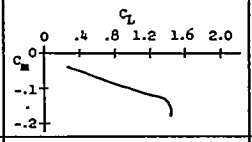	48
	.450 double slotted flap	$\delta_f = 30°$ 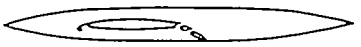	1.47*	29.4	5.47	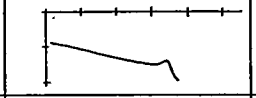	49
	.516 double slotted flap	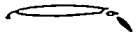	1.38	25.0	7.34	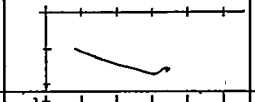	48
	.626 double slotted flap	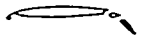	1.50	18.0	7.52	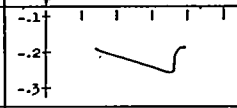	48
	.978 double slotted flap	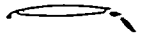	1.75	19.6	—	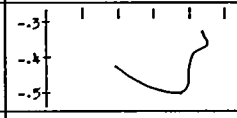	48
	Triangular flap	$\delta_f = 30°$ 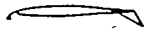	1.41	19.0	—	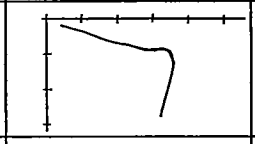	49
		$\delta_f = 30°$ 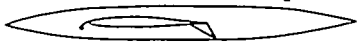	1.46	22.5	—	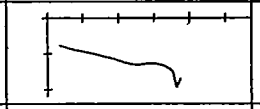	49
	.450 rotated split flap	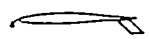	1.37	23.8	—	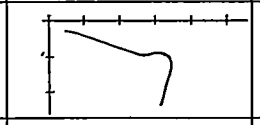	49
	.450 step split flap	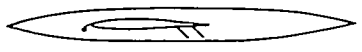	1.27*	31.2	—	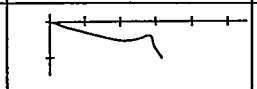	49
			1.38	31.0	—	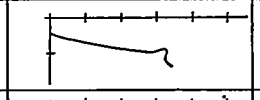	49
	.450 ext. split flap	$\delta_f = 15°$ 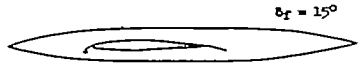	1.43	31.0	—	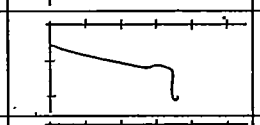	49
		$\delta_f = 30°$ 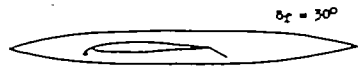	1.46	31.0	—	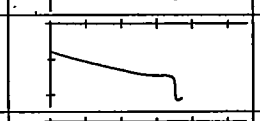	49
		$\delta_f = 45°$ 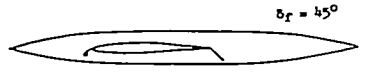	1.46	30.0	—	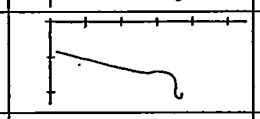	49
		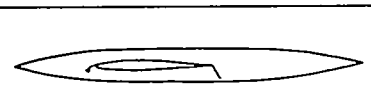	1.45	31.0	—	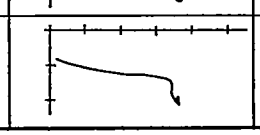	49

*$C_{L_{max}}$ not reached.

TABLE 34.—SUMMARY OF LONGITUDINAL STABILITY CHARACTERISTICS OF A WING WITH 47.7° OF LEADING-EDGE SWEEPBACK—Continued

Span of L.E. device (b/2)	Span of T.E. device (b/2)	Configuration	$C_{L_{max}}$	$\alpha_{C_{L_{max}}}$	L/D at 0.85 $C_{L_{max}}$	C_m characteristics	Reference
.375 L.E. flap	.600 ext. split flap	$\delta_f = 45°$	1.59	23.0	——		49
.425 L.E. flap	None		1.30	30.0	4.42		48
			1.41*	29.0	3.75		49
	.400 split flap		1.31*	25.0	6.36		48
	.450 split flap	$\delta_f = 15°$	1.43	29.0	——		49
		$\delta_f = 30°$	1.45	29.2	——		49
		$\delta_f = 45°$	1.36	25.0	——		49
			1.34	31.0	——		49
	.500 split flap		1.37*	22.0	5.54		48
	.600 split flap		1.38	21.4	——		49
	.450 double slotted flap	$\delta_f = 30°$	1.51*	29.0	5.94		49
	.516 double slotted flap		1.49	20.5	7.19		49
	Tri-angular flap	$\delta_f = 30°$	1.44	22.0	——		49
		$\delta_f = 30°$	1.47	30.0	——		49
	.450 rotated split flap		1.44	23.5	——		49

*$C_{L_{max}}$ not reached.

TABLE 34.—SUMMARY OF LONGITUDINAL STABILITY CHARACTERISTICS OF A WING WITH 47.7° OF LEADING-EDGE SWEEPBACK—Continued

Span of L.E. device (b/2)	Span of T.E. device (b/2)	Configuration	$C_{L_{max}}$	$\alpha_{C_{L_{max}}}$	L/D at 0.85 $C_{L_{max}}$	C_m characteristics	Reference
.425 L.E. flap	.450 step split flap	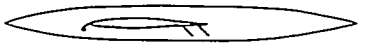	1.31	29.0	——	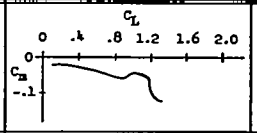	49
		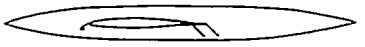	1.43	30.0	——	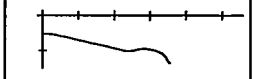	49
	.450 ext. split flap	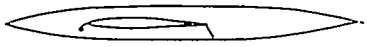	1.49	28.0	——	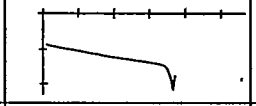	49
	.600 ext. split flap	$\delta_f = 30°$ 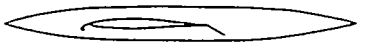	1.65	25.0	——	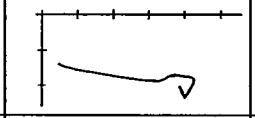	49
.475 L.E. flap	None		1.28*	25.0	5.07	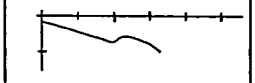	48
		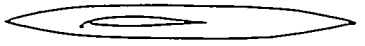	1.44	28.0	——	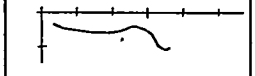	Unpublished
		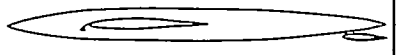 $i_t = -4.3°$ $\frac{2z}{b} = -.053$	1.50*	26.5	——	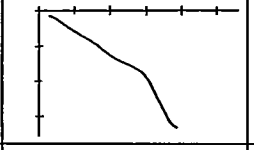	50
		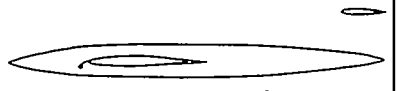 $i_t = -3.1°$ $\frac{2z}{b} = .382$	1.40*	26.1	——	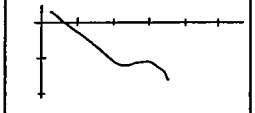	50
	.400 split flap	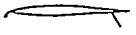	1.37*	25.0	5.69		48
		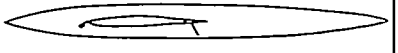	1.35*	25.5	5.45	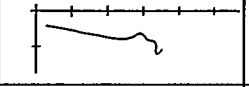	48
		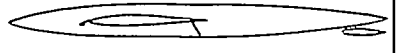 $i_t = -4.1°$ $\frac{2z}{b} = -.053$	1.54*	26.4	——	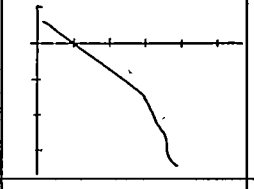	50
		$i_t = -3.1°$ $\frac{2z}{b} = .382$	1.41*	26.3	——	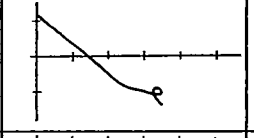	50
	.450 split flap	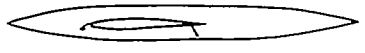	1.39	22.0	6.34	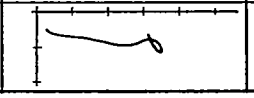	49

*$C_{L_{max}}$ not reached.

TABLE 34.—SUMMARY OF LONGITUDINAL STABILITY CHARACTERISTICS OF A WING WITH 47.7° OF LEADING-EDGE SWEEPBACK—Continued

Span of L.E. device (b/2)	Span of T.E. device (b/2)	Configuration	$C_{L_{max}}$	$\alpha_{C_{L_{max}}}$	L/D at 0.85 $C_{L_{max}}$	C_m characteristics	Reference
.475 L.E. flap	.500 split flap	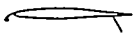	1.43	25.0	5.79	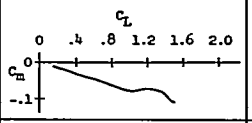	48
		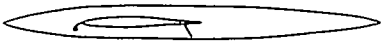	1.38	28.0	—	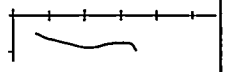	50
		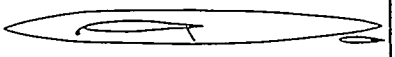 $i_t = -3.3°$ $\frac{2z}{b} = -.053$	1.51	27.3	—	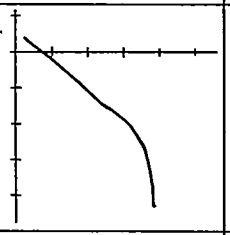	50
	.600 split flap	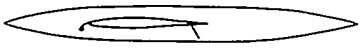	1.44	26.0	5.84	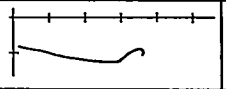	49
	.618 split flap	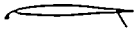	1.46	23.5	5.64	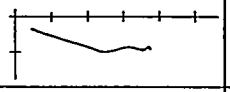	48
	.450 single slotted flap		1.49	25.0	5.77	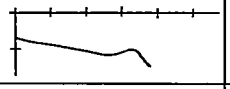	49
	.400 double slotted flap	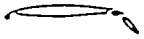	1.48	22.5	6.55	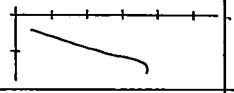	48
		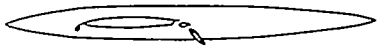	1.42*	26.0	6.85	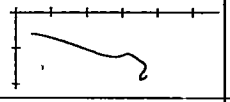	48
		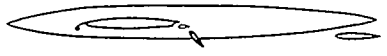 $i_t = -3.9°$ $\frac{2z}{b} = -.053$	1.54	26.0	—	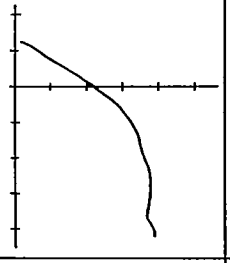	50
		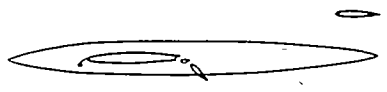 $i_t = -2.9°$ $\frac{2z}{b} = .150$	1.47*	26.2	—	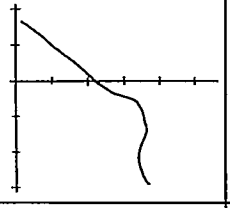	50
		$i_t = -3.1°$ $\frac{2z}{b} = .382$	1.43*	26.3	—	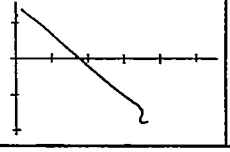	50

*$C_{L_{max}}$ not reached.

TABLE 34.—SUMMARY OF LONGITUDINAL STABILITY CHARACTERISTICS OF A WING WITH 47.7° OF LEADING-EDGE SWEEPBACK—Continued

Span of L.E. device (b/2)	Span of T.E. device (b/2)	Configuration	$C_{L_{max}}$	$\alpha_{C_{L_{max}}}$	L/D at 0.85 $C_{L_{max}}$	C_m characteristics	Reference
.473 L.E. flap	.450 double slotted flap	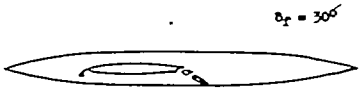 $\delta_f = 30°$	1.57	26.0	5.99	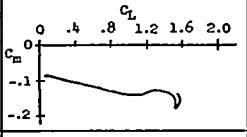	49
	.516 double slotted flap	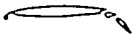	1.58	22.5	6.88	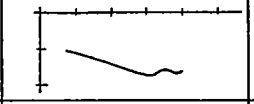	48
	.626 double slotted flap	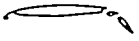	1.70	23.0	6.57	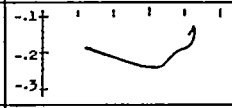	48
	Triangular flap	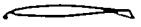 $\delta_f = 15°$	1.46	23.0	—	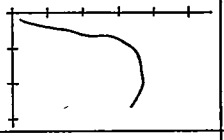	49
		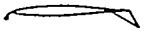 $\delta_f = 30°$	1.46	19.0	—	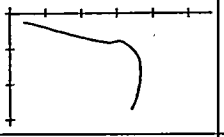	49
		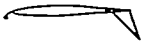 $\delta_f = 45°$	1.44	19.0	—	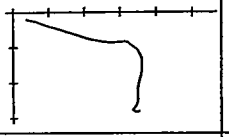	49
		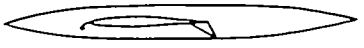 $\delta_f = 30°$	1.50	30.0	6.02	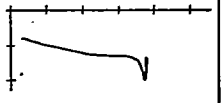	49
	.450 rotated split flap	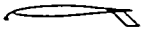	1.46	23.8	—	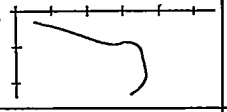	49
	.450 step split flap	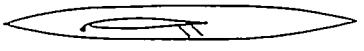	1.33	25.2	4.93	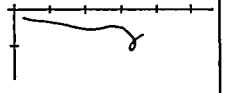	49
		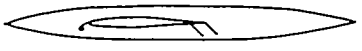	1.49	26.0	5.49	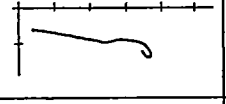	49
	.450 ext. split flap	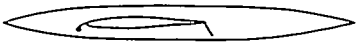	1.51	26.0	6.18	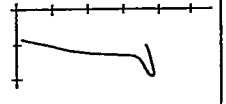	49
	.600 ext. split flap	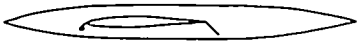 $\delta_f = 45°$	1.70	23.0	—	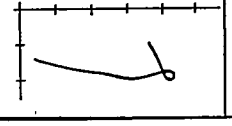	49

TABLE 34.—SUMMARY OF LONGITUDINAL STABILITY CHARACTERISTICS OF A WING WITH 47.7° OF LEADING-EDGE SWEEPBACK—Continued

Span of L.E. device (b/2)	Span of T.E. device (b/2)	Configuration	$C_{L_{max}}$	$\alpha_{C_{L_{max}}}$	L/D at 0.85 $C_{L_{max}}$	C_m characteristics	Reference
.525 L.E. flap	None	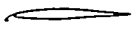	1.35*	27.0	4.99	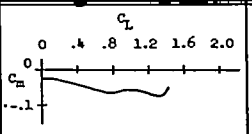	48
		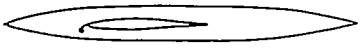	1.45	28.0	4.61	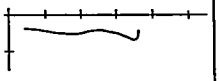	49
	.400 split flap	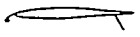	1.34	22.0	—	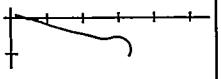	48
		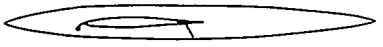	1.45	24.5	—	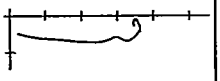	50
		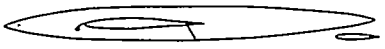 $i_t = -3.7°$ $\frac{2z}{b} = -.053$	1.54	24.5	—	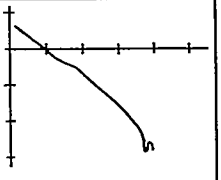	50
	.500 split flap	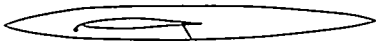	1.45	25.4	—	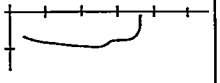	50
		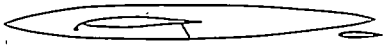 $i_t = -3.3°$ $\frac{2z}{b} = -.053$	1.57	28.3	—	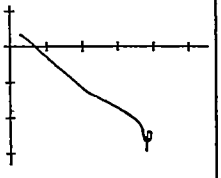	50
	.600 split flap	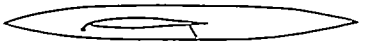	1.48	25.0	5.72	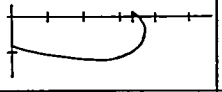	49
	.450 single slotted flap	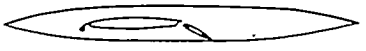	1.52	25.0	5.92	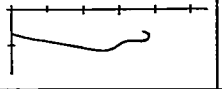	49
	.400 double slotted flap	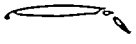	1.47	22.5	6.95	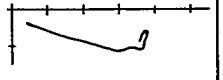	48
	.450 double slotted flap	$\delta_f = 30°$	1.62	25.0	5.98	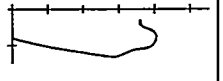	49
	.516 double slotted flap	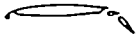	1.60	22.5	—	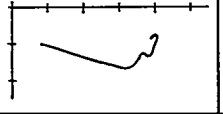	48
	Triangular flap	$\delta_f = 30°$ 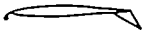	1.46	17.0	—	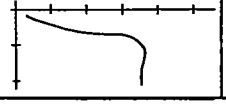	49

*$C_{L_{max}}$ not reached.

TABLE 34.—SUMMARY OF LONGITUDINAL STABILITY CHARACTERISTICS OF A WING WITH 47.7° OF LEADING-EDGE SWEEPBACK—Continued

Span of L.E. device (b/2)	Span of T.E. device (b/2)	Configuration	$C_{L_{max}}$	$\alpha_{C_{L_{max}}}$	L/D at 0.85 $C_{L_{max}}$	C_m characteristics	Reference
.525 L.E. flap	Tri-angular flap	$\delta_f = 30°$	1.55	21.5	——	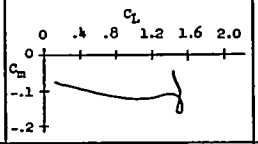	49
	.450 rotated split flap	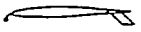	1.46	18.0	——	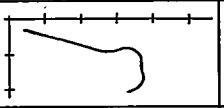	49
	.450 step split flap	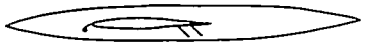	1.35	29.2	——	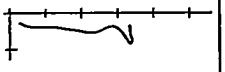	49
		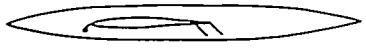	1.49	24.0	——	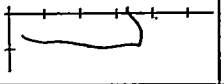	49
	.450 ext. split flap	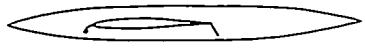	1.55	23.4	——	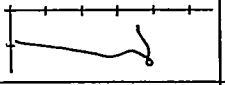	49
	.600 ext. split flap	$\delta_f = 45°$	1.67	23.8	——	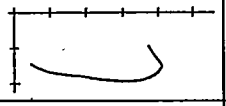	49
.575 L.E. flap	None	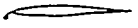	1.32	26.0	5.75	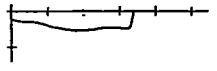	48
	.400 split flap	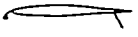	1.38	23.0	6.90	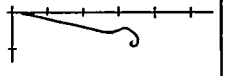	48
	.500 split flap	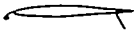	1.42	20.5	6.89	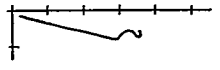	48
	.618 split flap		1.44	20.0	6.80	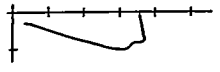	48
	.400 double slotted flap	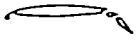	1.52	22.5	6.80	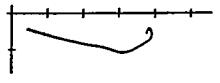	48
	.516 double slotted flap	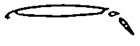	1.59	22.0	——	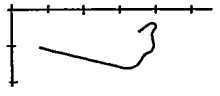	48
	.626 double slotted flap	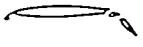	1.66	21.0	7.06	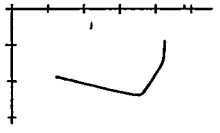	48
	Tri-angular flap	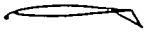 $\delta_f = 30°$	1.53	18.0	——	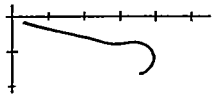	Un-published

TABLE 34.—SUMMARY OF LONGITUDINAL STABILITY CHARACTERISTICS OF A WING WITH 47.7° OF LEADING-EDGE SWEEPBACK—Continued

Span of L.E. device (b/2)	Span of T.E. device (b/2)	Configuration	$C_{L_{max}}$	$\alpha_{C_{L_{max}}}$	L/D at 0.85 $C_{L_{max}}$	C_m characteristics	Reference
.700 L.E. flap	None	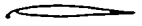	1.27	25.0	8.00	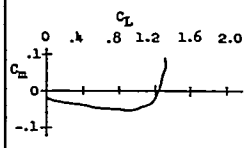	48
	.400 split flap	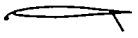	1.41	20.5	8.01	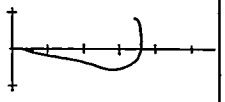	48
	.500 split flap	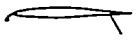	1.45	20.5	7.96	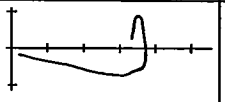	48
	.618 split flap	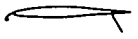	1.48	20.4	——	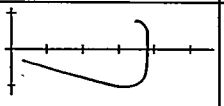	48
.975 L.E. flap	.618 split flap	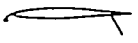	1.54	19.5	7.65	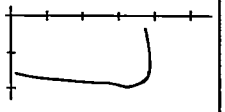	48
.375 L.E. droop	None	$\delta_n = 20°$ 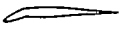	1.19	26.0	4.59.	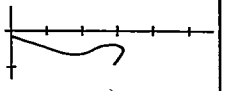	48
	.400 split flap	$\delta_n = 20°$ 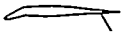	1.22	23.0	6.47	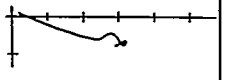	48
	.500 split flap	$\delta_n = 20°$ 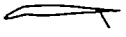	1.25	23.0	6.65	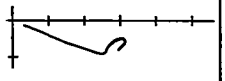	48
	.400 double slotted flap	$\delta_n = 20°$ 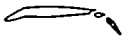	1.34	22.0	7.59	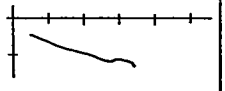	48
		$\delta_n = 20°$ 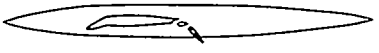	1.31	20.0	——	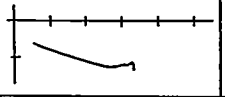	50
		$\delta_n = 20°$ 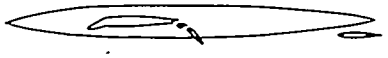 $i_t = -4.1°$ $\frac{2z}{b} = -.053$	1.44	26.2	——	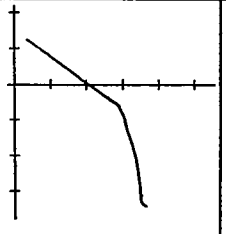	50
		$\delta_n = 20°$ 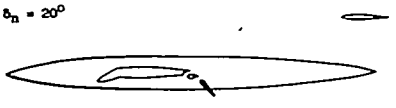 $i_t = -4.7°$ $\frac{2z}{b} = .382$	1.36	20.0	——	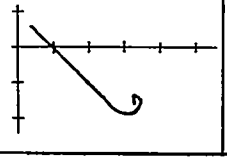	50

TABLE 34.—SUMMARY OF LONGITUDINAL STABILITY CHARACTERISTICS OF A WING WITH 47.7° OF LEADING-EDGE SWEEPBACK—Concluded

Span of L.E. device (b/2)	Span of T.E. device (b/2)	Configuration	$C_{L_{max}}$	$\alpha_{C_{L_{max}}}$	L/D at 0.85 $C_{L_{max}}$	C_m characteristics	Reference
.375 L.E. droop	.516 double slotted flap	$\delta_n = 20°$ 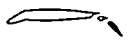	1.36	19.0	7.70	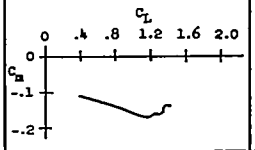	48
.475 L.E. droop	None	$\delta_n = 20°$ 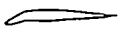	1.36	31.0	3.61	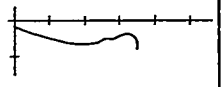	48
	.400 split flap	$\delta_n = 20°$ 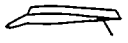	1.32	23.0	5.59	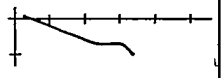	48
	.500 split flap	$\delta_n = 20°$ 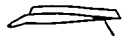	1.38*	25.0	5.32	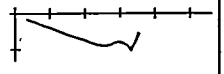	48
	.618 split flap	$\delta_n = 20°$ 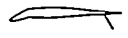	1.41	23.0	5.45	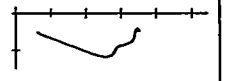	48
	.400 double slotted flap	$\delta_n = 20°$	1.47	23.5	5.67	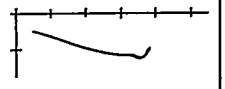	48
	.516 double slotted flap	$\delta_n = 20°$ 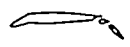	1.53	20.0	6.88	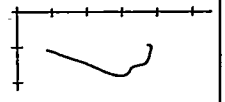	48
	.626 double slotted flap	$\delta_n = 20°$	1.58	20.5	7.47		48
.700 L.E. droop	.516 double slotted flap	$\delta_n = 20°$ 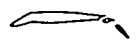	1.49	17.0	7.64	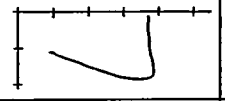	48
	.626 double slotted flap	$\delta_n = 20°$	1.57	15.5	7.61	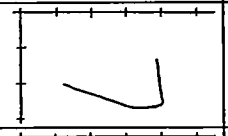	48
.375 L.E. droop	.400 double slotted flap	$\delta_n = 30°$ 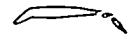	1.32	20.0	7.50	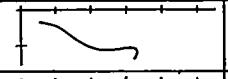	48
.475 L.E. droop	.400 double slotted flap	$\delta_n = 30°$	1.47	22.0	5.68	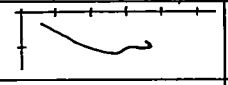	48
	.626 double slotted flap	$\delta_n = 30°$ 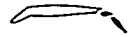	1.61	23.5	7.34	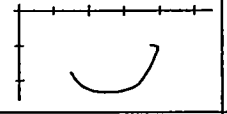	48
.700 L.E. droop	.626 double slotted flap	$\delta_n = 30°$	1.60	23.0	7.36		48

*$C_{L_{max}}$ not reached.

TABLE 35.—SUMMARY OF LONGITUDINAL STABILITY CHARACTERISTICS OF A WING WITH 48.1° OF LEADING-EDGE SWEEPBACK

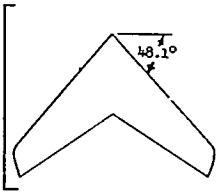

$\Lambda_{c/4} = 45°$ $A = 3.64$ $R_{max} = 18.0 \times 10^6$

$\lambda = 0.420$

Airfoil sections (variable)

Root: NACA 0015 (approximate)

Tip: NACA 23009 (approximate)

Span of L.E. device (b/2)	Span of T.E. device (b/2)	Configuration	$C_{L_{max}}$	$\alpha_{C_{L_{max}}}$	L/D at 0.85 $C_{L_{max}}$	C_m characteristics	Reference
None	None	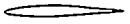	1.22	28.0	7.42	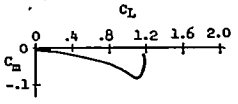	17
	.623 split flap	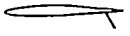	1.35	17.5	5.10	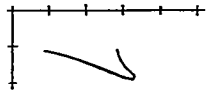	17
	.962 split flap	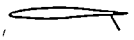	1.36	16.5	5.03	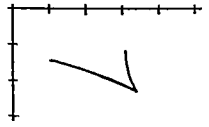	17

TABLE 36.—SUMMARY OF LONGITUDINAL STABILITY CHARACTERISTICS OF A WING WITH 48.4° OF LEADING-EDGE SWEEPBACK

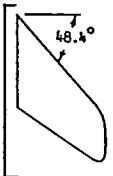

$\Lambda_{c/4} = 45°$ $A = 2.0$ $R_{max} = 12.0 \times 10^6$

$\lambda = 0.600$ $M_{max} = 0.20$

Airfoil sections (parallel to plane of symmetry)

Root: NACA 65A006

Tip: NACA 65A006

Span of L.E. device (b/2)	Span of T.E. device (b/2)	Configuration	$C_{L_{max}}$	$\alpha_{C_{L_{max}}}$	L/D at 0.85 $C_{L_{max}}$	C_m characteristics	Reference
None	None	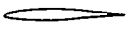	1.03	24.0	3.65	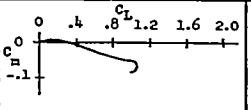	14
	.500 split flap	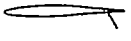	1.13	20.7	3.84	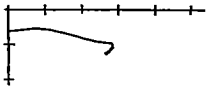	14

TABLE 37.—SUMMARY OF LONGITUDINAL STABILITY CHARACTERISTICS OF A WING WITH 48.6° OF LEADING-EDGE SWEEPBACK

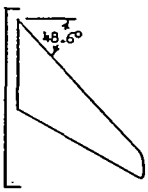

$\Lambda_{c/4} = 45°$ $A = 4.0$ $R_{max} = 11.9 \times 10^6$

$\lambda = 0.300$ $M_{max} = 0.20$

Airfoil sections (parallel to plane of symmetry)

Root: NACA 65A006

Tip: NACA 65A006

Span of L.E. device (b/2)	Span of T.E. device (b/2)	Configuration	$C_{L_{max}}$	$\alpha_{C_{L_{max}}}$	$\overline{L/D}$ at 0.85 $C_{L_{max}}$	C_m characteristics	Reference
None	None	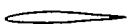	1.08	24.5	3.83	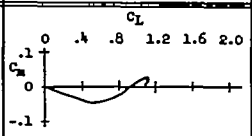	14
	.500 split flap	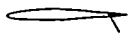	1.06	20.5	4.39	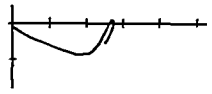	14

TABLE 38.—SUMMARY OF LONGITUDINAL STABILITY CHARACTERISTICS OF A WING WITH 52° OF LEADING-EDGE SWEEPBACK

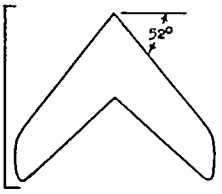

$\Lambda_{c/4} = 50°$ $A = 2.88$ $R_{max} = 11.0 \times 10^6$

$\lambda = 0.625$ $M_{max} \doteq 0.21$

Airfoil sections (perpendicular to 0.282 chord line)

Root: NACA 64_1-112

Tip: NACA 64_1-112

Span of L.E. device (b/2)	Span of T.E. device (b/2)	Configuration	$C_{L_{max}}$	$\alpha_{C_{L_{max}}}$	L/D at 0.85 $C_{L_{max}}$	C_m characteristics	Reference
None	None		1.12	27.1	5.26	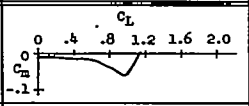	52
			1.14	26.0	4.97	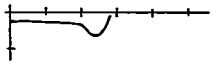	52
		$i_t = -3.2°$ $\frac{2x}{b} = .615$	1.14	25.0	—	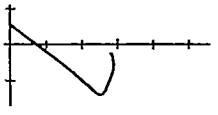	52
		$i_t = -3.1°$ $\frac{2x}{b} = .483$	1.13	26.0	—	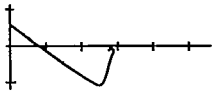	52
		$i_t = -3.2°$ $\frac{2x}{b} = .307$	1.15	27.0	—	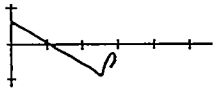	52
		$i_t = -4.1°$ $\frac{2x}{b} = .037$	1.25	27.0	—	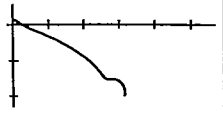	52
			1.17	26.6	4.48	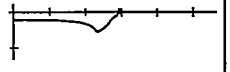	52
		$i_t = -3.2°$ $\frac{2x}{b} = .502$	1.15	26.0	—	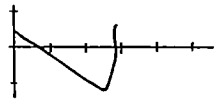	52
		$i_t = -3.1°$ $\frac{2x}{b} = .372$	1.16*	27.0	—	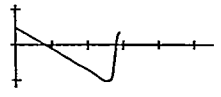	52
		$i_t = -3.2°$ $\frac{2x}{b} = .196$	1.21*	27.0	—	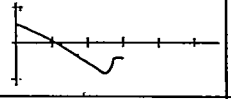	52
		$i_t = -4.1°$ $\frac{2x}{b} = -.074$	1.28*	26.0	—	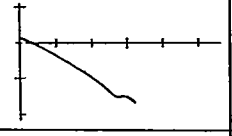	52
	.500 split flap		1.15	22.1	6.06	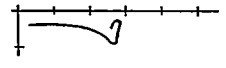	52

*$C_{L_{max}}$ not reached.

TABLE 38.—SUMMARY OF LONGITUDINAL STABILITY CHARACTERISTICS OF A WING WITH 52° OF LEADING-EDGE SWEEPBACK—Continued

Span of L.E. device (b/2)	Span of T.E. device (b/2)	Configuration	$C_{L_{max}}$	$^{a}C_{L_{max}}$	L/D at 0.85 $C_{L_{max}}$	C_m characteristics	Reference
None	.500 split flap	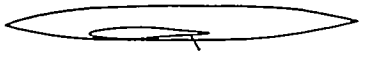	1.10	21.7	6.10	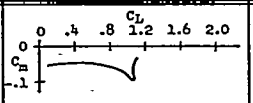	52
		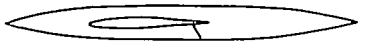	1.17	24.0	5.88	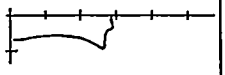	52
.250 L.E. flap	None	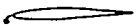	1.07	27.4	5.68	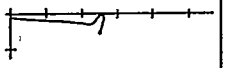	13
		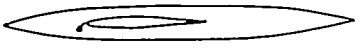	1.18	30.8	4.18	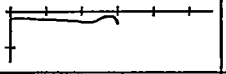	13
.350 L.E. flap	None	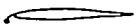	1.10	30.0	5.32	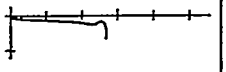	13
.400 L.E. flap	None	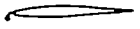	1.19	29.2	3.64	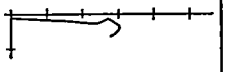	13
		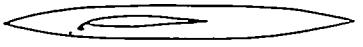	1.23	29.0	4.27	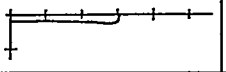	13
	.400 split flap	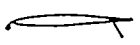	1.14	24.7	5.59	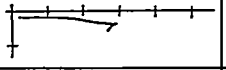	13
		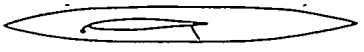	1.18	31.0	5.03	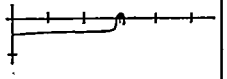	13
		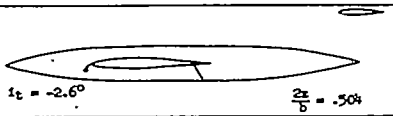	1.15	30.0	—	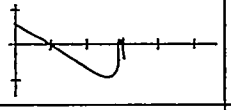	13
			1.25	31.0	—	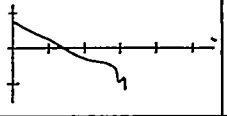	13
		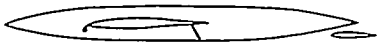	1.35*	31.0	—	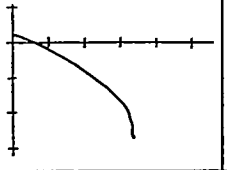	13
		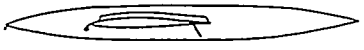	1.21*	30.4	4.29	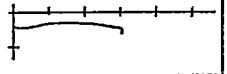	13
		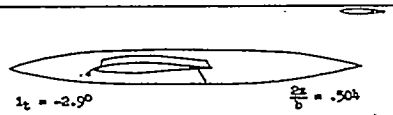	1.22*	30.6	—	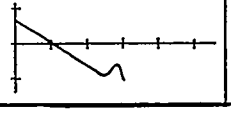	13

*$C_{L_{max}}$ not reached.

TABLE 38.—SUMMARY OF LONGITUDINAL STABILITY CHARACTERISTICS OF A WING WITH 52° OF LEADING-EDGE SWEEPBACK—Continued

Span of L.E. device (b/2)	Span of T.E. device (b/2)	Configuration	$C_{L_{max}}$	$\alpha_{C_{L_{max}}}$	L/D at 0.85 $C_{L_{max}}$	C_m characteristics	Reference
.400 L.E. flap	.400 split flap	$i_t = -2.8°$ $\frac{2z}{b} = .196$	1.24*	30.0	—	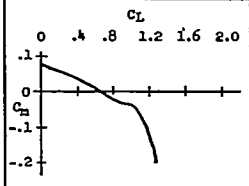	13
		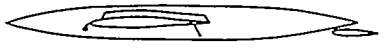 $i_t = -4.3°$ $\frac{2z}{b} = -.074$	1.58	30.4	—	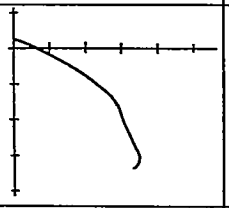	13
	.400 ext. split flap	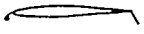	1.31	23.5	5.50	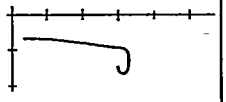	13
		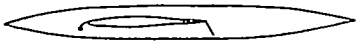	1.45	31.0	4.55	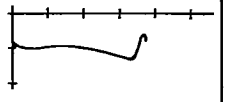	13
		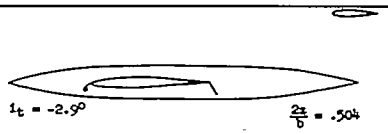 $i_t = -2.9°$ $\frac{2z}{b} = .504$	1.57	30.4	—	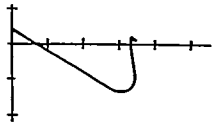	13
		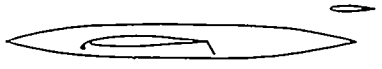 $i_t = -2.8°$ $\frac{2z}{b} = .196$	1.47	31.2	—	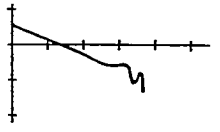	13
		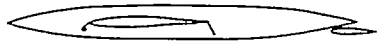 $i_t = -4.3°$ $\frac{2z}{b} = -.074$	1.59	30.2	—	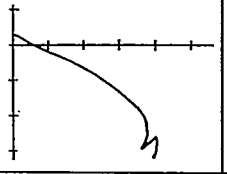	13
	.500 split flap	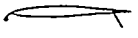	1.17	23.0	5.53	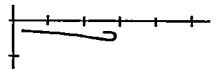	13
	.500 ext. split flap	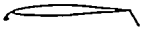	1.36	24.0	4.97	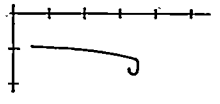	13
.450 L.E. flap	None	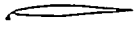	1.13	28.6	5.06	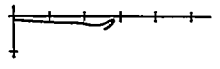	13
	.400 split flap	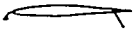	1.15	25.0	5.68	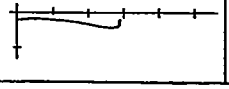	13

*$C_{L_{max}}$ not reached.

TABLE 38.—SUMMARY OF LONGITUDINAL STABILITY CHARACTERISTICS OF A WING WITH 52° OF LEADING-EDGE SWEEPBACK—Continued

Span of L.E. device (b/2)	Span of T.E. device (b/2)	Configuration	$C_{L_{max}}$	$\alpha_{C_{L_{max}}}$	L/D at 0.85 $C_{L_{max}}$	C_m characteristics	Reference
.450 L.E. flap	.400 ext. split flap	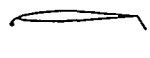	1.35	24.0	5.29	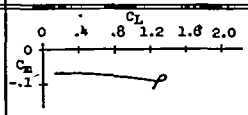	13
	.500 split flap	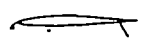	1.19	22.8	5.46	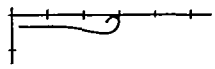	13
	.500 ext. split flap	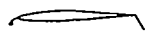	1.44	25.5	4.83	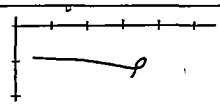	13
.375 L.E. flap	None	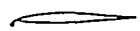	1.17*	28.2	5.13	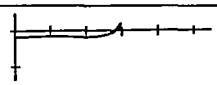	52
		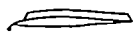	1.10*	28.2	6.37	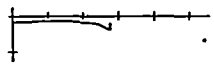	52
	.500 split flap	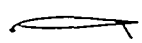	1.32	27.3	5.16	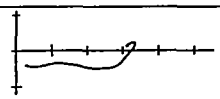	52
		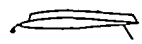	1.27	24.0	5.69	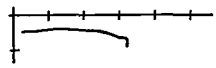	52
		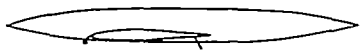	1.31	26.3	5.06	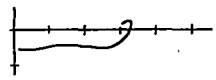	52
		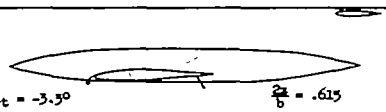 $i_t = -3.3°$ $\frac{2z}{b} = .615$	1.35	26.0	—	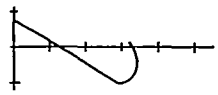	52
		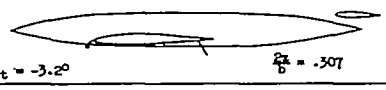 $i_t = -3.2°$ $\frac{2z}{b} = .307$	1.31	26.2	—	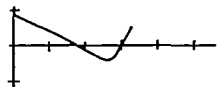	52
		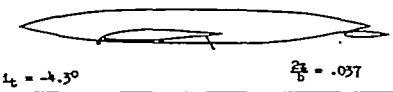 $i_t = -4.3°$ $\frac{2z}{b} = .037$	1.41	27.0	—	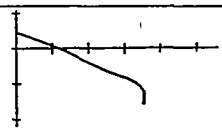	52
			1.31	24.3	5.24	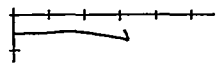	52
		$i_t = -3.3°$ $\frac{2z}{b} = .615$	1.33	23.0	—	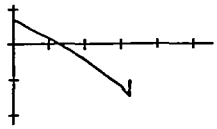	52
		$i_t = -3.2°$ $\frac{2z}{b} = .483$	1.30	24.0	—	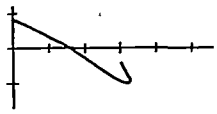	52

*$C_{L_{max}}$ not reached.

TABLE 38.—SUMMARY OF LONGITUDINAL STABILITY CHARACTERISTICS OF A WING WITH 52° OF LEADING-EDGE SWEEPBACK—Continued

Span of L.E. device (b/2)	Span of T.E. device (b/2)	Configuration	$C_{L_{max}}$	$\alpha_{C_{L_{max}}}$	L/D at 0.85 $C_{L_{max}}$	C_m characteristics	Reference
.575 L.E. flap	.500 split flap	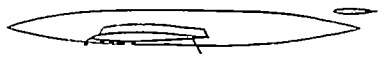 $i_t = -3.2°$ $\frac{2z}{b} = .307$	1.29	24.2	—	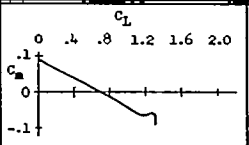	52
		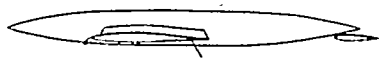 $i_t = -4.1°$ $\frac{2z}{b} = .037$	1.40*	27.4	—	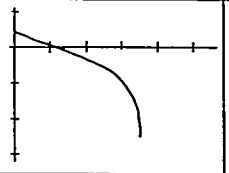	52
		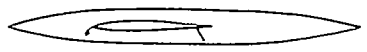	1.34	26.4	4.76	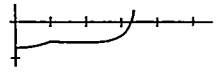	52
			1.39*	27.4	4.70	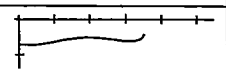	52
		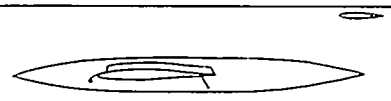 $i_t = -3.2°$ $\frac{2z}{b} = .502$	1.39*	27.4	—	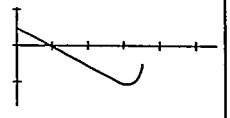	52
		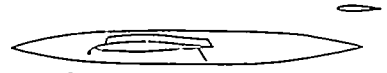 $i_t = -3.0°$ $\frac{2z}{b} = .372$	1.38*	27.4	—	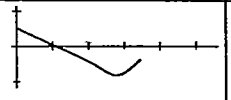	52
		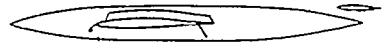 $i_t = -3.2°$ $\frac{2z}{b} = .196$	1.41*	27.4	—	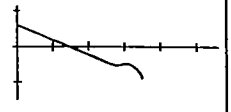	52
		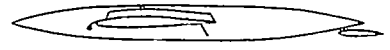 $i_t = -4.1°$ $\frac{2z}{b} = -.074$	1.48*	26.4	—	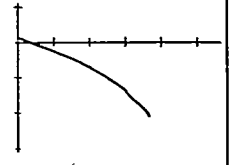	52
.725 L.E. flap	None	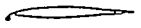	1.24*	28.2	5.29	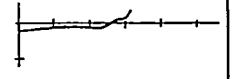	52
	.500 split flap	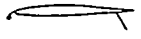	1.36	27.0	5.44	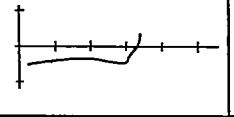	52

*$C_{L_{max}}$ not reached.

TABLE 38.—SUMMARY OF LONGITUDINAL STABILITY CHARACTERISTICS OF A WING WITH 52° OF LEADING-EDGE SWEEPBACK—Concluded

Span of L.E. device (b/2)	Span of T.E. device (b/2)	Chord of L.E. device ($\bar{c}$)	Configuration	$C_{L_{max}}$	$\alpha_{C_{L_{max}}}$	L/D at 0.85 $C_{L_{max}}$	C_m characteristics	Reference
.14 round L.E. chord ext.	None	.15		1.11	27.0	4.66	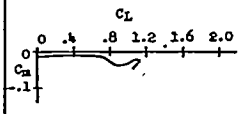	53
.23 round L.E. chord ext.	None	.15		1.18	29.5	4.67	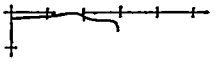	53
.43 round L.E. chord ext.	None	.075		1.16	25.0	4.88	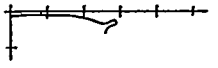	53
		.15		1.24	26.0	4.05	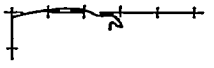	53
.43 sharp L.E. chord ext.	None	.075	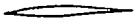	1.08	22.0	4.82	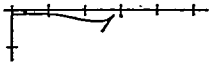	53
		.15		1.09	26.0	4.58	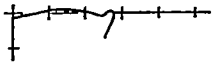	53

TABLE 39.—SUMMARY OF LONGITUDINAL STABILITY CHARACTERISTICS OF A WING WITH 52° OF LEADING-EDGE SWEEPBACK

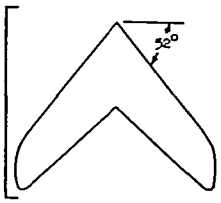

$\Lambda_{c/4} = 50.2°$ $A = 2.84$ $R_{max} = 9.7 \times 10^6$

$\lambda = 0.616$ $M_{max} = 0.19$

Airfoil sections (normal to line of maximum thickness)

Root: 9.8-percent-thick circular arc

Tip: 6.2-percent-thick circular arc

Span of L.E. device (b/2)	Span of T.E. device (b/2)	Configuration	$C_{L_{max}}$	$\alpha_{C_{L_{max}}}$	L/D at 0.85 $C_{L_{max}}$	C_m characteristics	Reference
None	None		1.04	24.5	3.58		54
			1.17	27.0	3.03		55
		$i_t = 2.6°$ $\frac{2z}{b} = .442$	1.18	30.0	—		55
		$i_t = 3.1°$ $\frac{2z}{b} = .136$	1.32	32.0	—		55
		$i_t = 2.2°$ $\frac{2z}{b} = -.132$	1.36	31.0	—		55
	.500 split flap		1.09	21.0	4.06		54
	.500 ext. split flap		1.29	22.0	4.05		54
.150 L.E. flap	None		1.06	26.0	3.23		54
.250 L.E. flap	None		1.06	27.5	3.23		54
			1.26	31.0	2.75		55
		$i_t = 2.9°$ $\frac{2z}{b} = .442$	1.31*	32.0	—		55

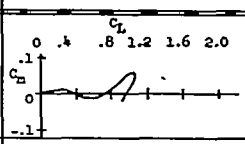

*$C_{L_{max}}$ not reached.

TABLE 39.—SUMMARY OF LONGITUDINAL STABILITY CHARACTERISTICS OF A WING WITH 52° OF LEADING-EDGE SWEEPBACK—Continued

Span of L.E. device (b/2)	Span of T.E. device (b/2)	Configuration	$C_{L_{max}}$	$\alpha_{C_{L_{max}}}$	L/D at 0.85 $C_{L_{max}}$	C_m characteristics	Reference
.250 L.E. flap	None	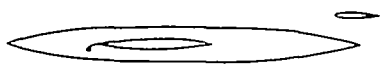 $i_t = 2.9°$ $\frac{2z}{b} = .136$	1.43*	32.0	—	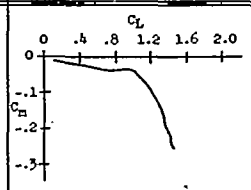	55
		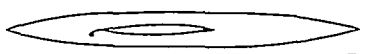 $i_t = 2.2°$ $\frac{2z}{b} = -.131$	1.43	30.0	—	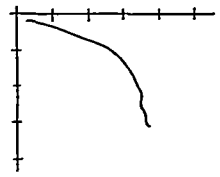	55
	.400 split flap	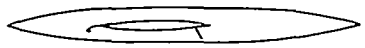	1.15*	32.0	—	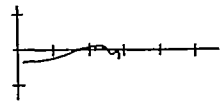	55
		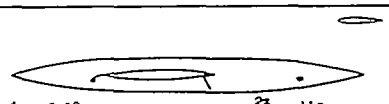 $i_t = 2.9°$ $\frac{2z}{b} = .442$	1.19*	32.0	—	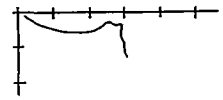	55
		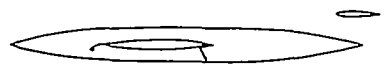 $i_t = 2.8°$ $\frac{2z}{b} = .136$	1.27*	32.0	—	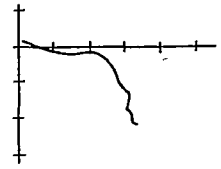	55
		$i_t = 2.2°$ $\frac{2z}{b} = -.132$	1.35*	32.0	—	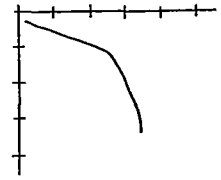	55
	.500 split flap	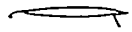	1.18	27.0	3.06	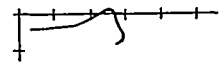	54
	.500 ext. split flap	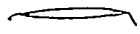	1.30	23.6	3.72	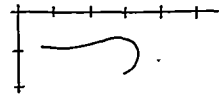	54
		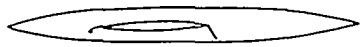	1.49*	32.0	—	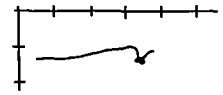	55
		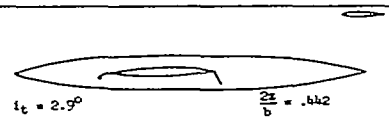 $i_t = 2.9°$ $\frac{2z}{b} = .442$	1.43*	32.0	—	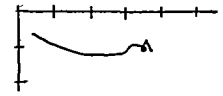	55

*$C_{L_{max}}$ not reached.

TABLE 39.—SUMMARY OF LONGITUDINAL STABILITY CHARACTERISTICS OF A WING WITH 52° OF LEADING-EDGE SWEEPBACK—Continued

Span of L.E. device (b/2)	Span of T.E. device (b/2)	Configuration	$C_{L_{max}}$	$\alpha_{C_{L_{max}}}$	L/D at 0.85 $C_{L_{max}}$	C_m characteristics	Reference
.250 L.E. flap	.500 ext. split flap	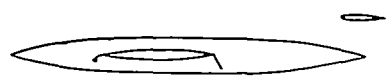 $i_t = 3.1°$ $\frac{2x}{b} = .136$	1.57*	32.0	—	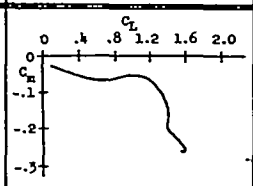	55
		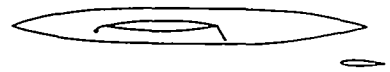 $i_t = 2.2°$ $\frac{2x}{b} = -.132$	1.68*	32.0	—	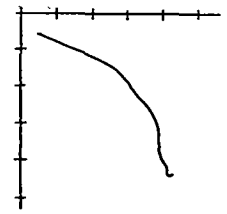	55
.350 L.E. flap	None	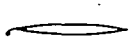	1.22*	31.2	2.40	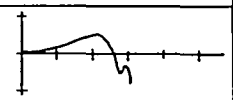	54
	.500 split flap	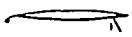	1.21	26.0	2.78	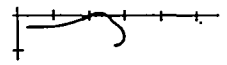	54
	.500 ext. split flap	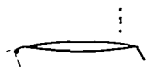	1.36	22.2	3.73	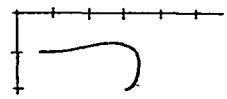	54
.450 L.E. flap	None	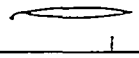	1.14*	28.1	3.21	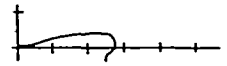	54
.550 L.E. flap	None	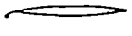	1.12	27.2	3.97	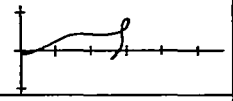	54
	.500 split flap	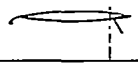	1.34	24.5	3.61	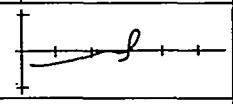	54
	.500 ext. split flap	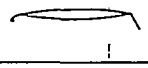	1.58	23.5	3.64	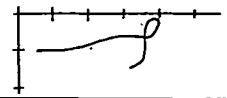	54
.250 L.E. droop	None	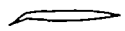	1.06	26.0	3.12	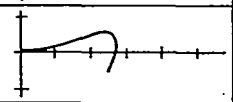	54
.450 L.E. droop	None	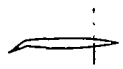	1.18	29.5	2.87	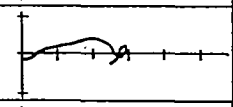	54
.600 L.E. droop	None	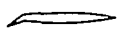	1.19	29.0	3.34	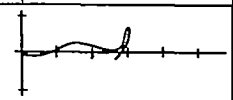	54

*$C_{L_{max}}$ not reached.

TABLE 39.—SUMMARY OF LONGITUDINAL STABILITY CHARACTERISTICS OF A WING WITH 52° OF LEADING-EDGE SWEEPBACK—Concluded

Span of L.E. device (b/2)	Span of T.E. device (b/2)	Chord of L.E. device ($\bar{c}$)	Configuration	$C_{L_{max}}$	$\alpha_{C_{L_{max}}}$	L/D at 0.85 $C_{L_{max}}$	C_m characteristics	Reference
.06 sharp L.E. chord ext.	None	.074	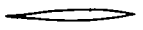	1.02	24.0	3.47	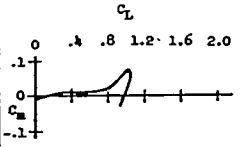	53
		.147	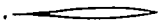	1.06	24.0	3.42	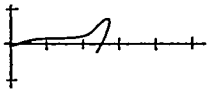	53
.25 sharp L.E. chord ext.	None	.074	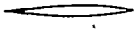	1.03	25.0	3.39	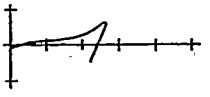	53
		.147		1.07	24.0	3.37	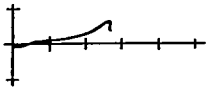	53
.25 sharp L.E. chord ext.	None	.074	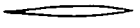	1.11	25.0	3.20	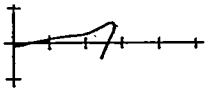	53
		.147		1.12	25.0	3.18	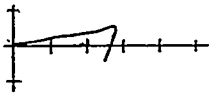	53

TABLE 40.—SUMMARY OF LONGITUDINAL STABILITY CHARACTERISTICS OF A WING WITH 60° OF LEADING-EDGE SWEEPBACK

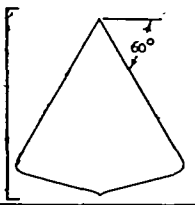

$\Lambda_{c/4} = 50.6°$ $A = 1.8$ $R_{max} = 5.3 \times 10^6$

$\lambda = 0$

Airfoil sections (parallel to plane of symmetry)

Root: NACA 0015-64 (approximate)

Tip: NACA 0015-64 (approximate)

Span of L.E. device (b/2)	Span of T.E. device (b/2)	Configuration	$C_{L_{max}}$	$\alpha_{C_{L_{max}}}$	L/D at 0.85 $C_{L_{max}}$	C_m characteristics	Reference
None	None	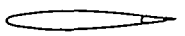	0.92	37.5	2.06	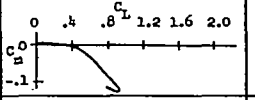	56
			0.61	23.0	—	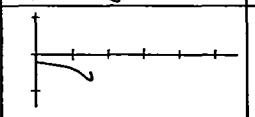	56
	.608 plain elevon flap	$\delta_f = -23°$	0.38	17.0	—	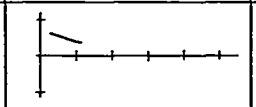	56
			0.57	17.0	—	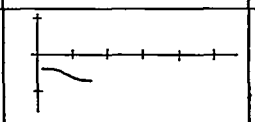	56
		$\delta_f = 23°$	0.60	17.0	—	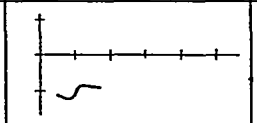	56
.553 sharp L.E.	None		1.25	40.0	2.15	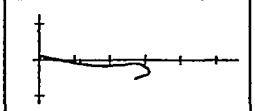	56
			1.01	32.5	—	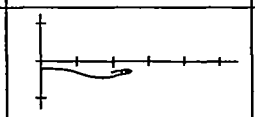	56
			1.29	41.0	—	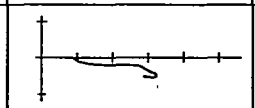	56
	.257 plain trim flap	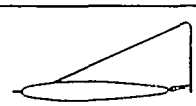 $\delta_f = -11°$	1.00	30.0	—	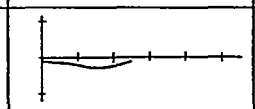	56
			1.03	30.0	—	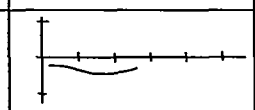	56
		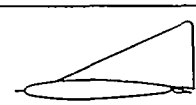 $\delta_f = 11°$	1.06	30.0	—	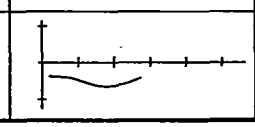	56

TABLE 40.—SUMMARY OF LONGITUDINAL STABILITY CHARACTERISTICS OF A WING WITH 60° OF LEADING-EDGE SWEEPBACK—Concluded

Span of L.E. device (b/2)	Span of T.E. device (b/2)	Configuration	$C_{L_{max}}$	$\alpha_{C_{L_{max}}}$	L/D at 0.85 $C_{L_{max}}$	C_m characteristics	Reference
.553 sharp L.E.	.608 plain elevon flap	$\delta_f = -25°$	0.88	33.0	—	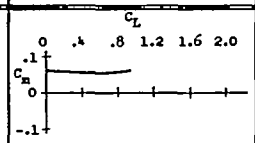	56
			1.04	33.0	—	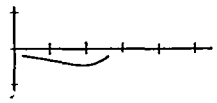	56
		$\delta_f = +25°$	1.05	33.0	—	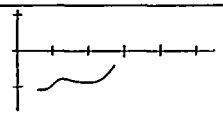	56
.726 faired sharp L.E.	None		1.32	40.0	—	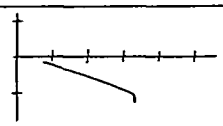	56
			1.28	40.0	—	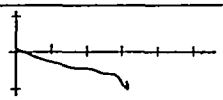	56
	.608 plain elevon flap	$\delta_f = -15°$	0.88	28.5	—	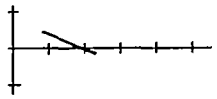	56
			0.96	28.5	—	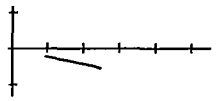	56
		$\delta_f = +15°$	0.97	28.5	—	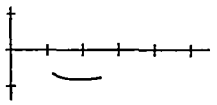	56

TABLE 41.—SUMMARY OF LONGITUDINAL STABILITY CHARACTERISTICS OF A WING WITH 60° OF LEADING-EDGE SWEEPBACK

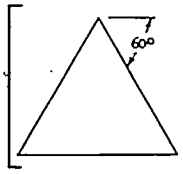

$\Lambda_{c/4} = 52.4°$ $A = 2.31$ $R_{max} = 9.61 \times 10^6$

$\lambda = 0$

Airfoil sections (parallel to plane of symmetry)

Root: 10-percent-thick circular arc

Tip: 10-percent-thick circular arc

Span of L.E. device (b/2)	Span of T.E. device (b/2)	Configuration	$C_{L_{max}}$	$\alpha_{C_{L_{max}}}$	L/D at 0.85 $C_{L_{max}}$	C_m characteristics	Reference
None	None		1.09	32.5	2.24	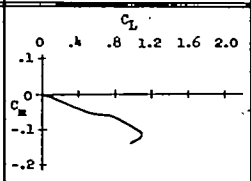	57
	.500 plain inboard flap	$\delta_f = 20°$ 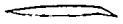	1.15	31.0	2.54	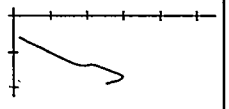	57
		$\delta_f = 40°$ 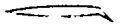	1.09	27.0	—	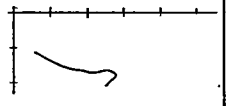	57
		$\delta_f = 60°$ 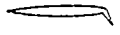	1.00	25.0	—	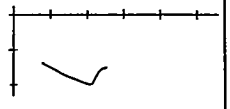	57
	1.000 plain flap	$\delta_f = 10°$	1.12	31.0	—	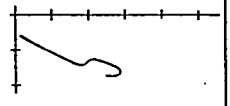	57
		$\delta_f = 20°$ 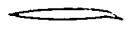	1.19	30.0	—	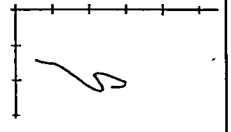	57
		$\delta_f = 30°$ 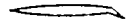	1.19	25.0	—	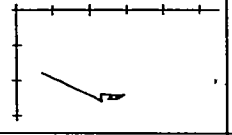	57
.500 inboard L.E. droop	None	$\delta_n = 20°$ 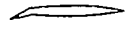	1.10	36.0	—	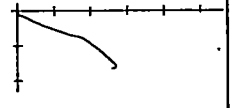	57
		$\delta_n = 40°$ 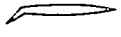	0.90	31.0	—	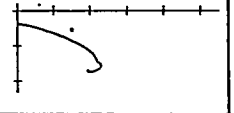	57

TABLE 41.—SUMMARY OF LONGITUDINAL STABILITY CHARACTERISTICS OF A WING WITH 60° OF LEADING-EDGE SWEEPBACK—Concluded

Span of L.E. device (b/2)	Span of T.E. device (b/2)	Configuration	$C_{L_{max}}$	$\alpha_{C_{L_{max}}}$	L/D at 0.85 $C_{L_{max}}$	C_m characteristics	Reference
.500 outboard L.E. droop	None	$\delta_n = 20°$ 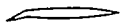	1.06	29.0	——	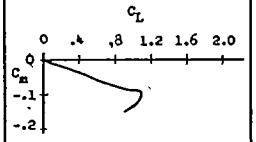	57
		$\delta_n = 30°$ 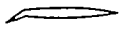	1.11	32.0	——	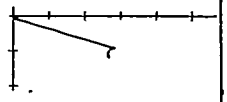	57
		$\delta_n = 40°$ 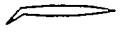	1.14	34.0	——	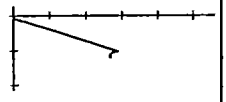	57
		$\delta_n = 50°$ 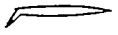	1.17	35.0	——	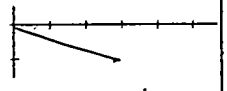	57
	.500 plain inboard flap	$\delta_n = 20°$ $\delta_f = 20°$ 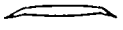	1.20	25.0	2.80	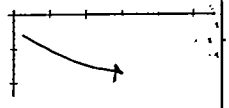	57
1.000 L.E. droop	None	$\delta_n = 10°$	1.12	35.0	——	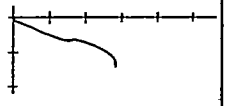	57
		$\delta_n = 20°$ 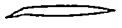	1.19	37.0	——	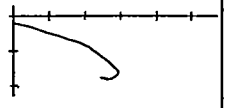	57
		$\delta_n = 30°$ 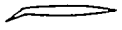	1.21	37.0	——	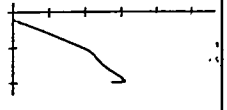	57
	.500 plain inboard flap	$\delta_n = 20°$ $\delta_f = 20°$ 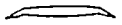	1.10	32.5	——	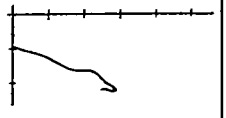	57
	1.000 plain flap	$\delta_n = 20°$ $\delta_f = 20°$ 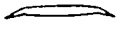	1.20	34.0	——	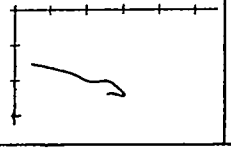	57

TABLE 42.—SUMMARY OF LONGITUDINAL STABILITY CHARACTERISTICS OF A WING WITH 60° OF LEADING-EDGE SWEEPBACK

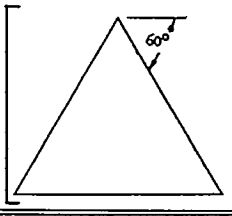

$\Lambda_{c/4} = 52.4°$ $A = 2.31$ $R_{max} = 16.4 \times 10^6$

$\lambda = 0$ $M_{max} = 0.13$

Airfoil sections (parallel to plane of symmetry)

Root: NACA 65-006.5

Tip: NACA 65-006.5

Span of L.E. device (b/2)	Span of T.E. device (b/2)	Configuration	$C_{L_{max}}$	$\alpha_{C_{L_{max}}}$	L/D at 0.85 $C_{L_{max}}$	C_m characteristics	Reference
None	None	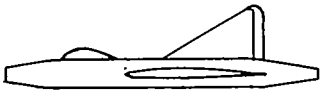	1.13	27.0	—	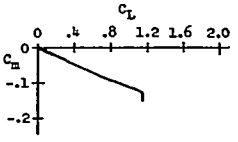	58
	.850 plain flap	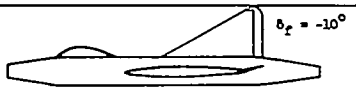	1.04	33.0	—	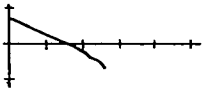	58

TABLE 43.—SUMMARY OF LONGITUDINAL STABILITY CHARACTERISTICS OF A WING WITH 60.9° OF LEADING-EDGE SWEEPBACK

$\Lambda_{c/4} = 60°$ $A = 4.0$ $R_{max} = 6.0 \times 10^6$

$\lambda = 0.600$ $M_{max} = 0.20$

Airfoil sections (parallel to plane of symmetry)

Root: NACA 65A006

Tip: NACA 65A006

Span of L.E. device (b/2)	Span of T.E. device (b/2)	Configuration	$C_{L_{max}}$	$\alpha_{C_{L_{max}}}$	L/D at 0.85 $C_{L_{max}}$	C_m characteristics	Reference
None	None	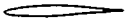	1.08	35.6	2.29	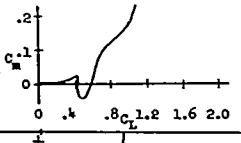	14
	.500 split flap		0.94	85.0	3.80	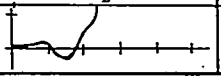	14

TABLE 44.—SUMMARY OF LONGITUDINAL STABILITY CHARACTERISTICS OF A WING WITH 63° OF LEADING-EDGE SWEEPBACK

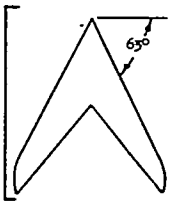

$\Lambda_{c/4}$ = 60.8° A = 3.5 R_{max} = 8.0 × 10^6

λ = 0.250

Airfoil sections (parallel to plane of symmetry)

Root: NACA 64A006

Tip: NACA 64A006

Span of L.E. device (b/2)	Span of T.E. device (b/2)	Configuration	$C_{L_{max}}$	$\alpha_{C_{L_{max}}}$	L/D at 0.85 $C_{L_{max}}$	C_m characteristics	Reference
None	None	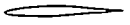	1.28	39.5	2.12	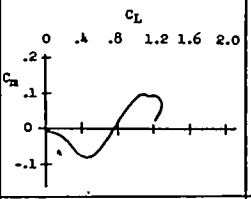	59
		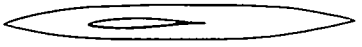	1.32	38.5	2.05	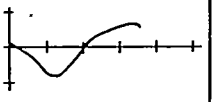	59
	.500 split flap	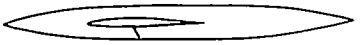	1.38	38.0	1.90	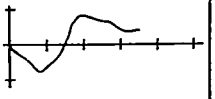	60
		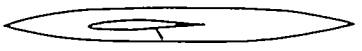	1.32	38.0	1.68	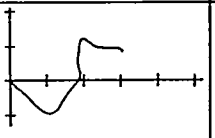	60
		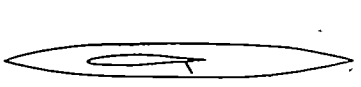	1.23	38.0	1.68	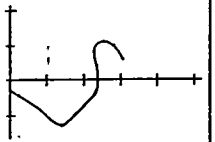	60
	.500 ext. split flap	$\delta_f = 0°$ 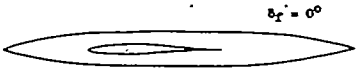	1.65*	38.5	2.06	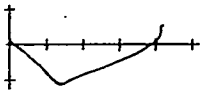	60
		$\delta_f = 25°$ 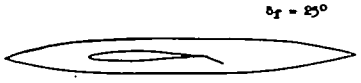	1.70	38.5	2.41	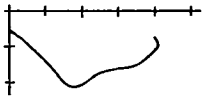	60
		$\delta_f = 45°$ 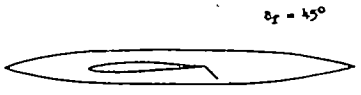	1.70	38.5	2.42	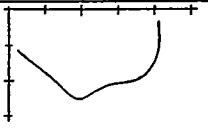	60
		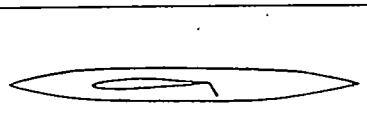	1.62	38.0	2.50	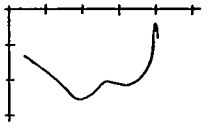	60

*$C_{L_{max}}$ not reached.

TABLE 44.—SUMMARY OF LONGITUDINAL STABILITY CHARACTERISTICS OF A WING WITH 63° OF LEADING-EDGE SWEEPBACK—Concluded

Span of L.E. device (b/2)	Span of T.E. device (b/2)	Configuration	$C_{L_{max}}$	$\alpha_{C_{L_{max}}}$	L/D at 0.85 $C_{L_{max}}$	C_m characteristics	Reference
None	.500 rotated split flap	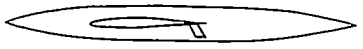	1.23	38.0	2.15	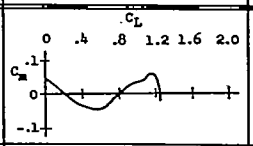	60
		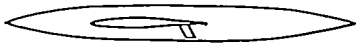	1.24	38.0	1.87	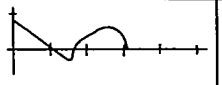	60
	.500 tri-angular flap	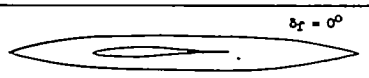	1.69	38.5	2.15	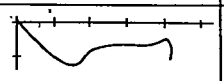	60
		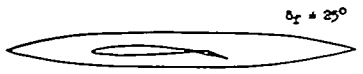	1.71	28.5	2.42	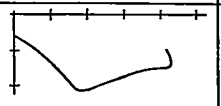	60
		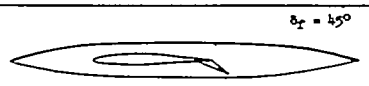	1.76	28.5	2.42	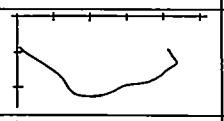	60
.500 L.E. flap	None	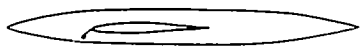	1.49*	38.1	—	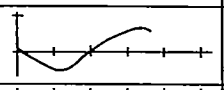	60
	.500 ext. split flap		1.65*	28.0	—	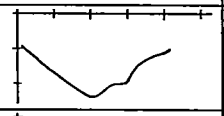	60
1.000 L.E. flap	None	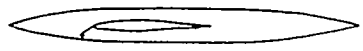	1.65*	38.2	—	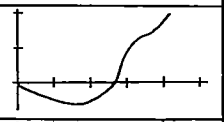	60
	.500 ext. split flap	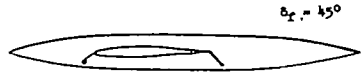	1.76*	28.3	2.72	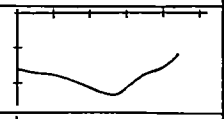	60
.500 L.E. droop	None	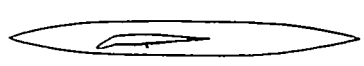	1.45	38.0	—	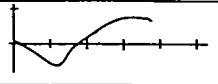	60
	.500 ext. split flap	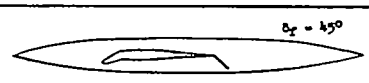	1.68	38.5	—		60
1.000 L.E. droop	None	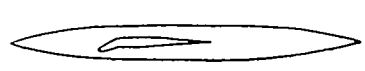	1.48*	38.1	2.07	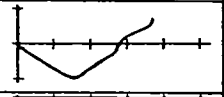	60
	.500 ext. split flap	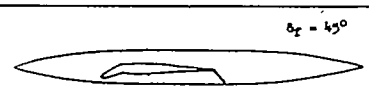	1.75*	38.5	2.52		60
.500 sharp L.E.	None	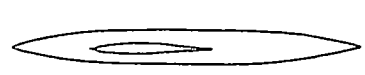	1.50	38.2	1.99	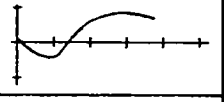	60
1.000 sharp L.E.	None	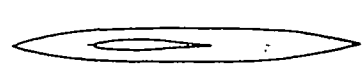	1.52	38.2	1.95	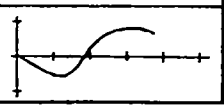	60

*$C_{L_{max}}$ not reached.

TABLE 45.—SUMMARY OF LONGITUDINAL STABILITY CHARACTERISTICS OF A WING WITH 63.03° OF LEADING-EDGE SWEEPBACK

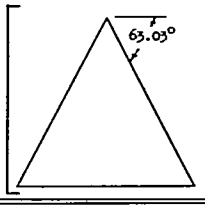

$\Lambda_{c/4} = 55.7°$ $A = 2.04$ $R_{max} = 15.0 \times 10^6$

$\lambda = 0$ $M_{max} = 0.18$

Airfoil sections (parallel to plane of symmetry)

Root: 5 percent thick at 0.20c hexagonal (faired)

Tip: 5 percent thick at 0.20c hexagonal (faired)

Span of L.E. device (b/2)	Span of T.E. device (b/2)	Configuration	$C_{L_{max}}$	$\alpha_{C_{L_{max}}}$	L/D at 0.85 $C_{L_{max}}$	C_m characteristics	Reference
None	None	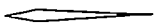	1.34	34.0	2.39	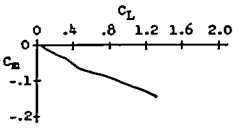	61
		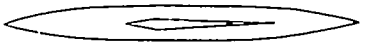	1.31*	31.0	2.41	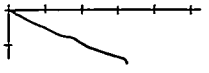	61
		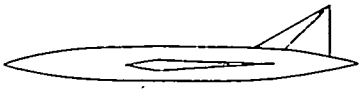	1.32*	20.0	2.34	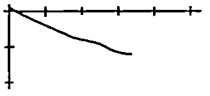	61
	.633 skewed tip flap	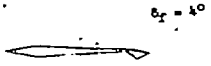	1.26*	30.0	2.49	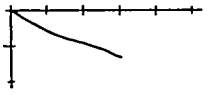	62
	1.000 plain flap		1.29*	28.0	—	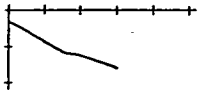	63
		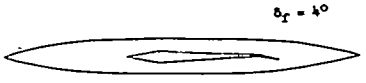	0.85*	18.0	—	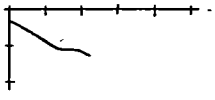	63
1.000 skewed L.E. flap	None	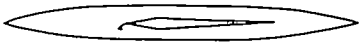	1.32	31.0	2.50	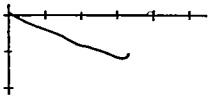	64
		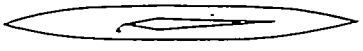	1.34	31.0	2.53	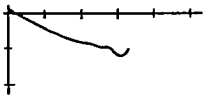	64

*$C_{L_{max}}$ not reached.

TABLE 46.—SUMMARY OF LONGITUDINAL STABILITY CHARACTERISTICS OF A WING WITH 63.43° OF LEADING-EDGE SWEEPBACK

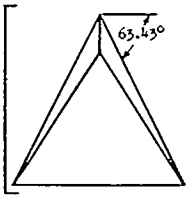

$\Lambda_{c/4} = 56.3°$ $A = 2.0$ $R_{max} = 32.3 \times 10^6$

$\lambda = 0$

Airfoil sections (parallel to plane of symmetry)

Root: 5 percent thick at 0.20c hexagonal (faired)

Tip: 5 percent thick at 0.20c hexagonal (faired)

Span of L.E. device (b/2)	Span of T.E. device (b/2)	Configuration	$C_{L_{max}}$	$\alpha_{C_{L_{max}}}$	L/D at 0.85 $C_{L_{max}}$	C_m characteristics	Reference
None	None	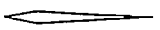	1.37	33.0	2.33	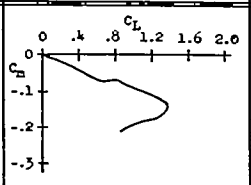	65
	.860 split flap	$\delta_f = 22°$ 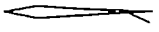	1.39	31.0	2.19	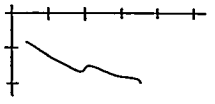	65
	.860 upper surface flap	$\delta_f = -22°$ 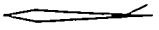	1.18	35.0	1.89	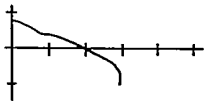	65
1.000 round L.E.	None	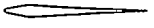	1.34	33.0	2.40	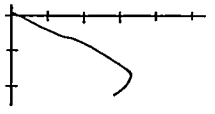	66
	.860 split flap	$\delta_f = 22°$ 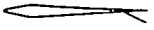	1.40	32.0	2.30	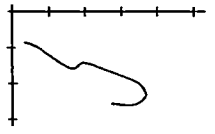	66
	.860 upper surface flap	$\delta_f = -22°$ 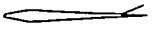	1.18	35.0	2.00	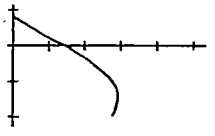	66
.860 L.E. flap	None	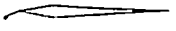	1.62	37.0	2.15	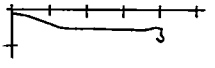	65
	.860 split flap	$\delta_f = 22°$ 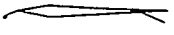	1.64	34.0	2.15	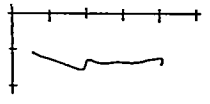	65
		$\delta_f = 44.5°$ 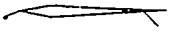	1.55	33.0	1.99	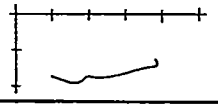	65

TABLE 47.—SUMMARY OF LONGITUDINAL STABILITY CHARACTERISTICS OF A WING WITH 63.43° OF LEADING-EDGE SWEEPBACK

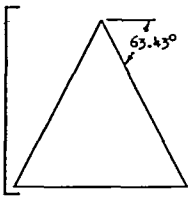

$\Lambda_{c/4} = 56.5°$ $A = 2.0$ $R_{max} = 15.3 \times 10^6$

$\lambda = 0$ $M_{max} = 0.13$

Airfoil sections (parallel to plane of symmetry)

Root: NACA 0005 (modified)

Tip: NACA 0005 (modified)

Span of L.E. device (b/2)	Span of T.E. device (b/2)	Configuration	$C_{L_{max}}$	$\alpha_{C_{L_{max}}}$	L/D at 0.85 $C_{L_{max}}$	C_m characteristics	Reference
None	1.000 plain flap	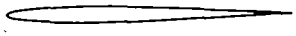	1.32	35.0	2.36	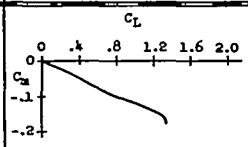	67
		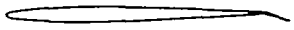	1.42	33.0	2.41	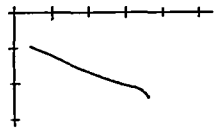	67
		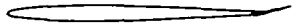	1.18	37.0	2.16	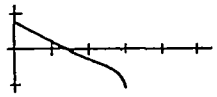	67

TABLE 48

Figure	Ordinate	Abscissa	Description
1	$\frac{c_l c}{C_L \bar{c}}$	$\frac{y}{b/2}$	Load distributions on wings having 0° and 45° of sweep.
2	c_l	α	Stall progression as indicated by section lift characteristics, $\Lambda_{c/4}=45°$.
3	C_L	C_m	Pitching-moment characteristics for a family of swept wings.
4	P, C_m, c_l	x/c, C_L, α	Effect of leading-edge separation on pressures, pitching moment, and lift.
5	L. E. radius	$\Lambda_{c/4}$	Boundary for leading-edge separation as defined by L. E. radius.
6	$C_{L_{inflection}}$	R	Reynolds number effect on inflection-lift coefficient.
7	C_L	C_m	Pitching-moment characteristics, L. E. separation present, for several swept wings.
8	C_L	C_m	Pitching-moment characteristics, L. E. separation present, for several aspect ratios.
9	C_L	C_m	Pitching-moment characteristics on delta wing with and without L. E. separation.
10	C_L	C_m	Effect of Reynolds number on mixed-flow separation.
11	C_L	R	Type of flow separation as influenced by Reynolds number.
12	A	$\Lambda_{c/4}$	Empirical stability boundary and its relation to constant area ratio.
13	$\frac{c_l c}{C_L \bar{c}}$	$\frac{y}{b/2}$	Load distributions for families of wings defined by constant area ratios.
14 (a) 14 (b)	c_l C_L	α C_m	Effects of fences on section lift and wing pitching-moment coefficients.
15	C_m	C_L	Effects of fences on the pitching-moment characteristics of several swept wings.
16	C_L	C_m	Effects of nacelles on the pitching-moment characteristics of a swept wing.
17	C_L, C_m	α	Effects of L. E. devices on the stall pattern of a swept wing.
18	L. E. flap span	T. E. flap span	Effects of L. E. and T. E. flaps on the pitching-moment characteristics of a swept wing.
19	A	$\Lambda_{c/4}$	Effect of stall-control devices on stability boundary of figure 12.
20	C_L	C_m	Boundary-layer control by suction on a swept wing.
21	C_m	C_L	Chord extensions on a swept wing.
22	C_m	C_L	Variable sweep.
23	C_L	C_m	Cambered and twisted swept wing.
24	C_L	C_m	Cambered and twisted swept wing with and without fences.
25	C_L	C_m	Cambered and twisted swept wing with L. E. flaps and fences.
26	ϵ	C_L	Horizontal-tail effectiveness at various vertical positions.

TABLE 48—Concluded

Figure	Ordinate	Abscissa	Description
27	$\frac{dw}{d\alpha}$	$\Lambda_{c/4}$	Rate of change of wake center with angle of attack.
28	$\frac{z}{b/2}$	ϵ	Downwash profiles behind a swept wing for several angles of attack.
29	ϵ, C_m	α	Correlation between downwash and horizontal tail effectiveness.
30	$C_{L_{\alpha_{calculated}}}$	$C_{L_{\alpha_{experiment}}}$	A comparison of experimental and calculated lift-curve slopes.
31	$\frac{C_{L_{max}}}{(C_{L_{max}})_{\Lambda=0}}$	$\Lambda_{c/4}$	Effect of leading-edge radius on maximum lift of swept wings.
32	$C_{L_{max}}$	$\Lambda_{c/4}$	Variations of maximum lift with sweep angle for several families of wings.
33	$C_{L_{max}}$	R	Reynolds number effect on the maximum lift of several swept wings.
34	$C_{L_{max}}$	A	Influence of aspect ratio on the maximum lift of several swept wings.
35	$\frac{C_{L_{inflection}}}{C_{L_{max}}}$	$\Lambda_{c/4}$	Influence of sweep and aspect ratio on the inflection lift coefficients of wings.
36	$\frac{\Delta C_{L(\alpha=0)}}{\Delta C_{L_{max}}}$	$\Lambda_{c/4}$	Influence of sweep on T. E. flap effectiveness.
37	ΔC_L	Flap span	Comparison of experimental and calculated linear-lift range flap effectiveness.
38	$\Delta C_{L(\alpha=0)}$	Various wings and flaps	Summary chart of lift increments due to various types of T. E. flaps on swept wings that are both stable and unstable.
39	$\Delta C_{L_{max}}$	Flap span	Effect of span and type of T. E. flaps on the maximum lift of two swept wings.
40	$\Delta C_{L_{max}}$	Various wings and flaps	Summary chart of maximum-lift increments due to various types of T. E. flaps on swept wings that are both stable and unstable.
41	$\frac{C_{D_{i_{elliptical}}}}{C_{D_i}}$	$\Lambda_{c/4}$	Calculated induced drags on swept wings.
42	$C_{D_{min}}$	$\Lambda_{c/4}$	Variation of minimum drag with sweep angle.
43	$C_{d_{wake}}$	C_l	Influence of sweep on the wake drag of an airfoil section.
44	C_{D_0}	C_L	Influence of sweep on the profile drag of a wing.
45	$\Delta C_{D_{0_e}}$	α	Influence of sweep on the effective profile drag of a wing with T. E. flaps.